New “Clickable” Reagents for Bioconjugate Chemistry

Thesis submitted in total fulfilment of the requirements of

Doctor of Philosophy

by

William Ian O’Malley

B. Form. Sci. (Hons)

Monash Institute of Pharmaceutical Sciences
Monash University
2016

Monash University

Declaration for thesis based or partially based on conjointly published or unpublished work

In accordance with Monash University Doctorate Regulation 17.2 Doctor of Philosophy and Research Master's regulations the following declarations are made:

I hereby declare that this thesis contains no material which has been accepted for the award of any other degree or diploma at any university or equivalent institution and that, to the best of my knowledge and belief, this thesis contains no material previously published or written by another person, except where due reference is made in the text of the thesis.

This thesis includes two original papers published in peer reviewed journals. The core theme of the thesis is the development of novel "clickable" reagents for bioconjugation. The ideas, development and writing up of the papers were the principal responsibility of myself, the candidate, working within the Monash Institute of Pharmaceutical Sciences under the supervision of Dr Bim Graham.

The inclusion of co-authors reflects the fact that the work came from active collaboration between researchers and acknowledges input into team-based research.

For Chapter 2, protein production was performed by Mr Elwy Abdelkader and Dr Choy-Theng Loh in association with Prof. Gottfried Otting (Research School of Chemistry, Australian National University). For Chapter 3, cellular uptake and (photo-)cytotoxicity studies were performed by Dr Riccardo Rubbiani in association with Prof. Gilles Gasser (Department of Chemistry, University of Zurich). For Chapter 5, all *in vivo* studies were conducted by Dr Frank Bergmann in association with Dr Holger Stephan (Institute of Radiopharmaceutical Cancer Research, Helmholtz Zentrum Dresden Rossendorf), with some of the radio stability studies being conducted by Dr Stephan's associates.

In the case of Chapters 2 and 3 my contribution to the work involved the following:

Thesis chapter	Publication title	Publication status	Nature and extent of candidate's contribution
2	Luminescent Alkyne-Bearing Terbium(III) Complexes and Their Application to Bioorthogonal Protein Labeling	Published	Synthesis and characterisation of synthetic compounds, evaluation of photophysical properties, interpretation of results, manuscript preparation
3	Cellular Uptake and Photo-Cytotoxicity of a Gadolinium(III)-DOTA-Naphthalimide Complex "Clicked" to a Lipidated Tat Peptide	Published	Synthesis and characterisation of synthetic compounds, evaluation of photophysical properties, interpretation of results, manuscript preparation

Signed: 

Date: 9/03/16

There is no denying that my PhD has been a long and sometimes troublesome road. As a result I feel very fortunate to those that have assisted me during this time, even at points were I may have not deserved it. First and foremost, I extend great thanks towards my supervisor, Dr Bim Graham, who has stuck with me throughout. Bim has been irreplaceable in my development as a professional, helping guide me towards my goals (sometimes with the carrot or the necessary stick!). I cannot thank him enough for all that he has done, from correcting my myriad of spelling and grammatical errors, to enjoying beer and paella with friends during a well-deserved break in Spain.

Second, I would like to thank those that directly aided in the work detailed in this thesis. I would like to extend my gratitude to all members of the Institute of Radiopharmaceutical Cancer Research located in Dresden Germany. Special thanks are made to Dr Holger Stephan and those of his research group for their assistance both during my time in Dresden as well as their continued support once back in Melbourne. Other collaborating individuals include Dr Riccardo Rubbiani, Prof. Gilles Gasser, Dr Kellie Tuck, Ms Margaret Aulsebrook, Prof. Leone Spiccia, Dr Choy-Theng Loh, Assoc. Prof. Michael Grace, Mr Elwy Abdeklader and Prof. Gottfried Otting who provided assistance in anything from performing toxicity studies to running NMR spectra.

Further acknowledgements are made on a slightly less professional note, thanking those that made my PhD experience at best a pleasure and at worst made things more bearable. Such people include Mr Ivan Troitsky, Mr Tom Day, Mr Michael Lee, Mr Luke Schembri, Dr Nicolas Barlow, Dr Jose Barreto, Ms Karina Pombo, Ms Lisa Barbaro, Dr Luke Adams, Dr James Swarbrick and any other I have met during my candidature. Special thanks must also be made to Ms Deborah Horne and the administration team at Monash for the gracious part time work they provided to me, allowing me to complete my PhD without significant financial hardship.

On a personal note, Philip and Susan O'Malley have been the greatest parents that anyone could hope for, their love is a constant reassurance and they have always displayed an interest and encouraged me in my pursuits, both professional and personal. By providing me with a solid support to fall back on when things get a bit too much, such as my car breaking down, their involvement in my PhD has been just as integral as anyone else. The rest of the immediate family have been pretty okay too. Other personal thanks are extended to my small, but close circle of friends, Mr Ben Lucas-Laws, Mr Alex Porlock, Mr John O'Connell and my wonderful girlfriend Ms Felicity Smith.

Finally, I extend my gratitude to Monash University and the Australian Government for the opportunity that has been provided to me and those in academia and education, both domestically and abroad.

Mohd A. Kamaruddin, Phuc Ung, Mohammed I. Hossain, Boonyarin Jarasrassamee, **William O'Malley**, Philip Thompson, Denis Scanlon, Heung-Chin Cheng and Bim Graham
A facile, click chemistry-based approach to assembling fluorescent chemosensors for protein tyrosine kinases.
Bioorg. Med. Chem. Lett. **2011**, *21*, 329-331.

José A. Barreto, **William O'Malley**, Manja Kubeil, Bim Graham, Holger Stephan and Leone Spiccia
Nanomaterials: Applications in Cancer Imaging and Therapy.
Adv. Mater. **2011**, 23 (12), H18–H40.

Karina P. García, Kristof Zarschler, Lisa Barbaro, José A. Barreto, **William O'Malley**, Leone Spiccia, Holger Stephan, and Bim Graham.
Zwitterionic-coated "Stealth" nanoparticles for biomedical applications: Recent advances in countering biomolecular corona formation and uptake by the mononuclear phagocyte system.
Small, **2014**, 10 (13), 2516–2529.

William I. O'Malley, Elwy H. Abdelkader, Margaret L. Aulsebrook, Riccardo Rubbiani, Choy-Theng Loh, Michael R. Grace, Leone Spiccia, Gilles Gasser, Gottfried Otting, Kellie L. Tuck and Bim Graham.
Luminescent alkyne-bearing terbium(III) complexes and their application to bioorthogonal protein labeling.
Inorg. Chem. **2016**, 55 (4), 1674–1682.

William I. O'Malley, Riccardo Rubbiani, Margaret L. Aulsebrook, Michael R. Grace, Leone Spiccia, Kellie L. Tuck, Gilles Gasser, and Bim Graham.
Cellular uptake and photo-cytotoxicity of a gadolinium(III)-DOTA-naphthalimide complex "clicked" to a lipidated tat peptide.
Molecules, **2016**, 21 (2), 194.

William I. O'Malley, Phuc Ung, Martin L. Williams, James Swarbrick and Bim Graham.
Magical luminescence: A lanthanide-based assay for psilocybin (Poster).
Monash Institute of Pharmaceutical Sciences: 6th Annual Postgraduate Research Symposium, **2011**, Parkville, Victoria, Australia.

William I. O'Malley, Linda Tjioe, Bim Graham.
"Clickable" lanthanide complexes for bioconjugation and the preparation of multi-modal imaging agents (Poster).
The Royal Australian Chemical Institute: Inorganic Division Conference, **2011**, Perth, Australia.
40th International Conference on Coordination Chemistry, **2012**, Valencia, Spain.

Bioorthogonal “click” chemistries represent a small but growing class of reliable “spring-loaded” reactions that occur exclusively between a pair of specific reaction partners, without interference from any of the native functional groups found in biological systems. These chemistries can be used to efficiently introduce a whole host of entities into biomolecules, ranging from targeting groups through to detectable molecules and functionalities that alter biodistribution characteristics.

This thesis describes the synthesis, utilisation and assessment of five new “clickable” imaging probes, spanning three different designs, with each bearing an alkyne functionality to facilitate highly-site specific tagging of azide-bearing (bio)molecules *via* the Cu(I)-catalysed click reaction.

The first set of tags are luminescent terbium(III) complexes incorporating cyclen-based chelators. Their utility for luminescent labelling was demonstrated through successful click conjugation to a small model azide compound as well as *E.coli* aspartate/glutamate-binding protein incorporating a genetically encoded *p*-azido-*L*-phenylalanine or *p*-(azidomethyl)-*L*-phenylalanine residue. Upon conjugation, one of the complexes displayed a significant luminescent enhancement (“light-up” effect), providing a simple indicator of successful ligation. The tags should prove useful for time-gated assay luminescence applications.

A second set of tags, also cyclen-based, were designed for potential bimodal imaging applications. These feature a fluorescent alkynyl-napthalimide group for optical detection, and a chelated Gd(III) ion to provide image contrast in MRI. As proof-of-concept, one of the complexes was clicked to a lipidated cell-penetrating peptide and uptake into tongue squamous carcinoma cells successfully visualised by fluorescence microscopy. The naphthalimide group was also found to impart photo-cytotoxic activity to the tagged peptide, suggesting that the tag may be a useful prototype building block for the production of theranostic agents.

The final class of tags, based upon the TACN macrocycle, were designed for chelation of the radionuclide ^{64}Cu and thereby the production of radiolabelled conjugates for imaging of tumours *via* positron emission tomography. Model ^{64}Cu chelates proved to be highly stable under physiological conditions, including in the presence of serum. By clicking one of the tags to a fluorescently-labelled bombesin peptide, a radiotracer designed for targeted imaging of prostate cancer was produced and evaluated in a small animal model. Although the peptide conjugate ultimately proved to have poor biodistribution characteristics, the "clickable" tags should prove useful for the development of better performing PET tracers in the future.

ACN	acetonitrile
ACPK	N^{ε}-(((1*R*,2*R*)-2-azidocyclo-pentyloxy)carbonyl)-*L*-lysine
Aha	azidohomoalanine
AlkK	N^{ε}-((prop-2-yn-1-yloxy)carbonyl)-*L*-lysine
AlkK2	N^{ε}-((pent-4-yn-1-yloxy)carbonyl)-*L*-lysine
Anl	azidonorleucine
AzK	N^{ε}-(2-azidoethoxy)carbonyl-*L*-lysine
BARAC	biarylazacyclooctynone
BBN	bombesin
BCN	bicyclo[6.1.0]nonyne
BCNK	N^{ε}-((1R,8S,9S)-bicyclo[6.1.0]non-4-yn-9-methyloxy)carbonyl)-*L*-lysine
Boc	*tert*-butyloxycarbonyl
Boc_2TACN	di-*tert*-butyloxycarbonyl-protected 1,4,7-triazacyclononane
BTTAA	2-[4-({*bis*[(1-*tert*-butyl-1H-1,2,3-triazol-4-yl)methyl]amino}methyl)-1H-1,2,3-triazol-1-yl]acetic acid
BTTES	2-[4-{(*bis*[(1-*tert*-butyl-1H-1,2,3-triazol-4-yl)methyl]amino)-methyl}-1H-1,2,3-triazol-1-yl]ethyl hydrogen sulphate
CoK1	N^{ε}-(cyclooct-2-yn-1-yloxy)carbonyl)-*L*-lysine
CoK2	N^{ε}-(2-(cyclooct-2-yn-1-yloxy)ethyl)carbonyl-*L*-lysine
CT	computer assisted tomography
CuAAC	copper-catalysed azide alkyne cycloaddition
Cy5	cyanine near-infrared (IR) fluorescence-emitting dye
cyclam	1,4,8,11-tetraazacyclotetradecane
cyclen	1,4,7,10-tetraazacyclododecane
DADT	diaminodithol

DIBO	dibenzocyclooctyne
DIFO	difluorocyclooctyne
DIPEA	*N*,*N*-diisopropylethylamine
DMPTACN	di(methylpyridyl)-1,4,7-triazacyclononane
DMF	dimethylfomamide
DMSO	dimethyl sulfoxide
DNA	deoxyribonucleic acid
DOTA	1,4,7,10-tetraazacyclododecane-1,4,7,10-tetraacetic acid
E. coli	*Escherichia coli*
EGF	epidermal growth factor
EGFr	epidermal growth factor receptor
EtcK	N^{ε}-(3-ethynyltetrahydrofuran-2-carbonyl)-*L*-lysine
Eth	ethynlphenylalanine
Fmoc	fluorenylmethyloxycarbonyl chloride
FRET	fluorescence resonance energy transfer
GFP	green fluorescent protein
GRP	gastrin-releasing peptide
GRPr	gastrin-releasing peptide receptor
HCTU	2-(6-chloro-1H-benzotriazole-1-yl)-1,1,3,3-tetramethylaminium hexafluorophosphate
HPLC	high performance liquid chromatography
Hpg	homopropargylglycine
HRMS	high resolution mass spectrometry
ITLC-SG	instant thin layer chromatography silica gel
LC-MS	liquid chromatography – mass spectrometry

Lp1A	lipoic acid ligase
LRET	luminescence resonance energy transfer
m-AzF	*m*-azidophenylanaline
m-Eth	*m*-ethynlphenylalanine
mDHFR	murine dihydrofolate reductase
MES	2-(*N*-morpholino)ethanesulphonic acid
MRI	magnetic resonance imaging
NHS	*N*-hydroxysuccinimide
NIR	near-infarred
NMR	nuclear magnetic resonance
NOTA	1,4,7-triazacyclononane-1,4,7-triacetic acid
o-AzbK	N^{ε}-(*o*-azidobenzyloxycarbonyl)-*L*-lysine
O/N	overnight
Orn(N_3)	azido-ornithine
p-AzMeF	*p*-azidomethylalanine
p-AzF	*p*-azidophenylanaline
PC-3	prostate cancer cell line-3
PEG	poly(ethylene glycol
PET	positron emission tomography
PrgF	*p*-propargyloxy-*L*-phenylalanine
PyBOP	benzotriazol-1-yl-oxytripyrrolidinophosphonium hexafluorophosphate
PylRS	pyrrolysine tRNA
RP-DCVC	reverse phase dry column vacuum chromatography
RT	room temperature
SPAAC	strain-promoted alkyne-azide cycloaddition

SPANC	strain-promoted alkyne-nitrone cycloaddition
SPS	solid-phase synthesis
SPPS	solid-phase peptide synthesiser
SUV_{mean}	absolute uptake values
TACN	1,4,7-triazacyclononane
TBTA	*tris*(benzyltriazolylmethyl)amine
TETA	1,4,8,11-tetraazacyclotetradecane-1,4,8,11-tetraacetic acid
TFA	trifluoroacetic acid
THF	tetrahydrofuran
THPTA	*tris*(3-hydroxypropyl-triazolylmethyl)amine
TLC	thin layer chromatography
TMAF	tetramethylammonium fluoride
TMS	trimethylsilyl
TMTH	3,3,6,6-tetramethylthiocycloheptyne
tRNA	transfer ribonucleic acid
TyrRS	tyrosyl tRNA synthetase
UAA	unnatural amino acid

CHAPTER 1:

INTRODUCTION

1.1 "Click" chemistry - an overview

Click chemistries represent a class of reliable "spring-loaded" reactions that ideally exclusively occur between a pair of reaction partners. The term "click chemistry" was first coined by Sharpless *et al.*[1] in 2001, with a stringent set of criteria imposed to determine if a reaction can be considered a click reaction. Such stringent criteria state that the reaction must be modular, wide in scope, high yielding, stereospecific (but not necessarily enantioselective) and only generate inoffensive by-products that are easily removed.[1] The processes and conditions of the reaction should also be relatively simple, requirements stating that the reaction be largely insensitive to the surrounding environment (i.e., not be adversely affected by oxygen or water) and proceed in either a complete absence of solvent or a solvent that is benign in nature and/or easily removed.[1] Initially, Sharpless proposed a repurposing of more traditional chemistries. These included: nucleophilic ring-opening reactions, such as those involving epoxides, aziridines, aziridinium ions and cyclic sulfates; non-aldol carbonyl chemistry, including the formation of oxime ethers, hydrazones and aromatic heterocycles;[2] additions to carbon-carbon multiple bonds, such as oxidative additions, as well as Michael additions of nucleophile reactants; and finally, cycloaddition reactions, encompassing 1,3-dipolar cycloaddition reactions and Diels-Alder reactions (**Figure 1**).[1]

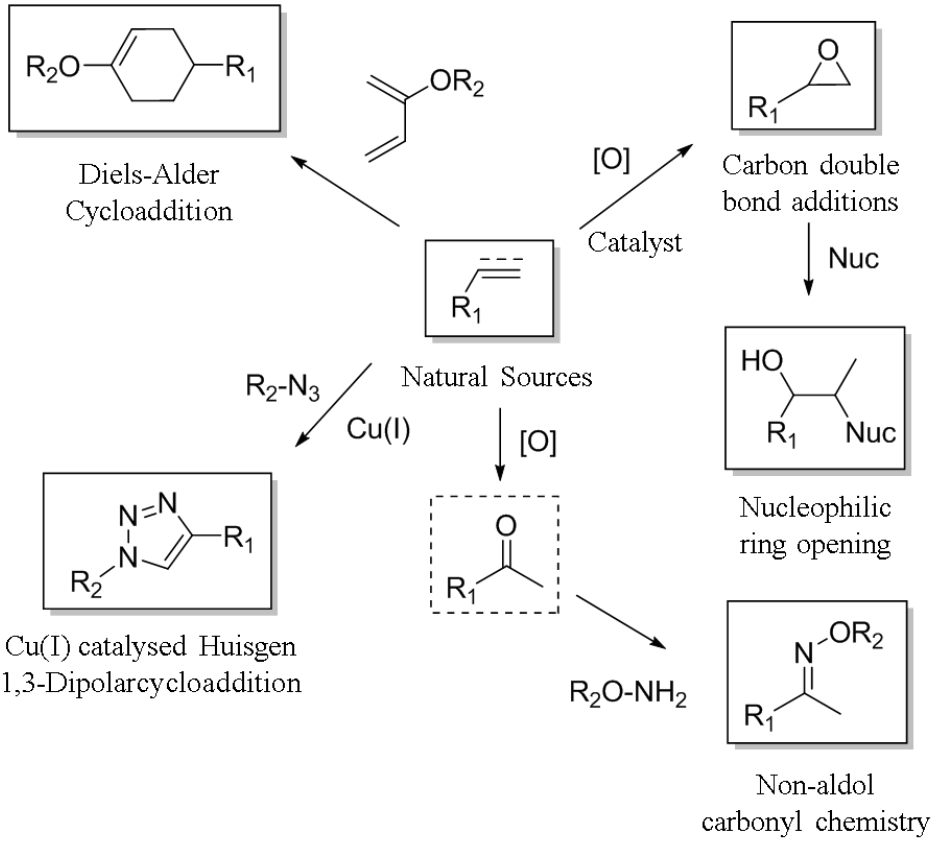

Figure 1. A series of reactions that satisfy click chemistry criteria. Reproduced from Moses *et al*.[3]

1.2 Copper-catalysed azide alkyne cycloaddition (CuAAC) - the "cream of the crop"

Of the reactions available, the Huisgen 1,3-dipolar cycloadditions[4] most ideally represent the properties of a click reaction. These modular fusion reactions between alkynes and azides generate five- and six-membered heterocycles and are very appealing due to the ease of synthesis/installation of the two reaction partners. The reaction participants also exhibit kinetic stability and a high tolerance to a wide range of functional groups and reaction conditions, allowing them to be installed when convenient and to remain unaffected by further synthetic reactions. Some concern exists regarding the potentially explosive or "shock-sensitive" nature of azides; this can be mitigated by observing the "rule of six", in which six carbon (or similarly sized) atoms per energetic functionality will typically provide sufficient dilution, rendering the compound relatively safe. Indeed, although azides are

thermodynamically favoured toward decomposition, azides generally remain unreactive until exposed to a dipolarophile.[5]

Whist all of these properties are beneficial, it was the remarkable discovery of copper(I) catalysis,[5,6] along with the beneficial effects of water upon the reaction, that thrust the Huisgen 1,3-dipolar azide-alkyne cycloaddition reaction into the limelight of click chemistry. This new "supercharged" version of the reaction requires no protecting groups, proceeds with almost complete conversion, generally requires no purification when utilised in the conjugation of small molecules, and is entirely selective for the 1,4-subsituted 1,2,3-triazole, as opposed to the thermally-induced reaction, which results in an approximate 1:1 ratio of the 1,4- and 1,5-substituted triazole stereoisomers (**Figure 2**).

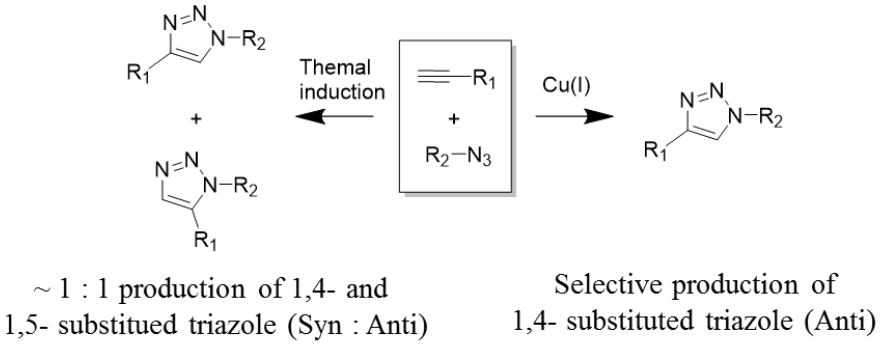

Figure 2. Comparison of the thermally-induced and copper(I)-catalysed Huisgen click reactions.

Due to all of these appealing properties, it is of no surprise that in common scientific vernacular "click chemistry" is almost synonymous with the Cu(I)-catalysed azide-alkyne cycloaddition (CuAAC) reaction. The reaction sequence of this remarkable reaction was investigated by Bock *et al.*[7] in 2006 through the analysis of a myriad of experimental results, resulting in the proposed mechanism shown in **Figure 3**.

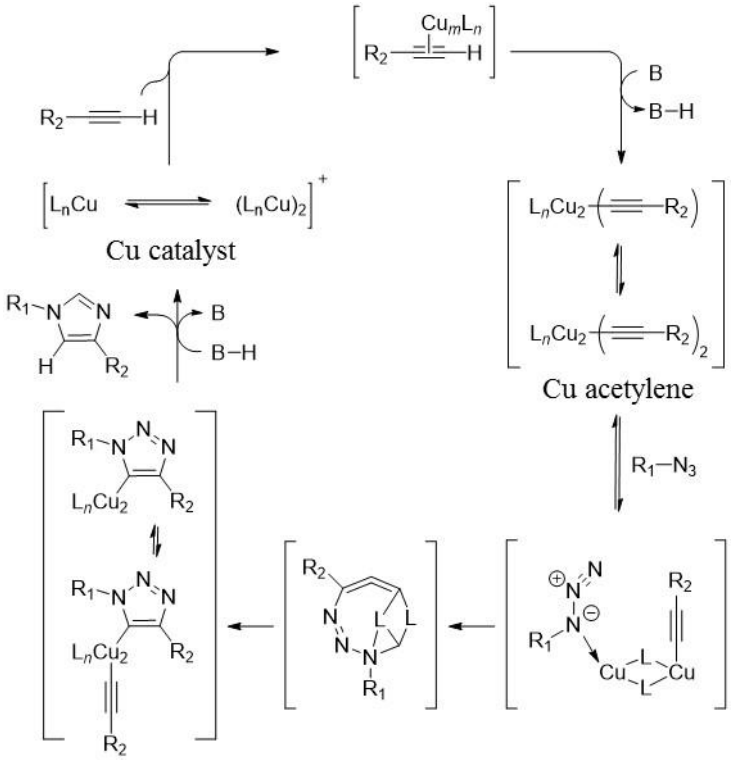

Figure 3. Reaction sequence and species involved in the CuAAC click reaction as proposed by Bock *et al.*[7]

1.2.1 CuAAC reaction promotors

Worthy of mention is the development and use of entities that assist the CuAAC reaction. As mentioned previously, the reaction exhibits a high tolerance to surrounding conditions, including the method of generation of the Cu(I) species. Sources of Cu(I) include the direct use of Cu(I) salts such as copper(I) iodide,[6] the *in situ* reduction of Cu(II) salts,[5] such as reduction of Cu(II)SO_4 with sodium ascorbate, and the comproportionation of Cu(0) and Cu(II).[8–10] The last decade has seen the development of a number of nitrogen-based, copper-binding ligands that aid the click reaction by stabilising the Cu(I) species, hindering any change in the oxidation state when placed under aerobic and aqueous conditions, thus promoting the desired transformation.[11] Specific examples of such ligands include *tris*-(benzyltriazolylmethyl)amine (TBTA),[11] the better performing *tris*(3-hydroxypropyltriazolylmethyl)amine (THPTA),[12] as well as 2-[4-{(*bis*[(1-*tert*-butyl-1H-1,2,3-

tri- azol-4-yl)methyl]amino)methyl}-1H-1,2,3-triazol-1-yl]acetic acid (BTTAA) and 2-[4-{(*bis*[(1-*tert*-butyl-1H-1,2,3-triazol-4-yl)methyl]amino)-methyl}-1H-1,2,3-triazol-1-yl]ethyl hydrogen sulphate (BTTES), the latter two of which are proposed to function the best when utilising CuAAC for bioconjugation.[13,14]

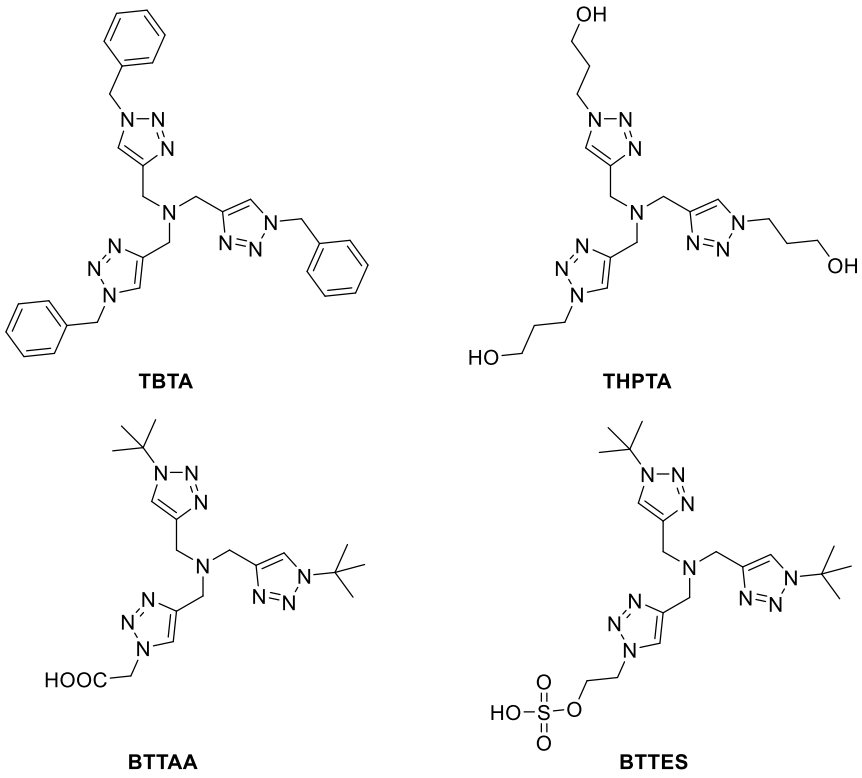

Figure 4. Selection of Cu(I)-complexing ligands commonly employed in CuAAC reactions.

1.3 Copper-free click chemistry

Whilst CuAAC is a very powerful reaction it is not without its drawbacks. The foremost of these is the necessary use of the copper catalyst. Use of the catalyst within an organic chemistry setting generally has little to no negative impact, however once the application shifts towards bioconjugation, compatibility issues emerge with some bioentities, causing the use of a metal catalyst to be highly undesirable. This has led to the development of so-called "copper-free click chemistries", including (but not limited to) strain-promoted alkyne-azide cycloaddition (SPAAC), strain-promoted alkyne-nitrone cycloaddition (SPANC) and inverse-

electron-demand Diels-Alder cycloadditions. These three reactions are discussed in more detail below.

1.3.1 Strain-promoted alkyne-azide cycloaddition (SPAAC)

Developed by Bettozzi and Boons, strain-promoted alkyne-azide cycloaddition (SPAAC) makes use of stained cyclooctynes to replace the alkyne in CuAAC. Due to intermolecular strain, these cyclooctynes (**Figure 5**, **A**) are able to readily react with azides in the absence of a metal catalyst at ambient temperatures.[15–18] SPAAC was initially described with the utilisation of cyclooctyne, the smallest of the isolatable cyclic alkynes. Further development has led to the discovery of more reactive cyclooctyne compounds (**Figure 5**, **B**) including derivatives of difluorocyclooctyne (DIFO),[19] bicyclo[6.1.0]nonyne (BCN),[20] dibenzocyclooctyne (DIBO),[18] biarylazacyclooctynone (BARAC), as well as the more recently developed thiacycloheptynes, such as 3,3,6,6-tetramethylthiocycloheptyne (TMTH).[21,22] Also of interest are cyclopropenones. These compounds transform to the corresponding dibenzocycloctynes upon exposure to light and have given rise to a light-sensitive version of SPAAC (**Figure 5**, **C**).[23–25]

SPAAC has been utilised in the synthesis of many conjugates, including proteins,[26] polymers,[27] dendrimers,[28] metal-organic frameworks[29] and functional surfaces,[30] as well as for labelling and imaging targeted biomolecules *in vivo*,[31,32] including in live mammalian cells[16] and zebrafish embryos.[33] SPAAC, however, is not without its disadvantages, possessing quite poor regioselectivity when compared to CuAAC. Further complications include undesirable reactivity of the cyclooctyne towards thiol-bearing cysteines, which can lead to non-specific labelling.[34] Additionally, cyclooctynes are quite difficult to synthesise, and although commercially available, are expensive, causing a significant barrier to entry for some research groups.

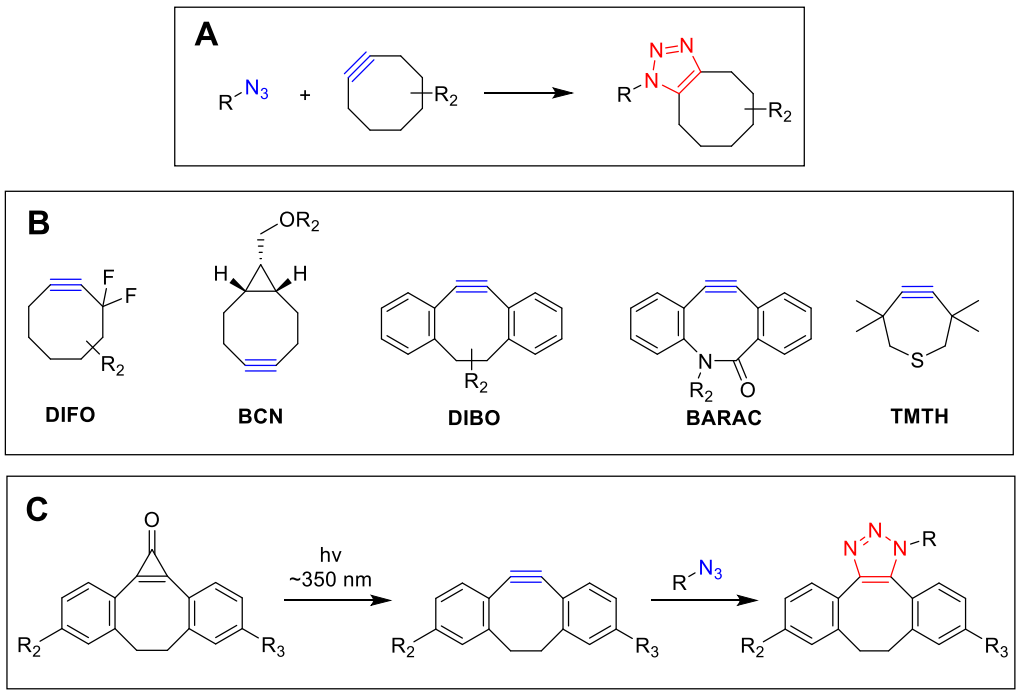

Figure 5. (**A**) Scheme for the SPAAC click reaction. (**B**) Developed reactive cyclooctyne compounds: DIFO,[19] BCN,[20] DIBO,[18] BARAC,[22] and TMTH.[21] (**C**) Scheme for a light-induced version of SPAAC.[25]

1.3.2 Strain-promoted alkyne-nitrone cycloaddition (SPANC)

Cyclooctynes, particularly benzannulated cyclooctynes, are also capable of reacting with substituted nitrones, at rates up to 30 times faster than comparable azides, resulting in the production of *N*-alkylated isoxazolines (**Scheme 1**).[35–37]

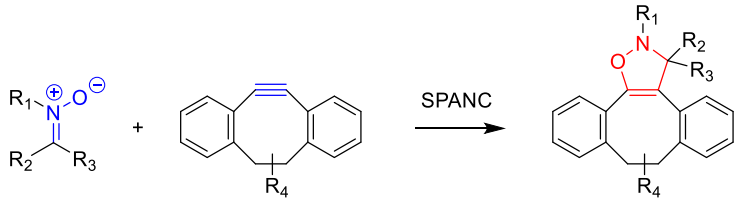

Scheme 1. Strain-promoted alkyne-nitrone 1,3-diploar cycloadditions (SPANC).

In one example, such a nitrone was installed onto the chemokine interleukin-8 *via* a one-pot, three-step protocol in which an *N*-terminus aldehyde was first introduced chemically with $NaIO_4$, then treated with *p*-methoxybenzenethiol, followed by *N*-methylhydroxylamine

and *p*-anisidine, to give the nitrone. This was then reacted with a cyclooctyne-bearing polyethyleneglycol (PEG) chain.[35] In another example, SPANC was utilised in the labelling of the epidermal growth factor receptor (EGFR), a commonly overexpressed receptor in breast cancer. An activated *N*-succinimidyl ester of a cyclic nitrone was first coupled to a lysine present on the surface of the EGFR. Fluorescent labelling was then achieved *via* a SPANC reaction with DIBO-biotin, followed by treatment with a streptavidin-coupled fluorophore.[38] The inherent instability of nitrones may limit the practical applications of SPANC.[36]

1.3.3. Inverse-electron-demand Diels-Alder cycloadditions

Classic Diels-Alder reactions involve a [4+2] cycloaddition between a conjugated, electron-rich, diene and an electron-poor dienophile (a strained alkene), forming a cyclohexene derivative as the product. An inverse-electron-demand Diels-Alder reaction, in contrast, occurs between an electron-rich dienophile (a strained alkene) and an electron-poor azadiene (a tetrazine) to yield a dihydropyridazine (**Figure 5**, **A**).[39] Investigation of these reactions in organic solvents demonstrated incredibly rapid reaction kinetics between *trans*-cyclooctene and a range of tetrazines, however instabilities of these initial tetrazines in aqueous media prevented their application within biological settings.[40] Work done more recently has identified the use of 3,6-diaryl-*s*-tetrazines as appropriate water-stable derivatives. One such derivative, 3,6-bipyridine-*s*-tetrazine, reacts rapidly with *trans*-cyclooctene, and has been successfully utilised in the modification of proteins *in vivo* (**Figure 5**, **B**).

Advantages of utilising inverse-electron-demand Diels-Alder reactions (particularly in regards to bioconjugation) include the lack of a requirement for potentially toxic catalysts, high selectivity, very rapid reaction kinetics, and an ability to tune reaction kinetics through variation of reagents.[41] Tetrazine-based inverse-electron-demand Diels-Alder reactions have been utilised in the synthesis of several biological conjugates, including labelling of antibodies with a tetrazine-based near-infrared (NIR) dye,[42] modification of proteins in both bacterial and

mammalian cells,[43–46] live cell imaging,[47] as well as the creation of magneto-fluorescent nanoparticles[48,49] and quantum dot conjugates.[50] This type of reaction also presents some interesting biomedical applications, largely surrounding tetrazine-based positron emission tomography[51,52] and ^{18}F scintigraphic imaging agents.[53,54]

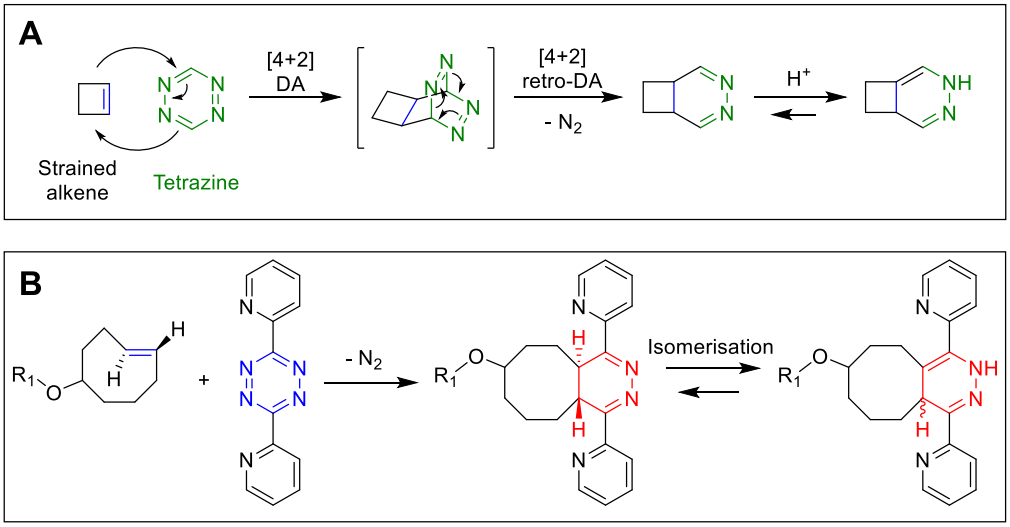

Figure 5. (**A**) Inverse-electron-demand Diels-Alder cycloaddition occurring between a strained alkene and 1,2,4,5-tetrazine, yielding a dihydropyridazine. (**B**) Reaction occurring between a strained cyclooctene and a 3,6-dipyridyltetrazine. Reproduced in part from Lang *et al.*[55]

1.4 Click chemistry for bioconjugation

Bioconjugation represents a host of reaction strategies with the objective of creating a stable covalent connection between two or more entities, with at least one of these being a biomolecule. The chemical modification of biomolecules is a field of great interest to chemists and biologists alike, allowing for the study of biomolecules in their native environment. Historically, bioconjugation has seen applications in the study of proteins,[56] enzyme functionality, tracking of cellular processes,[57] as well as the PEGylation of therapeutic proteins to improve *in vivo* characteristics,[58] and the modification of cancer-targeting agents with imaging motifs or therapeutic cytotoxins.[59]

Classically, protein/peptide bioconjugation has most often been performed using reactions that involve ligation to primary amine-containing lysine residues or thiol-containing

cysteine residues (**Figure 6**). Indeed, many of these chemistries remain invaluable bioconjugation tools. However, such techniques can prove troublesome when bioconjugates of precisely defined composition are required. For example, the utilisation of common chemical functionalities found within biological entities as reactive handles can sometimes require complicated global protective and deprotective measures to ensure that only the desired site is conjugated to. Reactions such as these can also be sensitive to the surrounding environment, with low tolerance to pH, solvent type, water and oxygen. As detailed earlier, click reactions are very specifically designed and selected to avoid these issues. They have proven to be highly useful within the field of bioconjugation, especially for the conjugation of small molecules to much larger biological entities.

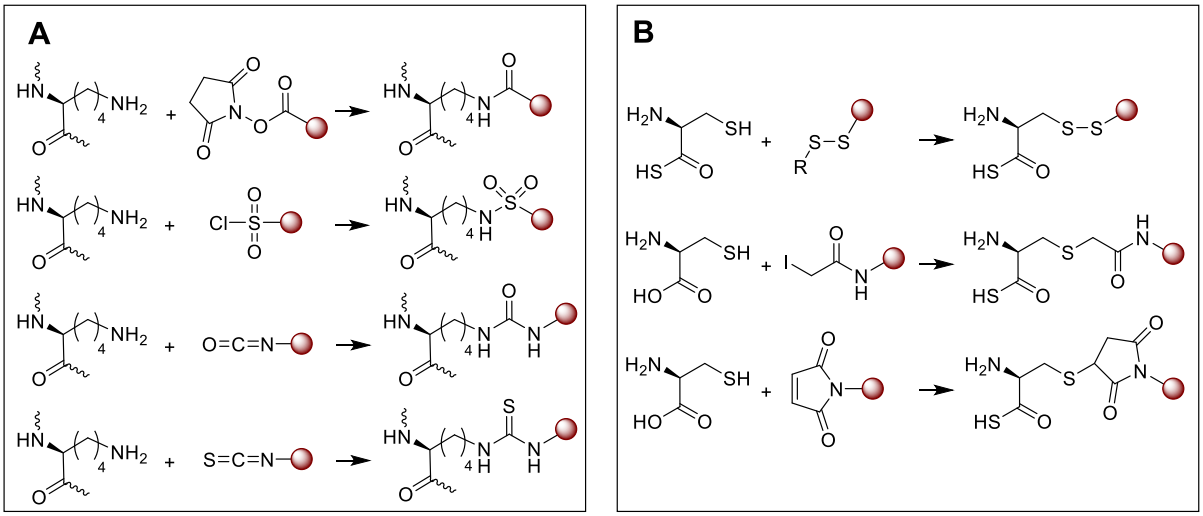

Figure 6. Classical reactions used for bioconjugation. (**A**) Modification of lysine residues with (top to bottom) *N*-hydroxysuccinimide-activated esters, sulfonyl chlorides, isocyanates and isothiocyanates. (**B**) Modification of cysteine residues through (top to bottom) disulphide exchange, alkylation with iodoacetamide reagents, and Michael additions with maleimides.

Click chemistries that have been employed for bioconjugation include the CuAAC and SPAAC reactions, thiol-ene reaction, thiol-Michael addition, oxime ligation, Diels-Alder reaction, Staudinger ligation and native chemical ligation (**Figure 7**). An excellent review by Tang *et al.*[60] describes the current applications of these click chemistries within the field of peptide bioconjugate synthesis. Of these reactions, those that are of particular interest are the

ones that are considered to be "bioorthogonal". Orthogonal chemistries boast a very valuable property: the two reactive participants are almost exclusively reactive towards each other. Bioorthogonal chemistries possess this quality but have the added benefit of not being reactive towards functional groups commonly found within biological systems. This type of chemistry allows for highly facile and specific bioconjugation to be executed as part of a late-stage labelling strategy for complex biological entities, including peptides and proteins. Of the various types of click chemistry mentioned, those that tend to best lend themselves to bioorthogonal bioconjugation are those that involve the azide conjugation handle, including CuAAC, SPAAC, Staudinger ligation and tandem [3+2] cycloaddition-retro-Diels-Alder (tandem crD-A).

From these available chemistries, the CuAAC reaction is of particular relevance for this project. As mentioned already, the reaction boasts tolerance of a wide range of solvents, it also proceeds readily under physiological conditions, and the formed triazole is highly stable. However, some factors must be taken in to consideration when determining the suitably of CuAAC for a specific application. The CuAAC reaction typically proceeds in near-quantitative to quantitative yields when used for organic synthesis, however this can drop to as low as 5% when employed for peptide synthesis. Yields tend to drop as peptides get longer, and peptide secondary folding can result in difficult to access reaction sites. Depending upon suitability, yields may be improved with microwave irradiation, increased temperature and introduction of reaction-promoting, copper-binding ligands such as BTTAA and BTTES. The copper catalyst used can also cause complications when used with specific biological entities, including protein denaturation,[61] as well as disruption of larger biological entities such as unravelling of DNA,[62] and cell cytotoxicity.[63] Purification to remove remaining copper salts, copper-binding ligands and any reducing agents such as sodium ascorbate must also be taken into consideration when assessing the suitability of CuAAC for a particular bioconjugation application.

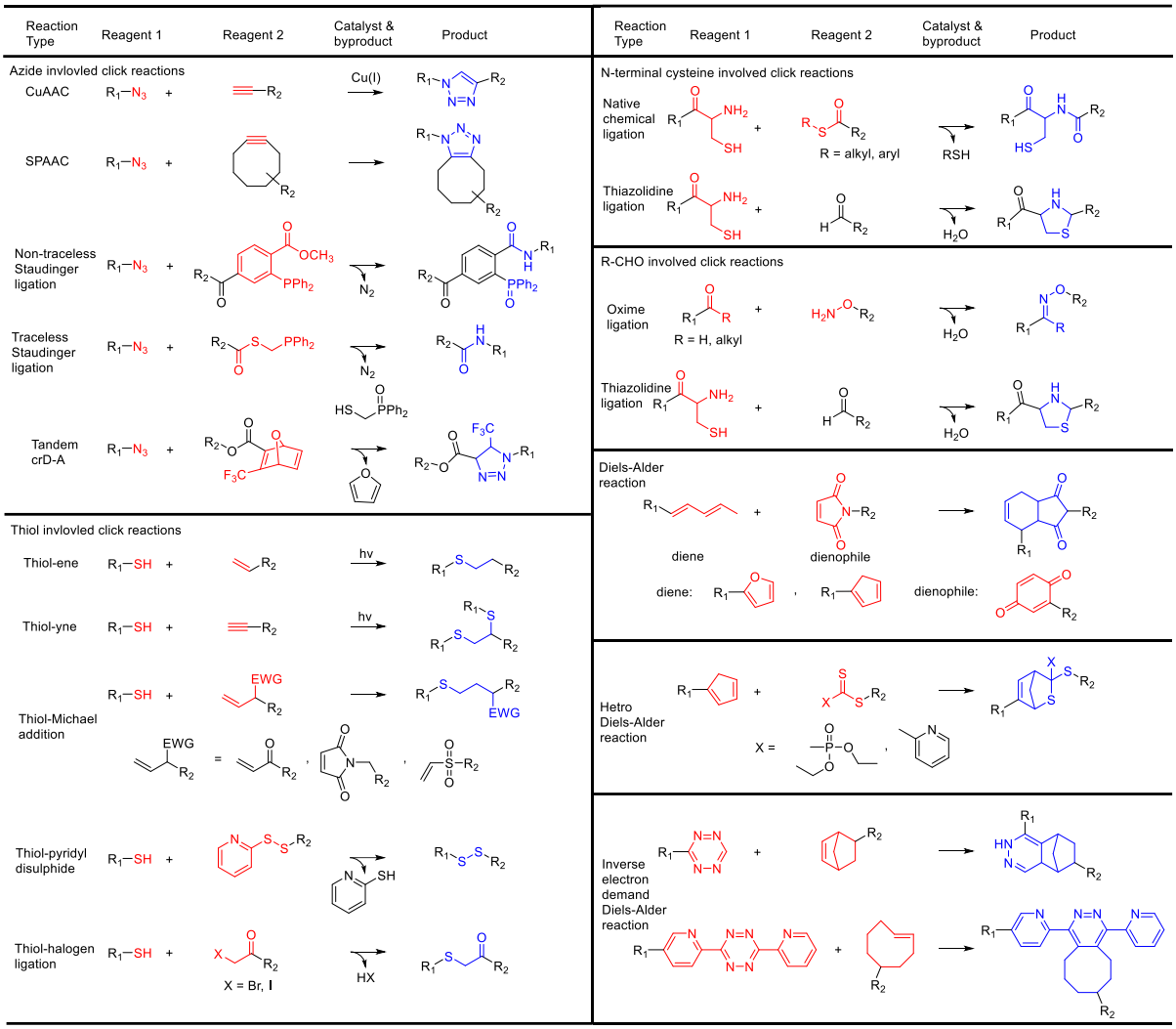

Figure 7. Summary of click reactions used for bioconjugation. Reproduced from Tang *et al.*[60]

1.5 Incorporation and application of "clickable" groups in peptides and proteins

Introduction of either azides or alkynes into peptides is most commonly achieved *via* the incorporation of azide- or alkyne-bearing amino acids into the peptide under standard peptide coupling conditions, either *via* solid- or liquid-phase peptide synthesis. A considerable library of such compounds exist, taking the form of terminal or non-terminal amino acids; examples and applications of a selection of these are shown in **Figure 8**.[64,65] It should be noted that, during solid phase synthesis, it is important to avoid the use of specific thiol scavengers such as 1,2-ethanedithiol during cleavage from the solid support, as this will induce reduction

of the azide to an amine, although dithiothreitol may prove suitable as a scavenger.[66] Applications of CuAAC in peptide synthesis and bioconjugation can range from a simple reaction between two amino acids to the construction of large biological entities. For example, Horne *et al.*[67] described the use of CuAAC in the synthesis of a dipeptidomimetic building block, which was in turn used in the construction of a cyclopeptide for the self-assembly of peptide nanotubes (**Figure 8**, **A**). The incorporation of the formed 1,2,3-triazole into the peptide was highly desirable for this application as it forced the cyclopeptide into a more planar structure, aiding nanotube formation.

The 1,2,3-tiazole has also proven useful in peptide synthesis as a β-turn mimetic. Such properties were investigated by Guan *et al*,[68] who studied the conjugation of two dipeptides (**Figure 8**, **B**), discovering that a 3-carbon linker was necessary for stable β-turn formation. CuAAC reactions have also been employed in the formation of cyclic peptides, an example being the Cu(I)-catalysed solid-phase cyclisation reported by Meldal and co-workers (**Figure 8**, **C**).[69] The same group also detailed the use of click chemistry in the liquid-phase synthesis of cyclic peptide as dipeptide surrogates.[70] Although less common, clickable groups can also be introduced through side chain modification, as shown, for example, in **Figure 8**, **D**, where a pent-2-en-4-ynyl alkyne conjugation handle was introduced, allowing for the conjugation of fluorescein-labelled histone peptide for monitoring enzyme activity.[64] Parrish *et al.*[71] demonstrated the post-transfer of a brominated peptide to an azido peptide in the grafting of an alkyne-containing PEG chain to a RGD-containing oligopeptide (**Figure 8**, **E**), although this method was quite involved, requiring multiple cycles of dialysis followed by freeze drying to isolate the peptide. A final example, **Figure 8**, **F**, involves the direct introduction of an amino acid bearing a side chain alkyne into a lipopeptide during standard solid-phase peptide synthesis (SPPS), which was utilised as a handle for PEGylation in the creation of potential solid-supported lipid bilayers and liposomal drug delivery platforms.[72]

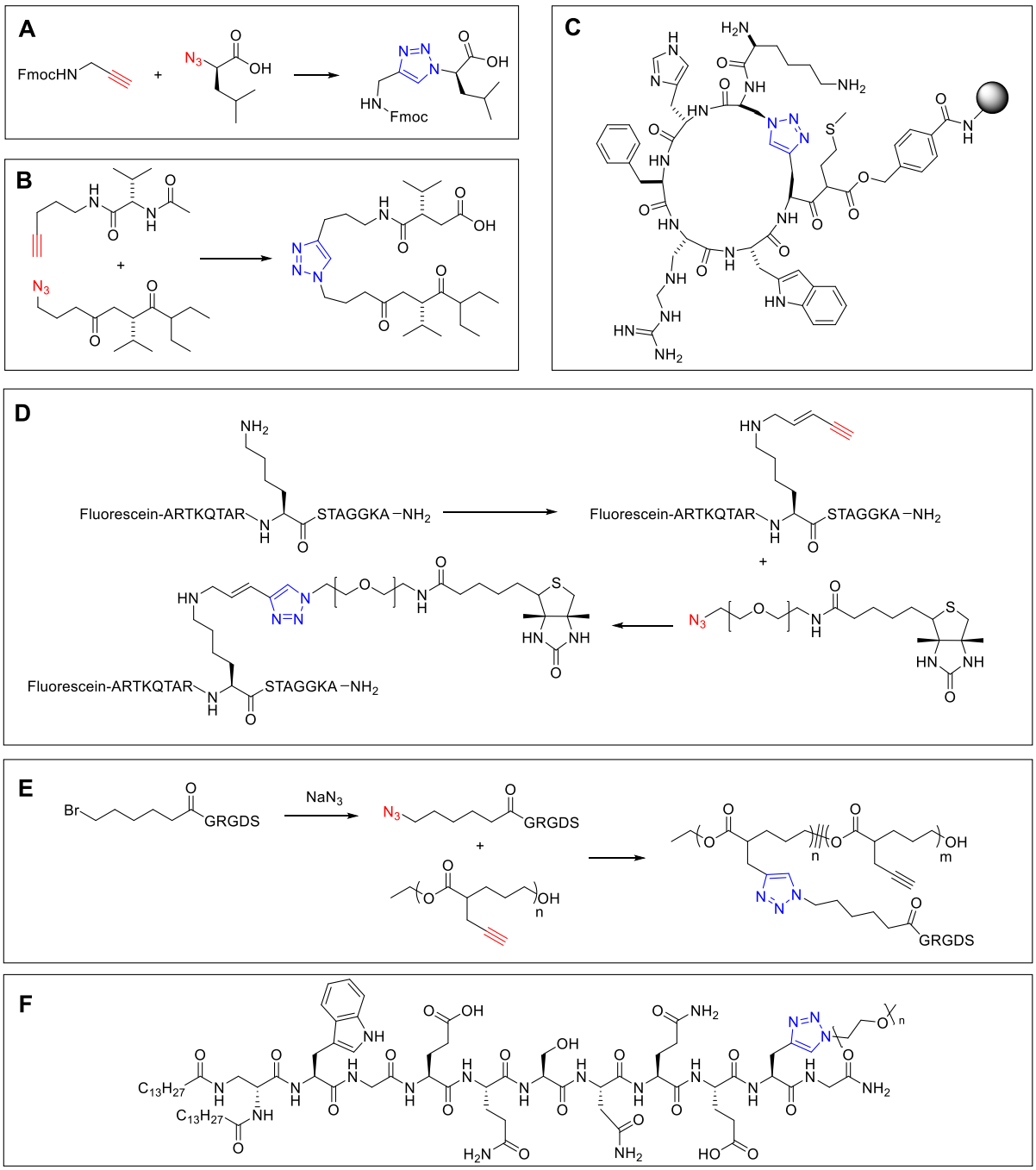

Figure 8. Examples of the application of CuAAC in the construction of peptide and peptide conjugates.

Introduction of CuAAC "clickable" groups into proteins presents a more significant challenge and must be performed with consideration, ensuring that no denaturation, disassembly or loss of biological activity occurs.[8] As mentioned before, the copper catalyst may have negative effects; for example, several proteins are known to chelate copper ion,

resulting in changes to the secondary structure. Wang *et al.*[73] successfully demonstrated the functionalisation of horse spleen apoferritin, attaching an *N*-hydroxysuccinimide activated ester of an alkyne to an exposed lysine residue. The alkyne-bearing protein was then conjugated *via* CuAAC to the pro-fluorophore 3-azidocoumarin (**Figure 9**, **A**),[74] which allowed for straightforward monitoring of the reaction. Another side chain modification method was employed by Corneslissen and Nolte in the click-enabled construction of polymer-protein bioconjugates as bioactive nanoassemblies.[75] This approach involved reacting a naturally occurring thiol (Cys-34) present on the surface of bovine serum albimun (BSA) with an alkyne-functionalised malemide to create a singly alkylated protein, which was then conjugated to azide-bearing polystyrene to create a biohybrid amphiphile (**Figure 9**, **B**). Such methods, although successful in their own right, still rely upon traditional conjugation techniques, and thus are susceptible to the same complications. Corneslissen and Nolte have more recently described a method involving cofactor reconstitution in the creation of further polymer-protein bioconjugates.[76] Use of the CuAAC reaction to synthesise a series of biohybrid triblock copolymers (**Figure 9**, **C**) was executed through the "clicking" of azide-bearing polymers with an alkyne-bearing heme.[76] The resulting bioconjugates were then reconstituted with either horse radish peroxidase or myoglobin. As described by the authors, such a method allows for site-specific conjugation, demonstrating significant advantages over direct clicking and preventing potentially damaging interactions between protein and the copper catalyst.

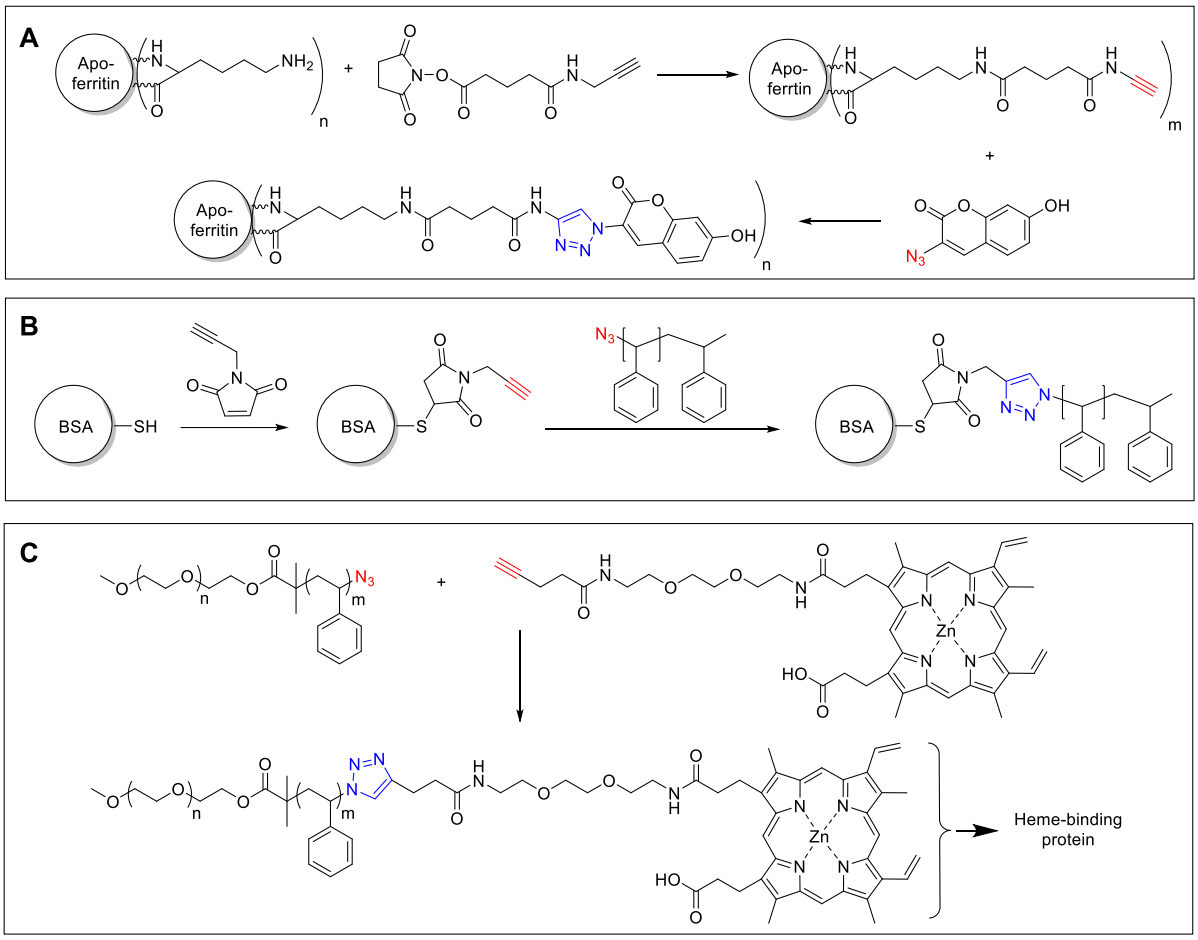

Figure 9. Examples of methods for the introduction of "clickable" sites into proteins and their applications.

Perhaps the most powerful methodologies for enabling CuAAC functionalisation of proteins are those reported by Schultz[77,78] and Tirrel.[79–81] These techniques employ modified bacterial and mammalian cells to insert, or metabolically replace a naturally occurring amino acid with an azide- or alkyne-bearing unnatural amino acid (UAA).[82–85] They are entirely independent of traditional protein bioconjugation methods, thus eliminating major weakness (as previously mentioned) and allowing for highly site-specific functionalisation. The group of Tirrell were successful in modifying a target protein through a method known as codon reassignment, in which methionine surrogates, azidohomoalanine (Aha) and homopropargylglycine (Hpg) are installed into proteins by co-opting the biosynthetic machinery of an *Escherichia coli* methionine auxotroph.[86,87] In one specific example, murine

dihydrofolate reductase (mDHFR) was modified to include Hpg. This was followed by isolation of the azido-protein and conjugation to an engineered phosphate-bearing antigenic peptide by Staudinger ligation, which proved to be highly selective even within a complex cell mixture.[80] Authors within the same group were also able to demonstrate direct modification of outer membrane proteins found on the cell surface of *E. coli via* site-directed mutagenesis of extracellularly exposed methionine residues to Aha.[81,88] CuAAC, along with a biotinylated alkyne, were utilised in the successful chemoselective modification of these cells. This clicking strategy was also applied to mammalian cells in which only the newly synthesised cells were mutated to contain Aha, allowing for selective labelling with a biotinylated alkyne affinity tag.[79] Another method described by Ting *et al.*[89] used a mutant strain of the lipoic acid ligase (LplA) enzyme from *E. coli.* to transfer an aryl azide onto a binding protein for photo-crosslinking applications. A similar technique by Plaks *et al.*[90] used Lp1A to insert a short azide-containing peptide into the internal loop regions of green fluorescent protein (GFP). Using this technique, the authors were able to successfully modify GFP through click chemistry, facilitating the site-specific attachment of PEG chains, alpha-*D*-mannopyranoside and palmitic acid, as well as immobilisation onto self-assembled monolayer surfaces containing DIBO.

Further research has seen the development of a flexible and selective methodology to install designer UAAs into the growing polypeptide chain by repurposing the "amber" stop codon (UAG) using orthogonal aminoactyl-tRNA synthetase/tRNA pairs.[55,91–94] This genetic code expansion has led to incorporation of UAAs containing clickable handles into proteins in *E. coli*, *Saccharomyces cerevisiae* and mammalian cells (**Figure 10**).[55] Simply described, incorporation of UAAs into a protein is enabled by firstly introducing the UAA into the growth medium, which is then specifically recognised by an orthogonal aminoacyl tRNA synthetase. The synthetase transfers the UAA to an orthogonal amber suppressor tRNA. Ribosomes, in

response to an amber codon (UAG), bind the UAA-bearing tRNA and subsequently incorporate the UAA into the growing protein chain. **Figure 11** shows a selection of "clickable" UAAs that have been incorporated into proteins using this technology.

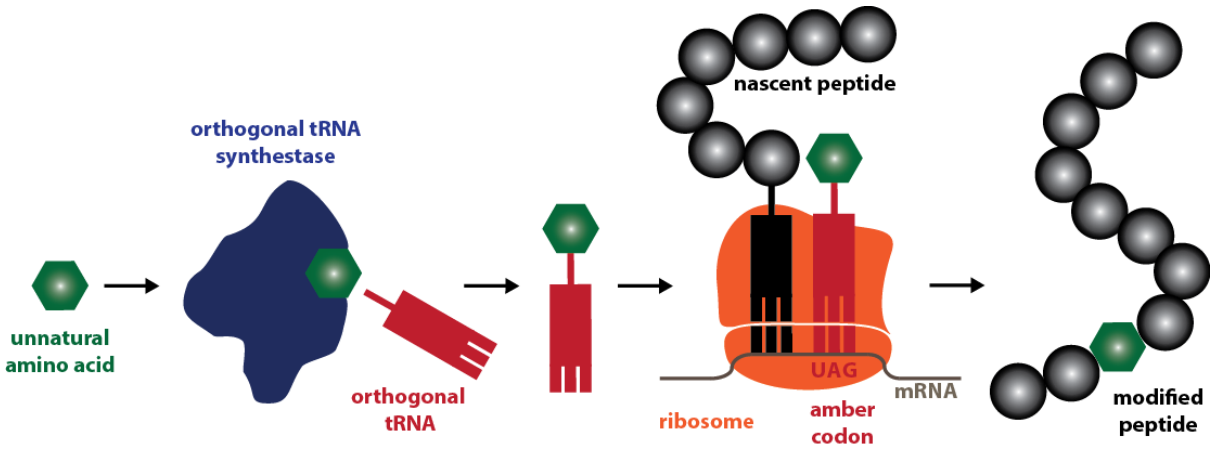

Figure 10. Incorporation of UAAs *via* genetic code expansion. A UAA is added to the growth medium, which is specifically recognised by an orthogonal aminoacyl tRNA synthetase and attached to an orthogonal amber suppressor tRNA. Responding to an amber codon (UAG), the ribosome binds the UAA-bearing tRNA and subsequently incorporates the UAA into the growing protein chain.

Schultz and co-workers have used mutants of the *E. coli* tyrosyl tRNA synthetase (*Ec*TyrRS)-tRNA$_{CUA}$ pair as well as the *Methanococcus jannaschii* tyrosyl-tRNA synthetase *Mj*TyrRS/tRNA$_{CUA}$ pair to genetically incorporate a range of azido- and alkyne-bearing tyrosine analogues into proteins (e.g., *p*-AzF, PrgF).[77,78,95–100] By way of example, azido- and alkyne-bearing tyrosine analogue UAAs were introduced into human superoxide dismutase, with the clicking of dansyl and fluorescein dyes confirming the presence of the UAAs.[77] Additional work yielded site-specific protein PEGylation for potential therapeutic applications.[78] Another system that has been used to exploit the UAG stop codon is the *Methanosarcina mazei* pyrrolysine (Pyl) aminoacyl-tRNA synthetase/tRNA pair[101,102] This pair has been used to introduce a range of azide- and alkyne-pyrrolysine analogues (e.g., EtcK, AlkK, AlkK2) into proteins for bioconjugation purposes.[101,103,104]

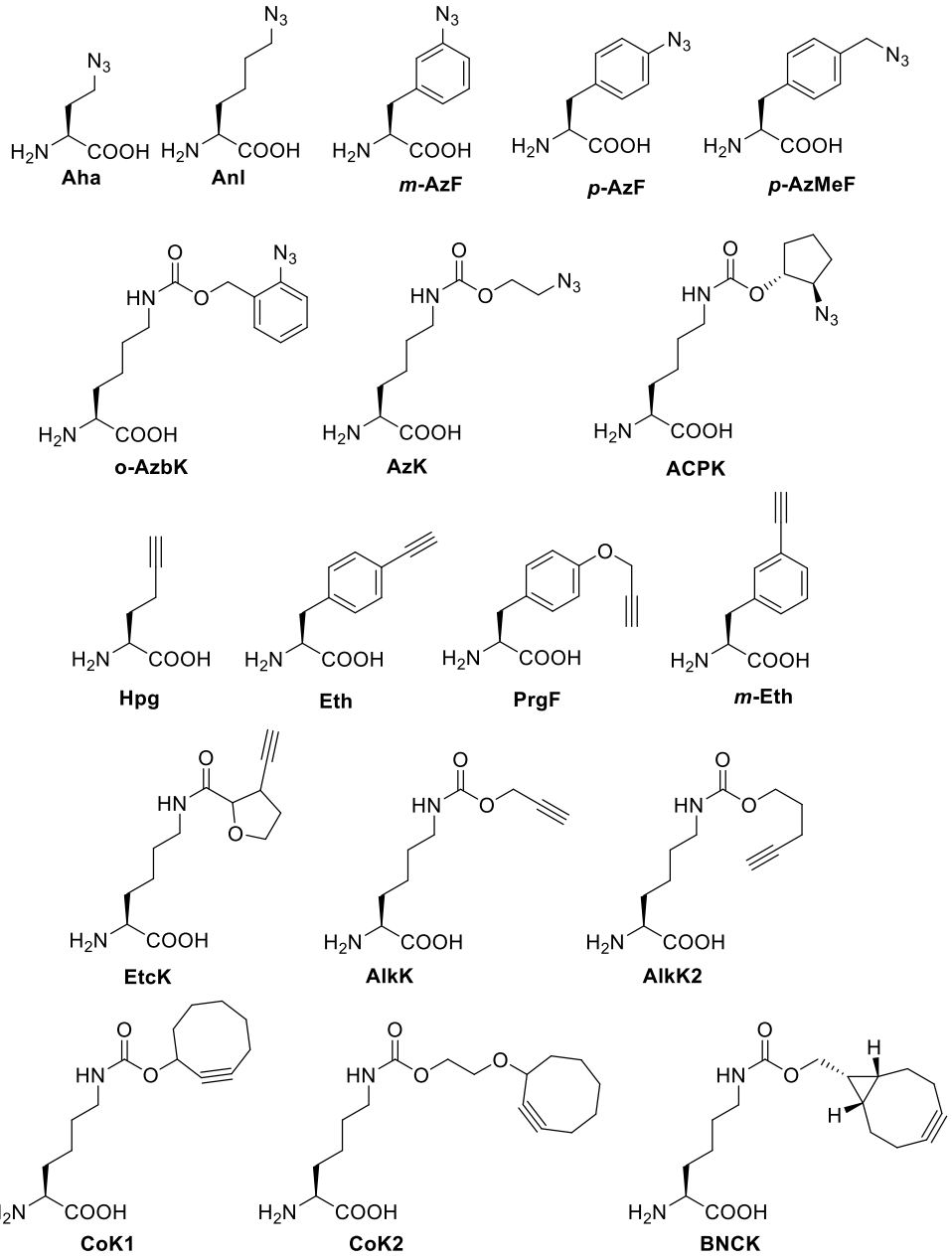

Figure 11. Selection of UAAs for click conjugation that have been introduced into recombinant proteins. Azide-bearing UAAs: Aha,[86,87] azidonorleucine (Anl),[105,106] *m*-AzF,[102] *p*-AzF,[77,97,98] *p*-azidomethylalanine (*p*-AzMeF),[107] N^{ε}-(*o*-azidobenzyloxycarbonyl)-*L*-lysine (*o*-AzbK),[108] N^{ε}-(2-azidoethoxy)carbonyl-*L*-lysine (AzK),[103] N^{ε}-(((1*R*,2*R*)-2-azidocyclo-pentyloxy)carbonyl)-*L*-lysine (ACPK).[109,110] Alkyne-bearing UAAs: Hpg,[86] ethynlphenylalanine (Eth),[86] PrgF,[77,95,96,100] *m*-ethynlphenylalanine (*m*-Eth),[102] EtcK,[101] N^{ε}-((prop-2-yn-1-yloxy)carbonyl)-*L*-lysine (AlkK),[103] N^{ε}-((pent-4-yn-1-yloxy)carbonyl)-*L*-lysine (AlkK2).[104] Strained cyclooctyne-bearing UAAs: CoK1,[111] CoK2,[111] BNCK.[46]

As discussed earlier, the use of a copper catalyst can interfere with bioentities, making its use undesirable. Consequently, cyclooctyne-bearing lysines, including N^{ε}-(cyclooct-2-yn-1-yloxy)carbonyl)-*L*-lysine (CoK1) and N^{ε}-(2-(cyclooct-2-yn-1-yloxy)ethyl)carbonyl-*L*-lysine (CoK2), have been developed for use with SPAAC conjugation.[111] These UAAs were genetically encoded into proteins in *E. coli* using an engineered PylRS/$tRNA_{CUA}$ pair and their functionality demonstrated through conjugation to an azido coumarin dye.[46,111] Further interest in copper-free click chemistry has seen the incorporation of a strained cyclooctene bicycle[6.1.0]nonyne-bearing lysine into proteins in *E. coli* and mammalian cells through engineered PylRS/$tRNA_{CUA}$ pairs.[46] The UAA in question, N^{ε}-((1R,8S,9S)-bicyclo[6.1.0]non-4-yn-9-methyloxy)carbonyl)-*L*-lysine (BCNK) could be applied with either SPAAC or inverse-electron-demand-Diels-Alder cycloadditions with tetrazine-bearing probes.[43,46]

1.6 "Clickable" reagents for bioconjugation

In many cases, the major challenge faced in using click chemistry (and more specifically CuAAC) for bioconjugation is the installation of the clickable group into the bio-entity, with the click partner being relatively easy to produce. The range of available molecules for click bioconjugation is therefore quite wide, including biotin derivatives, PEG chains, saccharides, fluorophores, lanthanide complexes, radiotracers, radiocomplexes and targeting moieties. The following sections will discuss some of the agents most relevant to this work, namely clickable fluorophores, luminescent lanthanide complexes, radiotracers and radiocomplexes.

1.6.1 Clickable fluorophores

Fluorescent tags are perhaps the largest family of small molecules that have been utilised in CuAAC bioconjugation, allowing for the production of fluorescent bioconjugates for bioimaging, biosensing and bioassay applications. Many common fluorophores have

proven amenable to either alkyne or azide modification, including, but in no way limited to, rhodamine,[112,113] cyanine,[114] difluoroboron chelates,[115] iminopyronin,[116] dansyl,[77,117] and fluorescein dyes[77,118,119] (**Figure 12**).

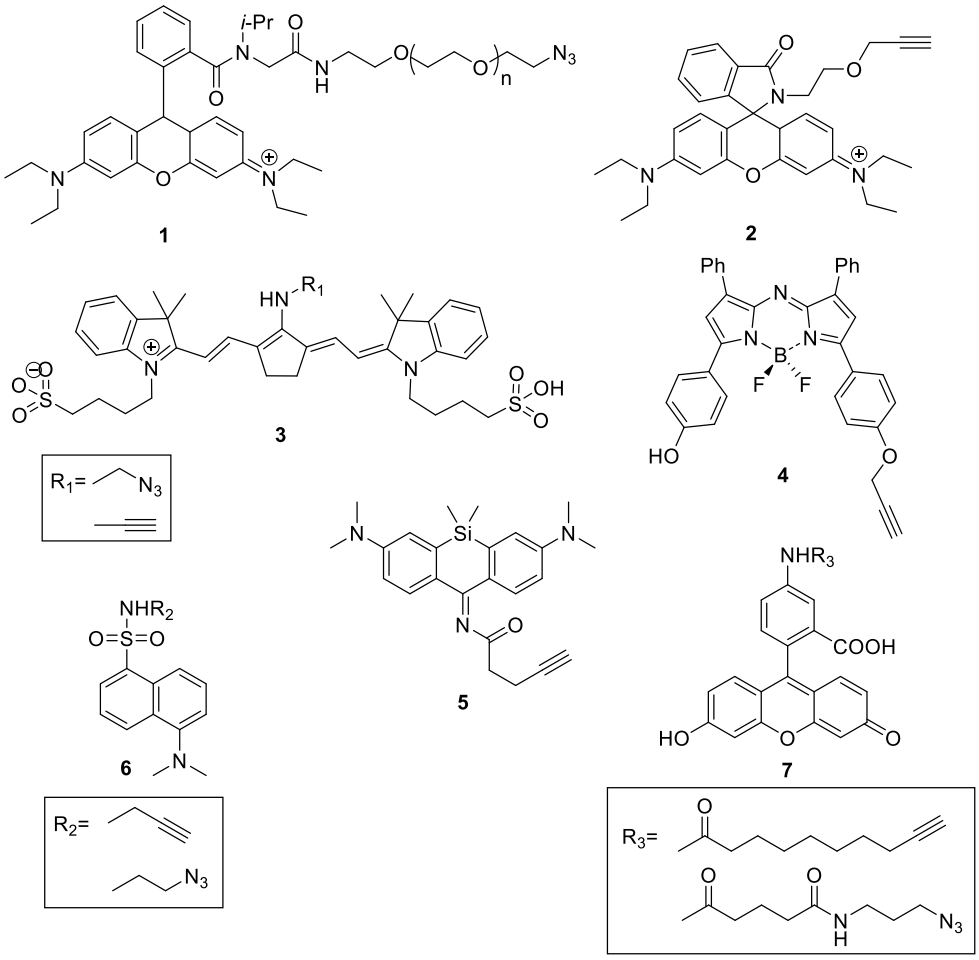

Figure 12. Examples of fluorophores modified for click conjugation, including rhodamine (**1**,[112] **2**[113]), cyanine (**3**),[114] difluoroboron chelates (**4**),[115] iminopyronin (**5**),[116] dansyl (**6**)[77,117] and fluorescein (**7**),[77,119] and derivatives.

Modification of fluorophores with azides can provide added benefits for labelling applications, the most notable of which is the capacity of azides to act as fluorescence "quenchers" through a photoinduced electron transfer (PET) effect.[90] Alkynes are also capable of exhibiting a quenching effect *via* an electron withdrawing effect.[120,121] This proves useful for imaging, since

once the triazole is formed upon clicking, the quenching effect is lost, effectively causing the fluorophore to "switch-on" or "light-up". Such a fluorogenic property is highly desirable from a labelling perspective as it can remove the necessity for a washing step to remove any unreacted fluorophore, often needed to ensure adequate sensitivity for imaging or detection. Use of such compounds also allows the progress of the conjugation reaction to be easily monitored.[122] Organic compounds that have been successfully used as clickable fluorogenic labelling agents include coumarin,[74,123–127] anthracene,[128,129] 1,8-napthalimide,[121] boron-dipyrromethene (BODIPY)[130,131] and benzothiazole[122,132] (**Figure 13**).

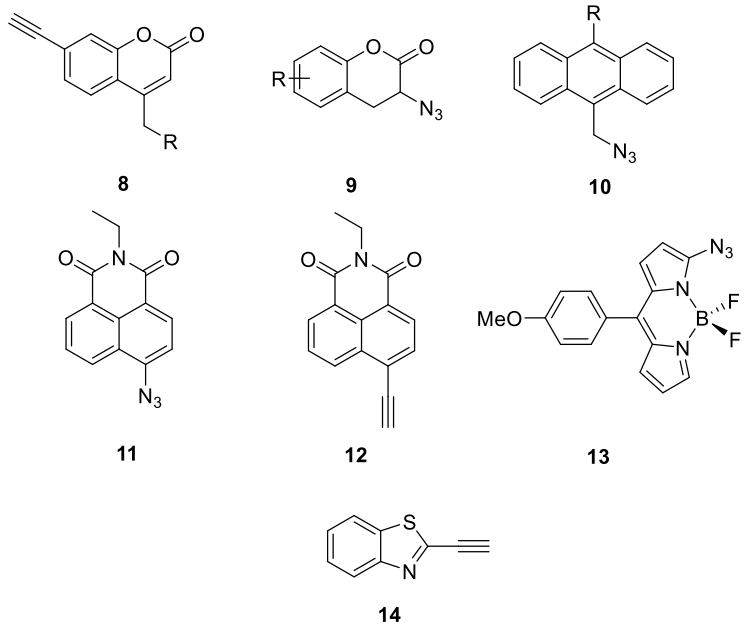

Figure 13. Examples of some "clickable" fluorogenic reagents, including azido- and alkynyl-coumarin (**8** & **9**),[74,126,133] azido-anthracene (**10**),[128,129] azido- and alkynyl- 1,8-napthalimide (**11** & **12**),[121] azido-BODIPY (**13**),[130] and alkynyl-benzothiazole (**14**).[122]

1.6.2 Luminescent lanthanide metal complexes for click conjugation

Lanthanide-based luminescent metal complexes represent a newer form of near IR-to-visible light-emitting probe that can provide a number of significant advantages over organic fluorophores, especially within a biological setting. Luminescence arising from lanthanides is

due to the excitation and subsequent decay to the ground state of 4*f* electrons. Such *f-f* transitions are Laporte forbidden, which causes any subsequent emissions to be very weak; consequently the direct excitation of lanthanide ions (especially in aqueous media, due quenching of lanthanide excited states) is not considered feasible for imaging applications.[134] This weakness can be overcome through the use of ligands specifically designed for harnessing lanthanide luminescence. These ligands consist loosely of three components: a multidentate chelating region that tightly binds the lanthanide ion, a suitable chromophore functioning as an antenna to transfer energy to the lanthanide metal ion *via* a Dexter or Förster energy transfer mechanism, and a reactive handle allowing conjugation to a (biological) molecule (**Figure 14**).[135,136]

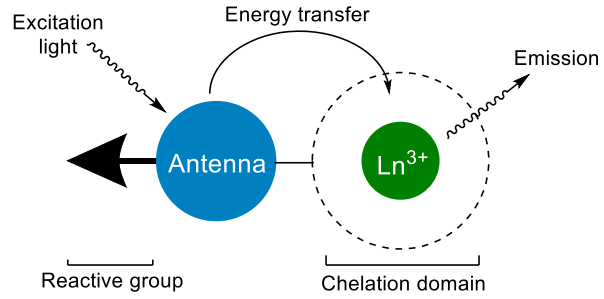

Figure 14: Representation of the general structure and function of a luminescent lanthanide complex.

The most commonly used lanthanide ions used for luminescence applications are Tb^{3+} and Eu^{3+}, as their respective green (450–650 nm) and red (550–750 nm) emissions fall within the visible light spectrum, however use has also been made of other lanthanides, including Nd^{3+}, Ho^{3+}, Er^{3+} and Yb^{3+}, which emit in the IR region. Advantages of luminescent lanthanide complexes (LLCs) include an extremely wide band of emission wavelengths and luminescence lifetimes that are of the order of milliseconds, far longer that the nanosecond lifetimes of organic dyes.[137,138] This characteristic allows LLCs to be used for time-gated imaging experiments (**Figure 15**), which essentially eliminates background fluorescence. LLCs also boast a large difference between absorption maxima of the antenna and the emission maxima

of the lanthanide ion (apparent Stokes shift). A large Stokes shift is very desirable as organic fluorophores, with their typically smaller shifts, can often experience complications pertaining to concentration-dependant self-absorption.

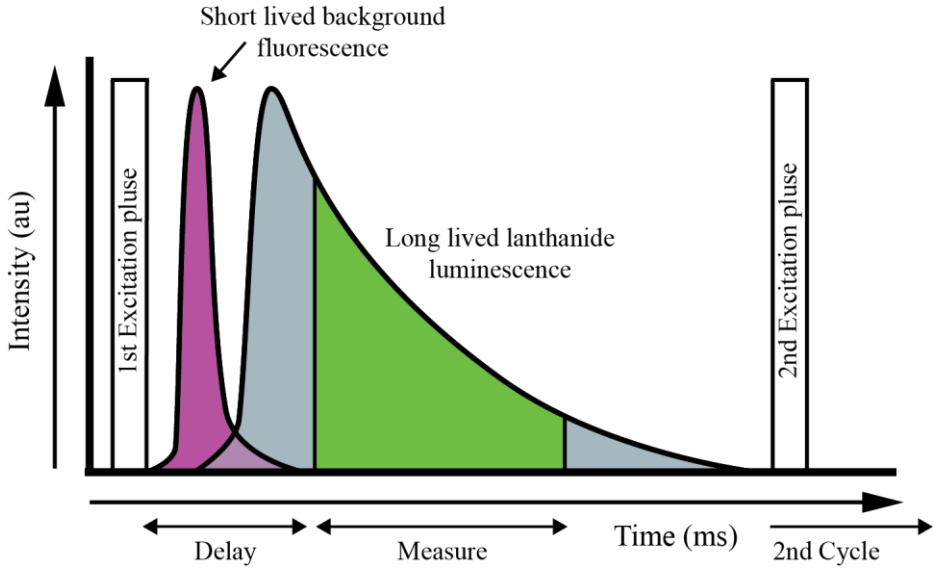

Figure 15. Principle of time-gated luminescence detection. At the start of an imaging cycle, a pulse of excitation radiation is applied, followed by a delay in which the short-lived background fluorescence is allowed to decay away. A measurement is then taken and the cycle repeated as many times as required.

An extensive range of LLCs have been reported to date.[139–141] Whist this number still remains small compared to the incredibly large library of organic fluorophores, the attractive qualities of lanthanide luminescence have led to the development of several commercially available probes. Typically, chelator groups used to bind the lanthanide ion incorporate 8–10 donor atoms to bind the ions as tightly as possible as well as avoid quenching of luminescence from co-ordinated water molecules.[142] One particularly common chelator is the multidentate macrocycle 1,4,7,10-tetraazacyclododecane-1,4,7,10-tetraacetic acid (DOTA), which has been coupled to numerous sensitising antenna groups, including carbostyril 124 (**15**),[143,144] acetophenone (**16**),[145] quinoline (**17**),[146] phenanthroline (**18**),[147,148] and bathocuproine (**19**).[140] Other examples include **20**, which incorporates a pyridine group that doubles in function, working as the antenna whilst also providing additional co-ordination to the metal ion.[149] The

terbium(III) complex, **21**, also incorporating a pyridine donor/antenna moiety, provides a very impressive quantum yield of 90% by occupying all nine of the available co-ordination sites around the metal.[150]

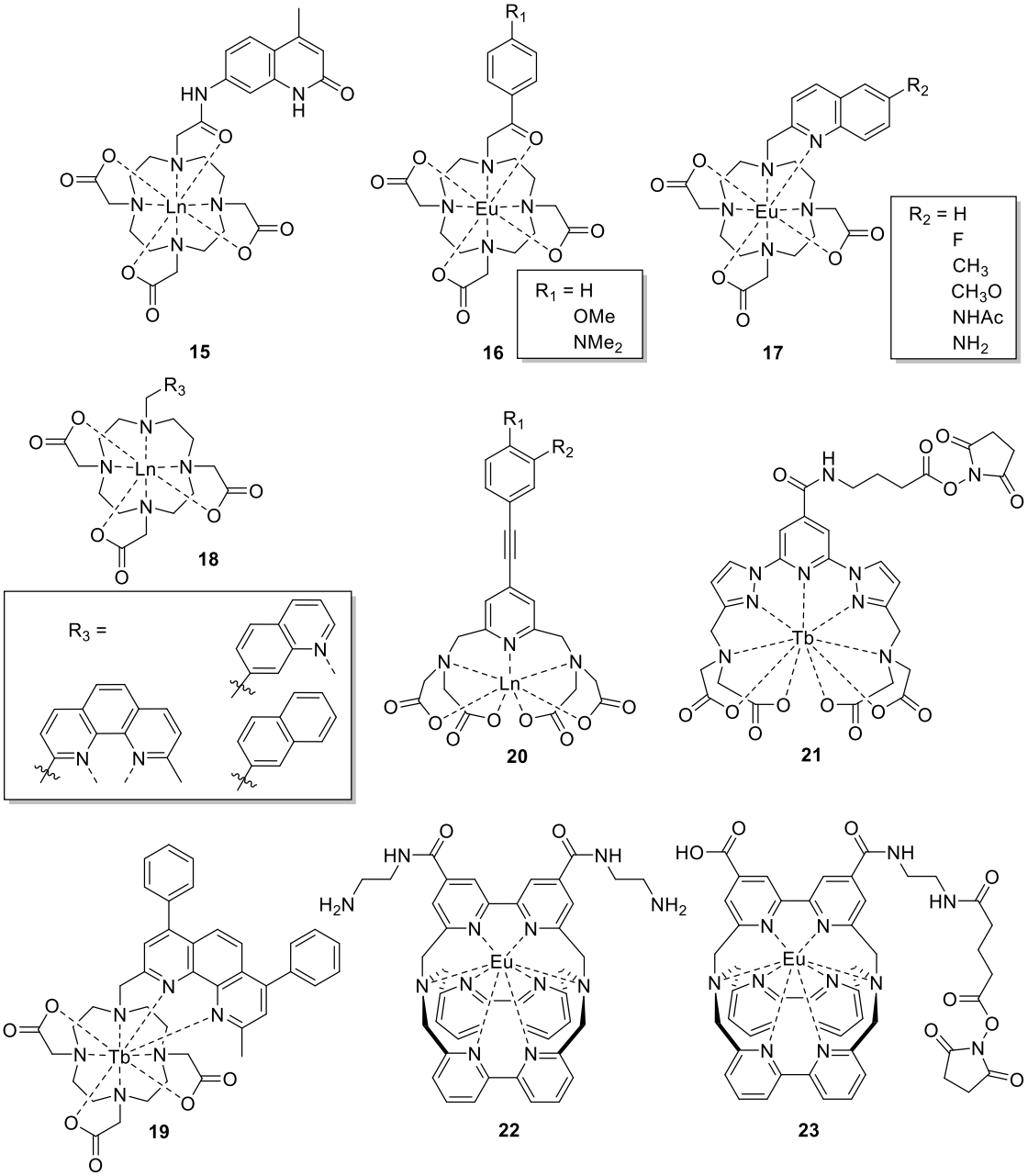

Figure 16. Selected examples of luminescent lanthanide complexes. **15**,[143,144] **16**,[145] **17**,[146] **18**,[147,148] **19**,[140] **20**,[149] **21**,[150] **22** & **23**.[151–153] Ln = Eu^{3+}/Tb^{3+}.

Worthy of mention is the commercial success of LLCs, predominantly in the form of lanthanide-based immunoassays designed to eliminate the background auto-fluorescence that

is a major problem without time-gating. In these assays, lanthanide-based complexes similar to **22** and **23**, act as the energy donor in a luminescence resonance energy transfer (LRET) pair, with the acceptor being either a fluorescent protein or small organic fluorophore.[151–153] As the use of lanthanide complexes in biological systems is so attractive, it makes them a prime candidate for bioconjugation *via* click chemistry. Such a method of bioconjugation may also allow the development of luminogenic lanthanide complexes, either through the quenching effect of an azide/alkyne group on the antenna, in a similar manner to organic fluorogenic compounds, or through structural changes upon clicking that result in the eviction of co-ordinated water molecules.

A number of lanthanide complexes with CuAAC functionalities do already exist in the literature, however many of these have only been utilised with CuAAC in the construction of larger non-biological entities, and many of them are non-luminescent.[154–158] Examples of clickable luminescent lanthanide complexes include **24**, an alkyne-bearing, cyclen macrocycle-based ligand used to prepare Eu^{3+} and Tb^{3+} complexes,[159] as well as **27**, an azidopyridine cyclen complex.[160] Other examples include alkyne- (**25**) and azide-functionalised pyridine (**26**) chelates,[161] as well as bispyridine- (**28**) and terpyridine-based complexes (**29**).[161]

Within our group, Dr Phuc Ung recently developed a number of clickable LLCs during his PhD studies.[162] Some of these complexes (**Figure 18**) exhibited increased luminescence upon clicking and were successfully employed in the labelling of a protein (ubiquitin) as well as the development of probes for adenosine receptors.

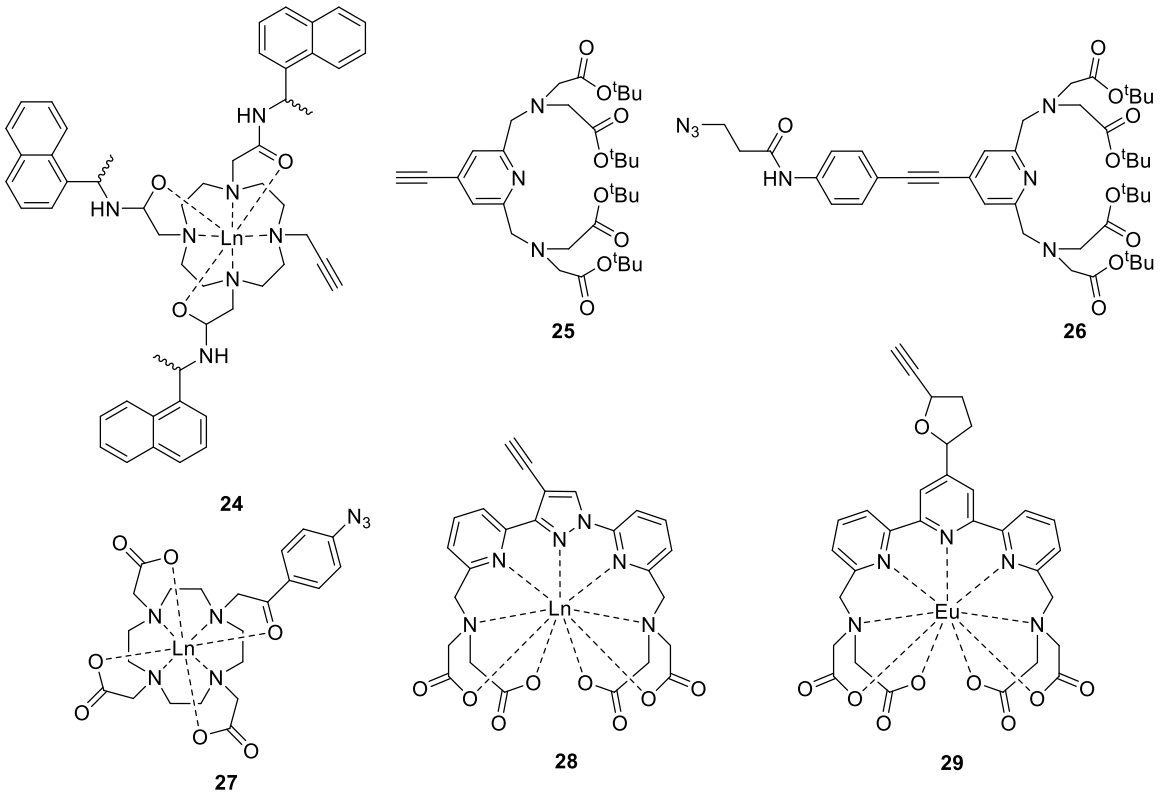

Figure 17. Selected examples of lanthanide complexes and lanthanide-binding ligands functionalised with azides or alkynes for click chemistry. **24**,[159] **27,**[160] **(25, 26, 28** and **29)**.[161]

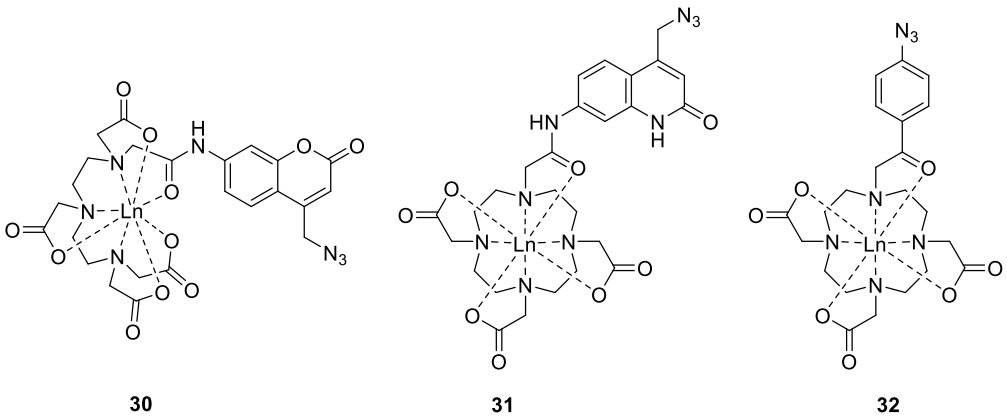

Figure 18. Series of clickable luminescent lanthanide complexes developed during Dr Ung's PhD; **30**, **31** and **32**.[162]

1.6.3 Applications of click chemistry in the synthesis of radiotracers

Radiotracers represent a class of probe in which radioisotopes are coupled with biologically active compounds, providing a unique methodology for the tracking of biochemical and biological events *in vivo*. Detecting the emissions of these radiotracers can be

either achieved through positron emission tomography (PET) or single-photon emission computed tomography (SPECT). Both of the techniques have been applied extensively for non-invasive diagnosis, staging and therapy in the fields of oncology, cardiology and neurology.[163–165]

Click chemistry presents a new tool in the synthesis of radiotracers. In addition to the advantages that click chemistry generally brings to conjugation and bioconjugation, the speed at which these reactions proceed is particularly attractive, given the limitations imposed by the short half-lives of the radioisotopes used in PET and SPECT.

Conceptually, the simplest method for radiotracer construction *via* click chemistry is through the application of small radiolabelled alkyne- and azide-containing building blocks in "hot click chemistry". Currently, the use of such building blocks has only been applied to the short-lived positron emitter fluorine-18 (^{18}F, $t_{1/2}$ = 109.8 min). These building blocks are commonly prepared through the nucleophilic displacement of tosyl groups, or other fast, simple chemistries, to give the corresponding fluoroalkyne or fluoroazide (**Figure 19, A**). A very large library of such compounds have been synthesised by various authors.[166–177]

Another approach for generating radiotracers is through the chelation of metal ion radionucleotides. In this regard, CuAAC can either be used for the conjugation of a chelation domain or in the construction of one. A prominent example of the latter is the "click-to-chelate" concept; this strategy employs click chemistry to create histidine-like polydentate chelating systems, with the formed 1,2,3-triazole providing one of the coordination sites. Such a system is highly appealing as it allows simultaneous formation of the chelator and conjugation to the biomolecule in a single high-yielding step. This methodology has been used in the construction of organometallic $^{99m}Tc(CO)_3$ radiotracers (**Figure 19**, **B**).[178–183] A second method involves the click conjugation of an already existing azide- or alkyne-bearing chelator to the molecule of interest. Complex **33** shows an alkyne-bearing, $^{99m}Tc(CO)_3$-binding dipyridylamine that was

conjugated to the drug Bicalutamide for imaging of prostate cancer.[180] Other alkyne examples include **34**, based upon the cyclen macrocycle and used in the preparation of an ^{111}In-labelled cyclic-RGD peptide;[166,184] **35**, another cyclen-based ligand, also coupled to a cyclic-RGD peptide, employed for tumour imaging of mice with ^{66}Gd;[167,185] and **36**, based upon 1,4,8,11-tetraazabicyclo[6.6.2]hexadecane-4,11-diacetic acid (CB-TE2A) and employed for ^{64}Cu-binding after clicking to a somatostatin peptide.[186,187] Finally, **37** shows a small azidopyridine-functionalised 1,4,7-triazacyclononane (TACN)-based ^{64}Cu-binding ligand successfully used in the construction of a multimodal probe targeting the epidermal growth factor receptor, a receptor often over-expressed in cancers.[188]

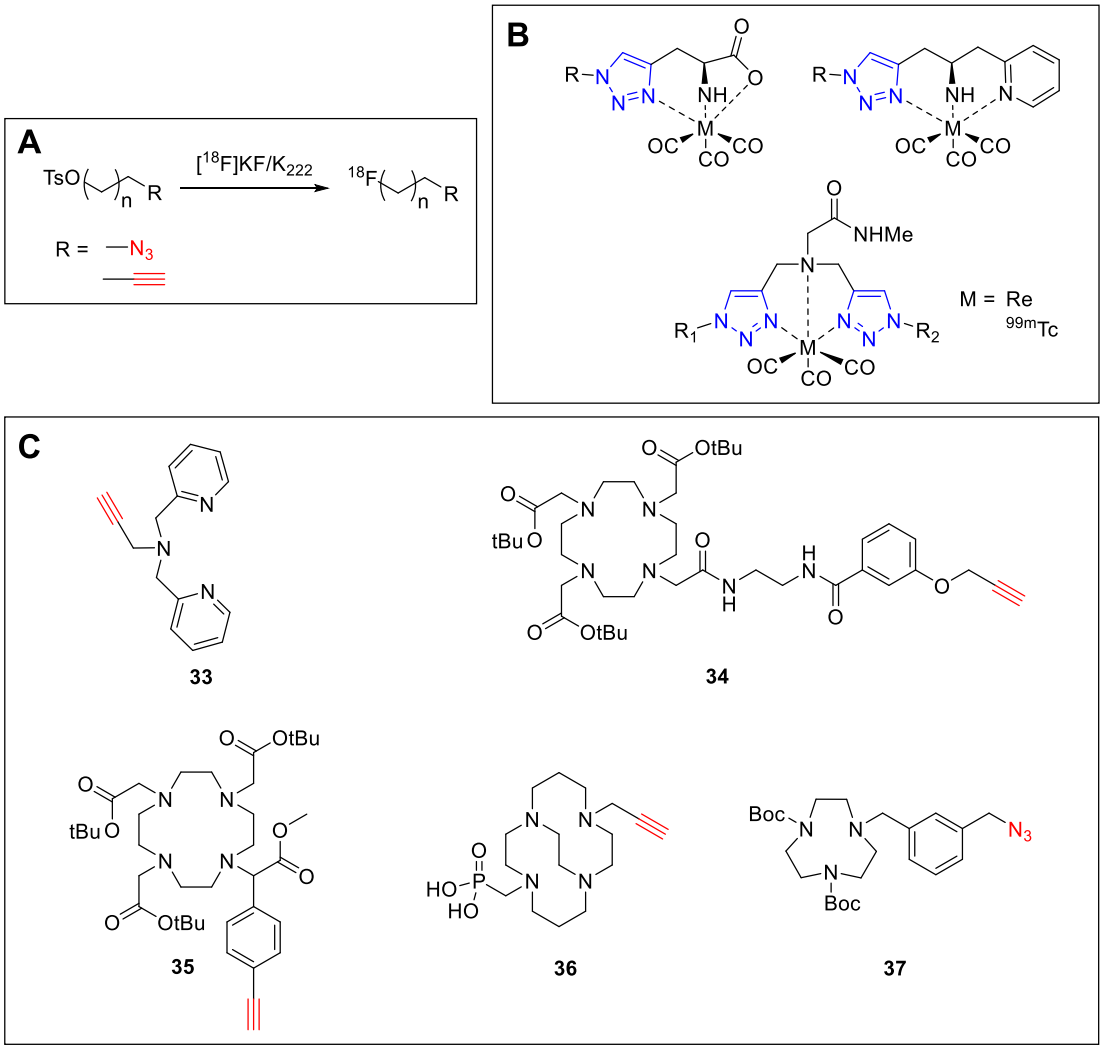

Figure 19. (**A**) Example of the synthesis of clickable ^{18}F radiolabels. (**B**) Examples of some "click-to-chelate" systems.[108] (**C**) Examples of clickable ligands for radiolabelling. **33**,[180] **34**,[166,184] **35**,[167,185] **36**,[186,187] and **37**.[188]

1.7 Scope of the current project

Click chemistry clearly provides a powerful tool for the construction of bioconjugates. Whilst a significant body of work exists, there remains considerable scope for further development of "clickable" agents that may assist in the development of bioconjugates for imaging, assay and therapeutic applications. This thesis details the design, synthesis and evaluation of three new types of click-conjugatable tags that incorporate either a metal ion complex or metal ion-chelating ligand within their structure. These have been developed to allow highly site-specific ligation of either i) a luminescent lanthanide complex, ii) a fluorescent and MRI-active label, or iii) radioactive ^{64}Cu to a biomolecule. In each case, the utility of the new tags has been successfully demonstrated through click conjugation to a "model" peptide or protein.

Each chapter within this thesis has its own compound numbering system and experimental section. Numbering of the figures as well as the referencing system is also reset at the start of each chapter. A brief summary of each chapter is provided below.

1.7.1 Chapter 2: Luminescent alkyne-bearing terbium(III) complexes and their application to bio-orthogonal protein labelling

Chapter 2, presented in the form of a published manuscript, details the synthesis and characterisation of two novel, terbium-based luminescent lanthanide complex labelling reagents featuring alkyne groups for conjugation *via* click chemistry (**Figure 20**, **A**). The results of a test conjugation with a model azide are presented, as well as a detailed analysis of the photophysical properties of these complexes, both pre-and post-clicking. This chapter further describes conjugation of these complexes to *E. coli* aspartate/glutamate-binding protein (DEBP) incorporating a genetically encoded *p*-azido-*L*-phenylalanine or *p*-(azidomethyl)-*L*-phenylalanine residue (**Figure 20**, **B**).

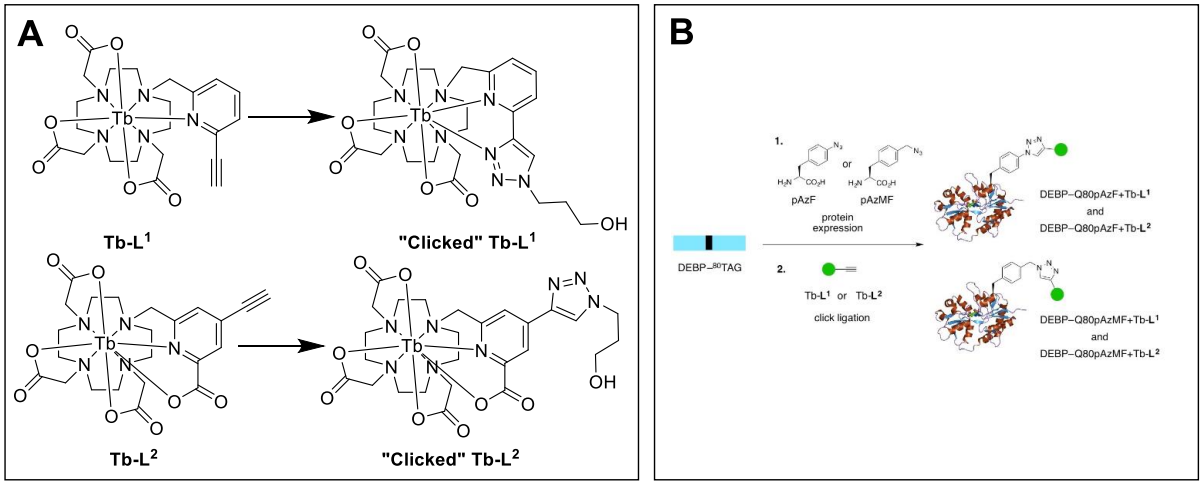

Figure 20. (**A**) Pre- and post-clicking structures of luminescent terbium tags developed during this study. (**B**) Genetically encoded incorporation of pAzF or pAzMF into DEBP in response to an amber stop codon (UAG) at position 80, and subsequent click ligation with luminescent terbium tags.

1.7.2 Chapter 3: Cellular uptake and photo-cytotoxicity of a gadolinium(III)-DOTA-naphthalimide complex "clicked" to a lipidated Tat peptide

Chapter 3, also presented in the form of a published manuscript, reports on the synthesis of the Gd(III) complex of a new bifunctional macrocyclic chelator featuring an alkynyl-naphthalimide fluorophore pendant. The photophysical properites of this complex pre-and post-clicking are also described. The utility of the tag is demonstrated through click conjugation to a cell-penetrating lipidated Tat peptide featuring an azido-*L*-lysine residue and the "theranostic" properties of this conjugate, arising from the fluorescence and photo-reactivity of the naphthalimide group, are presented.

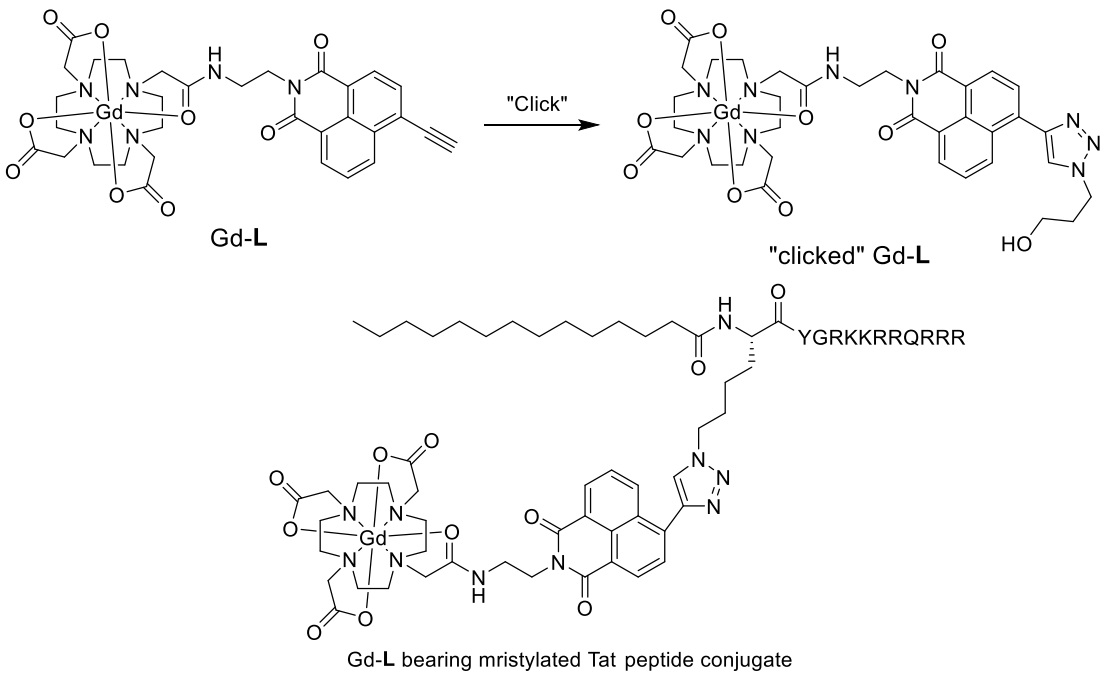

Figure 21. Pre-and post-clicking structures of the new Gd(III)-DOTA-naphthalimide complex, as well as the structure of the bifunctional Tat peptide conjugate developed during this study.

1.7.3 Chapter 4: Synthetic efforts towards to the development of additional clickable lanthanide complexes

Chapter 4 describes the results of additional work conducted on the development of clickable lanthanide complex tags, which did not appear in the preceding two published manuscripts. The synthesis and photophysical properties of a luminescent alkyne-bearing terbium complex of a nonadentate 1,4,7-triazacyclononane (TACN)-based macrocyclic ligand are described. Attempts to synthesise a second clickable napthalimide-bearing bifunctional macrocyclic chelator, akin to that described in Chapter 3, are also presented.

1.7.4 Chapter 5: Assembly of bombesin conjugates for bimodal PET-fluorescence imaging using "clickable" 1,4,7-triazacyclononane derivatives

Chapter 5 reports upon the synthesis of two clickable ^{64}Cu pro-chelators based upon the tridentate TACN macrocycle. These compounds were employed in the click-aided construction of multimodal imaging probes (**Figure 22**) incorporating a near-IR emitting cyanine dye and a bombesin peptide targeting the gastrin-releasing peptide receptor, which is over-expressed in prostate cancer. This chapter further reports upon the radio-stability, as well as the biodistribution of one of the probes *in vivo*.

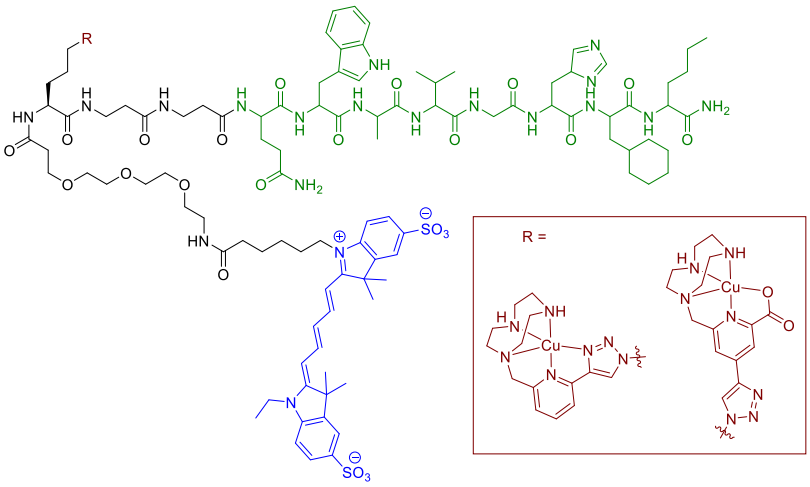

Figure 22. Structure of two bimodal imaging probes designed to target prostate cancer developed during this study. Green: bombesin derivative targeting the GRPr. Blue: near-IR emitting sulfo-Cy5 dye. Red: positron-emitting ^{64}Cu chelate.

1.7.5 Chapter 6: Summary and future work

Chapter 6 provides a critical summary of the results obtained during this work, including a discussion of unresolved issues and potential avenues for future work.

References

(1) Kolb, H. C.; Finn, M. G.; Sharpless, K. B. *Angew. Chem Int. Ed.* **2001**, *40* (11), 2004–2021.

(2) Kolb, H. C.; Sharpless, K. B. *Drug Discov. Today* **2003**, *8* (24), 1128–1137.

(3) Moses, J. E.; Moorhouse, A. D. *Chem. Soc. Rev.* **2007**, *36* (8), 1249–1262.

(4) Gothelf, K. V; Jørgensen, K. A. *Chem. Rev.* **1998**, *98* (2), 863–910.

(5) Rostovtsev, V. V.; Green, L. G.; Fokin, V. V.; Sharpless, K. B. *Angew. Chem Int. Ed.* **2002**, *41* (14), 2596–2599.

(6) Tornøe, C. W.; Christensen, C.; Meldal, M. *J. Org. Chem.* **2002**, *67* (9), 3057–3064.

(7) Bock, V. D.; Hiemstra, H.; van Maarseveen, J. H. *Eur. J. Org. Chem.* **2006**, *2006* (1), 51–68.

(8) Wang, Q.; Chan, T. R.; Hilgraf, R.; Fokin, V. V.; Sharpless, K. B.; Finn, M. G. *J. Am. Chem. Soc.* **2003**, *125* (11), 3192–3193.

(9) Himo, F.; Lovell, T.; Hilgraf, R.; Rostovtsev, V. V.; Noodleman, L.; Sharpless, K. B.; Fokin, V. V. *J. Am. Chem. Soc.* **2005**, *127* (1), 210–216.

(10) Diaz, D. D.; Punna, S.; Holzer, P.; McPherson, A. K.; Sharpless, K. B.; Fokin, V. V.; Finn, M. G. *J. Polym. Sci. Part A Polym. Chem.* **2004**, *42* (17), 4392–4403.

(11) Chan, T. R.; Hilgraf, R.; Sharpless, K. B.; Fokin, V. V. *Org. Lett.* **2004**, *6* (17), 2853–2855.

(12) Hong, V.; Presolski, S.; Ma, C.; Finn, M. A. G. *Angew. Chem Int. Ed.* **2009**, *48* (52), 9879–9883.

(13) Besanceney-Webler, C.; Jiang, H.; Zheng, T.; Feng, L.; Soriano del Amo, D.; Wang, W.; Klivansky, L. M.; Marlow, F. L.; Liu, Y.; Wu, P. *Angew. Chem Int. Ed.* **2011**, *50* (35), 8051–8056.

(14) Hao, Z.; Hong, S.; Chen, X.; Chen, P. R. *Acc. Chem. Res.* **2011**, *44* (9), 742–751.

(15) Agard, N. J.; Prescher, J. A.; Bertozzi, C. R. *J. Am. Chem. Soc.* **2004**, *126* (46), 15046–15047.

(16) Baskin, J. M.; Prescher, J. A.; Laughlin, S. T.; Agard, N. J.; Chang, P. V; Miller, I. A.; Lo, A.; Codelli, J. A.; Bertozzi, C. R. *Proc. Natl. Acad. Sci.* **2007**, *104* (43), 16793–16797.

(17) Agard, N. J.; Baskin, J. M.; Prescher, J. A.; Lo, A.; Bertozzi, C. R. *ACS Chem. Biol.* **2006**, *1* (10), 644–648.

(18) Ning, X.; Guo, J.; Wolfert, M. A.; Boons, G.-J. *Angew. Chem Int. Ed.* **2008**, *47* (12), 2253–2255.

(19) Codelli, J. A; Baskin, J. M.; Agard, N. J.; Bertozzi, C. R. *J. Am. Chem. Soc.* **2008**, *130* (34), 11486–11493.

(20) Dommerholt, J.; Schmidt, S.; Temming, R.; Hendriks, L. J. A; Rutjes, F. P. J. T.; Van Hest, J. C. M.; Lefeber, D. J.; Friedl, P.; Van Delft, F. L. *Angew. Chem Int. Ed.* **2010**, *49* (49), 9422–9425.

(21) De Almeida, G.; Sletten, E. M.; Nakamura, H.; Palaniappan, K. K.; Bertozzi, C. R. *Angew. Chem Int. Ed.* **2012**, *51* (10), 2443–2447.

(22) Gordon, C. G.; Mackey, J. L.; Jewett, J. C.; Sletten, E. M.; Houk, K. N.; Bertozzi, C. R. *J. Am. Chem. Soc.* **2012**, *134* (22), 9199–9208.

(23) Poloukhtine, A.; Popik, V. V. *J. Org. Chem.* **2003**, *68* (20), 7833–7840.

(24) Poloukhtine, A.; Popik, V. V. *J. Phys. Chem. A* **2006**, *110* (5), 1749–1757.

(25) Poloukhtine, A. A.; Mbua, N. E.; Wolfert, M. A.; Boons, G.-J.; Popik, V. V. *J. Am. Chem. Soc.* **2009**, *131* (43), 15769–15776.

(26) Yao, J. Z.; Uttamapinant, C.; Poloukhtine, A.; Baskin, J. M.; Codelli, J. A.; Sletten, E. M.; Bertozzi, C. R.; Popik, V. V.; Ting, A. Y. *J. Am. Chem. Soc.* **2012**, *134* (8), 3720–3728.

(27) Zheng, J.; Liu, K.; Reneker, D. H.; Becker, M. L. *J. Am. Chem. Soc.* **2012**, *134* (41), 17274–17277.

(28) Ornelas, C.; Broichhagen, J.; Weck, M. *J. Am. Chem. Soc.* **2010**, *132* (11), 3923–3931.

(29) Liu, C.; Li, T.; Rosi, N. L. *J. Am. Chem. Soc.* **2012**, *134* (46), 18886–18888.

(30) Manova, R.; van Beek, T. A.; Zuilhof, H. *Angew. Chem Int. Ed.* **2011**, *50* (24), 5428–5430.

(31) Koo, H.; Lee, S.; Na, J. H.; Kim, S. H.; Hahn, S. K.; Choi, K.; Kwon, I. C.; Jeong, S. Y.; Kim, K. *Angew. Chem Int. Ed.* **2012**, *51* (47), 11836–11840.

(32) Kim, Y.; Kim, S. H.; Ferracane, D.; Katzenellenbogen, J. A.; Schroeder, C. M. *Bioconjugate Chem.* **2012**, *23* (9), 1891–1901.

(33) Laughlin, S. T.; Baskin, J. M.; Amacher, S. L.; Bertozzi, C. R. *Science (80).* **2008**, *320* (5876), 664–667.

(34) van Geel, R.; Pruijn, G. J. M.; van Delft, F. L.; Boelens, W. C. *Bioconjugate Chem.* **2012**, *23* (3), 392–398.

(35) Ning, X.; Temming, R. P.; Dommerholt, J.; Guo, J.; Ania, D. B.; Debets, M. F.; Wolfert, M. A.; Boons, G. J.; van Delft, F. L. *Angew. Chem Int. Ed.* **2010**, *49* (17), 3065–3068.

(36) Debets, M. F.; van Berkel, S. S.; Dommerholt, J.; Dirks, A.; J.; Rutjes, F. P. J. T.; van Delft, F. L. *Acc. Chem. Res.* **2011**, *44* (9), 805–815.

(37) McKay, C. S.; Chigrinova, M.; Blake, J. A; Pezacki, J. P. *Org. Biomol. Chem.* **2012**, *10* (15), 3066–3070.

(38) McKay, C. S.; Blake, J. A; Cheng, J.; Danielson, D. C.; Pezacki, J. P. *Chem. Commun. (Camb).* **2011**, *47* (36), 10040–10042.

(39) Boger, D. L. *Chem. Rev.* **1986**, *86* (5), 781–793.

(40) Thalhammer, F.; Wallfahrer, U.; Sauer, J. *Tetrahedron Lett.* **1990**, *31* (47), 6851–6854.

(41) Blackman, M. L.; Royzen, M.; Fox, J. M. *J. Am. Chem. Soc.* **2008**, *130* (41), 13518–13519.

(42) Devaraj, N. K.; Weissleder, R.; Hilderbrand, S. A. *Communications* **2008**, 2297–2299.

(43) Lang, K.; Davis, L.; Wallace, S.; Mahesh, M.; Cox, D. J.; Blackman, M. L.; Fox, J. M.; Chin, J. W. *J. Am. Chem. Soc.* **2012**, *134* (25), 10317–10320.

(44) Plass, T.; Milles, S.; Koehler, C.; Szymański, J.; Mueller, R.; Wießler, M.; Schultz, C.; Lemke, E. A. *Angew. Chem - Int. Ed.* **2012**, *51* (17), 4166–4170.

(45) Lang, K.; Davis, L.; Torres-Kolbus, J.; Chou, C.; Deiters, A.; Chin, J. W. *Nat. Chem.* **2012**, *4* (4), 298–304.

(46) Borrmann, A.; Milles, S.; Plass, T.; Dommerholt, J.; Verkade, J. M. M.; Wiessler, M.; Schultz, C.; van Hest, J. C. M.; van Delft, F. L.; Lemke, E. A. *Chembiochem* **2012**, *13* (14), 2094–2099.

(47) Devaraj, N. K.; Hilderbrand, S.; Upadhyay, R.; Mazitschek, R.; Weissleder, R. *Angew. Chem* **2010**, *122* (16), 2931–2934.

(48) Haun, J. B.; Devaraj, N. K.; Hilderbrand, S. A; Lee, H.; Weissleder, R. *Nat. Nanotechnol.* **2010**, *5* (9), 660–665.

(49) Haun, J. B.; Devaraj, N. K.; Marinelli, B. S.; Lee, H.; Weissleder, R. *ACS Nano* **2011**, *5* (4), 3204–3213.

(50) Han, H. S.; Devaraj, N. K.; Lee, J.; Hilderbrand, S. A.; Weissleder, R.; Bawendi, M. G. *J. Am. Chem. Soc.* **2010**, *132* (23), 7838–7839.

(51) Zeglis, B. M.; Mohindra, P.; Weissmann, G. I.; Divilov, V.; Hilderbrand, S. A.; Weissleder, R.; Lewis, J. S. *Bioconjugate Chem.* **2011**, *22* (10), 2048–2059.

(52) Rossin, R.; Renart Verkerk, P.; van den Bosch, S. M.; Vulders, R. C. M.; Verel, I.; Lub, J.; Robillard, M. S. *Angew. Chem Int. Ed.* **2010**, *49* (19), 3375–3378.

(53) Li, Z.; Cai, H.; Hassink, M.; Blackman, M. L.; Brown, R. C. D.; Conti, P. S.; Fox, J. M. *Chem. Commun.* **2010**, *46* (42), 8043.

(54) Reiner, T.; Keliher, E. J.; Earley, S.; Marinelli, B.; Weissleder, R. *Angew. Chem Int. Ed.* **2011**, *50* (8), 1922–1925.

(55) Lang, K.; Chin, J. W. *Chem. Rev.* **2014**, *114* (9), 4764–4806.

(56) Glazer, A. N. *Annu. Rev. Biochem.* **1970**, *39* (1), 101–130.

(57) Stephanopoulos, N.; Francis, M. B. *Nat. Chem. Biol.* **2011**, *7* (12), 876–884.

(58) Veronese, F. M.; Pasut, G. *Drug Discov. Today* **2005**, *10* (21), 1451–1458.

(59) Wu, A. M.; Senter, P. D. *Nat. Biotechnol.* **2005**, *23* (9), 1137–1146.

(60) Tang, W.; Becker, M. L. *Chem. Soc. Rev.* **2014**, *43* (20), 7013–7039.

(61) Brewer, G. J. *Chem. Res. Toxicol.* **2010**, *23* (2), 319–326.

(62) Gierlich, J.; Burley, G. A.; Gramlich, P. M. E.; Hammond, D. M.; Carell, T. *Org. Lett.* **2006**, *8* (17), 3639–3642.

(63) Gaetke, L. *Toxicology* **2003**, *189* (1-2), 147–163.

(64) Peters, W.; Willnow, S.; Duisken, M.; Kleine, H.; Macherey, T.; Duncan, K. E.; Litchfield, D. W.; Lüscher, B.; Weinhold, E. *Angew. Chem Int. Ed.* **2010**, *49* (30), 5170–5173.

(65) Li, X. *Chem. - An Asian J.* **2011**, *6* (10), 2606–2616.

(66) Schneggenburger, P. E.; Worbs, B.; Diederichsen, U. *J. Pept. Sci.* **2010**, *16* (1), 10–14.

(67) Horne, W. S.; Stout, C. D.; Ghadiri, M. R. *J. Am. Chem. Soc.* **2003**, *125* (31), 9372–9376.

(68) Oh, K.; Guan, Z. *Chem. Commun. (Camb).* **2006**, *3* (c), 3069–3071.

(69) Roice, M.; Johannsen, I.; Meldal, M. *Qsar Comb. Sci.* **2004**, *23* (8), 662–673.

(70) Van Maarseveen, J. H.; Horne, W. S.; Ghadiri, M. R. *Org. Lett.* **2005**, *7* (4), 4503–4506.

(71) Parrish, B.; Breitenkamp, R. B.; Emrick, T. *J. Am. Chem. Soc.* **2005**, *127* (20), 7404–7410.

(72) Jølck, R. I.; Berg, R. H.; Andresen, T. L. *Bioconjugate Chem.* **2010**, *21* (5), 807–810.

(73) Zeng, Q.; Li, T.; Cash, B.; Li, S.; Xie, F.; Wang, Q. *Chem. Commun. (Camb).* **2007**, No. 14, 1453–1455.

(74) Sivakumar, K.; Xie, F.; Cash, B. M.; Long, S.; Barnhill, H. N.; Wang, Q. *Org. Lett.* **2004**, *6* (24), 4603–4606.

(75) Dirks, A. J.; van Berkel, S. S.; Hatzakis, N. S.; Opsteen, J. A.; van Delft, F. L.; Cornelissen, J. J. L. M.; Rowan, A. E.; van Hest, J. C. M.; Rutjes, F. P. J. T.; Nolte, R. J. M. *Chem. Commun.* **2005**, No. 33, 4172.

(76) Reynhout, I. C.; Cornelissen, J. J. L. M.; Nolte, R. J. M. *J. Am. Chem. Soc.* **2007**, *129* (8), 2327–2332.

(77) Deiters, A.; Cropp, T. A.; Mukherji, M.; Chin, J. W.; Anderson, J. C.; Schultz, P. G. *J. Am. Chem. Soc.* **2003**, *125* (39), 11782–11783.

(78) Deiters, A.; Cropp, T. A.; Summerer, D.; Mukherji, M.; Schultz, P. G. *Bioorganic Med. Chem. Lett.* **2004**, *14* (23), 5743–5745.

(79) Dieterich, D. C.; Link, A. J.; Graumann, J.; Tirrell, D. A.; Schuman, E. M. *Proc. Natl. Acad. Sci. U. S. A.* **2006**, *103* (25), 9482–9487.

(80) Kiick, K. L.; Saxon, E.; Tirrell, D. A; Bertozzi, C. R. *Proc. Natl. Acad. Sci. U. S. A.* **2002**, *99* (1), 19–24.

(81) Link, A. J.; Vink, M. K. S.; Tirrell, D. A. *J. Am. Chem. Soc.* **2004**, *126* (34), 10598–10602.

(82) Lutz, J.; Zarafshani, Z. *Adv. Drug Deliv. Rev.* **2008**, *60* (9), 958–970.

(83) Sletten, E. M.; Bertozzi, C. R. *Angew. Chem Int. Ed.* **2009**, *48* (38), 6974–6998.

(84) Chen, I.; Ting, A. Y. *Curr. Opin. Biotechnol.* **2005**, *16* (1), 35–40.

(85) Foley, T. L.; Burkart, M. D. *Curr. Opin. Chem. Biol.* **2007**, *11* (1), 12–19.

(86) Beatty, K. E.; Xie, F.; Wang, Q.; Tirrell, D. A. *J. Am. Chem. Soc.* **2005**, *127* (41), 14150–14151.

(87) Montclare, J. K.; Tirrell, D. A. *Angew. Chem Int. Ed.* **2006**, *45* (27), 4518–4521.

(88) Link, A. J.; Tirrell, D. A. *J. Am. Chem. Soc.* **2003**, *125* (37), 11164–11165.

(89) Baruah, H.; Puthenveetil, S.; Choi, Y.-A.; Shah, S.; Ting, A. Y. *Angew. Chem Int. Ed.*

2008, *47* (37), 7018–7021.

(90) Plaks, J. G.; Falatach, R.; Kastantin, M.; Berberich, J. A.; Kaar, J. L. *Bioconjugate Chem.* **2015**, *26* (6), 1104–1112.

(91) Park, H.S.; Hohn, M. J.; Umehara, T.; Guo, L.T.; Osborne, E. M.; Benner, J.; Noren, C. J.; Rinehart, J.; Soll, D. *Science (80).* **2011**, *333* (6046), 1151–1154.

(92) Chin, J. W. *Science (80).* **2003**, *301* (5635), 964–967.

(93) Wu, N.; Deiters, A.; Cropp, T. A.; King, D.; Schultz, P. G. *J. Am. Chem. Soc.* **2004**, *126* (44), 14306–14307.

(94) Neumann, H.; Peak-Chew, S. Y.; Chin, J. W. *Nat. Chem. Biol.* **2008**, *4* (4), 232–234.

(95) Young, T. S.; Ahmad, I.; Brock, A.; Schultz, P. G. *Biochemistry* **2009**, *48* (12), 2643–2653.

(96) Liu, W.; Brock, A.; Chen, S.; Chen, S.; Schultz, P. G. *Nat. Methods* **2007**, *4* (3), 239–244.

(97) Chin, J. W.; Santoro, S. W.; Martin, A. B.; King, D. S.; Wang, L.; Schultz, P. G. *J. Am. Chem. Soc.* **2002**, *124* (31), 9026–9027.

(98) Tian, F.; Tsao, M.L.; Schultz, P. G. *J. Am. Chem. Soc.* **2004**, *126* (49), 15962–15963.

(99) Chakraborty, A.; Wang, D.; Ebright, Y. W.; Korlann, Y.; Kortkhonjia, E.; Kim, T.; Chowdhury, S.; Wigneshweraraj, S.; Irschik, H.; Jansen, R.; Nixon, B. T.; Knight, J.; Weiss, S.; Ebright, R. H. *Science* **2012**, *337* (6094), 591–595.

(100) Deiters, A.; Schultz, P. G. *Bioorg. Med. Chem. Lett.* **2005**, *15* (5), 1521–1524.

(101) Li, X.; Fekner, T.; Ottesen, J.; Chan, M. *Angew. Chem* **2009**, *121* (48), 9348–9351.

(102) Wang, Y.S.; Fang, X.; Chen, H.Y.; Wu, B.; Wang, Z. U.; Hilty, C.; Liu, W. R. *ACS Chem. Biol.* **2013**, *8* (2), 405–415.

(103) Nguyen, D. P.; Lusic, H.; Neumann, H.; Kapadnis, P. B.; Deiters, A.; Chin, J. W. *J. Am. Chem. Soc.* **2009**, *131* (25), 8720–8721.

(104) Li, J.; Lin, S.; Wang, J.; Jia, S.; Yang, M.; Hao, Z.; Zhang, X.; Chen, P. R. *J. Am. Chem. Soc.* **2013**, *135* (19), 7330–7338.

(105) Tanrikulu, I. C.; Schmitt, E.; Mechulam, Y.; Goddard, W. A; Tirrell, D. A. *Pnas* **2009**, *106* (36), 15285–15290.

(106) Ngo, J. T.; Champion, J. A.; Mahdavi, A.; Tanrikulu, I. C.; Beatty, K. E.; Connor, R. E.; Yoo, T. H.; Dieterich, D. C.; Schuman, E. M.; Tirrell, D. A. *Nat. Chem. Biol.* **2009**, *5* (10), 715–717.

(107) Xiao, H.; Nasertorabi, F.; Choi, S.; Han, G. W.; Reed, S. A.; Stevens, R. C.; Schultz, P. G. *Proc. Natl. Acad. Sci. USA* **2015**, *112* (22), 6961–6966.

(108) Yanagisawa, T.; Ishii, R.; Fukunaga, R.; Kobayashi, T.; Sakamoto, K.; Yokoyama, S. *Chem. Biol.* **2008**, *15* (11), 1187–1197.

(109) Hao, Z.; Song, Y.; Lin, S.; Yang, M.; Liang, Y.; Wang, J.; Chen, P. R. *Chem. Commun.* **2011**, *47* (15), 4502–4504.

(110) Lin, S.; Zhang, Z.; Xu, H.; Li, L.; Chen, S.; Li, J.; Hao, Z.; Chen, P. R. *J. Am. Chem.*

Soc. **2011**, *133* (50), 20581–20587.

(111) Plass, T.; Milles, S.; Koehler, C.; Schultz, C.; Lemke, E. A. *Angew. Chem Int. Ed.* **2011**, *50* (17), 3878–3881.

(112) Brauch, S.; Henze, M.; Osswald, B.; Naumann, K.; Wessjohann, L. A.; van Berkel, S. S.; Westermann, B. *Org. Biomol. Chem.* **2012**, *10* (5), 958–965.

(113) Li, K.-B.; Wang, H.; Zang, Y.; He, X.; Li, J.; Chen, G.; Tian, H. *ACS Appl. Mater. Interfaces* **2014**, *6* (22), 19600–19605.

(114) Kele, P.; Li, X.; Link, M.; Nagy, K.; Herner, A.; Lőrincz, K.; Béni, S.; Wolfbeis, O. S. *Org. Biomol. Chem.* **2009**, *7* (17), 3486.

(115) Murtagh, J.; Frimannsson, D. O.; O'Shea, D. F. *Org. Lett.* **2009**, *11* (23), 5386–5389.

(116) Horváth, P.; Šebej, P.; Šolomek, T.; Klán, P. *J. Org. Chem.* **2015**, *80* (3), 1299–1311.

(117) Padalkar, V. S.; Patil, V. S.; Sekar, N. *Chem. Cent. J.* **2011**, *5* (10), 77.

(118) Nwe, K.; Brechbiel, M. W. *Cancer Biother. Radiopharm.* **2009**, *24* (3), 289–302.

(119) Crisp, G. T.; Gore, J. *Tetrahedron* **1997**, *53* (4), 1505–1522.

(120) Zhou, Z.; Fahrni, C. J. *J. Am. Chem. Soc.* **2004**, *126* (29), 8862–8863.

(121) Sawa, M.; Hsu, T.-L.; Itoh, T.; Sugiyama, M.; Hanson, S. R.; Vogt, P. K.; Wong, C.-H. *Proc. Natl. Acad. Sci. U. S. A.* **2006**, *103* (33), 12371–12376.

(122) Qi, J.; Han, M. S.; Chang, Y. C.; Tung, C. H. *Bioconjugate Chem.* **2011**, *22* (9), 1758–1762.

(123) Zhou, Z.; Fahrni, C. J. *J. Am. Chem. Soc.* **2004**, *126* (29), 8862–8863.

(124) Beatty, K. E.; Liu, J. C.; Xie, F.; Dieterich, D. C.; Schuman, E. M.; Wang, Q.; Tirrell, D. A. *Angew. Chem* **2006**, *118* (44), 7524–7527.

(125) Li, K.; Lee, L.; Lu, X.; Wang, Q. *Biotechniques* **2010**, *49* (1), 525–527.

(126) Jewett, J. C.; Bertozzi, C. R. *Org. Lett.* **2011**, *13* (22), 5937–5939.

(127) Uttamapinant, C.; Tangpeerachaikul, A.; Grecian, S.; Clarke, S.; Singh, U.; Slade, P.; Gee, K. R.; Ting, A. Y. *Angew. Chem* **2012**, *124* (24), 5954–5958.

(128) Xie, F.; Sivakumar, K.; Zeng, Q.; Bruckman, M. A.; Hodges, B.; Wang, Q. *Tetrahedron* **2008**, *64* (13), 2906–2914.

(129) Seela, F.; Pujari, S. S. *Bioconjugate Chem.* **2010**, *21* (9), 1629–1641.

(130) Wang, C.; Xie, F.; Suthiwangcharoen, N.; Sun, J.; Wang, Q. *Sci. China Chem.* **2012**, *55* (1), 125–130.

(131) Chauhan, D. P.; Saha, T.; Lahiri, M.; Talukdar, P. *Tetrahedron Lett.* **2014**, *55* (1), 244–247.

(132) Qi, J.; Tung, C.H. *Bioorg. Med. Chem. Lett.* **2011**, *21* (1), 320–323.

(133) Du Ý, L.; Ni Ý, N.; Li, M.; Wang, B. *Tetrahedron Lett.* **2010**, *51* (8), 1152–1154.

(134) Gunnlaugsson, T.; Leonard, J. P. *Chem. Commun.* **2005**, No. 25, 3114–3131.

(135) Parker, D. *Chem. Soc. Rev.* **2004**, *33* (3), 156.

(136) Parker, D.; Williams, J. A. G. *J. Chem. Soc. Dalt. Trans.* **1996**, No. 18, 3613.

(137) Beeby, A.; Botchway, S. W.; Clarkson, I. M.; Faulkner, S.; Parker, A. W.; Parker, D.; Williams, J. A. G. *J. Photochem. Photobiol. B Biol.* **2000**, *57* (2-3), 83–89.

(138) Charbonnière, L.; Ziessel, R.; Guardigli, M.; Roda, A.; Sabbatini, N.; Cesario, M. *J. Am. Chem. Soc.* **2001**, *123* (10), 2436–2437.

(139) Faulkner, S.; Pope, S. J. A.; Burton-Pye, B. P. *Appl. Spectrosc. Rev.* **2005**, *40* (1), 1–31.

(140) Armelao, L.; Quici, S.; Barigelletti, F.; Accorsi, G.; Bottaro, G.; Cavazzini, M.; Tondello, E. *Coord. Chem. Rev.* **2010**, *254* (5-6), 487–505.

(141) Bünzli, J. C. G. *Chem. Rev.* **2010**, *110* (5), 2729–2755.

(142) Beeby, A.; Clarkson, I. M.; Dickins, R. S.; Faulkner, S.; Parker, D.; Royle, L.; de Sousa, A. S.; Williams, J. a. G.; Woods, M. *J. Chem. Soc. Perkin Trans. 2* **1999**, *2* (3), 493–504.

(143) Li, M.; Selvin, P. R. *J. Am. Chem. Soc.* **1995**, *117* (31), 8132–8138.

(144) Xiao, M.; Selvin, P. R. *J. Am. Chem. Soc.* **2001**, *123* (29), 7067–7073.

(145) Beeby, A.; Bushby, L. M.; Maffeo, D.; Gareth Williams, J. A. *J. Chem. Soc. Dalt. Trans.* **2002**, No. 1, 48–54.

(146) Hanaoka, K.; Kikuchi, K.; Kobayashi, S.; Nagano, T. *J. Am. Chem. Soc.* **2007**, *129* (44), 13502–13509.

(147) Caravan, P.; Ellison, J. J.; McMurry, T. J.; Lauffer, R. B. *Chem. Rev.* **1999**, *99* (9), 2293–2352.

(148) Quici, S.; Cavazzini, M.; Raffo, M. C.; Botta, M.; Giovenzana, G. B.; Ventura, B.; Accorsi, G.; Barigelletti, F. *Inorganica Chim. Acta* **2007**, *360* (8), 2549–2557.

(149) Takalo, H.; Hanninen, E.; Kankare, J. *Helv. Chim. Acta* **1993**, *76* (2), 877–883.

(150) Starck, M.; Kadjane, P.; Bois, E.; Darbouret, B.; Incamps, A.; Ziessel, R.; Charbonnière, L. J. *Chem. - A Eur. J.* **2011**, *17* (33), 9164–9179.

(151) Gudgin Dickson, E. F.; Pollak, A.; Diamandis, E. P. *Pharmacol. Ther.* **1995**, *66* (2), 207–235.

(152) Hemmilä, I.; Dakubu, S.; Mukkala, V. M.; Siitari, H.; Lövgren, T. *Anal. Biochem.* **1984**, *137* (2), 335–343.

(153) Hagan, A. K.; Zuchner, T. *Anal. Bioanal. Chem.* **2011**, *400* (9), 2847–2864.

(154) Jauregui, M.; Perry, W. S.; Allain, C.; Vidler, L. R.; Willis, M. C.; Kenwright, A. M.; Snaith, J. S.; Stasiuk, G. J.; Lowe, M. P.; Faulkner, S. *Dalton Trans.* **2009**, 6283–6285.

(155) Szijjarto, C.; Pershagen, E.; Borbas, K. E. *Dalt. Trans* **2012**, *41* (25), 7660–7669.

(156) Stasiuk, G. J.; Lowe, M. P. *Dalt. Trans.* **2009**, No. 44, 9725–9727.

(157) Tropiano, M.; Kilah, N. L.; Morten, M.; Rahman, H.; Davis, J. J.; Beer, P. D.; Faulkner, S. *J. Am. Chem. Soc.* **2011**, *133* (31), 11847–11849.

(158) Viguier, R. F. H.; Hulme, A. N. *J. Am. Chem. Soc.* **2006**, *128* (35), 11370–11371.

(159) Molloy, J. K.; Kotova, O.; Peacock, R. D.; Gunnlaugsson, T. *Org. Biomol. Chem.* **2012**, *10* (2), 314–322.

(160) Tropiano, M.; Kenwright, A. M.; Faulkner, S. *Chem. A Eur. J.* **2015**, *21* (15), 5697–5699.

(161) Ketola, J.; Katajisto, J.; Hakala, H.; Hovinen, J. *Helv. Chim. Acta* **2007**, *90* (3), 607–615.

(162) Ung, P. Lanthanide Tags for Luminescence Applications and Paramagnetic NMR Spectroscopy, Monash University, **2013**.

(163) Phelps, M. E. *J. Nucl. Med.* **2000**, *41* (4), 661–681.

(164) Wester, H. *Clin. Cancer Res.* **2007**, *13* (12), 3470–3481.

(165) Rahmim, A.; Zaidi, H. *Nucl. Med. Commun.* **2008**, *29* (3), 193–207.

(166) Mamat, C.; Ramenda, T.; Wuest, F. *Mini. Rev. Org. Chem.* **2009**, *6* (1), 21–34.

(167) Wängler, C.; Schirrmacher, R.; Bartenstein, P.; Wängler, B. *Curr. Med. Chem.* **2010**, *17*, 1092–1116.

(168) Marik, J.; Sutcliffe, J. L. *Tetrahedron Lett.* **2006**, *47* (37), 6681–6684.

(169) Sirion, U.; Kim, H. J.; Lee, J. H.; Seo, J. W.; Lee, B. S.; Lee, S. J.; Oh, S. J.; Chi, D. Y. *Tetrahedron Lett.* **2007**, *48* (23), 3953–3957.

(170) Sephton, S. M.; Dennler, P.; Leutwiler, D. S.; Mu, L.; Wanger-Baumann, C. A.; Schibli, R.; Krämer, S. D.; Ametamey, S. M. *Am. J. Nucl. Med. Mol. Imaging* **2012**, *2* (1), 14–28.

(171) Li, Z.-B.; Wu, Z.; Chen, K.; Chin, F. T.; Chen, X. *Bioconjugate Chem.* **2007**, *18* (6), 1987–1994.

(172) Glaser, M.; Morrison, M.; Solbakken, M.; Arukwe, J.; Karlsen, H.; Wiggen, U.; Champion, S.; Kindberg, G. M.; Cuthbertson, A. *Bioconjugate Chem.* **2008**, *19* (4), 951–957.

(173) Ross, T. L.; Honer, M.; Lam, P. Y. H.; Mindt, T. L.; Groehn, V.; Schibli, R.; Schubiger, P. A.; Ametamey, S. M. *Bioconjugate Chem.* **2008**, *19* (12), 2462–2470.

(174) Devaraj, N. K.; Keliher, E. J.; Thurber, G. M.; Nahrendorf, M.; Weissleder, R. *Bioconjugate Chem.* **2009**, *20* (2), 397–401.

(175) Hausner, S. H.; Marik, J.; Gagnon, M. K. J.; Sutcliffe, J. L. *J. Med. Chem.* **2008**, *51* (19), 5901–5904.

(176) Maschauer, S.; Haubner, R.; Kuwert, T.; Prante, O. *Mol. Pharm.* **2014**, *11* (2), 505–515.

(177) Glaser, M.; Robins, E. G. *J. Label. Compd. Radiopharm.* **2009**, *52* (10), 407–414.

(178) Mindt, T. L.; Müller, C.; Melis, M.; de Jong, M.; Schibli, R. *Bioconjugate Chem.* **2008**, *19* (8), 1689–1695.

(179) Mindt, T. L.; Struthers, H.; Brans, L.; Anguelov, T.; Schweinsberg, C.; Maes, V.; Tourwé, D.; Schibli, R. *J. Am. Chem. Soc.* **2006**, *128* (47), 15096–15097.

(180) Moore, A. L.; Bučar, D. K.; MacGillivray, L. R.; Benny, P. D. *Dalt. Trans.* **2010**, *39*

(8), 1926.

(181) Struthers, H.; Spingler, B.; Mindt, T. L.; Schibli, R. *Chem. - A Eur. J.* **2008**, *14* (20), 6173–6183.

(182) Wang, C.; Zhou, W.; Yu, J.; Zhang, L.; Wang, N. *Nucl. Med. Commun.* **2012**, *33* (1), 84–89.

(183) Ferro-Flores, G.; Rivero, I. A.; Santos-Cuevas, C. L.; Sarmiento, J. I.; Arteaga de Murphy, C.; Ocampo-García, B. E.; García-Becerra, R.; Ordaz-Rosado, D. *Appl. Radiat. Isot.* **2010**, *68* (12), 2274–2278.

(184) Dijkgraaf, I.; Rijnders, A. Y.; Soede, A.; Dechesne, A. C.; van Esse, G. W.; Brouwer, A. J.; Corstens, F. H. M.; Boerman, O. C.; Rijkers, D. T. S.; Liskamp, R. M. J. *Org. Biomol. Chem.* **2007**, *5* (6), 935.

(185) Knör, S.; Modlinger, A.; Poethko, T.; Schottelius, M.; Wester, H. J.; Kessler, H. *Chem. - A Eur. J.* **2007**, *13* (21), 6082–6090.

(186) Cai, Z.; Ouyang, Q.; Zeng, D.; Nguyen, K. N.; Modi, J.; Wang, L.; White, A. G.; Rogers, B. E.; Xie, X.-Q.; Anderson, C. J. *J. Med. Chem.* **2014**, *57* (14), 6019–6029.

(187) Cai, Z.; Li, B. T. Y.; Wong, E. H.; Weisman, G. R.; Anderson, C. J. *Dalt. Trans.* **2015**, *44* (9), 3945–3948.

(188) Viehweger, K.; Barbaro, L.; García, K. P.; Joshi, T.; Geipel, G.; Steinbach, J.; Stephan, H.; Spiccia, L.; Graham, B. *Bioconjugate Chem.* **2014**, *25* (5), 1011–1022.

CHAPTER 2:

LUMINESCENT ALKYNE-BEARING TERBIUM(III) COMPLEXES AND THEIR APPLICATION TO BIOORTHOGONAL PROTEIN LABELING

Declaration for Thesis Chapter 2.

Declaration by candidate

In the case of Chapter 2 the nature and extent of my contribution to the work was the following:

Nature of contribution	Extent of contribution (%)
Synthesis and characterisation of synthetic compounds, evaluation of photophysical properties, interpretation of results, manuscript preparation.	75%

The following co-authors contributed to the work. If co-authors are students at Monash University, the extent of their contribution in percentage terms must be stated:

Name	Nature of contribution	Extent of contribution (%) for student co-authors only
Elwy Abdelkader	Protein synthesis	
Margaret Aulsebrook	Compound characterisation	5%
Riccardo Rubbiani	Compound characterisation	
Choy-Theng Loh	Protein synthesis	
Michael Grace	Research guidance, manuscript review	
Leone Spiccia	Research guidance, manuscript review	
Gilles Gasser	Research guidance, manuscript review	
Gottfried Otting	Research guidance, manuscript review	
Kellie Tuck	Research guidance, experimental design, manuscript review	
Bim Graham	Research guidance, experimental design, interpretation of results, manuscript review	

The undersigned hereby certify that the above declaration correctly reflects the nature and extent of the candidate's and co-authors' contributions to this work.

Candidate's Signature		**Date 9/3/16**
Main Supervisor's Signature	[redacted]	**Date 8/3/16**

Inorganic Chemistry

Article

pubs.acs.org/IC

Luminescent Alkyne-Bearing Terbium(III) Complexes and Their Application to Bioorthogonal Protein Labeling

William I. O'Malley,[†] Elwy H. Abdelkader,[‡] Margaret L. Aulsebrook,[⊥] Riccardo Rubbiani,[∥] Choy-Theng Loh,[‡] Michael R. Grace,[⊥] Leone Spiccia,[⊥] Gilles Gasser,[∥] Gottfried Otting,[‡] Kellie L. Tuck,*[,⊥] and Bim Graham*[,†]

[†]Monash Institute of Pharmaceutical Sciences, Monash University, Parkville VIC 3052, Australia

[‡]Research School of Chemistry, Australian National University, Canberra ACT 2601, Australia

[⊥]School of Chemistry, Monash University, Clayton VIC 3800, Australia

[∥]Department of Chemistry, University of Zurich, Winterthurerstrasse 190, CH-8057 Zurich, Switzerland

Supporting Information

ABSTRACT: Two new bifunctional macrocyclic chelate ligands that form luminescent terbium(III) complexes featuring an alkyne group for conjugation to (bio)molecules via the Cu(I)-catalyzed "click" reaction were synthesized. Upon ligation, the complexes exhibit a significant luminescent enhancement when excited at the λ_{max} of the "clicked" products. To demonstrate the utility of the complexes for luminescent labeling, they were conjugated in vitro to *E. coli* aspartate/glutamate-binding protein incorporating a genetically encoded *p*-azido-L-phenylalanine or *p*-(azidomethyl)-L-phenylalanine residue. The complexes may prove useful for time-gated assay applications.

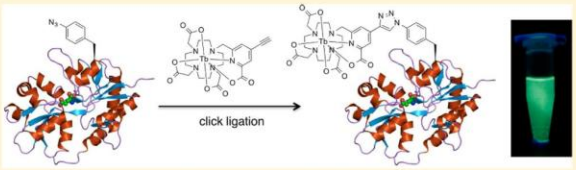

INTRODUCTION

The luminescent properties of the lanthanide(III) ions have been of long-standing interest. In the early 1950s, a number of these ions began to be exploited as phosphor dopants in the production of cathode ray tube-style televisions.[1] More recently, luminescent lanthanide complexes (LLCs), particularly those of terbium(III) (green luminescence) and europium(III) (red luminescence), have found widespread application in research, drug discovery, and clinical environments as imaging agents, sensors, and bioassay components.[2−11] As labels and probes LLCs offer a number of distinct advantages over the more traditionally used organic fluorophores. Salient features include large Stokes shifts, which reduce self-quenching effects, narrow emission bands that are environmentally insensitive, and very long-lived excited-state lifetimes (in the order of milliseconds).[10−14] The latter property, in particular, has proven instrumental to the development of ultrasensitive time-resolved fluorescence immunoassays,[6,9,15,16] which incorporate a time delay between sample excitation and emission detection to eliminate interference from short-lived "background" fluorescence.

The development of LLCs for labeling of biomolecules requires careful attention to ligand design. High-denticity (hepta- to nonadentate) ligands incorporating "hard" and/or "borderline" donor atoms are generally required to ensure that the lanthanide ion is stably bound and that the number of aqua ligands is minimized so as to reduce deactivation of the emissive state through O−H vibrations.[3,6,10,11,13,14] Second, since f−f transitions involving the 4f electrons of lanthanides are parity-forbidden,[12] a suitable sensitizing "antenna" group (typically a heteroaromatic ring system) must be incorporated to improve accessibility of the lanthanide excited state via a process that involves absorption of radiation by the antenna to promote it to an excited ligand singlet state (S_1), followed by intersystem crossing (ISC) to an excited triplet state (T_1), and finally, energy transfer to the metal center to populate its excited state.[3,6,10,11,13,14] The desirable traits for an effective antenna group include a high extinction coefficient, efficient $S_1 \rightarrow T_1$ ISC rate, and close proximity to the lanthanide center. The excited state of the antenna must be higher than that of the lanthanide ion for energy transfer to be thermodynamically favored.

In addition to the above, an LLC requires a suitable reactive group within its ligand structure to allow conjugation to a target biomolecule. Over the past few decades, a wide array of LLCs featuring amine- and thiol-reactive groups have been reported, and many of these have been successfully used to label proteins via lysine and cysteine side-chains.[17] While appropriate for many applications, the frequent occurrence of amine and thiol functionalities leads to nonspecific, inhomogeneous labeling. Alternative approaches that avoid this issue include the use of lanthanide-binding peptide motifs (including genetically encoded ones)[18] and self-labeling protein tagging strategies (e.g., SNAP-tag technology).[19] So-called "bioorthogonal" conjugation chemistries and labeling strategies afford the

Received: November 11, 2015

DOI: 10.1021/acs.inorgchem.5b02605
Inorg. Chem. XXXX, XXX, XXX−XXX

Scheme 1. Synthesis[a] of Tb-L1 and a Model Clicked Derivative

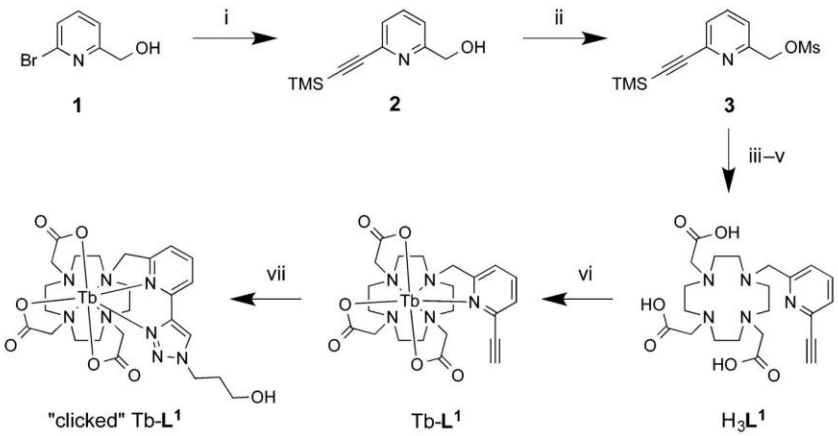

[a](i) $Pd(PPh_3)_2Cl_2$, TMS acetylene, CuI, Et_3N, THF, N_2 atmosphere, RT, 2 h, 75%; (ii) MsCl, DIPEA, DCM, 0 °C to RT, 30 min, 96%; (iii) $^tBu_3DO_3A{\cdot}HBr$, DIPEA, MeCN, reflux, O/N; (iv) KF, MeCN/H_2O, RT, 2 h; (v) TFA, DCM, RT, O/N, 23% (over steps iii–v); (vi) $Tb(OTf)_3$, H_2O, NaOH (pH 8–9), 90 °C, 2 h, quantitative (57% isolated); (vii) 3-azido-1-propanol, $CuSO_4$, THPTA, sodium ascorbate, H_2O/MeCN, pH 7, RT, O/N, quantitative (22% isolated).

Scheme 2. Synthesis[a] of Tb-L^2 and a Model Clicked Derivative

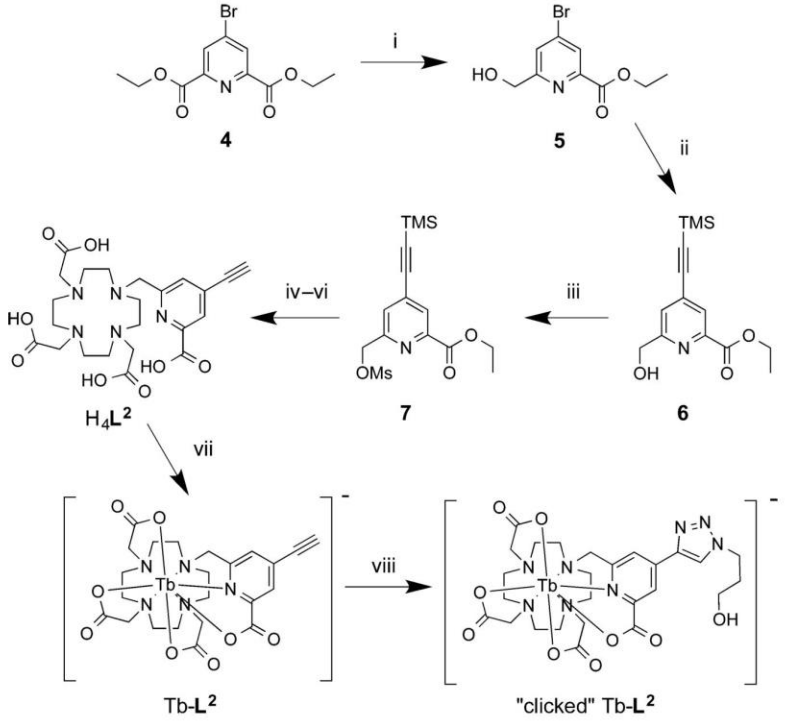

[a](i) $NaBH_4$, EtOH, reflux, 15 min, 48%; (ii) $Pd(PPh_3)_2Cl_2$, TMS acetylene, CuI, Et_3N, THF, N_2 atmosphere, RT, 2 h, 85%; (iii) MsCl, DIPEA, DCM, 0 °C to RT, 30 min, quantitative; (iv) DIPEA, MeCN, reflux, O/N; (v) 1 M NaOH, MeCN, RT, 2 h; (vi) TFA, DCM, RT, O/N, 28% (over steps iv–vi); (vii) $Tb(OTf)_3$, H_2O, NaOH (pH 8–9), 90 °C, 2 h, quantitative (49% isolated); (viii) 3-azido-1-propanol, $CuSO_4$, THPTA, sodium ascorbate, water/MeCN, pH 7, RT, O/N, quantitative (37% isolated).

opportunity for site-specific labeling. Currently, however, there are very few reports of the incorporation of LLCs into biomolecules using such technologies.[20−22]

Among the bioorthogonal reactions, the Cu(I)-catalyzed azide−alkyne cycloaddition reaction ("click reaction")[23] and its copper-free variant−strain-promoted azide−alkyne cycloaddition (SPAAC)[24,25] have proven particularly useful for the production of well-defined bioconjugates, both because of the highly specific and robust nature of these reactions as well as the existence and continued development of increasingly

DOI: 10.1021/acs.inorgchem.5b02605
Inorg. Chem. XXXX, XXX, XXX−XXX

sophisticated methods to introduce azide or alkyne groups into proteins and other biomolecules.[26−31] In particular, orthogonal suppressor-tRNA/aminoacyl-tRNA-synthetase pairs have provided an effective tool for the site-specific incorporation of unnatural amino acids bearing azide- and alkyne-bearing side chains into recombinantly expressed proteins.[30,31] A number of alkyne- and azide-bearing lanthanide complexes have been described,[21,22,32−36] and a recent study reports the use of SPACC to conjugate an azide-bearing LLC to a protein featuring cyclooctyne groups attached to surface lysine residues.[22] Fully site-specific protein labeling with an LLC using a genetically encoded unnatural amino acid, however, has not yet been reported.

Building on our recent work on "clickable" lanthanide complexes for paramagnetic NMR and electron paramagnetic resonance spectroscopic studies of proteins,[37−39] we report herein the synthesis of two new stable luminescent alkyne-bearing terbium(III) complexes and demonstrate their facile conjugation to a protein—the *E. coli* aspartate/glutamate-binding protein[39]—using either a *p*-azido-L-phenylalanine or *p*-(azidomethyl)-L-phenylalanine residue installed by stop codon reassignment.

RESULTS AND DISCUSSION

Synthesis of Ligands and Complexes. Key to the synthesis of the new macrocyclic ligands $\mathbf{L^1}$ and $\mathbf{L^2}$ was the preparation of two functionalized pyridine compounds designed to serve as sensitizing antenna groups as well as coordinating groups and reactive handles for conjugation. As shown in Scheme 1, preparation of the first of these involved a Sonogashira reaction between (6-bromopyridin-2-yl)methanol (**1**) and trimethylsilylacetylene (TMS acetylene) to install a protected alkyne group,[40] followed by mesitylation to facilitate coupling to the macrocyclic ring of *tert*-butyl-protected 1,4,7,10-tetraazacyclododecane-1,4,7-triacetic acid (^{t}Bu$_3$DO$_3$A).[41] Subsequent removal of the TMS and *tert*-butyl protecting groups using KF and trifluoroacetic acid (TFA), respectively, afforded ligand $H_3\mathbf{L^1}$.

The synthesis of $\mathbf{L^2}$ (Scheme 2) commenced with reduction of one of the ester groups of diethyl 4-bromopyridine-2,6-dicarboxylate (**4**)[42] to a hydroxyl according to a literature procedure.[43] A Sonogashira reaction with TMS acetylene was then used to replace the bromo substituent with a protected alkyne group, before mesitylation of the hydroxyl group to enable attachment of the pyridine-based antenna to ^{t}Bu$_3$DO$_3$A.[44] Hydrolytic cleavage of the TMS and ethyl ester groups using NaOH, followed by removal of the *tert*-butyl protecting groups using TFA, afforded $H_4\mathbf{L^2}$.[45] Both of the ligands were obtained in excellent purity (>95%) after preparative HPLC.

The terbium(III) complexes of $\mathbf{L^1}$ and $\mathbf{L^2}$ were prepared by heating slightly basic aqueous solutions (pH 8−9) of the ligands with 2 equiv of terbium(III) triflate for 2 h (Schemes 1 and 2). After this time, LC-MS analysis indicated near-quantitative complexation. Preparative HPLC was then used to purify the complexes to >95% purity (it was necessary to employ 0.1% formic acid in HPLC buffers, rather than the more traditionally used 0.1% TFA, to prevent decomplexation during purification).

To assess the luminescent properties of the terbium(III) complexes post-clicking, they were conjugated to 3-azido-1-propanol as a model azide compound in aqueous solution. As per well-established protocols, $CuSO_4$ (0.1 equiv) was utilized as the copper source, sodium ascorbate (1.0 equiv) as the reducing agent, and tris(3-hydroxypropyl-triazolylmethyl)amine (THTPA; 0.2 equiv) as a Cu(I)-stabilizing ligand.[46,47] After the mixture was stirred overnight, conversion to the clicked products was quantitative according to LC-MS analysis. The complexes were again isolated in >95% purity following preparative HPLC.

Photophysical Properties of Complexes. The spectral properties of the four isolated terbium(III) complexes were measured in aqueous solution buffered at pH 7.4 with 100 mM HEPES. Table 1 summarizes the data, while absorbance and emission spectra of the complexes are shown in Figures 1 and 2, respectively.

Table 1. Photophysical Data for Terbium(III) Complexes Measured in 100 mM HEPES, pH 7.4 (298 K)

complex	absorption λ_{max} (ε [M^{-1} cm^{-1}])	Φ^a (%)	brightness ($\varepsilon \times \Phi$/1000 [M^{-1} cm^{-1}])
Tb-$\mathbf{L^1}$	287 (6700)	13	0.87
clicked Tb-$\mathbf{L^1}$	300 (10 800), 250 sh (10 300)	21	2.3
Tb-$\mathbf{L^2}$	297 (7800), 250 sh (12 200)	22	1.7
clicked Tb-$\mathbf{L^2}$	274 (15 900)	19	3.0

[a]Quantum yields were measured relative to quinine sulfate.[48] The estimated relative error is 10−15%.

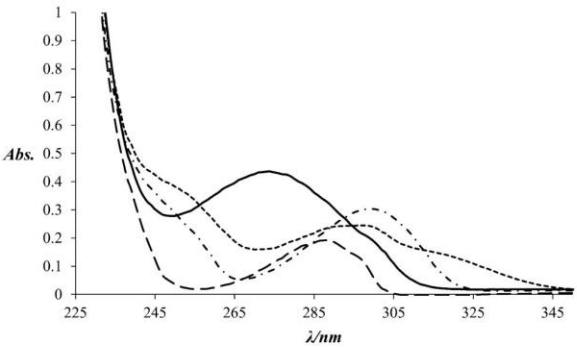

Figure 1. Absorbance spectra of terbium(III) complexes (25 μM) in 100 mM HEPES, pH 7.4 (298 K). Dashed line: Tb-$\mathbf{L^1}$, dot-dashed line: clicked Tb-$\mathbf{L^1}$, dotted line: Tb-$\mathbf{L^2}$, solid line: clicked Tb-$\mathbf{L^2}$.

Complex Tb-$\mathbf{L^1}$ exhibits an absorbance maximum at 287 nm, assigned to a $\pi \rightarrow \pi^*$ ligand-centered transition, which shifts to 300 nm in the corresponding clicked complex. Complex Tb-$\mathbf{L^2}$ displays poorly resolved bands at ca. 250 and 300 nm, while the clicked derivative features a more pronounced absorption band centered at 274 nm, assigned to a combination of $\pi \rightarrow \pi^*$ and n $\rightarrow \pi^*$ ligand-centered transitions.[49,50] All complexes exhibit almost identical luminescence emission profiles consisting of four bands between ca. 470 and 630 nm, corresponding to transitions from the $^5D_4$ excited state to the ^7F_J (J = 6−3) levels, with the $^5D_4 \rightarrow {}^7F_5$ green emission (545 nm) being the most prominent one (Figure 2).[14] The overall quantum yields (Φ) range between 13 and 22% and compare favorably with those of many other luminescent terbium(III) complexes developed for imaging and assay applications.[51]

It was anticipated that the triazole group formed upon clicking of the alkyne group within Tb-$\mathbf{L^1}$ would coordinate to

DOI: 10.1021/acs.inorgchem.5b02605
Inorg. Chem. XXXX, XXX, XXX−XXX

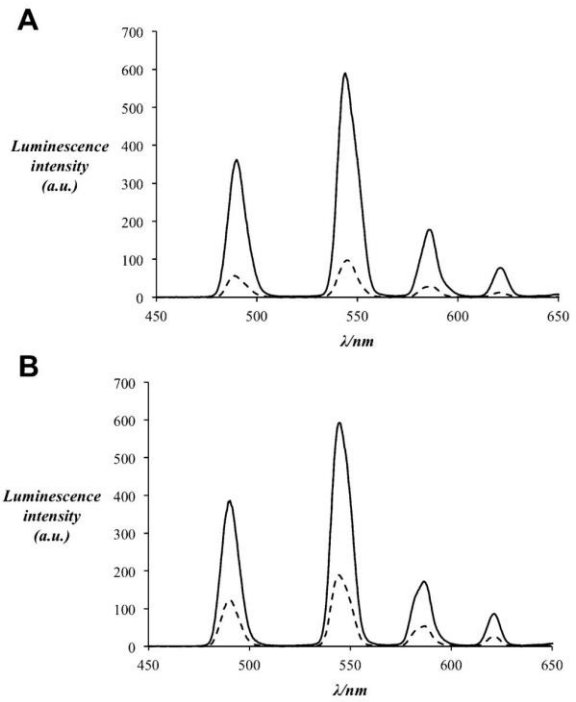

Figure 2. Luminescence emission spectra of terbium(III) complexes (25 μM) in 100 mM HEPES, pH 7.4 (298 K). (A) Tb-$\mathbf{L^1}$ (dashed line) and clicked Tb-$\mathbf{L^1}$, complex (solid line) excited at 300 nm. (B) Tb-$\mathbf{L^2}$ (dashed line) and clicked Tb-$\mathbf{L^2}$ complex (solid line) excited at 274 nm.

the terbium(III) center, forming a five-membered chelate ring, as shown in Scheme 1. To confirm this, measurements of the luminescence lifetimes (τ) of Tb-$\mathbf{L^1}$ and the clicked product were conducted in both H_2O and D_2O (Figures S1–S4) to estimate the number of water molecules in the primary coordination sphere (q) according to the equation of Parker and co-workers, $q = 5 \times (1/\tau(H_2O) - 1/\tau(D_2O) - 0.06)$.[52] The q value reduces from approximately one (0.84) to zero (−0.14) upon clicking of the complex. The higher luminescence quantum yield of the clicked derivative is also consistent with ejection of an aqua ligand by the triazole group, since coordinated water molecules are well-known to cause radiationless O−H vibronic deactivation of the luminescent excited state of terbium(III) complexes.[52]

In the case of the clicked and non-clicked Tb-$\mathbf{L^2}$ complexes, the quantum yields are essentially the same; however, the clicked complex has a higher brightness value (Table 1) due its higher molar absorptivity (15 900 M^{-1} cm^{-1} at λ_{max} = 274 nm vs 7800 M^{-1} cm^{-1} at λ_{max} = 297 nm for Tb-$\mathbf{L^2}$).

Figure 3 shows a photograph of solutions of the complexes (25 μM) irradiated with a common laboratory TLC lamp (254 nm). Interestingly, Tb-$\mathbf{L^1}$ is almost completely nonemissive under these conditions, while the clicked derivative displays bright green luminescence due to a much larger absorptivity at this particular wavelength (Figure 1). Likewise, a luminescent "switch on" effect is observed when these two complexes are irradiated at 300 nm (Figure 2A), the λ_{max} of the clicked product, providing a simple indicator of successful ligation of the Tb-$\mathbf{L^1}$ complex. In the case of Tb-$\mathbf{L^2}$ and its clicked derivative, both complexes exhibit bright green luminescence

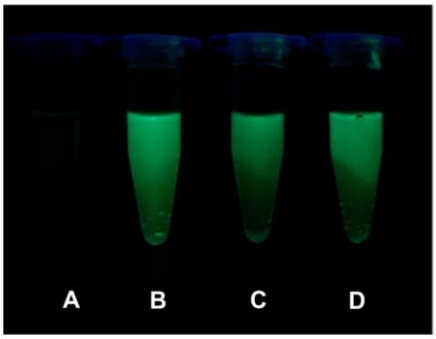

Figure 3. Photograph of solutions of the terbium(III) complexes (25 μM) in 100 mM HEPES, pH 7.4 (298 K), irradiated with a common laboratory TLC lamp (254 nm). (A) Tb-$\mathbf{L^1}$. (B) Clicked Tb-$\mathbf{L^1}$. (C) Tb-$\mathbf{L^2}$. (D) Clicked Tb-$\mathbf{L^2}$.

under 254 nm irradiation (Figure 3) due to their similar absorptivities at this wavelength (Figure 1). However, the clicked complex is significantly more emissive than Tb-$\mathbf{L^2}$ when irradiated at 274 nm, its λ_{max} (Figure 2B).

Conjugation of Complexes to a Protein. To demonstrate the utility of the new complexes for highly site-specific introduction of luminescent labels into proteins, we investigated their ligation to *E. coli* aspartate/glutamate-binding protein (DEBP),[53] incorporating a single copy of either a *p*-azido-L-phenylalanine (pAzF)[54] or *p*-(azidomethyl)-L-phenylalanine (pAzMF)[55] residue at position Q80, which is highly solvent-exposed (Figure 4).[39] Protein samples were produced from PCR-amplified DNA by cell-free expression,[56] with the unnatural amino acids introduced site-specifically in response to an "amber" stop codon (TAG) using the well-established orthogonal tRNA/*p*-cyano-L-phenylalanyl-tRNA synthetase system.[54] Click labeling was performed at pH 8 using $CuSO_4$, sodium ascorbate and 2-[4-({bis[(1-*tert*-butyl-1*H*-1,2,3-triazol-4-yl)methyl]amino}-methyl)-1*H*-1,2,3-triazol-1-yl]acetic acid) (BTTAA),[57] with 150 mM NaCl added to prevent protein precipitation.[37]

After incubation at room temperature for 16 h, mass spectrometry indicated near-quantitative ligation of the complexes (Figure 4B,C). Successful protein labeling was also evident from the luminescence observed upon irradiation of the protein samples with a TLC lamp (254 nm) following spin dialysis to remove unreacted tag molecules (Figure S5), as well as from the luminescence emission spectra (Figures S6 and S7).

■ CONCLUSION

In conclusion, we have developed two terbium(III) complexes that can be readily conjugated to azide-bearing molecules via the Cu(I)-catalyzed click reaction to introduce a luminescent label. Among various methods for incorporating azide groups into (bio)molecules, biosynthetic routes based on unnatural amino acids offer exciting prospects for site-specific tagging, opening the door to time-resolved luminescence resonance energy transfer experiments for distance measurements and monitoring biomolecular interactions. The tags possess favorable photophysical properties and can be ligated in near-quantitative yield. We therefore anticipate that they will prove useful for luminescent assay applications.

DOI: 10.1021/acs.inorgchem.5b02605
Inorg. Chem. XXXX, XXX, XXX−XXX

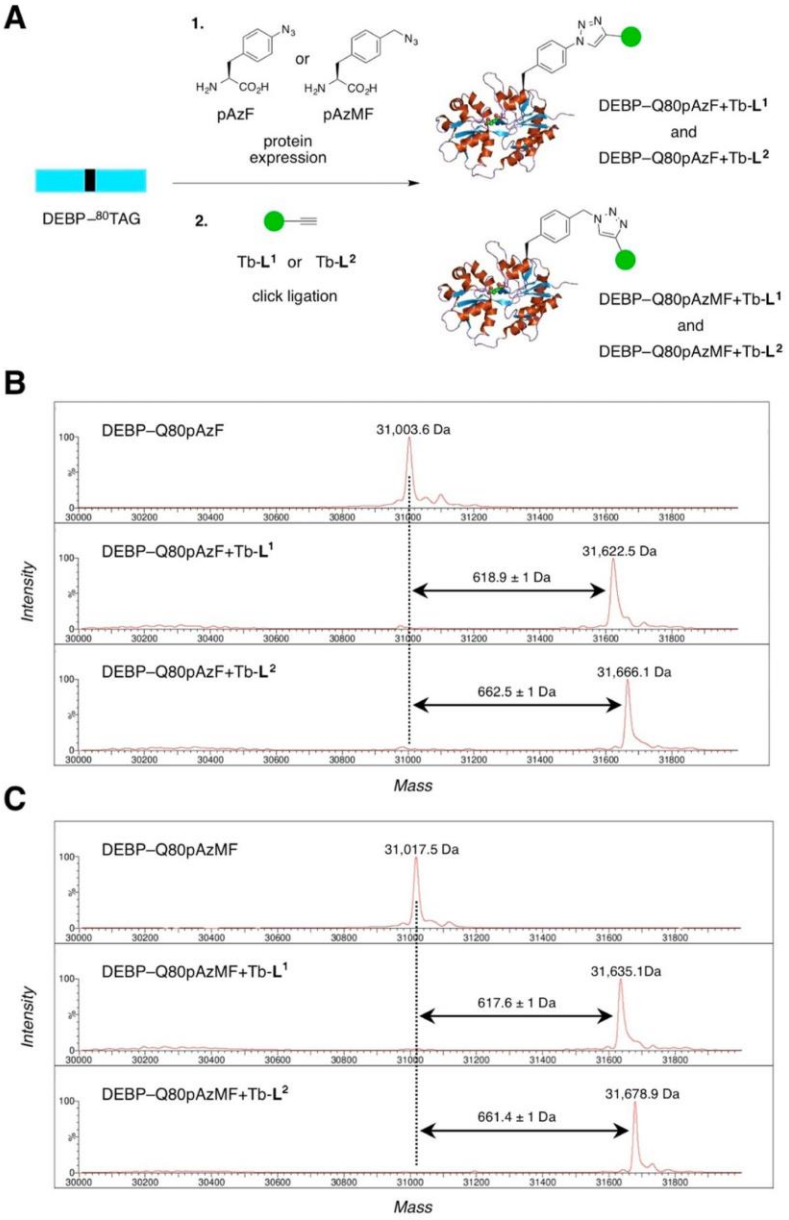

Figure 4. (A) Genetically encoded incorporation of pAzF or pAzMF into DEBP, in response to an amber stop codon (TAG) at position 80, and subsequent click ligation with Tb-**L**^{1} and Tb-**L**^{2}. (B) MS analysis of DEBP-Q80AzF shows a single major signal at 31 003.6 Da. Reaction of DEBP-Q80AzF with Tb-**L**^{1} (Tb-**L**^{2}) shows a single major signal at 31 622.5 Da (31 666.1 Da), consistent with the expected mass increase of 618.1 Da (662.1 Da) from selective reaction with Tb-**L**^{1} (Tb-**L**^{2}). (C) MS analysis of DEBP-Q80AzMF shows a single major signal at 31 017.5 Da. Reaction of DEBP-Q80AzMF with Tb-**L**^{1} (Tb-**L**^{2}) shows a single major signal at 31 635.1 Da (31 678.9 Da), again consistent with the expected mass increase from selective reaction with Tb-**L**^{1} (Tb-**L**^{2}).

■ EXPERIMENTAL SECTION

Materials and Methods. All chemicals were purchased from Sigma-Aldrich Pty, Matrix Scientific, or Merck Group Ltd. and used without purification. 1,4,7,10-Tetraazacyclododecane-1,4,7-triacetic acid (^{t}Bu$_3$DO$_3$A·HBr)[41] diethyl 4-bromopyridine-2,6-dicarboxylate (**4**),[42] tris(3-hydroxypropyl-triazolylmethyl)amine (THTPA),[46,47] 2-[4-({bis[(1-*tert*-butyl-1*H*-1,2,3-triazol-4-yl)methyl]amino}-methyl)-1*H*-1,2,3-triazol-1-yl]acetic acid) (BTTAA),[57] *p*-azido-L-phenylalanine (pAzF)[54] and *p*-(azidomethyl)-L-phenylalanine (pAzMF)[55] were synthesized as per reported literature procedures. All solvents were reagent grade. Flash chromatography was performed using Merck 38 Silica gel 60, 230−400 mesh ASTM. Thin layer chromatography (TLC) was performed on Merck Silica Gel 60 F254 plates. TLC plates were visualized using a UV lamp at 254 nm or through the use of $KMnO_4$ or ninhydrin staining agent. ^{1}H and ^{13}C nuclear magnetic resonance (NMR) spectra were recorded using an Avance III Nanobay 400 MHz Bruker spectrometer coupled to the BACS 60 automatic sample changer at 400.13 and 100.61 MHz, respectively. Data acquisition and processing was managed using Topspin software package version 3. Additional processing was handled with

DOI: 10.1021/acs.inorgchem.5b02605
Inorg. Chem. XXXX, XXX, XXX−XXX

MestReNova software (PC). Chemical shifts (δ) were measured in parts per million referenced to an internal standard of residual solvent. Spectroscopic data are given using the following abbreviations: s, singlet; d, doublet; app. t, apparent triplet; q, quartet; m, multiplet; br, broad; *J*, coupling constant. Elemental analyses were performed by the Campbell Microanalytical Laboratory, Otago, New Zealand. Analytical high-performance liquid chromatography (HPLC) was performed on an Agilent 1260 series modular HPLC equipped with the following modules: G1312B binary pump, G1316A thermostated column compartment equipped with an Agilent Eclipse Plus C18 3.5 μm, 4.6 × 100 mm column and a G1312B diode array detector. The following elution protocol was used: 0−10 min, gradient from 5% solvent B/95% solvent A to 100% solvent B (solvent A = 99.9% H_2O, 0.1% TFA, and solvent B = 99.9% MeCN, 0.1% TFA, except in the case of analysis of the LLCs, where solvent A = 99.9% H_2O, 0.1% formic acid, and solvent B = 99.9% MeCN, 0.1% formic acid); flow rate = 1 mL min^{-1}. Preparative HPLC purification was performed on an Agilent 1260 modular Prep HPLC equipped with the following modules: G1361A prep pump, G2260A prep automatic liquid sampler, G1364B fraction collector, G1315D diode array detector, and a Luna C8 5 μm, 100 Å AXIA, 250 × 21.2 mm column. The following elution protocol was used: 0−5 min, 100% solvent C; 5−30 min, gradient from 100% solvent C to 20% solvent C/80% solvent D (solvent C = 99.9% H_2O, 0.1% formic acid, and solvent D = 99.9% MeCN, 0.1% formic acid); flow rate = 20 mL min^{-1}. Reversed-phase silica dry column vacuum chromatography (RP-DCVC) was performed using reversed-phase silica (C18 bonded, 10 μm, 60 Å) purchased from Grace Davison and loaded into a sintered Buchner funnel (50 × 50 mm ID). Elution was performed with 100% solvent C (200 mL), followed by a 5% incremental stepwise gradient from 0 to 80% solvent D (50 mL of each solvent C/D mixture). Fractions were collected under vacuum into a separating funnel and then into test tubes. Collected fractions were analyzed by analytical HPLC. Liquid chromatography-mass spectrometry (LC-MS) was performed using an Agilent 6100 Series Single Quad LC-MS coupled to an Agilent 1200 Series HPLC with the following mass spectrometry conditions: multimode electrospray ionization (ESI) mode, 300 °C drying gas temperature, 200 °C vaporizing temperature, capillary voltage of 2000 V (positive), capillary voltage of 4000 V (negative), scan range between 100−1000 *m*/*z* with an 0.1 second step size and a 10 min acquisition time. High-resolution mass spectrometric (HRMS) analyses were performed on a Waters LCT TOF LC-MS mass spectrometer coupled to a 2795 Alliance Separations module. All data were acquired and mass corrected via a dual-spray Leucine Enkephaline reference sample. Mass spectra were generated by averaging the scans across each peak and background subtraction of the TIC. Acquisition and analysis were performed using the MassLynx software version 4.1. The mass spectrometer conditions were as follows: ESI mode, desolvation gas flow of 550 L h^{-1}, desolvation temperature of 250 °C, source temperature of 110 °C, capillary voltage of 2400 V, sample cone voltage of 60 V, scan range acquired between 100−1500 *m*/*z*, one second scan times, and internal reference ions for positive ion mode (Leucine Enkephaline) of 556.2771. Protein mass spectrometry was performed on a Waters LCT Premier XE mass spectrometer. The mass spectrometer conditions were as follows: ES+ polarity, capillary voltage of 1000−4500 V, sample cone voltage of 50−200 V, desolvation gas flow of 450 L h^{-1}, desolvation temperature of 150 °C and source temperature of 80 °C. Acquisition and analysis were performed using the MassLynx software version 4.1. Absorbance spectra were recorded on a Varian Cary 50 Bio UV−vis spectrophotometer using a 1 cm path length quartz cuvette. Luminescence emission spectra were acquired using a Varian Cary Eclipse fluorescence spectrophotometer using a 1 cm path length quartz cuvette and the following settings: phosphorescence mode, total decay time = 0.02 s, number of flashes = 1, delay time = 0.1 ms, gate time = 5 ms, excitation slit width = 1 nm, emission slit width = 1 nm, data interval = 1 nm, averaging time = 0.015 s.

Syntheses. *(6-((Trimethylsilyl)ethynyl)pyridin-2-yl)methanol (**2**).* (6-Bromo-2-pyridinyl)methanol (**1**) (4.00 g, 21.2 mmol), TMS acetylene (4.42 mL, 31.9 mmol), $Pd(PPh_3)_2Cl_2$ (746 mg, 1.06 mmol), CuI (405 mg, 2.13 mmol), and Et_3N (5.7 g, 8.9 mL, 64 mmol) were dissolved in dry THF (50 mL) and stirred at room temperature (RT) for 2 h under a N_2 atmosphere. The solution was combined with H_2O (100 mL) and extracted with EtOAc (2 × 100 mL). The combined extracts were dried over $MgSO_4$ and evaporated in vacuo to produce a dark brown crude solid, which was subjected to silica gel chromatography (30% EtOAc in petroleum spirits) to yield the product as an off-white solid (R_f = 0.2). Yield: 3.30 g, 75%. ^{1}H NMR ($CDCl_3$) δ 7.63 (t, *J* = 7.8 Hz, 1H), 7.36 (d, *J* = 7.6 Hz, 1H), 7.23 (d, *J* = 7.8 Hz, 1H), 4.73 (s, 2H), 0.27 (s, 9H). ^{13}C NMR ($CDCl_3$) δ 159.92, 142.07, 136.88, 126.27, 120.11, 103.58, 95.37, 64.51, −0.15. HRMS (ESI): *m*/*z* calcd for $[M + H]^+$, M = $C_{11}H_{15}NOSi$: 206.0996, found: 206.0993. Analytical HPLC: 99% purity (254 nm).

*2-(Bromomethyl)-6-((trimethylsilyl)ethynyl)pyridine (**3**).* *N*,*N*-Diisopropylethylamine (DIPEA; 1.35 mL, 7.79 mmol) was added to an ice-cooled solution of **2** (800 mg, 3.90 mmol) in dichloromethane (DCM; 25 mL) under N_2. With rapid stirring, methanesulfonyl chloride (MsCl) (669 mg, 452 μL, 5.84 mmol) was then added in a dropwise fashion. The mixture was stirred for 30 min at RT, washed with H_2O (2 × 25 mL), and dried over $MgSO_4$, and the solvent was removed in vacuo to yield the product as a brown solid. Yield: 1.05 g, 96%. ^{1}H NMR ($CDCl_3$) δ 7.73 (app. t, *J* = 7.8 Hz, 1H), 7.45 (d, *J* = 7.8 Hz, 1H), 7.44 (d, *J* = 7.8 Hz, 1H), 5.32 (s, 2H), 3.09 (s, 3H), 0.26 (s, 9H). ^{13}C NMR ($CDCl_3$) δ 154.43, 142.98, 137.85, 127.69, 121.90, 103.02, 96.71, 71.30, 38.32, 0.00. HRMS (ESI): *m*/*z* calcd for $[M + H]^+$, M = $C_{12}H_{17}NO_3SSi$: 284.0771, found: 284.0765. Analytical HPLC: 92% purity (254 nm).

*2,2′,2″-(10-((5-Ethynylpyridin-3-yl)methyl)-1,4,7,10-tetraazacyclododecane-1,4,7-triyl)triacetic acid (H_3**L**^{1}).* Compound **3** (500 mg, 1.86 mmol), ^{t}Bu$_3$DO$_3$A·HBr[41] (740 mg, 1.24 mmol), and DIPEA (321 mg, 740 μL, 2.49 mmol) were dissolved in MeCN (10 mL), and the solution was refluxed overnight (O/N). The solvent was then removed in vacuo, and the residue was subjected to silica gel chromatography (5% MeOH in DCM) to separate the coupled intermediate product (R_f = 0.3) as a glassy yellow solid. Yield: 350 mg, 40%. LC-MS (ESI): *m*/*z* 702.6 $[M + H]^+$ (100%). To remove the TMS protecting group, this compound (700 mg, 1.00 mmol) was dissolved in a mixture of 1 M aqueous KF (1.50 mL, 1.50 mmol) and MeCN (10 mL), and the solution was stirred for 2 h at RT. The solvent was then removed in vacuo, the resulting yellow residue redissolved in water (10 mL), and the TMS-deprotected product was extracted into DCM (2 × 10 mL). After it was dried over $MgSO_4$, the solvent was removed in vacuo to yield an amber glass solid. Yield: 560 mg, 89%. LC-MS (ESI): *m*/*z* 630.50 $[M + H]^+$ (100%). Removal of the ^{t}Bu groups was then affected by dissolving this compound (550 mg, 0.87 mmol) in a 1:1 (v/v) mixture of TFA/DCM (5 mL) and stirring at RT O/N. Removal of the bulk of the TFA/DCM under a stream of N_2 produced a thick oily brown residue that was subjected to RP-DCVC to yield the product as a fluffy white solid after lyophilization. Yield: 260 mg, 64% (23% over three steps). ^{1}H NMR (MeOD) δ 7.81 (app. t, *J* = 7.8 Hz, 1H), 7.64 (d, *J* = 7.8 Hz, 1H), 7.53 (d, *J* = 7.7 Hz, 1H), 4.40 (br, s 2H), 4.40−3.56 (br, 6H), 3.76 (s, 1H), 3.56−2.83 (br, 16 H). ^{13}C NMR (MeOD) δ 161.96, 161.61, 161.27, 160.93, 141.84, 138.27, 127.27, 124.59, 121.16, 118.25, 115.34, 112.43, 81.61, 79.04, 57.49, 54.02, 53.29, 50.66−49.11 (br set of signals). HRMS (ESI): *m*/*z* calcd for $[M + H]^+$, M = $C_{22}H_{31}N_5O_6$: 462.2353, found: 462.2357. Analytical HPLC: 97% purity (254 nm).

*Ethyl 4-bromo-6-(hydroxymethyl)picolinate (**5**).* To a refluxing solution of diethyl 4-bromopyridine-2,6-dicarboxylate (**4**)[42] (10.00 g, 33.10 mmol) in EtOH (150 mL) was added $NaBH_4$ (250 mg, 6.62 mmol). After 15 min, the mixture was analyzed by TLC (30% EtOAc in petroleum spirits) to assess the extent of consumption of **4** (product R_f = 0.4). Further portions of $NaBH_4$ (250 mg, 6.62 mmol) were added until **4** had been completely consumed, after which point the reaction was quenched with acetone (20 mL), and the solvent was removed in vacuo. The resulting off-white solid was redissolved in EtOAc (100 mL) and washed with water (2 × 100 mL). The organic layer was then dried over $MgSO_4$, and the solvent was removed in vacuo to yield the product as a white solid. Yield: 4.14 g, 48%. ^{1}H NMR ($CDCl_3$) δ 8.10 (d, *J* = 1.6 Hz, 1H), 7.75 (d, *J* = 1.7 Hz, 1H),

DOI: 10.1021/acs.inorgchem.5b02605
Inorg. Chem. XXXX, XXX, XXX−XXX

```
MHHHHHHMEN LYFQGMAAGS TLDKIAKNGV IVVGHRESSV PFSYYDNQQK VVGYSQDYSN  60
AIVEAVKKKL NKPDLQVKLI PITSQNRIPL LQNGTFDFEC GSTTNNVERQ KQAAFSDTIF 120
VVGTRLLTKK GGDIKDFANL KDKAVVVTSG TTSEVLLNKL NEEQKMNMRI ISAKDHGDSF 180
RTLESGRAVA FMMDDALLAG ERAKAKKPDN WEIVGKPQSQ EAYGCMLRKD DPQFKKLMDD 240
TIAQVQTSGE AEKWFDKWFK NPIPPKNLNM NFELSDEMKA LFKEPNDKAL N          291
```

Figure 5. Amino acid sequence of the DEBP construct used. The TEV cleavage site is underlined. The location of the amber stop mutation introduced for site-specific incorporation of unnatural amino acids is shaded in gray.

4.82 (s, 2H), 4.42 (q, J = 7.1 Hz, 2H), 3.92 (s, 1H), 1.39 (t, J = 7.1 Hz, 3H). ^{13}C NMR ($CDCl_3$) δ 164.03, 162.33, 148.29, 134.54, 127.16, 127.07, 64.44, 62.45, 14.31. HRMS (ESI): m/z calcd for $[M + H]^+$, M = $C_9H_{10}NO_3Br$: 259.9917, found: 259.9913. Analytical HPLC: 91% purity (254 nm).

*Ethyl 6-(hydroxymethyl)-4-((trimethylsilyl)ethynyl)picolinate (**6**).* Compound **5** (4.00 g, 15.4 mmol), TMS acetylene (2.29 g, 3.20 mL, 23.1 mmol), $Pd(PPh_3)_2Cl_2$ (540 mg, 0.77 mmol), CuI (293 mg, 1.54 mmol), and Et_3N (4.67 g, 6.43 mL, 46.1 mmol) were dissolved in dry THF (100 mL) and stirred at RT for 2 h under a N_2 atmosphere. The solvent was then removed in vacuo to give a black solid, which was subjected to silica gel chromatography (50% EtOAc in petroleum spirits) to yield the product as a viscous orange oil (R_f = 0.5). Yield: 3.63 g, 85%. ^{1}H NMR ($CDCl_3$) δ 7.95 (d, J = 1.3 Hz, 1H), 7.54 (d, J = 1.3 Hz, 1H), 4.80 (s, 2H), 4.40 (q, J = 7.1 Hz, 2H), 1.38 (t, J = 7.1 Hz, 3H), 0.23 (s, 9H). ^{13}C NMR ($CDCl_3$) δ 164.98, 161.13, 147.69, 133.55, 126.30, 101.99, 101.64, 64.85, 62.52, 14.66, 0.00. HRMS (ESI): m/z calcd for $[M + H]^+$, M = $C_{14}H_{19}NO_3Si$: 278.1207, found: 278.1195. Analytical HPLC: 93% purity (254 nm).

*Ethyl 6-(bromomethyl)-4-((trimethylsilyl)ethynyl)picolinate (**7**).* DIPEA (931 mg, 1.26 mL, 7.22 mmol) was added to an ice-cooled, N_2-blanketed solution of **6** (1.10 g, 3.61 mmol) dissolved in DCM (50 mL). With rapid stirring, MsCl (783 mg, 592 μL, 5.42 mmol) was then added in a dropwise fashion. The mixture was stirred for 30 min at RT, washed with H_2O (2 × 50 mL), and dried over $MgSO_4$, and the solvent was removed in vacuo to yield the product as a yellow oil (1.28 g, quantitative). ^{1}H NMR ($CDCl_3$) δ 8.08 (d, J = 1.4 Hz, 1H), 7.65 (d, J = 1.4 Hz, 1H), 5.40 (s, 2H), 4.49 (A of AB quartet, J = 7.1 Hz, 1H), 4.45 (B of AB quartet, J = 7.1 Hz, 1H), 3.17 (s, 3H), 1.43 (t, J = 7.1 Hz, 3H), 0.28 (s, 9H). ^{13}C NMR ($CDCl_3$) δ 164.29, 154.76, 148.28, 134.10, 127.18, 126.98, 103.04, 100.80, 70.71, 62.44, 38.25, 14.41, −0.30. HRMS (ESI): m/z calcd for $[M + H]^+$, M = $C_{15}H_{21}NO_5SSi$: 356.0982, found: 356.0966. Analytical HPLC: 91% purity (254 nm).

*2,2′,2″-(10-((6-Carboxy-4-ethynylpyridin-2-yl)methyl)-1,4,7,10-tetraazacyclododecane-1,4,7-triyl)triacetic acid (**H_4L^2**).* Compound **7** (300 mg, 0.88 mmol), ^{t}Bu$_3$DO$_3$A·HBr (350 mg, 0.59 mmol), and DIPEA (152 mg, 204 μL, 1.18 mmol) were dissolved in MeCN (10 mL), and the solution was refluxed O/N. The solvent was then removed in vacuo, and the residue was subjected to silica gel chromatography (5% MeOH in DCM) to separate the coupled intermediate product (R_f = 0.2) as a glassy yellow solid. Yield: 290 mg, 63%. LC-MS (ESI): m/z 774.52 $[M + H]^+$ (100%). To remove the TMS protecting group and hydrolyze the ethyl ester, this compound (250 mg, 0.32 mmol) was dissolved in a mixture of 1,4-dioxane (5 mL) and 1 M NaOH (1.29 mL, 1.29 mmol), and the solution was stirred for 3 h at RT. The solvent was then removed in vacuo, and the oily yellow residue was stirred in a 1:1 (v/v) mixture of TFA/DCM (5 mL) at RT O/N to remove the ^{t}Bu groups. Removal of the bulk of the TFA/DCM under a stream of N_2 produced a thick oily brown residue that was subjected to RP-DCVC to yield the product as a white solid after lyophilization. Yield: 95 mg, 44%. ^{1}H NMR (MeOD) δ 8.09 (d, J = 1.1 Hz, 1H), 7.81 (d, J = 1.2 Hz, 1H), 4.40 (br s, 2H), 4.07 (s, 1H), 3.92−3.69 (br, 6H), 3.64−2.96 (br, 16H). ^{13}C NMR (MeOD) δ 167.25, 149.55, 134.58, 131.15, 128.06, 119.64, 116.73, 85.95, 80.95, 57.83, 55.19, 54.60, 51.09. HRMS (ESI): m/z calcd for $[M + H]^+$, M = $C_{23}H_{31}N_5O_8$: 506.2251, found: 506.2259. Analytical HPLC: 98% purity (254 nm).

*Tb-**L^1**.* Ligand H_3**L^1** (40 mg, 79 μmol) and $Tb(OTf)_3$ (72 mg, 120 μmol) were dissolved in Milli-Q H_2O (5 mL), and the pH was adjusted to 8−9 with 2 M NaOH. The stirred mixture was heated at 90 °C for 2 h, after which time LC-MS analysis showed near-quantitative complexation. After the pH was adjusted to near-neutral with 2 M HCl, RP-DCVC was used to separate the product, which was isolated as a white solid after lyophilization. Yield: 40 mg, 57%. Anal. Calcd for $[C_{22}H_{28}N_5O_6Tb].5H_2O$: C, 37.35; H, 5.41; N, 9.90. Found: C, 37.48; H, 5.36; N, 9.69%. HRMS (ESI): m/z calcd for $[M + H]^+$, M = $C_{22}H_{28}N_5O_6Tb$: 618.1371, found: 618.1381. Analytical HPLC: 95% purity (254 nm).

*Tb-**L^2** (H^+ counterion).* This complex was prepared in the same fashion as Tb-**L^1** from H_4**L^2** (100 mg, 217 μmol) and $Tb(OTf)_3$ (197 mg, 325 μmol). Yield: 66 mg, 49%. Anal. Calcd for H-$[C_{23}H_{27}N_5O_8Tb]$·TFA·$4H_2O$: C, 35.43; H, 4.40; N, 8.26. Found: C, 35.47; H, 4.41; N, 8.57%. HRMS (ESI): m/z calcd for $[M + 2H]^+$, M = $C_{23}H_{27}N_5O_8Tb$: 662.1270, found: 662.1277. Analytical HPLC: 96% purity (254 nm).

*Clicked Tb-**L^1**.* Ligand H_3**L^1** (30 mg, 65 μmol) and $Tb(OTf)_3$ (59 mg, 97 μmol) were dissolved in Milli Q water (5 mL), and the pH was adjusted to 8−9 with 2 M NaOH. After the pH was adjusted to near-neutral with 2 M HCl, 3-azidopropan-1-ol (7.9 mg, 78 μmol), sodium ascorbate (6.4 mg, 32 μmol), $CuSO_4$ (1.0 mg, 6.5 μmol), and THPTA[46,47] (5.6 mg, 13 μmol) were added, and the mixture was stirred at RT O/N, after which time LC-MS analysis showed near-quantitative click ligation. RP-DCVC was used to separate the product, which was isolated as a white solid after lyophilization. Yield: 11 mg, 22%. Anal. Calcd for $[C_{25}H_{35}N_8O_7Tb]$·$4H_2O$: C, 37.98; H, 5.48; N, 14.17. Found: C, 37.89; H, 5.20; N, 14.12%. HRMS (ESI): m/z calcd for $[M + H]^+$, M = $C_{25}H_{35}N_8O_7Tb$: 719.1960, found: 719.1970. Analytical HPLC: 98% purity (254 nm).

*Clicked Tb-**L^2** (H^+ counterion).* This complex was prepared in the same fashion as the clicked Tb-**L^1** complex from H_4**L^2** (30 mg, 60 μmol), $Tb(OTf)_3$ (55 mg, 90 μmol), 3-azidopropan-1-ol (7.9 mg, 78 μmol), sodium ascorbate (6.4 mg, 32 μmol), $CuSO_4$ (1.0 mg, 6.5 μmol), and THPTA (5.6 mg, 13 μmol). Yield: 17 mg, 37%. Anal. Calcd for $H[C_{26}H_{34}N_8O_9Tb]$·$4H_2O$: C, 37.42; H, 5.19; N, 13.43. Found: C, 37.20; H, 5.09; N, 13.51%. HRMS (ESI): m/z calcd for $[M + 2H]^+$, M = $C_{26}H_{34}N_8O_9Tb$: 763.1859, found: 763.1870. Analytical HPLC: 96% purity (254 nm).

Quantum Yield Determinations. Complexes were prepared at a range on concentrations in a 100 mM HEPES buffer at pH 7.4, and absorbance and luminescence emission spectra were recorded. Quantum yields (Φ) were then determined, using quinine sulfate in 0.1 M sulfuric acid as the reference compound (Φ = 54%),[48] according to the following equation:

$$\Phi_X = \Phi_{ST} \times (\mathrm{Grad}_x/\mathrm{Grad}_{ST}) \times (\eta_X/\eta_{ST})^2$$

where Φ is the quantum yield, X and ST denote the sample and reference, respectively, Grad is the gradient of the integrated luminescence versus absorbance plot, and η represents the refractive index of the solvent.

Protein Synthesis. The wild-type gene of the *E. coli* aspartate/glutamate-binding protein (DEBP)[53] without periplasmic leader sequence was cloned into the pETMCSIII vector[58] with an N-terminal His_6 tag followed by a tobacco etch virus (TEV) protease recognition site (Figure 5). DEBP-containing pAzF[54] or pAzMF[55] at position Q80 were produced from PCR-amplified DNA by cell-free

DOI: 10.1021/acs.inorgchem.5b02605
Inorg. Chem. XXXX, XXX, XXX−XXX

protein synthesis using RF1-depleted S30 extract, using established protocols.[56]

For the cell-free reactions, the final concentrations were 0.5 mg mL^{-1} total tRNA containing optimized suppressor tRNA[59] (inner buffer), 50 mM *p*-cyano-L-phenylalanine-specific aminoacyl-tRNA synthetase (*p*CNF-RS)[54] (inner buffer) and 1 mM of the unnatural amino acid (inner and outer buffer). DEBP Q80AzF and DEBP Q80AzMF were produced from linear PCR-amplified double-stranded DNA with eight-nucleotide single-stranded overhangs containing an amber stop codon at position Q80.[54a] All cell-free reactions were incubated at 30 °C for 16 h.

Protein Purification. The synthesized proteins were purified using a 1 mL Ni-NTA column (GE Healthcare, USA) according to the manufacturer's protocol. Subsequently, the N-terminal His_6 tag was removed by treating the purified proteins with His_6-tagged TEV protease[60] at 4 °C for 16 h in a buffer of 25 mM Tris-HCl, pH 8, 500 mM sodium chloride, and 2 mM 2-mercaptoethanol. The cleaved proteins were separated from the His_6 tag and TEV protease by running the solution again over a Ni-NTA column and then dialyzed against click buffer (50 mM sodium phosphate, 150 mM sodium chloride, pH 8) at 4 °C. Finally, DEBP-Q80AzF and DEBP-Q80AzMF were concentrated using an Amicon ultrafiltration centrifugal tube with a molecular weight cutoff (MWCO) of 10 kDa.

Protein Conjugation. The solutions of mutant protein in click buffer (50 mM sodium phosphate, pH 8, 150 mM sodium chloride) were added to solutions of the tag, followed by addition of a premixed solution of $CuSO_4$ and BTTAA,[57] aminoguanidine, glycerol, and finally ascorbic acid, to yield a total reaction volume of 0.5 mL. The final concentrations were 0.05 mM protein, 0.5 mM tag, 0.3 mM $CuSO_4$, 1.5 mM BTTAA, 5 mM aminoguanidine, 0.5 mM glycerol, and 5 mM ascorbic acid.[37] The reaction was performed in a glovebox under N_2 atmosphere at room temperature with stirring for 16 h. The reaction was terminated by the addition of EDTA to a final concentration of 2 mM and stirring for 30 min in air. The buffer was exchanged to 50 mM sodium phosphate, pH 7, and concentrated by ultrafiltration using an Amicon centrifugal filter tube (10 kDa MWCO). The incorporation of pAzF and pAzMF into DEBP and the products of the click reactions were confirmed by mass spectrometry.

■ ASSOCIATED CONTENT

Supporting Information

The Supporting Information is available free of charge on the ACS Publications website at DOI: 10.1021/acs.inorgchem.5b02605.

Luminescence lifetime measurements, luminescence data for labeled protein samples, NMR spectral data of reported compounds, and LC traces for ligands, complexes, and peptide conjugates. (PDF)

■ AUTHOR INFORMATION

Corresponding Authors

*Phone: +61 3 9905 4510. Fax: +61 3 9905 4597. E-mail: kellie.tuck@monash.edu. Web: kellietuckgroup.com. (K.L.T.)

*Phone: +61 3 9903 9706. Fax: +61 3 9903 9582. E-mail: bim.graham@monash.edu. Web: bimgrahamgroup.com. (B.G.)

Notes

The authors declare no competing financial interest.

■ ACKNOWLEDGMENTS

Financial support by the Australian Research Council (DP120100561 and DP150100383 to B.G. and G.O., FT130100838 to B.G., and DP130100816 to L.S.), the Swiss National Science Foundation (Professorship Nos. PP00P2_133568 and PP00P2_157545 to G.G.), the Stiftung für wissenschaftliche Forschung of the Univ. of Zurich (G.G.), the UBS Promedica Stiftung (R.R. and G.G.), the Novartis Jubilee Foundation (R.R. and G.G.), and the Univ. of Zurich (G.G.) is gratefully acknowledged. The authors thank the Center for Microscopy and Image Analysis of the Univ. of Zurich for access to state-of-the-art equipment.

■ REFERENCES

(1) Ozawa, L.; Itoh, M. *Chem. Rev.* **2003**, *103*, 3835−3856.
(2) Selvin, P. R. *Annu. Rev. Biophys. Biomol. Struct.* **2002**, *31*, 275−302.
(3) Bünzli, J.-C. G.; Piguet, C. *Chem. Soc. Rev.* **2005**, *34*, 1048−1077.
(4) Hemmilä, I.; Laitala, V. *J. Fluoresc.* **2005**, *15*, 529−542.
(5) Montgomery, C. P.; Murray, B. S.; New, E. J.; Pal, R.; Parker, D. *Acc. Chem. Res.* **2009**, *42*, 925−937.
(6) Moore, E. G.; Samuel, A. P. S.; Raymond, K. N. *Acc. Chem. Res.* **2009**, *42*, 542−552.
(7) Thibon, A.; Pierre, V. C. *Anal. Bioanal. Chem.* **2009**, *394*, 107−120.
(8) Bünzli, J.-C. G. *Chem. Rev.* **2010**, *110*, 2729−2755.
(9) Zwier, J. M.; Bazin, H.; Lamarque, L.; Mathis, G. *Inorg. Chem.* **2014**, *53*, 1854−1866.
(10) Heffern, M. C.; Matosziuk, L. M.; Meade, T. J. *Chem. Rev.* **2014**, *114*, 4496−4539.
(11) Amoroso, A. J.; Pope, S. J. A. *Chem. Soc. Rev.* **2015**, *44*, 4723−4772.
(12) Werts, M. H. *Sci. Prog.* **2005**, *88*, 101−131.
(13) Leonard, J. P.; Nolan, C. B.; Stomeo, F.; Gunnlaugsson, T. *Top. Curr. Chem.* **2007**, *281*, 1−43.
(14) Bünzli, J.-C. G.; Eliseeva, S. V. Lanthanide Luminescence: Photophysical, Analytical and Biological Aspects. In *Springer Series on Fluorescence;* Hänninen, P., Härmä, H., Eds.; Springer Verlag: Berlin, Germany, 2011; Vol. *7*, pp 1−46.
(15) Hemmilä, I. *J. Biomol. Screening* **1999**, *4*, 303−307.
(16) Mathis, G. *J. Biomol. Screening* **1999**, *4*, 309−313.
(17) See, for example, (a) Heyduk, E.; Heyduk, T. *Anal. Biochem.* **1997**, *248*, 216−227. (b) Weibel, N.; Charbonnière, L. J.; Guardigli, M.; Roda, A.; Ziessel, R. *J. Am. Chem. Soc.* **2004**, *126*, 4888−4896. (c) Ge, P.; Selvin, P. R. *Bioconjugate Chem.* **2008**, *19*, 1105−1111. (d) Hovinen, J.; Guy, P. M. *Bioconjugate Chem.* **2009**, *20*, 404−421. (e) Starck, M.; Kadjane, P.; Bois, E.; Darbouret, B.; Incamps, A.; Ziessel, R.; Charbonnière, L. J. *Chem. - Eur. J.* **2011**, *17*, 9164−9179. (f) Xu, J.; Corneillie, T. M.; Moore, E. G.; Law, G.-L.; Butlin, N. G.; Raymond, K. N. *J. Am. Chem. Soc.* **2011**, *133*, 19900−19910.
(18) (a) MacManus, J. P.; Hogue, C. W.; Marsden, B. J.; Sikorska, M.; Szabo, A. G. *J. Biol. Chem.* **1990**, *265*, 10358−10366. (b) Nitz, M.; Franz, K. J.; Maglathlin, R. L.; Imperiali, B. *ChemBioChem* **2003**, *4*, 272−276. (c) Nitz, M.; Sherawat, M.; Franz, K. J.; Peisach, E.; Allen, K. N.; Imperiali, B. *Angew. Chem., Int. Ed.* **2004**, *43*, 3682−3685. (d) Ancel, L.; Niedzwiecka, A.; Lebrun, C.; Gateau, C.; Delangle, P. C. *R. Chim.* **2013**, *16*, 515−523. (e) Pazos, E.; Vázquez, M. E. *Biotechnol. J.* **2014**, *9*, 241−252.
(19) (a) Maurel, D.; Comps-Agrar, L.; Brock, C.; Rives, M.-L.; Bourrier, E.; Ayoub, M. A.; Bazin, H.; Tinel, N.; Durroux, T.; Prézeau, L.; Trinquet, E.; Pin, J.-P. *Nat. Methods* **2008**, *5*, 561−567. (b) Comps-Agrar, L.; Maurel, D.; Rondard, P.; Pin, J.-P.; Trinquet, E.; Prézeau, L. *Methods Mol. Biol.* **2011**, *756*, 201−214.
(20) Hovinen, J. *Chem. Biodiversity* **2006**, *3*, 296−303.
(21) Ketola, J.; Jaakkola, L.; Hovinen, J. *Lett. Org. Chem.* **2008**, *5*, 444−449.
(22) Candelon, N.; Hadade, N. D.; Matache, M.; Canet, J.-L.; Cisnetti, F.; Funeriu, D. P.; Nauton, L.; Gautier, A. *Chem. Commun.* **2013**, *49*, 9206−9208.
(23) Kolb, H. C.; Finn, M. G.; Sharpless, K. B. *Angew. Chem., Int. Ed.* **2001**, *40*, 2004−2021.
(24) Baskin, J. M.; Prescher, J. A.; Laughlin, S. T.; Agard, N. J.; Chang, P. V.; Miller, I. A.; Lo, A.; Codelli, J. A.; Bertozzi, C. R. *Proc. Natl. Acad. Sci. U. S. A.* **2007**, *104*, 16793−16797.
(25) Jewett, J. C.; Bertozzi, C. R. *Chem. Soc. Rev.* **2010**, *39*, 1272−1279.

DOI: 10.1021/acs.inorgchem.5b02605
Inorg. Chem. XXXX, XXX, XXX−XXX

(26) Hodgson, D. R. W.; Sanderson, J. M. *Chem. Soc. Rev.* **2004**, *33*, 422−430.
(27) van Swieten, P. F.; Leeuwenburgh, M. A.; Kessler, B. M.; Overkleeft, H. S. *Org. Biomol. Chem.* **2005**, *3*, 20−27.
(28) Prescher, J. A.; Bertozzi, C. R. *Nat. Chem. Biol.* **2005**, *1*, 13−21.
(29) Zhang, G.; Zheng, S.; Liu, H.; Chen, P. R. *Chem. Soc. Rev.* **2015**, *44*, 3405−3417.
(30) Liu, C. C.; Schultz, P. G. *Annu. Rev. Biochem.* **2010**, *79*, 413−444.
(31) Lang, K.; Chin, J. W. *Chem. Rev.* **2014**, *114*, 4764−4806.
(32) Viguier, R. F. H.; Hulme, A. N. *J. Am. Chem. Soc.* **2006**, *128*, 11370−11371.
(33) Jauregui, M.; Perry, W. S.; Allain, C.; Vidler, L. R.; Willis, M. C.; Kenwright, A. M.; Snaith, J. S.; Stasiuk, G. J.; Lowe, M. P.; Faulkner, S. *Dalton Trans.* **2009**, *32*, 6283−6285.
(34) Do-Thanh, C.-L.; Rowland, M. M.; Best, M. D. *Tetrahedron* **2011**, *67*, 3803−3808.
(35) Szíjjártó, C.; Pershagen, E.; Borbas, K. E. *Dalton Trans.* **2012**, *41*, 7660−7669.
(36) Molloy, J. K.; Kotova, O.; Peacock, R. D.; Gunnlaugsson, T. *Org. Biomol. Chem.* **2012**, *10*, 314−322.
(37) Loh, C.-T.; Ozawa, K.; Tuck, K. L. T.; Barlow, N.; Huber, T.; Otting, G.; Graham, B. *Bioconjugate Chem.* **2013**, *24*, 260−268.
(38) Loh, C.-T.; Graham, B.; Abdelkader, E. H.; Tuck, K. L.; Otting, G. *Chem. - Eur. J.* **2015**, *21*, 5084−5092.
(39) Abdelkader, E. H.; Feintuch, A.; Yao, X.; Adams, L. A.; Aurelio, L.; Graham, B.; Goldfarb, D.; Otting, G. *Chem. Commun.* **2015**, *51*, 15898−15901.
(40) D'Amora, A.; Fanfoni, L.; Cozzula, D.; Guidolin, N.; Zangrando, E.; Felluga, F.; Gladiali, S.; Benedetti, F.; Milani, B. *Organometallics* **2010**, *29*, 4472−4485.
(41) Raghunand, N.; Guntle, G. P.; Gokhale, V.; Nichol, G. S.; Mash, E. A.; Jagadish, B. *J. Med. Chem.* **2010**, *53*, 6747−6757.
(42) Wang, Y.; Cooper, C. G. F.; Luisi, B. S.; Moulton, B.; MacDonald, J. C. *J. Chem. Crystallogr.* **2007**, *37*, 299−308.
(43) Schäferling, M.; Ääritalo, T.; Soukka, T. *Chem. - Eur. J.* **2014**, *20*, 5298−5308.
(44) The ethyl ester analogue of compound **6** has been reported previously: Soulié, M.; Latzko, F.; Bourrier, E.; Placide, V.; Butler, S. J.; Pal, R.; Walton, J. W.; Baldeck, P. L.; Le Guennic, B.; Andraud, C.; Zwier, J. M.; Lamarque, L.; Parker, D.; Maury, O. *Chem. - Eur. J.* **2014**, *20*, 8636−8646.
(45) A lanthanide-chelating ligand similar to $\mathbf{L^2}$, but featuring a substituted phenylethynyl group attached to the 4-position of the pyridine ring rather than a conjugatable terminal alkyne, has been reported: D'Aléo, A.; Allali, M.; Picot, A.; Baldeck, P. L.; Toupet, L.; Andraud, C.; Maury, O. *C. R. Chim.* **2010**, *13*, 681−690 The extended conjugation provided by the phenylethynyl group provided an efficient antenna for sensitization of Eu(III) luminescence in this case..
(46) Chan, T. R.; Hilgraf, R.; Sharpless, K. B.; Fokin, V. V. *Org. Lett.* **2004**, *6*, 2853−2855.
(47) Hong, V.; Presolski, S. I.; Ma, C.; Finn, M. G. *Angew. Chem., Int. Ed.* **2009**, *48*, 9879−9883.
(48) Melhuish, W. H. *J. Phys. Chem.* **1961**, *65*, 229−235.
(49) Renaud, F.; Piguet, C.; Bernardinelli, G.; Bünzli, J.-C. G.; Hopfgartner, G. *Chem. - Eur. J.* **1997**, *3*, 1660−1667.
(50) Nonat, A.; Gateau, C.; Fries, P. H.; Mazzanti, M. *Chem. - Eur. J.* **2006**, *12*, 7133−7150.
(51) Brunet, E.; Juanes, O.; Rodriguez-Ubis, J. C. *Curr. Chem. Biol.* **2007**, *1*, 11−39.
(52) Beeby, A.; Clarkson, I. M.; Dickins, R. S.; Faulkner, S.; Parker, D.; Royle, L.; de Sousa, A. S.; Williams, J. A. G.; Woods, M. J. *J. Chem. Soc., Perkin Trans. 2* **1999**, 493−503.
(53) Hu, Y.; Fan, C.-P.; Fu, G.; Zhu, D.; Jin, Q.; Wang, D.-C. *J. Mol. Biol.* **2008**, *382*, 99−111.
(54) Young, D. D.; Young, T. S.; Jahnz, M.; Ahmad, I.; Spraggon, G.; Schultz, P. G. *Biochemistry* **2011**, *50*, 1894−1900.
(55) Zimmerman, E. S.; Heibeck, T. H.; Gill, A.; Li, X.; Murray, C. J.; Madlansacay, M. R.; Tran, C.; Uter, N. T.; Yin, G.; Rivers, P. J.; Yam, A. Y.; Wang, W. D.; Steiner, A. R.; Bajad, S. U.; Penta, K.; Yang, W.; Hallam, T. J.; Thanos, C. D.; Sato, A. K. *Bioconjugate Chem.* **2014**, *25*, 351−361.
(56) (a) Wu, P. S. C.; Ozawa, K.; Lim, S. P.; Vasudevan, S. G.; Dixon, N. E.; Otting, G. *Angew. Chem., Int. Ed.* **2007**, *46*, 3356−3358. (b) Apponyi, M.; Ozawa, K.; Dixon, N.; Otting, G. In *Structural Proteomics;* Kobe, B., Guss, M., Huber, T., Eds.; Humana Press, 2008; Vol. *426*, pp 257−268. (c) Loscha, K. V.; Herlt, A. J.; Qi, R.; Huber, T.; Ozawa, K.; Otting, G. *Angew. Chem., Int. Ed.* **2012**, *51*, 2243−2246.
(57) Besanceney-Webler, C.; Jiang, H.; Zheng, T.; Feng, L.; Soriano del Amo, D.; Wang, W.; et al. *Angew. Chem., Int. Ed.* **2011**, *50*, 8051−8056.
(58) Neylon, C.; Brown, S. E.; Kralicek, A. V.; Miles, C. S.; Love, C. A.; Dixon, N. E. *Biochemistry* **2000**, *39*, 11989−11999.
(59) Young, T. S.; Ahmad, I.; Yin, J. A.; Schultz, P. G. *J. Mol. Biol.* **2010**, *395*, 361−374.
(60) Cabrita, L. D.; Gilis, D.; Robertson, A. L.; Dehouck, Y.; Rooman, M.; Bottomley, S. P. *Protein Sci.* **2007**, *16*, 2360−2367.

DOI: 10.1021/acs.inorgchem.5b02605
Inorg. Chem. XXXX, XXX, XXX−XXX

Supporting Information

Luminescent Alkyne-Bearing Terbium(III) Complexes and their Application to Bioorthogonal Protein Labeling

William I. O'Malley, Elwy H. Abdelkader, Margaret L. Aulsebrook, Riccardo Rubbiani, Choy-Theng Loh, Michael R. Grace, Leone Spiccia, Gilles Gasser, Gottfried Otting, Kellie L. Tuck, Bim Graham

Contents **Pages**

Luminescence lifetime measurements

Lifetime measurements were performed on a Varian Cary Eclipse fluorescence spectrophotometer using a 1 cm path length quartz cuvette and the following settings: total decay time = 30 ms, number of flashes = 1, delay time = 0.1 ms, gate time = 0.1 ms, excitation slit width = 5 nm, emission slit width = 5 nm, number of cycles = 100. Samples were prepared at 10 μM concentration in both H_2O and D_2O. Samples were excited at their respective λ_{max}: 287 nm for Tb-**L**^{1} and 300 nm for "clicked" Tb-**L**^{1}. Emission intensity was recorded at 543 nm. The resulting luminescence decay curves were fitted to following equation using the SigmaPlot software:

$$I_t = I_0 * \exp(-t/\tau)$$

where I_t is the intensity at time t after the excitation flash, I_0 is the initial intensity at t = 0, and τ is the luminescence lifetime.

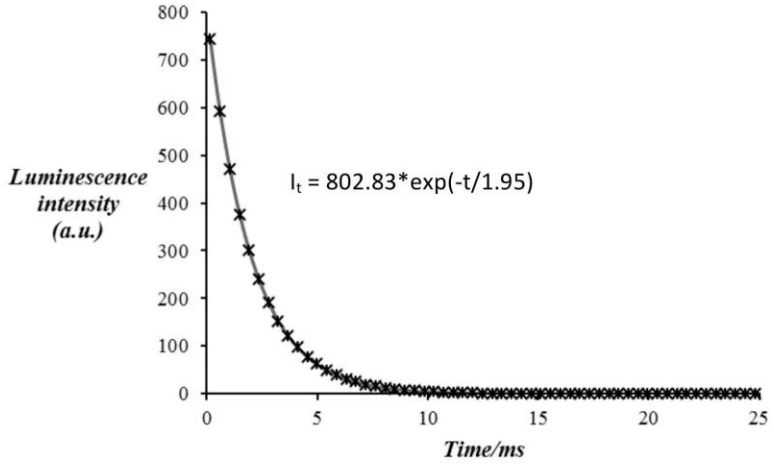

Figure S1. Luminescence decay for Tb-**L**[1] in H_2O; τ = 1.95 ms. Experimental data points are marked by crosses (with only one in every four data points shown to aid clarity) and the fitted curve is shown as a solid gray line.

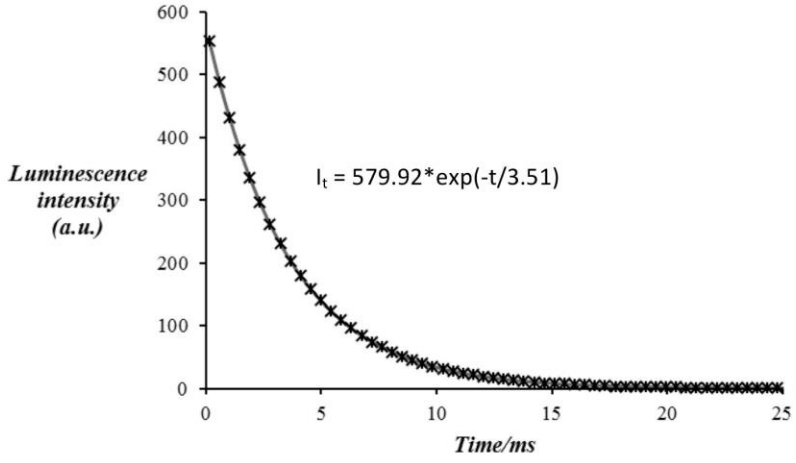

Figure S2. Luminescence decay for Tb-**L**[1] in D_2O; τ = 3.51 ms. Experimental data points are marked by crosses (with only one in every four data points shown to aid clarity) and the fitted curve is shown as a solid gray line.

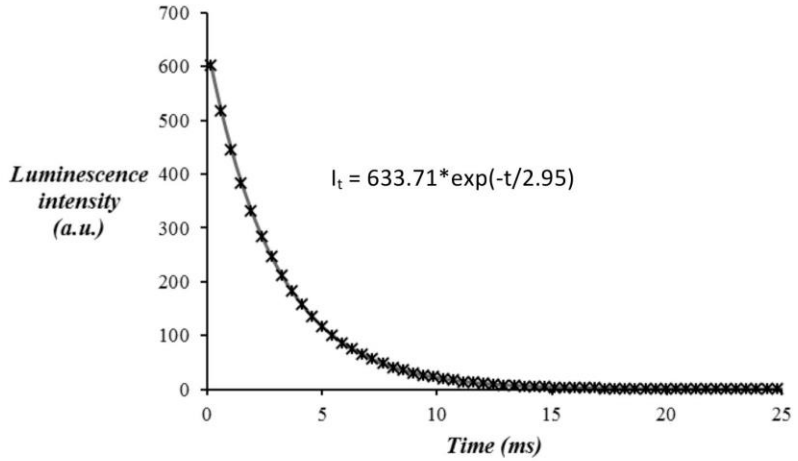

Figure S3. Luminescence decay for clicked Tb-**L**[1] in H_2O; τ = 2.95 ms. Experimental data points are marked by crosses (with only one in every four data points shown to aid clarity) and the fitted curve is shown as a solid gray line.

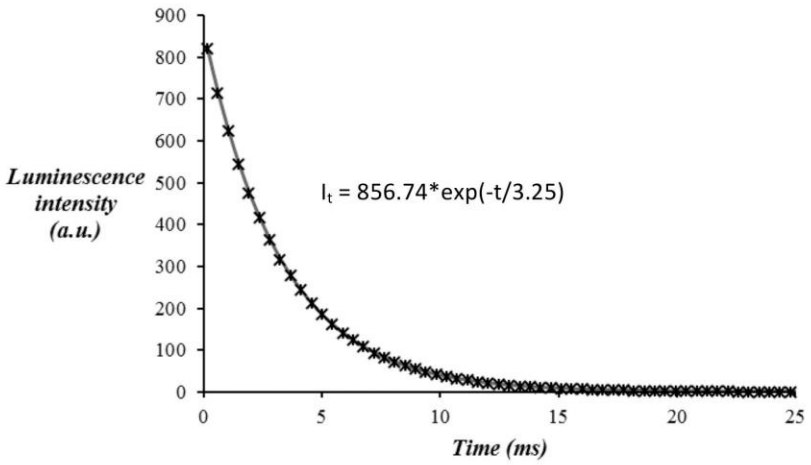

Figure S4. Luminescence decay for clicked Tb-**L**[1] in D_2O; τ = 3.25 ms. Experimental data points are marked by crosses (with only one in every four data points shown to aid clarity) and the fitted curve is shown as a solid gray line.

Luminescence of labeled protein samples

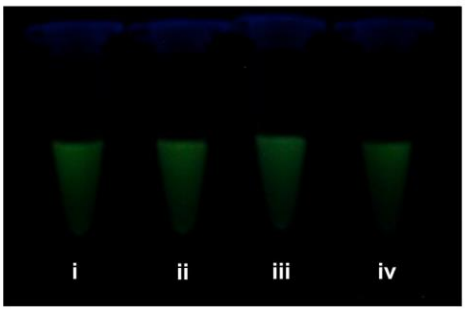

Figure S5. Photograph of spin-dialyzed solutions of labelled DEBP samples (*ca.* 10 μM in H_2O) irradiated with a common laboratory TLC lamp (254 nm): (i) DEBP-Q80AzF+Tb-**L**^{1}, (ii) DEBP-Q80AzF+Tb-**L**^{2}, (iii) DEBP-Q80AzMF+Tb-**L**^{1}, (iv) DEBP-Q80AzMF+Tb-**L**^{2}.

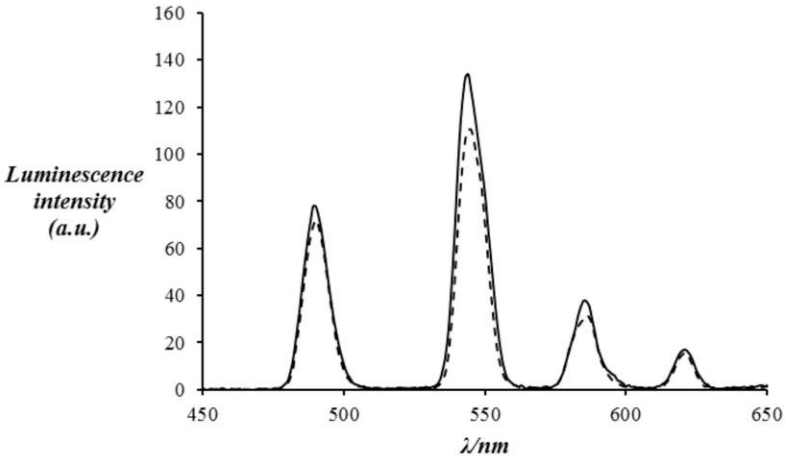

Figure S6. Luminescence emission spectra of DEBP-Q80AzF+Tb-**L**^{1} (*ca.* 10 μM in H_2O) excited at 300 nm (dashed line) and DEBP-Q80AzF+Tb-**L**^{2} (*ca.* 10 μM in H_2O) excited at 274 nm (solid line).

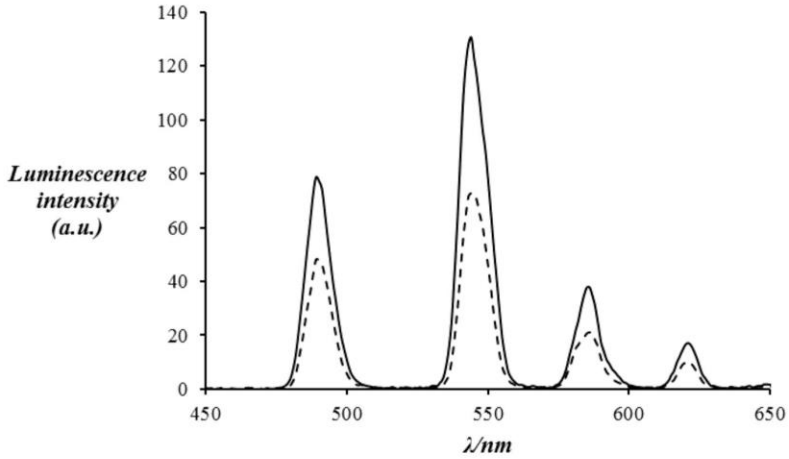

Figure S7. Luminescence emission spectra of DEBP-Q80AzMF+Tb-$\mathbf{L^1}$ (*ca.* 10 μM in H_2O) excited at 300 nm (dashed line) and DEBP-Q80AzMF+Tb-$\mathbf{L^2}$ (*ca.* 10 μM in H_2O) excited at 274 nm (solid line).

NMR spectra of reported compounds

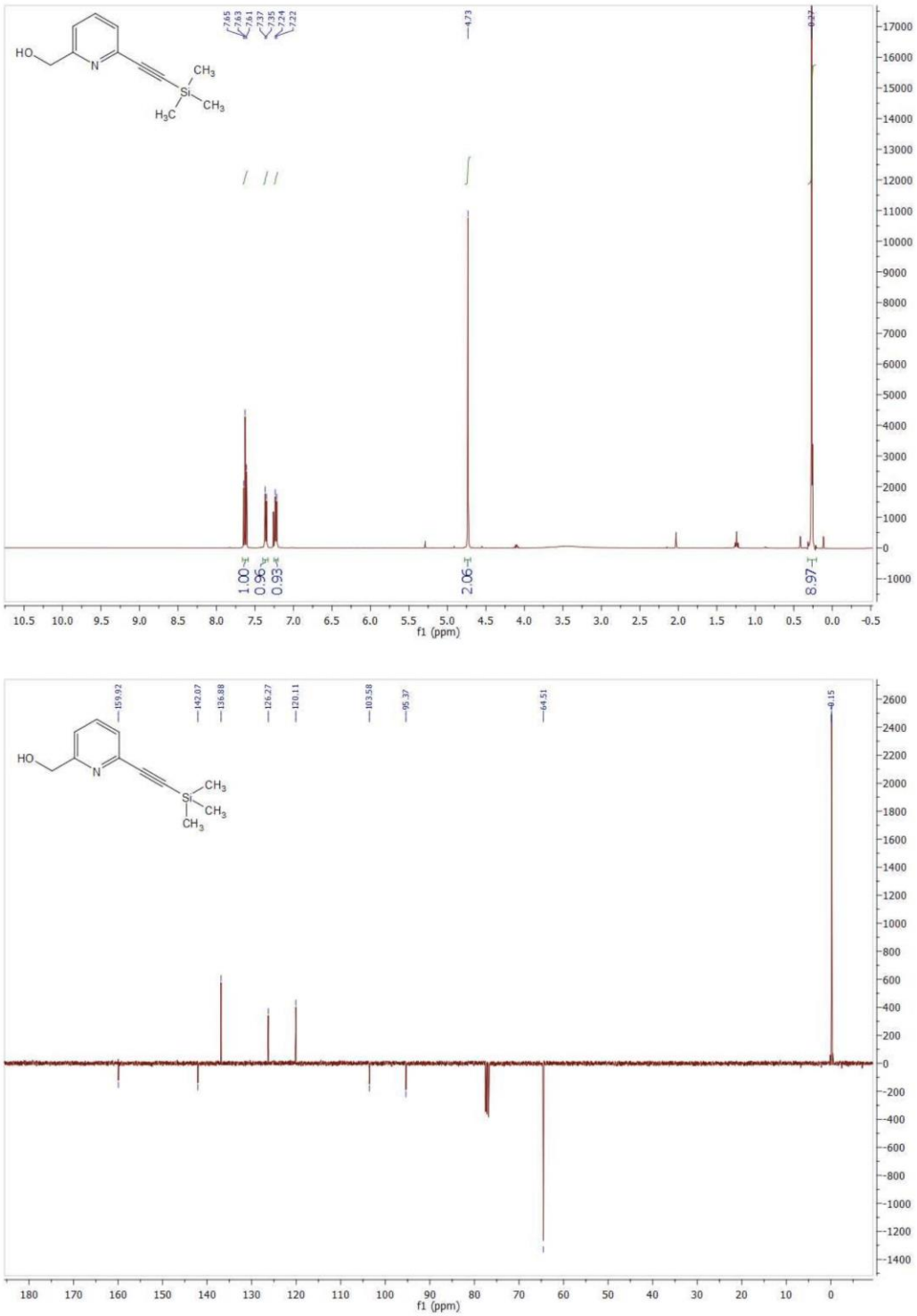

Figure S8. ^{1}H and ^{13}C NMR spectra of **2** in $CDCl_3$.

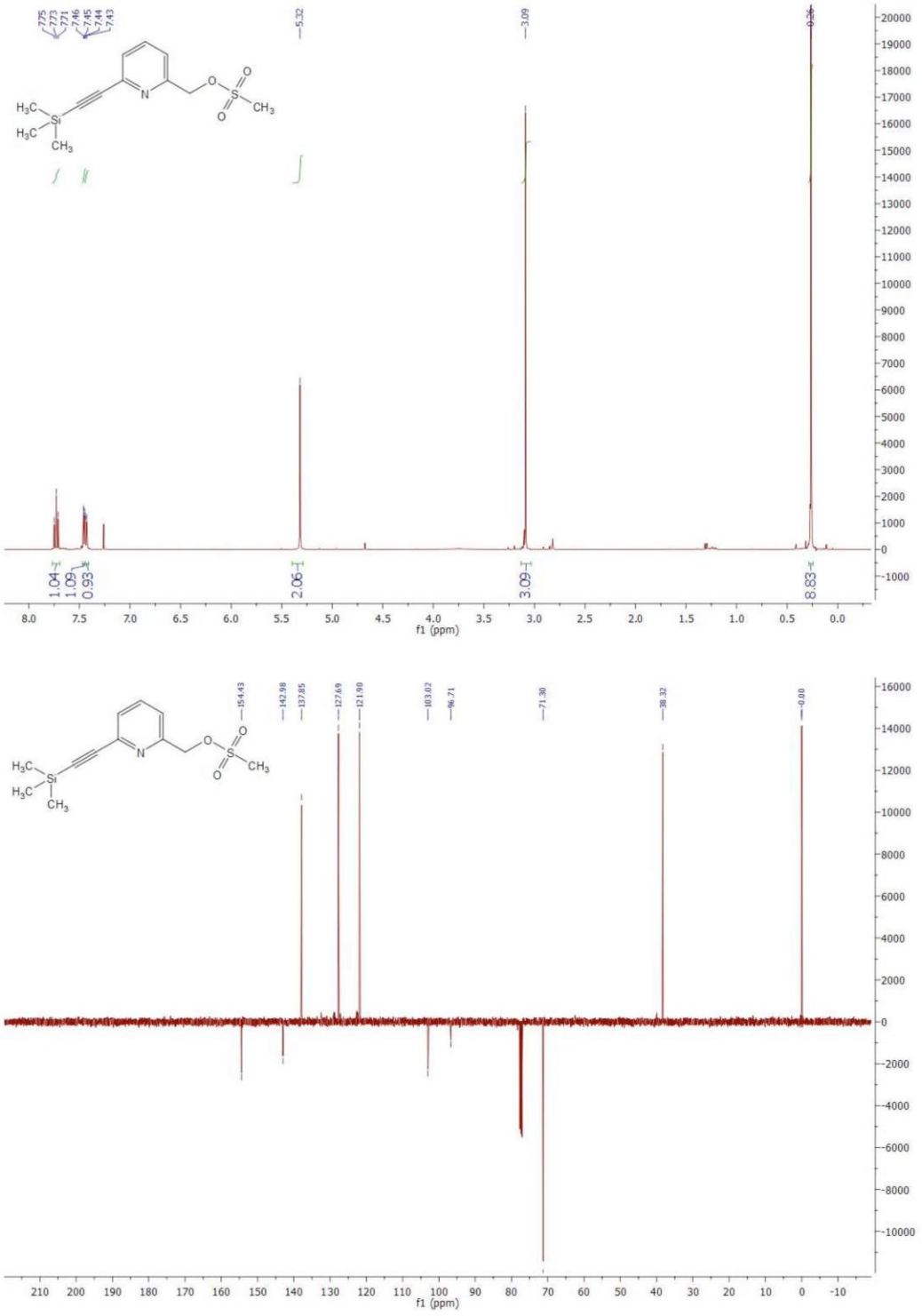

Figure S9. ^{1}H and ^{13}C NMR spectra of **3** in $CDCl_3$.

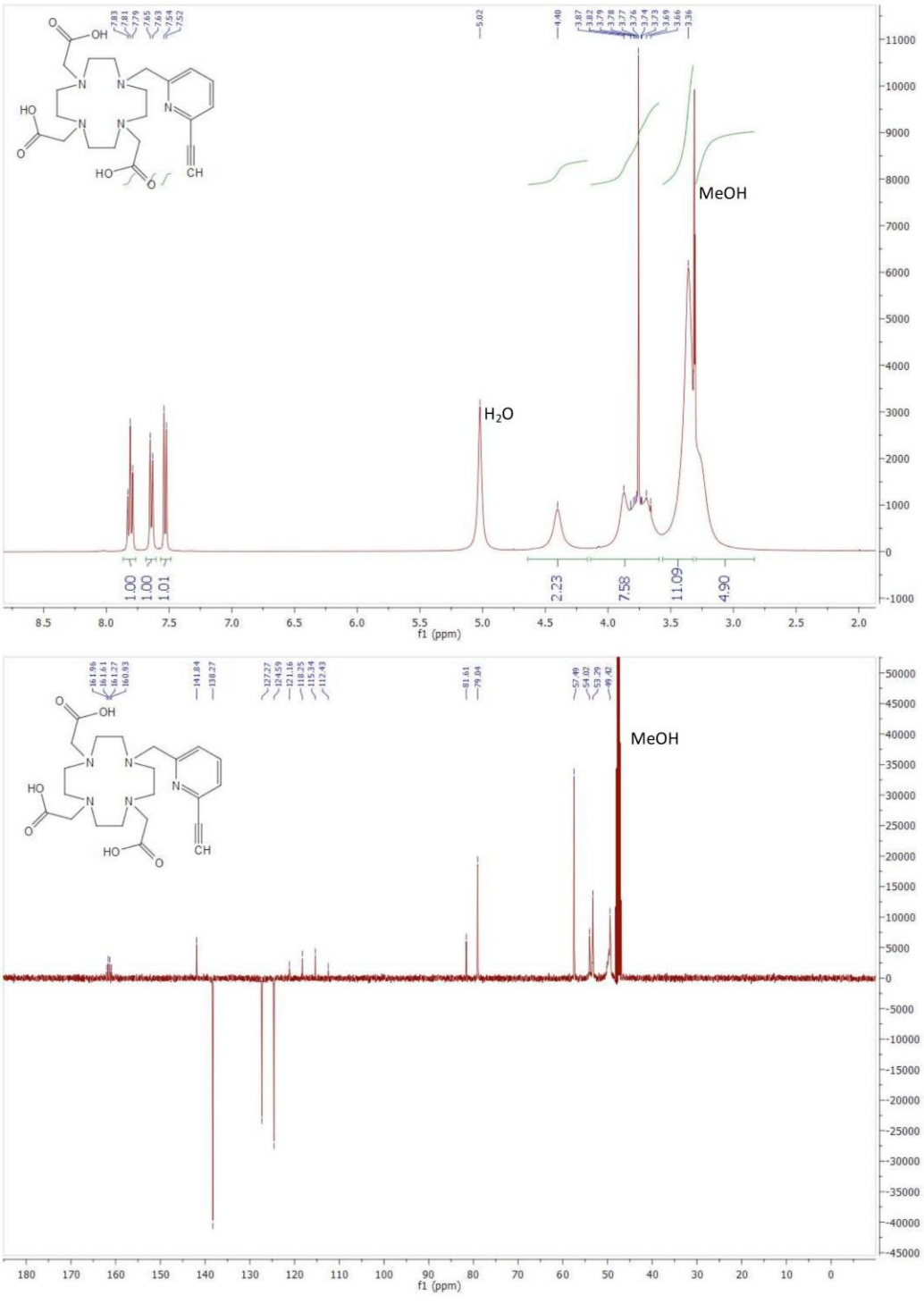

Figure S10. ^{1}H and ^{13}C NMR spectra of $H_3\mathbf{L^1}$ in MeOD.

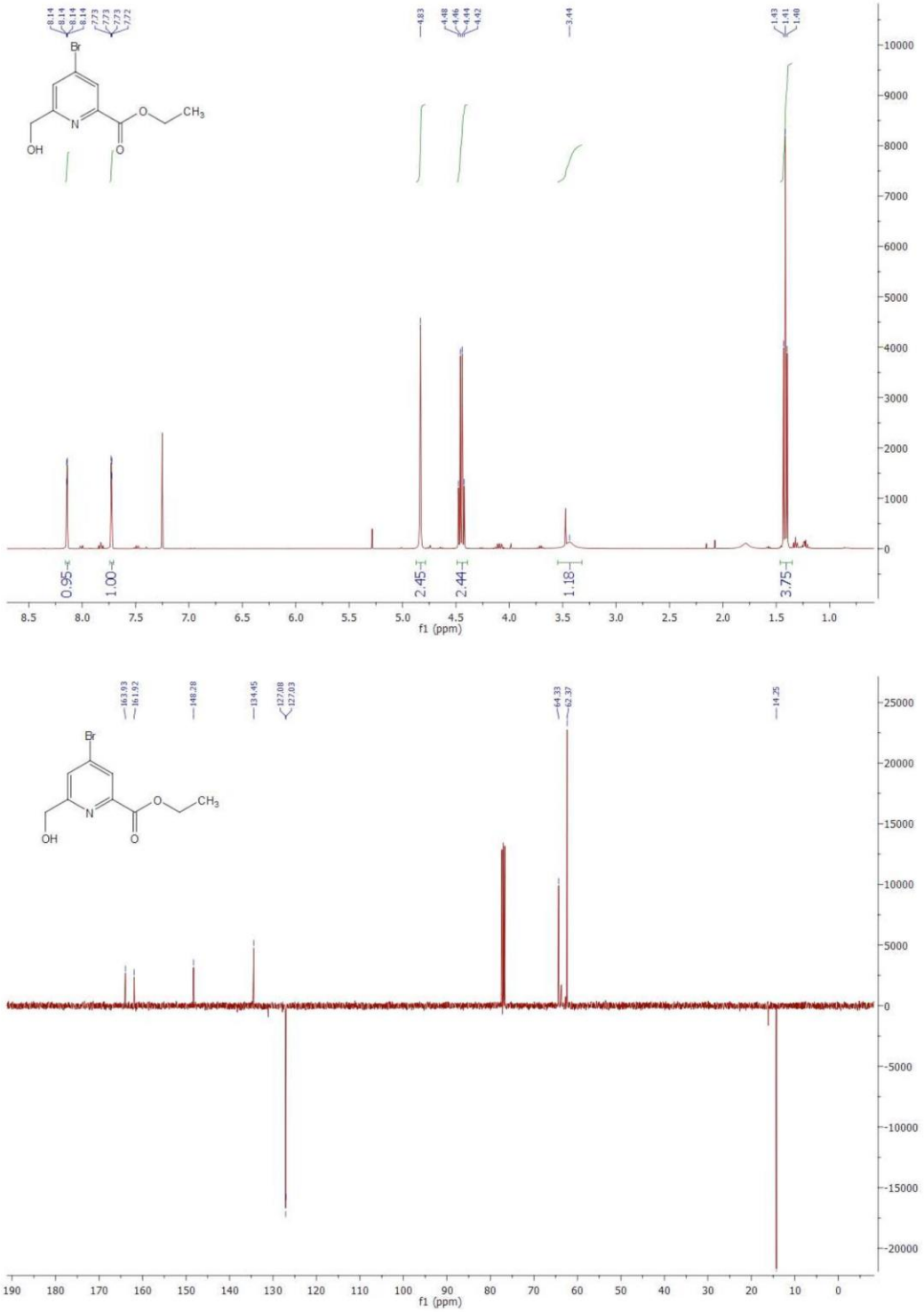

Figure S11. ^{1}H and ^{13}C NMR spectra of **5** in $CDCl_3$.

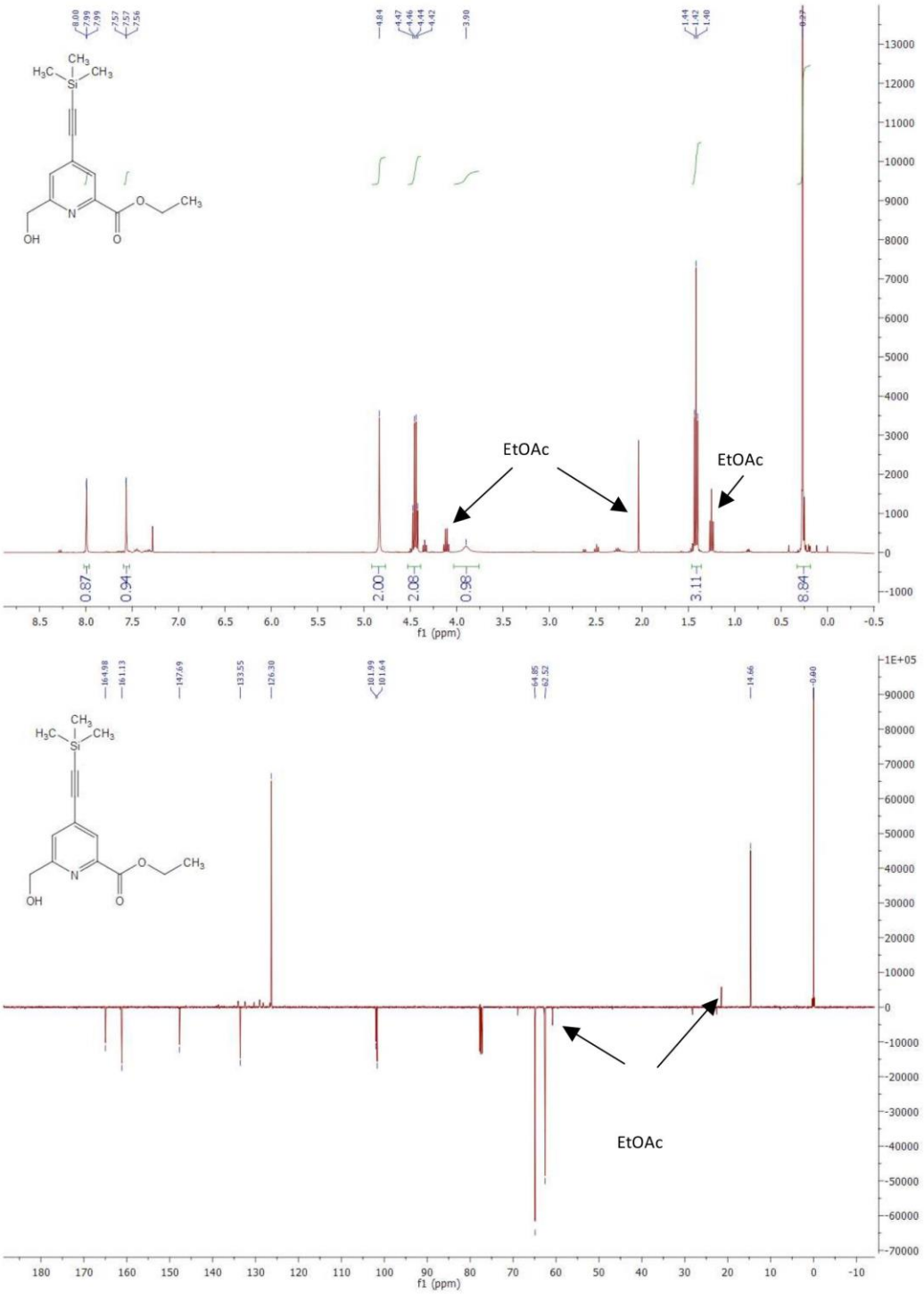

Figure S12. ^{1}H and ^{13}C NMR spectra of **6** in $CDCl_3$.

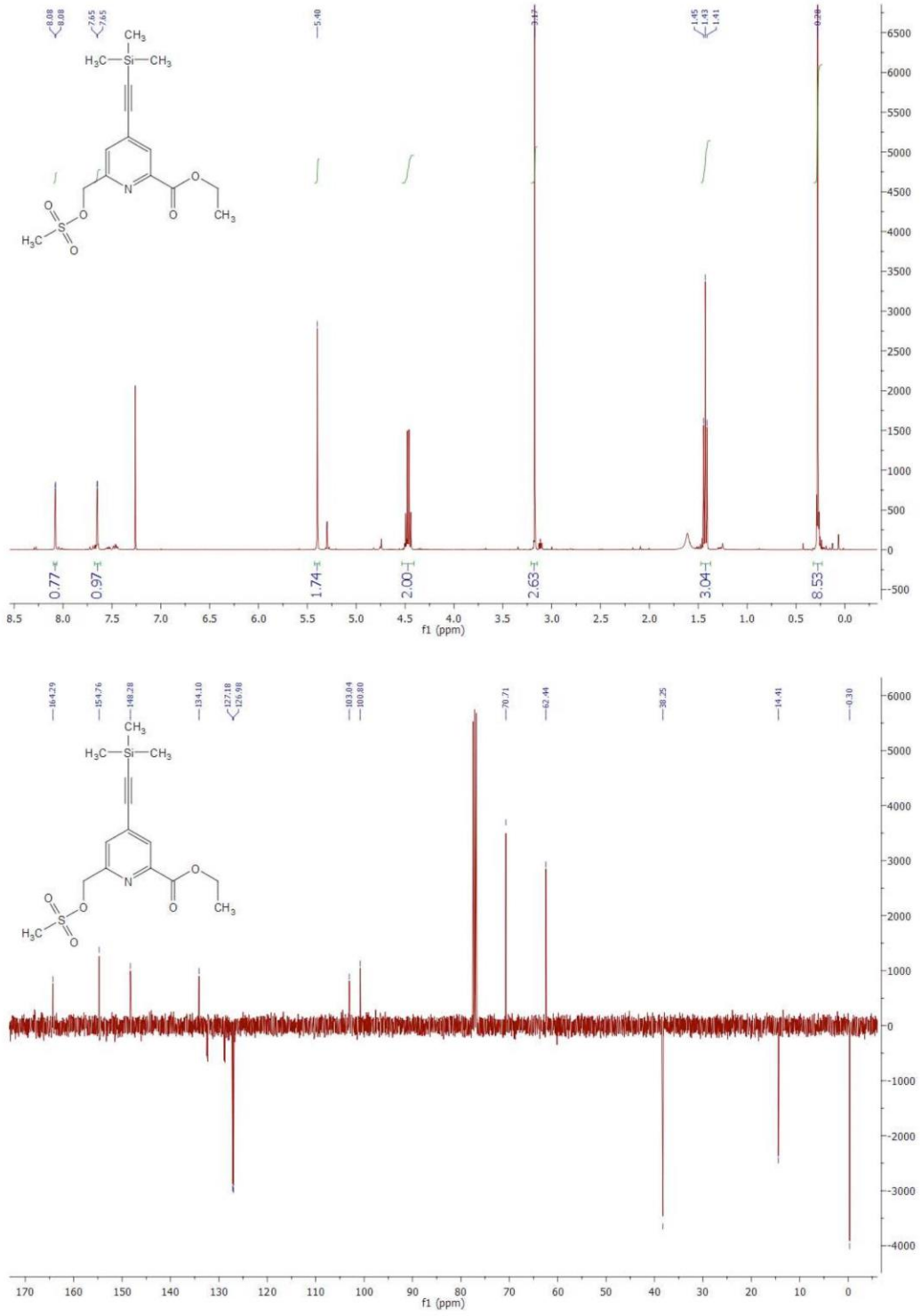

Figure S13. ^{1}H and ^{13}C NMR spectra of **7** in $CDCl_3$.

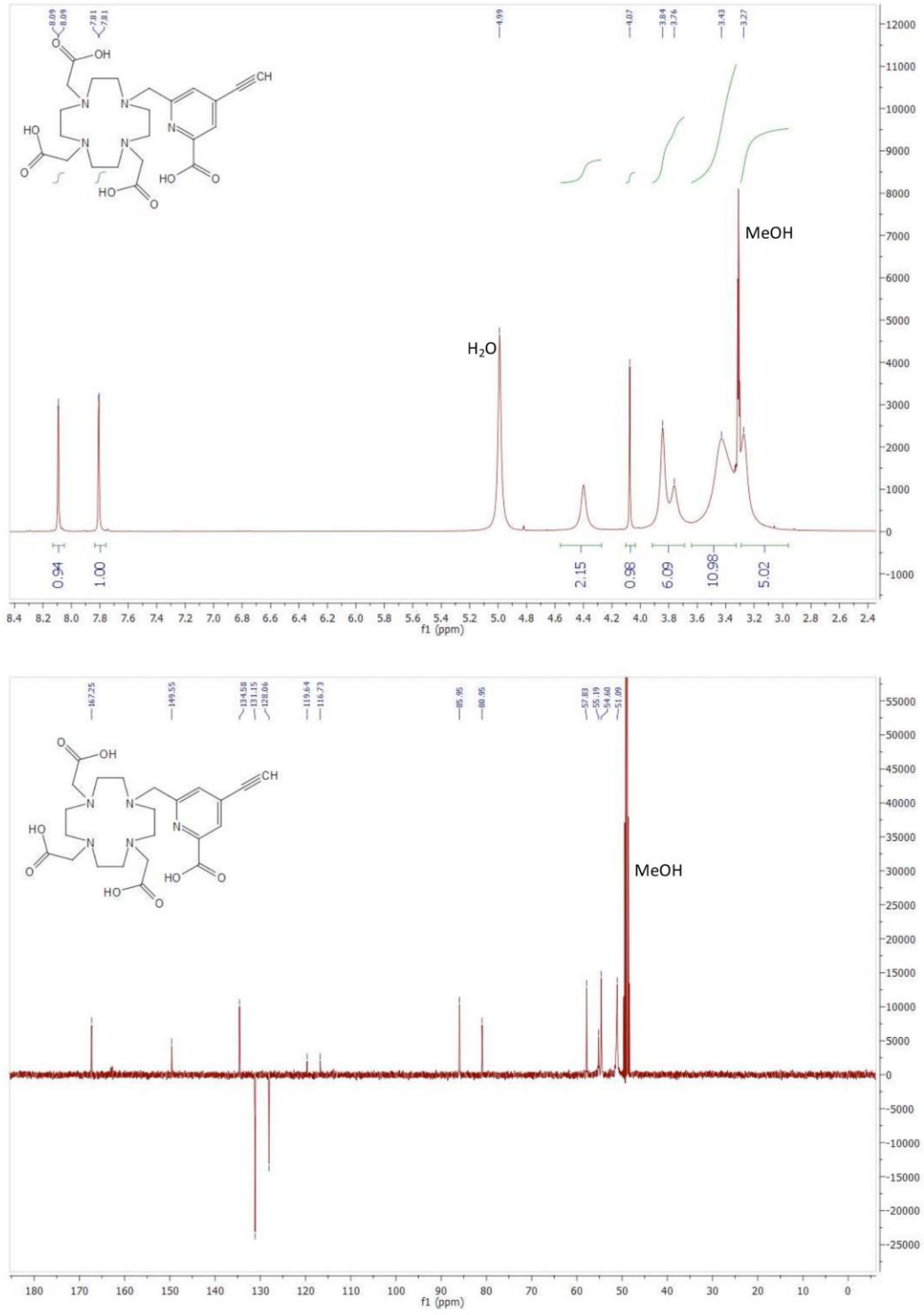

Figure S14. ^{1}H and ^{13}C NMR spectra of $H_4\mathbf{L^2}$ in MeOD.

LC traces for ligands

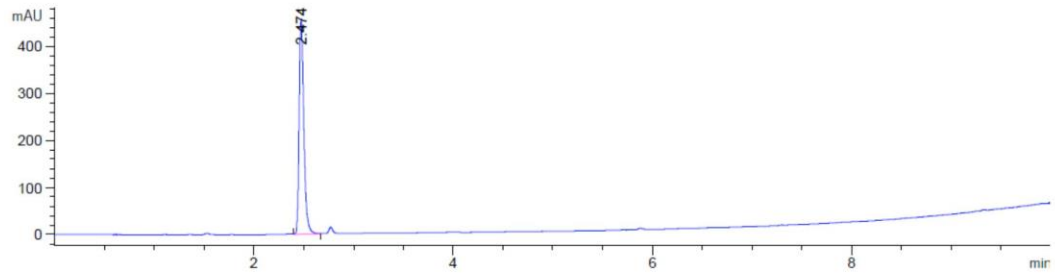

Figure S15. LC trace for H_3L^1.

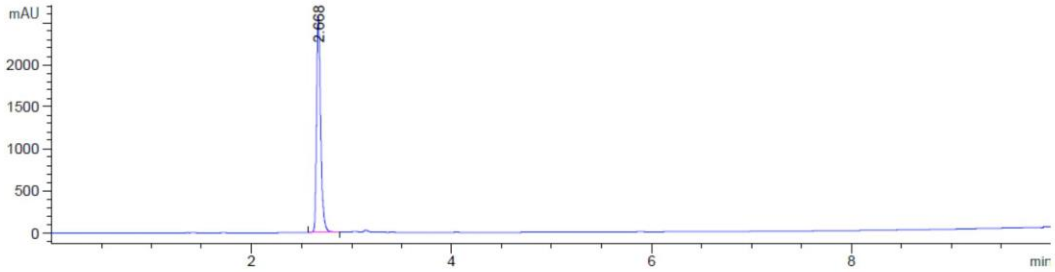

Figure S16. LC trace for H_4L^2.

LC traces for terbium(III) complexes

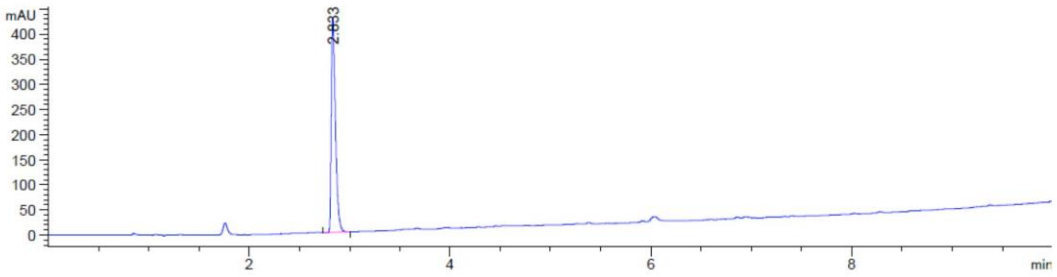

Figure S17. LC trace for Tb-L^1.

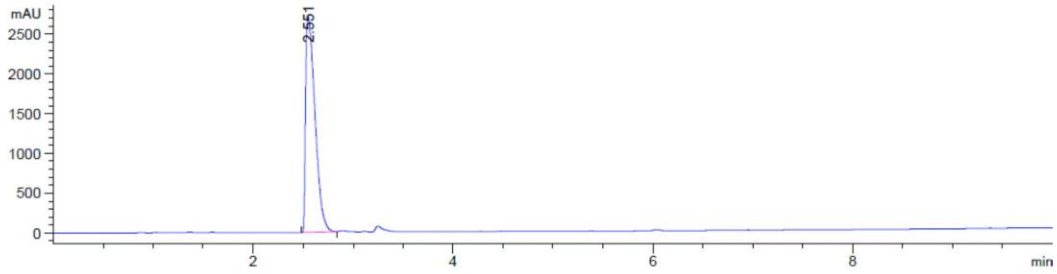

Figure S18. LC trace for Tb-L^2.

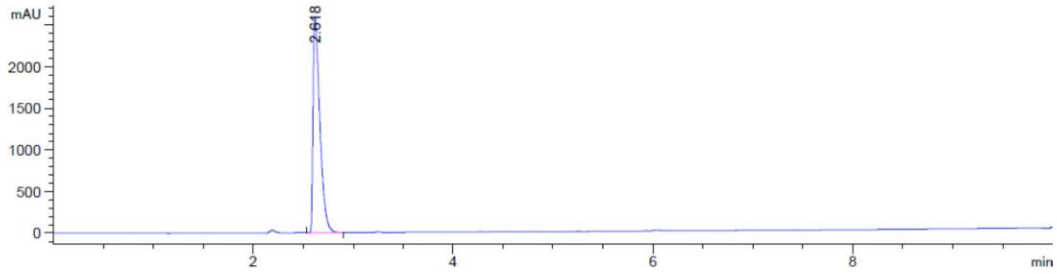

Figure S19. LC trace for clicked Tb-L^1.

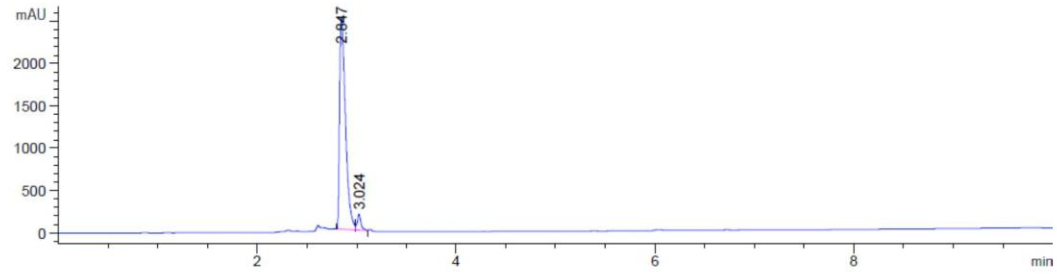

Figure S20. LC trace for clicked Tb-L^2.

CHAPTER 3:

CELLULAR UPTAKE AND PHOTO-CYTOTOXICITY OF A GADOLINIUM(III)-DOTA-NAPHTHALIMIDE COMPLEX "CLICKED" TO A LIPIDATED TAT PEPTIDE

Declaration for Thesis Chapter 3.

Declaration by candidate

In the case of Chapter 3 the nature and extent of my contribution to the work was the following:

Nature of contribution	Extent of contribution (%)
Synthesis and characterisation of synthetic compounds, evaluation of photophysical properties, interpretation of results, manuscript preparation.	65%

The following co-authors contributed to the work. If co-authors are students at Monash University, the extent of their contribution in percentage terms must be stated:

Name	Nature of contribution	Extent of contribution (%) for student co-authors only
Margaret Aulsebrook	Compound characterisation.	5%
Riccardo Rubbiani	Cell uptake and cytotoxicity studies	
Michael Grace	Research guidance, manuscript review	
Leone Spiccia	Research guidance, manuscript review	
Gilles Gasser	Research guidance, experimental design, manuscript review	
Kellie Tuck	Research guidance, experimental design, manuscript review	
Bim Graham	Research guidance, experimental design, interpretation of results, manuscript review	

The undersigned hereby certify that the above declaration correctly reflects the nature and extent of the candidate's and co-authors' contributions to this work.

Candidate's Signature		**Date 9/3/16**
Main Supervisor's Signature	[redacted]	**Date 8/3/16**

molecules

MDPI

Article

Cellular Uptake and Photo-Cytotoxicity of a Gadolinium(III)-DOTA-Naphthalimide Complex "Clicked" to a Lipidated Tat Peptide

William I. O'Malley [1,†], Riccardo Rubbiani [2,†], Margaret L. Aulsebrook [3], Michael R. Grace [3], Leone Spiccia [3], Kellie L. Tuck [3,*], Gilles Gasser [2,*] and Bim Graham [1,*]

1 Monash Institute of Pharmaceutical Sciences, Monash University, Parkville VIC 3163, Australia; william.o'malley@monash.edu

2 Department of Chemistry, University of Zurich, Winterthurerstrasse 190, Zurich CH-8057, Switzerland; riccardo.rubbiani@chem.uzh.ch

3 School of Chemistry, Monash University, Clayton VIC 3800, Australia; margaret.aulsebrook@monash.edu (M.L.A.); mike.grace@monash.edu (M.R.G.); leone.spiccia@monash.edu (L.S.)

* Correspondence: kellie.tuck@monash.edu (K.L.T.); gilles.gasser@chem.uzh.ch (G.G.); bim.graham@monash.edu (B.G.); Tel.: +61-3-9905-4510 (K.L.T.); +41-44-635-46-30 (G.G.); +61-3-9903-9706 (B.G.)

† These authors contributed equally to this work.

Academic Editor: Wiktor Szymański

Received: 12 December 2015 ; Accepted: 2 February 2016 ; Published: 5 February 2016

Abstract: A new bifunctional macrocyclic chelator featuring a conjugatable alkynyl-naphthalimide fluorophore pendant group has been prepared and its Gd(III) complex coupled to a cell-penetrating lipidated azido-Tat peptide derivative using Cu(I)-catalysed "click" chemistry. The resulting fluorescent conjugate is able to enter CAL-33 tongue squamous carcinoma cells, as revealed by confocal microscopy, producing a very modest anti-proliferative effect (IC_{50} = 93 μM). Due to the photo-reactivity of the naphthalimide moiety, however, the conjugate's cytotoxicity is significantly enhanced (IC_{50} = 16 μM) upon brief low-power UV-A irradiation.

Keywords: cell-penetrating peptide; fluorescence; gadolinium complex; photo-cytotoxicity; theranostic

1. Introduction

There continues to be much interest in the development of molecular imaging agents, including ones that can be detected by more than one imaging modality ("multi-modal imaging agents") [1–5]. This is particularly so within the field of oncology, where imaging agents are used extensively for the screening, diagnosis, staging, planning of treatment, post-treatment assessment and surveillance of cancer [6,7]. Another area that has seen rapid growth over the last decade is the development of agents that can be used for both imaging and therapy ("theranostics"), allowing for image-guided drug delivery, *in vivo* detection of drug release/activation, and/or monitoring of patient's response to therapy [8–10]. Designs range from small molecules and (bio)conjugates [11] through to multi-functional nanoparticulate systems [12,13].

The most advanced theranostic designs are engineered to be stimuli-responsive, with activation of therapeutic activity/drug release occurring in response to endogenous triggers (e.g., pH change, hypoxia, elevated enzyme activity) or external stimuli (e.g., heat, light). This allows for controlled dosing and/or reduced exposure of non-diseased cells/tissue to cytotoxic species [14,15]. The development of *photo-responsive* systems, in particular, has received considerable attention, since light, as a stimulus, is generally non-invasive and can be readily manipulated, enabling

drug activation/release to be controlled both spatially and temporally with extreme precision. Photo-responsiveness is often achieved by loading bioactive cargo into carrier (nano)materials that are amenable to dissociation/structural change upon exposure to light [16–18]. Alternatively, light-activated pro-drugs may be employed in the construction of photo-responsive theranostic designs. These include photo-sensitisers, which generate cytotoxic singlet oxygen ($^1O_2$) in response to light and form the basis of photo-dynamic therapy (PDT) [19–21], and photo-activated chemotherapeutic (PACT) agents, which induce cell death through mechanisms such as light-mediated ligand ejection, DNA crosslinking and uncaging [22–27]. As an added benefit, many PDT and PACT agents are luminescent, providing a ready means of detection [28–30].

The development of increasingly elaborate and sophisticated multi-modal imaging agent and theranostic designs, including photo-responsive ones, has been aided by the advent of "bio-orthogonal" chemistries, such as the Cu(I)-catalysed azide-alkyne cycloaddition reaction ("click reaction") [31,32] and its Cu-free variant—strain-promoted azide-alkyne cycloaddition (SPAAC) [33,34]. These allow for the late-stage introduction of moieties into highly functionalised molecules (small molecules, peptides, proteins) [35–38] and nanoparticles [39–41], as well as the controlled stepwise elaboration of hetero-multifunctional scaffolds [42–44], without the need for complex protection group strategies. The widespread adoption of bio-orthogonal labelling technologies in the biological and biomedical sciences has also seen an expanding toolbox of "clickable" compounds (fluorophores, cross-linkers, macrocyclic chelators, *etc.*) become available to researchers interested in multi-functional imaging and therapeutic agents. Indeed, many such "building blocks" are now commercially available.

We have a particular interest in the development of metal complex-based agents for imaging and therapy, including photo-cytotoxic complexes for potential application as new PDT and PACT agents [45–52]. During the course of our work, a number of "clickable" metal complexes/chelators have been developed and employed in the synthesis of peptide conjugates with tumour-targetting, cell-penetrating and/or organelle-specific localising properties [53–56]. Additionally, we have incorporated alkyne-bearing metal complexes into proteins via click conjugation to unnatural amino acids to facilitate protein structural investigations [57–59]. Many other research groups have likewise reported alkyne- and azide-bearing metal complexes/chelators for a range of biological and biomedical applications [60–64].

As part of an effort to generate new photo-activated theranostics and multi-modal imaging agents, we have now developed a new macrocyclic gadolinium(III) complex of a 1,4,7,10-tetraazacyclodocane-1,4,7,10-tetraacetic acid (DOTA) derivative featuring a conjugatable alkynyl-napthalimide pendant. Naphthalimide derivatives are widely employed as fluorescent dyes and are known to be photo-reactive [65–71], while Gd(III)-DOTA-type complexes are well-established MRI contrast agents [72–74]. To demonstrate its utility, the complex has been conjugated to a "model" peptide—a lipidated, azide-bearing derivative of the cell-penetrating "Tat" peptide, derived from the HIV-1 "Trans-Activator of Transcription" protein [75]. We show that the "clicked" naphthalimide moiety can be used for fluorescence tracking and results in a photo-cytotoxic effect when cellular entry of the complex is facilitated by conjugation to the Tat peptide.

2. Results and Discussion

2.1. Synthesis of Ligand and Gd(III) Complexes

The synthesis of the ligand, L, commenced with a condensation reaction between commercially-available 4-bromo-1,8-naphthalic anhydride and *N*-Boc-1,2-ethylenediamine, followed by a Sonogashira reaction of the product (1) with trimethylsilyl (TMS) acetylene to install a TMS-protected alkyne group in place of the bromo substituent (Scheme 1). Following Boc-deprotection of 2 with trifluoroacetic acid (TFA), the exposed amine of 3 was reacted with bromoacetyl bromide to produce the bromoacetamide derivative, 4. Compound 4 was subsequently coupled to *tert*-butyl-protected 1,4,7,10-tetraazacyclododecane-1,4,7-triacetic acid (^{t}Bu$_3$DO3A) [76]. Lastly, the

TMS and ^{t}Bu groups were removed using KF and TFA, respectively, to yield L, which was purified by preparative HPLC.

The Gd(III) complex, Gd-L, was prepared by heating a neutral (pH 6.5–7.5) aqueous solution of the ligand with two equiv. of gadolinium(III) acetate for 2 h, after which time LC-MS analysis indicated near-quantitative complexation. Preparative HPLC was then used to purify the complex to >95% purity.

As an initial test, Gd-L was conjugated to 3-azido-1-propanol as a model azide in aqueous solution. $CuSO_4$ (0.1 equiv.) was utilised as the copper source, sodium ascorbate (1 equiv.) as the reducing agent and *tris*(3-hydroxypropyl-triazolylmethyl)amine (THTPA) (0.2 equiv.) as a Cu(I)-stabilising ligand [77,78]. After stirring overnight, conversion to the clicked product was near-quantitative according to LC-MS analysis. The complex was again isolated in >95% purity following preparative HPLC.

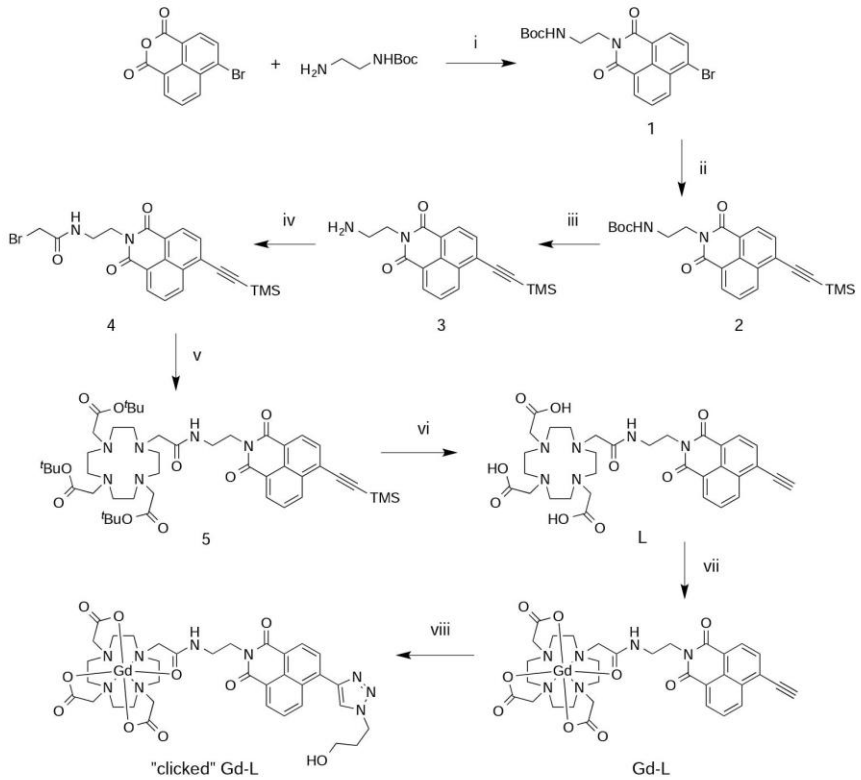

Scheme 1. Synthesis of ligand and Gd(III) complexes. (i) DMF, 80 °C, overnight (O/N), 91%; (ii) TMS acetylene, $Pd(PPh_3)_2Cl_2$, CuI, Et_3N, THF, N_2 atmosphere, RT, 3 h, 48%; (iii) TFA, DCM, RT, 4 h, 96%; (iv) bromoacetyl bromide, Na_2CO_3, acetone, RT, 3 h, 59%; (v) $^{t}Bu_3DO_3A.HBr$, DIPEA, ACN, reflux, O/N, 81%; (vi) (a) KF, H_2O/ACN, RT, 2 h; (b) TFA, DCM, RT, O/N, 71% (over two steps); (vii) $Gd(OAc)_3$, water/ACN, 70 °C, 2 h, quant. (53% isolated); (viii) 3-azido-1-propanol, $CuSO_4$, sodium ascorbate, THPTA, water/ACN, pH 7, RT, O/N, quant. (47% isolated).

2.2. Photo-Physical Properties of Complexes

The spectral properties of the two Gd(III) complexes were measured in aqueous solution buffered at pH 7.4 with 100 mM HEPES. Table 1 summarises the data, while absorbance and fluorescence emission spectra of the complexes are shown in Figure 1.

Click conjugation of the Gd-L complex is associated with a slight bathochromic shift (6 nm) in the absorbance band arising from *π-π* transitions within the naphthalimide group. A much larger shift

(54 nm) is observed for the fluorescence emission band and the fluorescence quantum yield is increased by *ca.* 70%. These findings are in accordance with those reported for a simple *N*-ethyl naphthalimide derivative bearing an alkyne at the 8-position [79].

Table 1. Photo-physical data for Gd(III) complexes measured in 100 mM HEPES, pH 7.4 (298 K).

Complex	Absorption λ_{max} (ε ($M^{-1}cm^{-1}$))	Emission λ_{max}	Φ [a] (%)	Brightness ($\varepsilon \times \Phi/1000$ ($M^{-1}cm^{-1}$))
Gd-L	356 (22,500)	417	35%	7.9
"Clicked" Gd-L	362 (19,200)	471	59%	11.3

[a] Quantum yield measured relative to quinine sulphate [80].

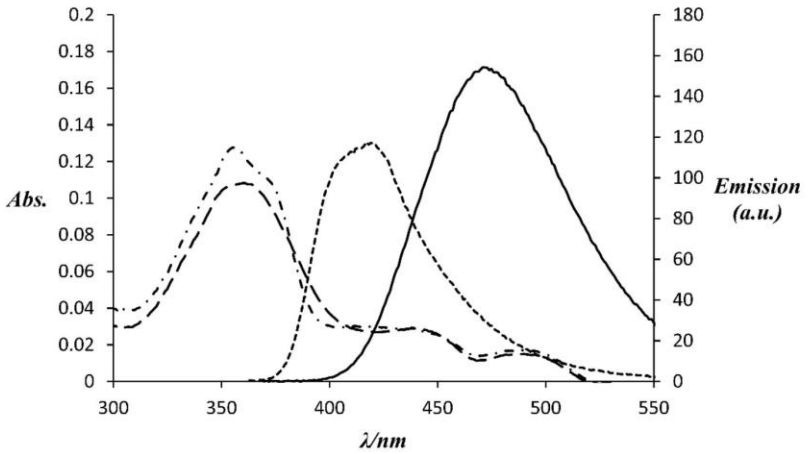

Figure 1. Absorbance and fluorescence emission spectra of Gd(III) complexes (5 μM) in 100 mM HEPES, pH 7.4 (298 K). Dot-dashed line: absorbance of Gd-L, dotted line: emission of Gd-L excited at 356 nm, dashed line: absorbance of "clicked" Gd-L, solid line: emission of "clicked" Gd-L excited at 362 nm.

2.3. Conjugation of Complex to Lipidated Tat Peptide

To demonstrate its utility, the Gd-L complex was ligated to a derivative of the cell-penetrating Tat peptide featuring a myristic acid tail at its N-terminus (to aid with cellular uptake) and an internal azido-L-lysine residue (Figure 2). We have previously attached a luminescent rhenium(I) complex to this lipidated peptide and visualised uptake of the resulting conjugate into cells via fluorescence microscopy [55]. Stirring the peptide with Gd-L in the presence of $CuSO_4$, sodium ascorbate and THPTA at room temperature overnight led to essentially quantitative conversion, as judged by LC-MS analysis. The product was isolated in 90% purity following preparative HPLC.

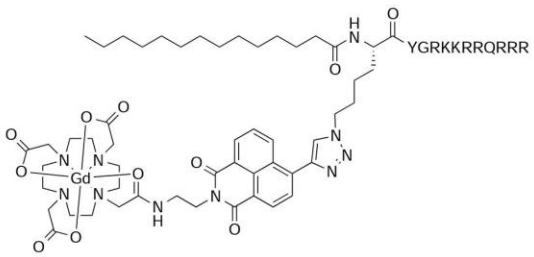

Figure 2. Structure of Gd-L-bearing myristylated Tat peptide conjugate.

2.4. (Photo-)cytotoxicity of Complexes and Conjugate

The cytotoxic properties of Gd-L, "clicked" Gd-L and the Gd-L-Tat peptide conjugate were assessed on CAL-33 tongue squamous carcinoma cells, either in the dark or combined with short exposure to a low-power dose of UV-A radiation (350 nm, 2.58 J·cm^{-2}, 10 min). As the results in Table 2 indicate, the Gd-L and "clicked" Gd-L complexes exerted essentially no cytotoxic effect under either of these conditions, with measured IC_{50} values >100 μM in all cases. The Tat conjugate also produced only a very modest anti-proliferative effect when incubated with cells in the dark ($IC_{50} \approx 93$ μM). However, a six-fold enhancement in cytotoxicity ($IC_{50} \approx 16$ μM) was observed when the conjugate was exposed to UV-A radiation (see also Figure 3). These results reflect, first of all, that the myristylated Tat peptide aids considerably with cellular uptake [55,81]. Secondly, the observed photo-cytotoxicity of the conjugate is consistent with previous reports of the photo-reactivity of naphthalimide derivatives towards biological molecules, including proteins and nucleic acids [65–71].

Table 2. Anti-proliferative effects of the Gd(III) complexes and Tat peptide conjugate on CAL-33 cancer cells in the dark and upon light irradiation at 350 nm for 10 min (2.58 J·cm^{-2}).

Compound	IC_{50} (Dark) [a] (μM)	IC_{50} (UV-A) [a] (μM)	PI [b] (x-Fold)
Gd-L	>100	>100	n.a.
"clicked" Gd-L	>100	>100	n.a.
Gd-L-Tat conjugate	93 ± 3	16 ± 6	5.8

[a] expressed as mean ± standard error of independent experiments; [b] PI = photo-toxic index = IC_{50} (UV-A)/IC_{50} (dark). n.a. = not applicable.

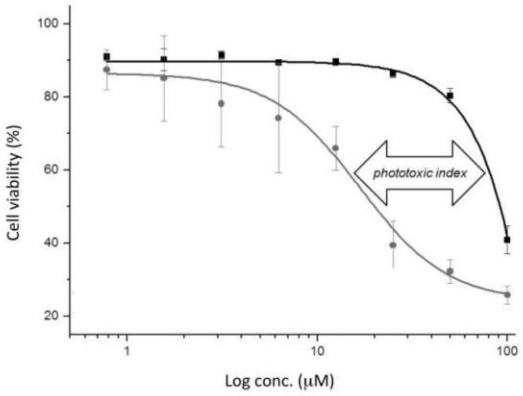

Figure 3. Dose-response curves for the anti-proliferative effect of Gd-L-Tat peptide conjugate on CAL-33 cells in the dark (black line) and upon UV-A irradiation (at 350 nm for 10 min, 2.58 J·cm^{-2}; grey line).

2.5. Cellular Uptake of Complexes and Conjugates

The ability of the two Gd(III) complexes and the Tat conjugate to enter CAL-33 cells was assessed using confocal fluorescence microscopy (Figure 4). Although the optimal excitation and emission wavelengths for the naphthalimide fluorophore are 356 and 417 nm for Gd-L and 362 and 471 nm for "clicked" Gd-L, respectively (Table 1), the compounds could also be reliably detected using the microscope's "hybrid 1 red wavelength" channel (excitation: 405 nm; emission: 600−800 nm) because of the brightness of the naphthalimide fluorophore, combined with the broadness of its absorption and emission peaks. For cells incubated with "clicked" Gd-L, only extremely weak fluorescence was observed (panels 2b and 3b), while cells treated with Gd-L were essentially non-fluorescent (panels 2c and 3c), indicating that these complexes are not able to enter CAL-33 cells. In contrast, for

cells incubated with the Gd-L-Tat peptide conjugate there was clear evidence of uptake and localisation within the cytoplasmic regions of the cells (panel 3d). This is consistent with the results of previous studies, which have shown that myristylated Tat is an effective cell-penetrating agent [55,81]. The experiments were performed at 100 μM, a concentration that resulted in a clear Gd-L-Tat signal. At this dose, it was possible to observe the early stages of induced cellular stress, in good agreement with the cytotoxicity investigation. It is worthwhile noting that, besides cytosolic uptake, Gd-L-Tat also displayed some punctate accumulation in regions ascribable to the cell nucleoli (panels 2d and 3d). Overall, the confocal microscopy results help to rationalise the cytotoxicity data: the conjugate is the only compound that exerts a cytotoxic effect because it is the only compound to enter the CAL-33 cells.

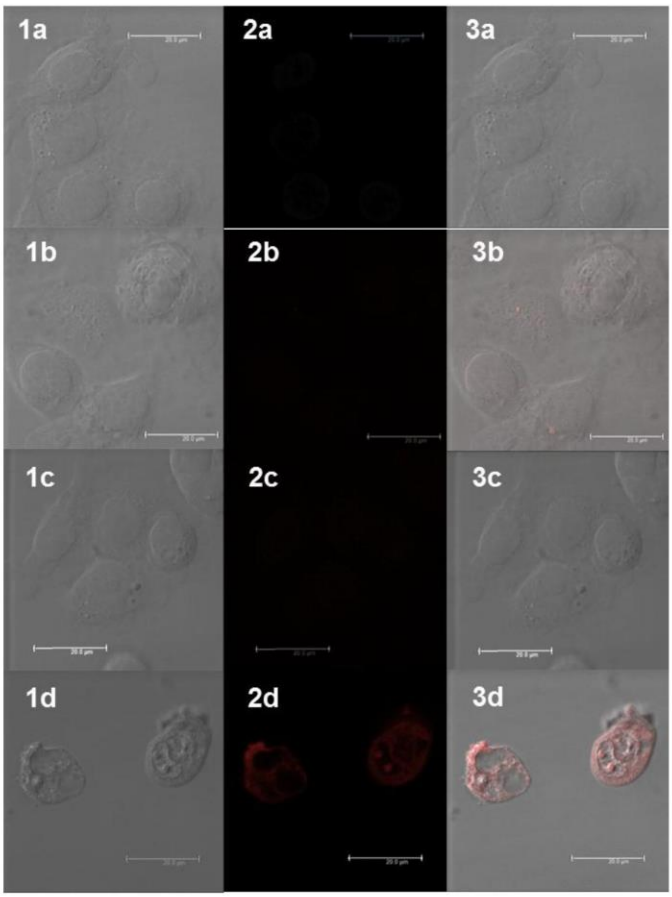

Figure 4. Confocal fluorescence microscopic images of CAL-33 cells incubated with Gd(III) complexes or conjugate for 4 h: (**1a**) DIC (differential interference contrast) image of the untreated Cal-33 cells; (**2a**) visualisation of background fluorescence in untreated CAL-33 cells using the excitation/emission wavelength settings (hybrid 1 channel) employed for detection of the Gd(III) compounds; (**3a**) merged image of the DIC and hybrid 1 channel images of untreated cells; (**1b**) DIC image of the CAL-33 cells treated with 100 μM of "clicked" Gd-L; (**2b**) visualisation of "clicked" Gd-L in cells; (**3b**) merged image of the DIC and hybrid 1 channel images of cells treated with "clicked" Gd-L; (**1c**) DIC image of the CAL-33 cells treated with 100 μM of Gd-L; (**2c**) visualisation of Gd-L in cells; (**3c**) merged image of the DIC and hybrid 1 channel images of cells treated with Gd-L; (**1d**) DIC image of the CAL-33 cells treated with 100 μM of Gd-L-Tat peptide conjugate; (**2d**) visualisation of Gd-L-Tat peptide conjugate in cells; (**3d**) merged image of the DIC and hybrid 1 channel images of cells treated with Gd-L-Tat peptide conjugate. The scale bars represent 20 μm.

3. Experimental Section

3.1. Materials and Methods

All chemicals were purchased from Sigma-Aldrich Pty (St. Louis, MO, USA), Matrix Scientific (Columbia, SC, USA), or Merck Group Ltd (Darmstadt, Germany) and used without purification. 1,4,7,10-Tetraazacyclododecane-1,4,7-triacetic acid ($^{t}Bu_3$DO3A.HBr) [76] and *tris*(3-hydroxypropyltriazolylmethyl)amine (THTPA) [77,78], were synthesised as per reported literature procedures. All solvents were reagent, analytical or HPLC grade.

Flash chromatography was carried out using Merck 38 Silica gel 60, 230–400 mesh ASTM. Thin layer chromatography (TLC) was performed on Merck Silica Gel 60 F254 plates. TLC plates were visualised using a UV lamp at 254 nm or through the use of $KMnO_4$ or ninhydrin staining agent.

Elemental analyses were performed by the Campbell Microanalytical Laboratory, Otago, New Zealand.

^{1}H and ^{13}C nuclear magnetic resonance (NMR) spectra were recorded using an Avance III Nanobay 400 MHz Bruker spectrometer (Billerica, MA, USA) coupled to the BACS 60 automatic sample changer at 400.13 MHz and 100.61 MHz, respectively. Data acquisition and processing was managed using Topspin software package version 3. Additional processing was handled with MestReNova software (PC). Chemical shifts (δ) were measured in parts per million, referenced to an internal standard of residual solvent. Spectroscopic data are given using the following abbreviations: s, singlet; d, doublet; dd, doublet of doublets; ddd, doublet of doublet of doublets; dt, doublet of triplets; t, triplet; m, multiplet; J, coupling constant.

Analytical high-performance liquid chromatography (HPLC) was carried out on an Agilent 1260 series modular HPLC (Santa Clara, CA, USA) equipped with the following modules: G1312B binary pump, G1316A thermostated column compartment equipped with an Agilent Eclipse Plus C18 3.5 µm, 4.6 × 100 mm column and a G1312B diode array detector. The following elution protocol was used: 0–10 min, gradient from 5% solvent B/95% solvent A to 100% solvent B (solvent A = 99.9% H_2O, 0.1% TFA, and solvent B = 99.9% acetonitrile (ACN), 0.1% TFA, except in the case of the analysis of Gd complexes, where solvent A = 99.9% H_2O, 0.1% formic acid, and solvent B = 99.9% ACN, 0.1% formic acid); flow rate = 1 mL·min^{-1}.

Preparative HPLC purification was carried out on an Agilent 1260 modular Prep HPLC equipped with the following modules: G1361A prep pump, G2260A prep automatic liquid sampler, G1364B fraction collector, G1315D diode array detector, and a Luna C8 5 µm, 100 Å AXIA, 250 × 21.2 mm column. The following elution protocol was used: 0–5 min, 100% solvent C; 5–30 min, gradient from 100% solvent A to 20% solvent C/80% solvent D (solvent C = 99.9% H_2O, 0.1% formic acid; solvent D = 99.9% ACN, 0.1% formic acid); flow rate = 20 mL·min^{-1}.

High-resolution mass spectrometric (HRMS) analyses were performed on a Waters LCT TOF LC-MS mass spectrometer (Milford, MA, USA) coupled to a 2795 Alliance Separations module. All data were acquired and mass corrected via a dual-spray Leucine Enkephaline reference sample. Mass spectra were generated by averaging the scans across each peak and background subtracted of the TIC. Acquisition and analysis were performed using the MassLynx software version 4.1. The mass spectrometer conditions were as follows: electrospray ionisation (ESI) mode, desolvation gas flow of 550 L·h^{-1}, desolvation temperature of 250 °C, source temperature of 110 °C, capillary voltage of 2400 V, sample cone voltage of 60 V, scan range acquired between 100–1500 m/z, one sec scan times and internal reference ions for positive ion mode (Leucine Enkephaline) of 556.2771.

Liquid chromatography-mass spectrometry (LC-MS) was performed using an Agilent 6100 Series Single Quad LC-MS coupled to an Agilent 1200 Series HPLC with the following mass spectrometer conditions: multimode-ESI mode, 300 °C drying gas temperature, 200 °C vaporising temperature, capillary voltage of 2000 V (positive), capillary voltage of 4000 V (negative), scan range between 100–1000 m/z with an 0.1 s step size and a 10 min acquisition time.

Analysis of the peptide conjugates was performed on a Shimadzu modular LC-MS system (Kyoto, Japan) equipped with the following modules: LC-20AD liquid chromatograph system, SPD-M20A diode array detector, CTO-20A column oven equipped with a Luna 3 micron C8(2) 3 µm, 100 Å, 100 × 2.0 mm column and a LC-MS-2020 system, operating in positive mode with an m/z scan range of 200–2000.

Absorbance spectra were recorded on a Varian Cary 50 Bio UV-Vis spectrophotometer (Palo Alto, CA, USA) using a 1 cm-path length quartz cuvette. Fluorescence emission spectra were acquired using a Varian Cary Eclipse fluorescence spectrophotometer using a 1 cm-path length quartz cuvette.

3.2. Synthetic Procedures

3.2.1. *tert-Butyl 2-(6-bromo-1,3-dioxo-1H-benzo[de]isoquinolin-2(3H)-yl)ethylcarbamate* (**1**)

4-Bromo-1,8-napthalic anhydride (3.00 g, 10.8 mmol) and *N*-(*tert*-butoxycarbonyl)-1, 2-ethylenediamine (1.91 g, 11.9 mmol) were dissolved in DMF (30 mL) and stirred at 80 °C overnight (O/N). The solution was then allowed to cool to room temperature (RT), before being poured into ice-cold water to produce a yellow precipitate, which was collected via vacuum filtration, washed several times with cold H_2O and dried in a vacuum desiccator overnight. Yield: 4.12 g, 91%. ^{1}H-NMR (DMSO-d_6) δ 8.62–8.39 (m, 2H), 8.26 (d, J = 7.2 Hz, 1H), 8.17 (d, J = 7.5 Hz, 1H), 7.95 (t, J = 7.4 Hz, 1H), 6.87 (s, 1H), 4.10 (s, 2H), 3.25 (d, J = 4.1 Hz, 2H), 1.19 (s, 9H). ^{13}C-NMR (DMSO-d_6) δ 163.05, 163.00, 155.77, 132.36, 131.38, 131.25, 130.76, 129.71, 128.83, 128.71, 128.39, 122.99, 122.23, 77.46, 37.63, 28.04. LC-MS (ESI): m/z 319.21 $[M - Boc + H]^+$ (100%). Analytical HPLC: 89% purity (254 nm).

3.2.2. *tert-Butyl 2-(1,3-dioxo-6-((trimethylsilyl)ethynyl)-1H-benzo[de]-isoquinolin-2(3H)-yl)ethylcarbamate* (**2**)

Compound 1 (4.00 g, 9.54 mmol), TMS acetylene (1.12 g, 1.49 mL, 11.5 mmol), $Pd(PPh_3)_2Cl_2$ (334 mg, 0.48 mmol), CuI (182 mg, 0.95 mmol) and Et_3N (2.90 g, 4.00 mL, 28.6 mmol) were all dissolved in dry THF (100 mL) and stirred at RT for 2 h under a N_2 atmosphere. The solution was combined with H_2O (100 mL) and extracted with dichoromethane (DCM) (3 × 100 mL). The combined extracts were dried over $MgSO_4$ and evaporated *in vacuo* to produce a dark brown-black solid, which was subjected to silica gel chromatography (10% EtOAc in DCM,) to yield the product as a pale yellow solid (R_f = 0.6). Yield: 1.99 g, 48%. ^{1}H-NMR (DMSO-d_6) δ 8.52 (dd, J = 13.6, 7.8 Hz, 2H), 8.39 (d, J = 7.6 Hz, 1H), 7.91 (t, J = 8.0 Hz, 2H), 6.80 (t, J = 6.2 Hz, 1H), 4.13 (t, J = 5.8 Hz, 2H), 3.27 (dd, J = 11.6, 5.9 Hz, 2H), 1.21 (s, 9H), 0.34 (s, 9H). ^{13}C-NMR (DMSO-d_6) δ 163.20, 162.91, 155.67, 131.27, 131.01, 130.93, 130.85, 129.53, 127.86, 127.34, 125.68, 122.81, 122.39, 104.51, 101.07, 77.32, 37.63, 27.97, −0.37. LC-MS (ESI): m/z 337.11 $[M - Boc + H]^+$ (100%). Analytical HPLC: 94% purity (254 nm).

3.2.3. *2-(2-Aminoethyl)-6-((trimethylsilyl)ethynyl)-1H-benzo[de]isoquinoline-1,3(2H)-dione* (**3**)

Compound 2 (2.00 g, 4.58 mmol) was stirred in a 1:4 (v/v) mixture of DCM and TFA at RT for 4 h. The DCM and the bulk of the TFA were then removed *in vacuo*, leaving a thick orange liquid. Upon the addition of H_2O (50 mL), a yellow precipitate formed, which was collected via vacuum filtration, washed several times with cold H_2O and dried in a vacuum desiccator overnight. Yield: 1.48 g, 96%. ^{1}H-NMR (400 MHz, DMSO-d_6) δ 8.50 (ddd, J = 8.3, 7.8, 1.0 Hz, 2H), 8.36 (d, J = 7.6 Hz, 1H), 7.95 (dt, J = 7.4, 4.0 Hz, 2H), 4.30 (t, J = 5.8 Hz, 2H), 3.26–3.06 (m, 2H), 0.36 (s, 9H). ^{13}C-NMR (101 MHz, DMSO-d_6) δ 163.70, 163.41, 131.55, 131.32, 131.13, 130.90, 129.80, 128.34, 127.31, 125.79, 122.78, 122.37, 105.07, 101.16, 37.61, 37.51, −0.25. LC-MS (ESI): m/z 337.10 $[M + H]^+$. Analytical HPLC: 91% purity (254 nm).

3.2.4. *2-Bromo-N-(2-(1,3-dioxo-6-((trimethylsilyl)ethynyl)-1H-benzo[de]isoquinolin-2(3H)-yl)ethyl)acetamide* (**4**)

Compound 3 (1.50 g, 4.46 mmol), bromoacetyl bromide (1.80 g, 777 µL, 8.92 mmol) and Na_2CO_3 (1.42 g, 13.4 mmol) were dissolved in acetone (50 mL) and stirred at RT for 2 h. The solvent was

removed *in vacuo* to produce a brown solid. Purification via silica gel chromatography (20% EtOAc in petroleum spirits) yielded the product as a pale yellow solid (R_f = 0.1). Yield: 1.21 g, 59%. ^{1}H-NMR (DMSO-d_6) δ 8.55–8.46 (m, 2H), 8.36 (dd, J = 7.6, 3.2 Hz, 1H), 7.98–7.91 (m, 2H), 4.13 (t, J = 6.3 Hz, 2H), 3.71 (d, J = 14.0 Hz, 2H), 3.54–3.34 (m, 2H), 0.35 (s, 9H). ^{13}C-NMR (DMSO-d_6) δ 131.63, 131.45, 131.23, 130.12, 128.67, 127.62, 125.90, 125.81, 123.20, 123.10, 122.82, 122.70, 105.20, 105.12, 101.53, 61.66, 37.26, 36.67, 29.64, 0.06. LC-MS (ESI): m/z 457.00 (100%) $[M + H]^+$. Analytical HPLC: 97% purity (254 nm).

3.2.5. *tri-tert-Butyl 2,2′,2″-(10-(2-((2-(1,3-Dioxo-6-((trimethylsilyl)ethyn-yl)-1H-benzo[de]isoquinolin-2(3H)-yl)ethyl)amino)-2-oxoethyl)-1,4,7,10-tetraazacyclododecane-1,4,7-triyl)triacetate* (**5**)

Compound 4 (350 mg, 0.76 mmol), ^{t}Bu$_3$DO$_3$A.HBr (414 mg, 0.70 mmol), and DIPEA (180 mg, 242 µL, 1.39 mmol) were dissolved in ACN (50 mL) and the mixture refluxed overnight. The solvent was removed *in vacuo* and the residue subjected to silica gel chromatography (5% MeOH in DCM) to isolate the product as a glassy yellow solid (R_f = 0.1). Yield: 460 mg, 81%. ^{1}H-NMR ($CDCl_3$) δ 8.56 (dd, J = 8.4, 1.1 Hz, 1H), 8.53 (dd, J = 7.3, 1.1 Hz, 1H), 8.41 (d, J = 7.6 Hz, 1H), 7.81 (d, J = 7.6 Hz, 1H), 7.76 (dd, J = 8.3, 7.4 Hz, 1H), 4.37–1.97 (broad set of overlapping signals, 28H), 1.42 (d, J = 2.9 Hz, 27H), 0.33 (s, 9H). ^{13}C-NMR ($CDCl_3$) δ 172.51, 172.19, 164.34, 164.02, 132.61, 131.85, 131.74, 131.18, 130.49, 128.00, 127.61, 127.46, 122.75, 122.16, 105.53, 101.26, 81.86, 81.81, 56.49, 55.76, 54.23, 42.60, 39.61, 38.36, 28.24, 28.06, 27.99, −0.08. LC-MS (ESI): m/z 446.47 $[M + 2H]^{2+}$ (100%). Analytical HPLC: 93% purity (254 nm).

3.2.6. *2,2′,2″-(10-(2-((2-(6-Ethynyl-1,3-dioxo-1H-benzo[de]isoquinolin-2(3H)-yl)ethyl)amino)-2-oxoethyl)-1,4,7,10-tetraazacyclododecane-1,4,7-triyl)triacetic acid* (L)

Compound 5 (320 mg, 0.36 mmol) and KF (42 mg, 0.72 mmol) were dissolved in 1:1 (v/v) mixture of H_2O and ACN (10 mL) and the solution stirred for 3 h at RT. The solvent was removed *in vacuo* and the remaining residue dissolved in a 1:1 (v/v) mixture of TFA and DCM and stirred O/N at RT. After removal of the TFA and DCM using a nitrogen stream, the crude product was purified by preparative HPLC. Lypholisation yielded a fluffy orange solid. Yield: 167 mg, 71%. ^{1}H-NMR (CD_3OD) δ 8.73 (dd, J = 8.4, 1.1 Hz, 1H), 8.62 (dd, J = 7.3, 1.1 Hz, 1H), 8.52 (d, J = 7.6 Hz, 1H), 8.00 (d, J = 7.6 Hz, 1H), 7.93 (dd, J = 8.4, 7.4 Hz, 1H), 4.42 (s, 1H), 4.49–3.00 (broad set of overlapping signals, 28H). ^{13}C-NMR (CD_3OD) δ 164.40, 164.08, 132.07, 131.78, 131.39, 130.00, 127.79, 127.69, 126.68, 122.65, 122.31, 118.15, 115.24, 39.21, 37.74. HRMS (ESI): m/z calc'd for $[M + H]^+$, M = $C_{32}H_{38}N_6O_9$: 651.2779, found: 651.2773. Analytical HPLC: 96% purity (254 nm).

3.2.7. Gd-L

Ligand L (38 mg, 47 µmol) and $Gd(OAc)_3$ (39 mg, 120 µmol) were dissolved in MilliQ H_2O (5 mL) and the pH adjusted to *ca.* 7 with 2 M NaOH. The resulting solution was stirred at 70 °C for 2 h, after which time LC-MS showed complete complexation. The product was purified via preparative HPLC and isolated as a fluffy orange solid following lyophilisation. Yield: 20 mg, 53%. Anal. Calc'd for $C_{32}H_{35}N_6O_9Gd \cdot 6H_2O$: C, 42.10; H, 5.19; N, 9.20. Found: C, 42.09; H, 5.06; N, 9.11. HRMS (ESI): m/z calc'd for $[M + H]^+$, M = $C_{32}H_{35}N_6O_9Gd$: 806.1785, found: 806.1779. Analytical HPLC: 96% purity (254 nm).

3.2.8. "Clicked" Gd-L

Ligand L (38 mg, 47 µmol) and $Gd(OAc)_3$ (39 mg, 120 µmol) were dissolved in MilliQ H_2O (5 mL) and pH adjusted to *ca.* 7 with 2 M NaOH. The resulting solution was stirred at 70 °C for 2 h. After this time, the pH of the solution was readjusted to *ca.* 7, then 3-azidopropan-1-ol (9.6 mg, 95 µmol), sodium ascorbate (18.7 mg, 95 µmol), $CuSO_4$ (0.7 mg, 5 µmol) and THPTA (4.3 mg, 10 µmol) added and the mixture stirred at RT O/N. The product was purified by preparative HLPC and isolated as a fluffy orange solid after lyophilisation. Yield: 20 mg, 47%. Anal. Calc'd for $C_{35}H_{42}N_9O_{10}Gd \cdot 6H_2O$:

C, 41.45; H, 5.37; N, 12.43. Found: C, 41.82; H, 5.27; N, 12.36. HRMS (ESI): m/z calc'd for $[M + H]^+$ M = $C_{35}H_{42}N_9O_{10}Gd$: 907.2374, found: 907.2413. Analytical HPLC: 96% purity (254 nm).

3.2.9. Peptide Conjugation

To a solution of Myr-Lys(N_3)-YGRKKRRQRRR [55] (10 mg, 5.2 µmol) in MilliQ water (5 mL) was added Gd-L (10 mg, 12 µmol), followed by $CuSO_4$ (0.8 mg, 5 µmol), THPTA (4.5 mg, 10 µmol) and sodium ascorbate (3.1 mg, 16 µmol). The pH was then adjusted to 6–7 with 1 M HCl and the mixture stirred O/N at RT. Peptide LC-MS analysis showed near-complete consumption of starting peptide after this time. The product was isolated as a white solid following preparative HPLC and lyophilisation. Peptide LC-MS (ESI): m/z 986.95 $[M + 2TFA + H]^{3+}$, 90% purity (214 nm).

3.3. Quantum Yield Determinations

Complexes were prepared at a range on concentrations in a 100 mM HEPES buffer at pH 7.4, and absorbance and fluorescence emission spectra recorded. Quantum yields (Φ) were then determined, using quinine sulphate in 0.1 M sulfuric acid as the reference compound (Φ = 54%) [80], according to the following equation:

$$\Phi_X = \Phi_{ST} \times (Grad_x/Grad_{ST}) \times (\eta_X/\eta_{ST})^2$$

where Φ is the quantum yield, X and ST denote the sample and reference, respectively, Grad is the gradient of the integrated fluorescence *vs.* absorbance plot, and η represents the refractive index of the solvent.

3.4. Cell Culture

Tongue squamous carcinoma cells (CAL-33) were cultured in phenol red-free RPMI medium (Gibco) supplemented with 10% fetal calf serum (FCS, Gibco), 1% glutamax (Gibco), 100 U penicillin mL^{-1}, 100 µg streptomycin mL^{-1} at 37 °C and 6% CO_2.

3.5. Cytotoxicity Studies

Cytotoxicity studies of the effect of irradiation on CAL-33 cells treated with Gd-L, "clicked" Gd-L and the Gd-L-Tat peptide conjugate were performed via a fluorimetric cell viability assay using resazurin (Promocell GmbH). Briefly, one day before treatment, cells were plated in triplicate into 96-well plates at a density of 4×10^3 cells$\cdot$ well^{-1} in 100 µL of medium. After addition of increasing concentrations of the test compound, cells were incubated for 4 h, then the medium was replaced with fresh medium devoid of compound. The plates were irradiated for 10 min at 350 nm (2.58 J$\cdot$ cm^{-2}) in a Rayomet Chamber Reactor. Upon further incubation at 37 °C in 6% CO_2 for 44 h, the medium was removed and complete medium (100 µL) containing resazurin (0.2 mg$\cdot$ mL^{-1} final concentration) was added. After 4 h of incubation at 37 °C in 6% CO_2, the fluorescence of the intensely red fluorescent resorufin product was quantified using a SpectraMax M5 microplate reader (excitation: 540 nm; emission: 590 nm).

3.6. Cellular Uptake Studies

Cellular uptake and localisation of Gd-L, "clicked" Gd-L and the Gd-L-Tat peptide conjugate was assessed by confocal fluorescence microscopy. CAL-33 cells were grown on 18-mm Menzel-gläser coverslips at a density of 2×10^5 cells$\cdot$ mL^{-1} and incubated for 4 h with one of the compounds (100 µM). Cells were fixed in 4% formaldehyde in phosphate-buffered saline (PBS), washed with PBS and H_2O, and mounted on slides for viewing. Fixed cells were viewed on a CLSM Leica SP5 microscope (Heerbrugg, Switzerland), with the compounds visualised using the hybrid 1 red wavelength selection on the microscope (excitation: 405 nm; emission: 600−800 nm). It should be noted that there is the possibility that fixation may change the cellular localisation of fluorescent molecules as they may be washed out or redistributed.

4. Conclusions

In conclusion, we have developed a new Gd(III)-DOTA-naphthalimide complex that can be readily conjugated to azide-bearing molecules via the Cu(I)-catalysed click reaction to introduce a fluorescent and photo-cytotoxic label. Whilst the photo-physical properties of the naphthalimide group are not optimal for PDT, the complex represents a useful prototype building block for the facile construction of new theranostic agents for combined PDT and optical imaging. By virtue of the Gd centre, the complex could also serve as an effective MRI contrast agent if incorporated into appropriate *in vivo* imaging agent designs. Future work will include measurement of the proton nuclear magnetic relaxation dispersion of the "clicked" Gd-L complex to confirm this capability. Since MRI is a very insensitive technique, it will also be important to establish conjugate designs that are able to deliver sufficient concentrations of Gd-L to desired sites (e.g., diseased tissue) to provide adequate image contrast *in vivo*.

Supplementary Materials: The following are available online at http://www.mdpi.com/1420-3049/21/2/194/s1. NMR spectra of reported compounds, LC traces for final ligand, Gd(III) complexes and peptide conjugate.

Acknowledgments: Financial support by the Australian Research Council (DP120100561, DP150100383 and FT130100838 to B.G., and DP130100816 to L.S.), the Swiss National Science Foundation (Professorships N° PP00P2_133568 and PP00P2_157545 to G.G.), the Stiftung für Wissenschaftliche Forschung of the University of Zurich (G.G.), the UBS Promedica Stiftung (R.R. and G.G.), the Novartis Jubilee Foundation (R.R. and G.G.) and the University of Zurich (G.G.) is gratefully acknowledged. The authors thank the Center for Microscopy and Image Analysis of the University of Zurich for access to state-of-the-art equipment.

Author Contributions: M.R.G., L.S., K.L.T., G.G. and B.G. conceived and designed the experiments; W.O., R.R. and M.L.A. performed the experiments; W.O., R.R., M.R.G., L.S., K.L.T., G.G. and B.G. analyzed the data; W.O., R.R., L.S., K.L.T., G.G. and B.G. wrote the paper.

Conflicts of Interest: The authors declare no conflict of interest.

Abbreviations

The following abbreviations are used in this manuscript:

ACN:	acetonitrile
BOC:	*tert*-butoxycarbonyl
$^{t}Bu_3$DO3A:	*tert*-butyl-protected 1,4,7,10-tetraazacyclodocane-1,4,7,10-tetraacetic acid
d:	doublet
dd:	doublet of doublets
ddd:	doublet of doublet of doublets
dt:	doublet of triplets
DCM:	dichloromethane
DIC:	differential interference contrast
DIPEA:	*N*,*N*-diisopropylethylamine
DMF:	*N*,*N*-dimethylformamide
DOTA:	1,4,7,10-tetraazacyclodocane-1,4,7,10-tetraacetic acid
ESI:	electrospray ionization
HEPES:	4-(2-hydroxyethyl)-1-piperazineethanesulfonic acid
HPLC:	high-performance liquid chromatography
HRMS:	high-resolution mass spectrometry
IC_{50}:	half maximal inhibitory concentration
J:	coupling constant
LC-MS:	liquid chromatography-mass spectrometry
m:	multiplet
MRI:	magnetic resonance imaging
NMR:	nuclear magnetic resonance NMR

O/N:	overnight
PBS:	phosphate-buffered saline
PDT:	photo-dynamic therapy
PI:	photo-toxic index
RT:	room temperature
R_f:	retention factor
s:	singlet
SPAAC:	strain-promoted azide-alkyne cycloaddition
t:	triplet
TAT:	trans-activator of transcription
THF:	tetrahydrofuran
TFA:	trifluoroacetic acid
THPTA:	*tris*(3-hydroxypropyl-triazolylmethyl)amine
TLC:	thin layer chromatography
TMS:	trimethylsilyl
UV-A:	ultraviolet A radiation
Φ:	quantum yield

References

1. Lee, S.Y.; Jeon, S.I.; Jung, S.; Chung, I.J.; Ahn, C.-H. Targeted multimodal imaging modalities. *Adv. Drug Del. Rev.* **2014**, *76*, 60–78. [CrossRef] [PubMed]
2. Melendez-Alafort, L.; Muzzio, P.C.; Rosato, A. Optical and multimodal peptide-based probes for *in vivo* molecular imaging. *Anticancer Agents Med. Chem.* **2012**, *12*, 476–499. [CrossRef] [PubMed]
3. Kobayashi, H.; Longmire, M.R.; Ogawa, M.; Choyke, P.L. Rational chemical design of the next generation of molecular imaging probes based on physics and biology: Mixing modalities, colors and signals. *Chem. Soc. Rev.* **2011**, *40*, 4626–4648. [CrossRef] [PubMed]
4. Louie, A. Multimodality imaging probes: Design and challenges. *Chem. Rev.* **2010**, *10*, 3146–3195. [CrossRef] [PubMed]
5. Jennings, L.E.; Long, N.J. "Two is better than one"—Probes for dual-modality molecular imaging. *Chem. Commun.* **2009**, 3511–3524. [CrossRef] [PubMed]
6. Fass, L. Imaging and cancer: A review. *Mol. Oncol.* **2008**, *2*, 115–152. [CrossRef] [PubMed]
7. Glasspool, R.M.; Evans, T.R. Clinical imaging of cancer metastasis. *Eur. J. Cancer* **2000**, *36*, 1661–1670. [CrossRef]
8. Palekar-Shanbhag, P.; Jog, S.V.; Chogale, M.M.; Gaikwad, S.S. Theranostics for cancer therapy. *Curr. Drug Deliv.* **2013**, *10*, 357–362. [CrossRef] [PubMed]
9. Lammers, T.; Rizzo, L.Y.; Storm, G.; Kiessling, F. Personalized nanomedicine. *Clin. Cancer Res.* **2012**, *18*, 4889–4894. [CrossRef] [PubMed]
10. Kelkar, S.S.; Reineke, T.M. Theranostics: Combining imaging and therapy. *Bioconjugate Chem.* **2011**, *22*, 1879–1903. [CrossRef] [PubMed]
11. Kumar, R.; Shin, W.S.; Sunwoo, K.; Kim, W.Y.; Koo, S.; Bhuniya, S.; Kim, J.S. Small conjugate-based theranostic agents: An encouraging approach for cancer therapy. *Chem. Soc. Rev.* **2015**, *44*, 6670–6683. [CrossRef] [PubMed]
12. Lim, E.-K.; Kim, T.; Paik, S.G.; Haam, S.; Huh, Y.-M.; Lee, K. Nanomaterials for theranostics: Recent advances and future challenges. *Chem. Rev.* **2015**, *115*, 327–394. [CrossRef] [PubMed]
13. Muthu, M.S.; Leong, D.T.; Mei, L.; Feng, S.-S. Nanotheranostics—Application and further development of nanomedicine strategies for advanced theranostics. *Theranostics* **2014**, *4*, 660–677. [CrossRef] [PubMed]
14. Wang, Y.; Shim, M.S.; Levinson, N.S.; Sung, H.-W.; Xia, Y. Stimuli-responsive materials for controlled release of theranostic agents. *Adv. Funct. Metar.* **2014**, *24*, 4206–4220. [CrossRef] [PubMed]

15. Caldorera-Moore, M.E.; Liechty, W.B.; Peppas, N.A. Responsive theranostic systems: Integration of diagnostic imaging agents and responsive controlled release drug delivery carriers. *Acc. Chem. Res.* **2011**, *44*, 1061–1070. [CrossRef] [PubMed]
16. Bansal, A.; Zhang, Y. Photocontrolled nanoparticle delivery systems for biomedical applications. *Acc. Chem. Res.* **2014**, *47*, 3052–3060. [CrossRef] [PubMed]
17. Salvatore, S. Photoactivated nanomaterials for biomedical release applications. *J. Mater. Chem.* **2012**, *22*, 301–318.
18. Rai, P.; Mallidi, S.; Zheng, X.; Rahmanzadeh, R.; Mir, Y.; Elrington, S.; Khurshid, A.; Hasan, T. Development and applications of photo-triggered theranostic agents. *Adv. Drug Deliv. Rev.* **2010**, *62*, 1094–1124. [CrossRef] [PubMed]
19. Schmitt, J.; Heitz, V.; Sour, A.; Bolze, F.; Kessler, P.; Flamigni, L.; Ventura, B.; Bonnet, C.S.; Tóth, E. A theranostic agent combining a two-photon-absorbing photosensitizer for photodynamic therapy and a gadolinium(III) complex for MRI detection. *Chem. Eur. J.* **2016**. [CrossRef] [PubMed]
20. Dixit, S.; Novak, T.; Miller, K.; Zhu, Y.; Kenney, M.E.; Broome, A.M. Transferrin receptor-targeted theranostic gold nanoparticles for photosensitizer delivery in brain tumors. *Nanoscale* **2015**, *7*, 1782–1790. [CrossRef] [PubMed]
21. Truillet, C.; Lux, F.; Moreau, J.; Four, M.; Sancey, L.; Chevreux, S.; Boeuf, G.; Perriat, P.; Frochot, C.; Antoine, R.; *et al*. Bifunctional polypyridyl-Ru(II) complex grafted onto gadolinium-based nanoparticles for MR-imaging and photodynamic therapy. *Dalton Trans.* **2013**, *42*, 12410–12420. [CrossRef] [PubMed]
22. Cao, Y.; Pan, R.; Xuan, W.; Wei, Y.; Liu, K.; Zhou, J.; Wang, W. Photo-triggered fluorescent theranostic prodrugs as DNA alkylating agents for mechlorethamine release and spatiotemporal monitoring. *Org. Biomol. Chem.* **2015**, *13*, 6742–6748. [CrossRef] [PubMed]
23. Karaoun, N.; Renfrew, A.K. A luminescent ruthenium(II) complex for light-triggered drug release and live cell imaging. *Chem. Commun.* **2015**, 14038–14041. [CrossRef] [PubMed]
24. Knoll, J.D.; Turro, C. Control and utilization of ruthenium and rhodium metal complex excited states for photoactivated cancer therapy. *Coord. Chem. Rev.* **2015**, *282*, 110–126. [CrossRef] [PubMed]
25. Mari, C.; Pierroz, V.; Leonidova, A.; Ferrari, S.; Gasser, G. Towards selective light-activated Ru^{II}-based prodrug candidates. *Eur. J. Inorg. Chem.* **2015**, *23*, 3879–3891. [CrossRef]
26. Leonidova, A.; Pierroz, V.; Rubbiani, R.; Lan, Y.; Schmitz, A.G.; Kaech, A.; Sigel, R.K.O.; Ferrari, S.; Gasser, G. Photo-induced uncaging of a specific Re(I) organometallic complex in living cells. *Chem. Sci.* **2014**, *5*, 4044–4056. [CrossRef]
27. Dai, Y.; Xiao, H.; Liu, J.; Yuan, Q.; Ma, P.A.; Yang, D.; Li, C.; Cheng, Z.; Hou, Z.; Yang, P.; *et al*. *In vivo* multimodality imaging and cancer therapy by near-infrared light-triggered trans-platinum pro-drug-conjugated upconverison nanoparticles. *J. Am. Chem. Soc.* **2013**, *135*, 18920–18929. [CrossRef] [PubMed]
28. Shi, G.; Monro, S.; Hennigar, R.; Colpitts, J.; Fong, J.; Kasimova, K.; Yin, H.; DeCoste, R.; Spencer, C.; Chamberlain, L.; *et al*. Ru(II) dyads derived from α-oligothiophenes: A new class of potent and versatile photosensitizers for PDT. *Coord. Chem. Rev.* **2015**, *282*, 127–138. [CrossRef]
29. Ma, D.-L.; He, H.-Z.; Leung, K.-H.; Chan, D.S.-H.; Leung, C.-H. Bioactive luminescent transition-metal complexes for biomedical applications. *Angew. Chem. Int. Ed.* **2013**, *52*, 7666–7682. [CrossRef] [PubMed]
30. Yua, A.; Wu, J.; Tang, X.; Zhao, L.; Xu, F.; Hu, Y. Application of near-infrared dyes for tumor imaging, photothermal, and photodynamic therapies. *J. Pharm. Sci.* **2013**, *102*, 6–28.
31. Meldal, M.; Tornø, C.W. Cu-catalyzed azide-alkyne cycloaddition. *Chem. Rev.* **2008**, *108*, 2952–3015. [CrossRef] [PubMed]
32. Kolb, H.C.; Finn, M.G.; Sharpless, K.B. Click chemistry: Diverse chemical function from a few good reactions. *Angew. Chem. Int. Ed.* **2001**, *40*, 2004–2021. [CrossRef]
33. Jewett, J.C.; Bertozzi, C.R. Cu-free click cycloaddition reactions in chemical biology. *Chem. Soc. Rev.* **2010**, *39*, 1272–1279. [CrossRef] [PubMed]
34. Baskin, J.M.; Prescher, J.A.; Laughlin, S.T.; Agard, N.J.; Chang, P.V.; Miller, I.A.; Lo, A.; Codelli, J.A.; Bertozzi, C.R. Copper-free click chemistry for dynamic *in vivo* imaging. *Proc. Natl. Acad. Sci. USA* **2007**, *104*, 16793–16797. [CrossRef] [PubMed]

35. Kim, H.L.; Sachin, K.; Jeong, H.J.; Choi, W.; Lee, H.S.; Kim, D.W. F-18 labeled RGD probes based on bioorthogonal strain-promoted click reaction for PET imaging. *ACS Med. Chem. Lett.* **2015**, *6*, 402–407. [CrossRef] [PubMed]
36. Li, G.; Xing, Y.; Wang, J.; Conti, P.S.; Chen, K. Near-infrared fluorescence imaging of CD13 receptor expression using a novel Cy5.5-labeled dimeric NGR peptide. *Amino Acids* **2014**, *46*, 1547–1556. [CrossRef] [PubMed]
37. Zeng, D.; Zeglis, B.M.; Lewis, J.S.; Anderson, C.J. The growing impact of bioorthogonal click chemistry on the development of radiopharmaceuticals. *J. Nucl. Med.* **2013**, *54*, 829–832. [CrossRef] [PubMed]
38. Chen, K.; Wang, X.; Lin, W.-Y.; Shen, C.K.-F.; Yap, L.-P.; Hughes, L.D.; Conti, P.S. Strain-promoted catalyst-free click chemistry for rapid construction of ^{64}Cu-labeled PET imaging probes. *ACS Med. Chem. Lett.* **2012**, *3*, 1019–1023. [CrossRef] [PubMed]
39. Lee, D.E.; Na, J.H.; Lee, S.; Kang, C.M.; Kim, H.N.; Han, S.J.; Kim, H.; Choe, Y.S.; Jung, K.H.; Lee, K.C.; *et al*. Facile method to radiolabel glycol chitosan nanoparticles with ^{64}Cu via copper-free click chemistry for MicroPET imaging. *Mol. Pharm.* **2013**, *10*, 2190–2198. [CrossRef] [PubMed]
40. Zhang, P.; Liu, S.; Gao, D.; Hu, D.; Gong, P.; Sheng, Z.; Deng, J.; Ma, Y.; Cai, L. Click-functionalized compact quantum dots protected by multidentate-imidazole ligands: Conjugation-ready nanotags for living-virus labeling and imaging. *J. Am. Chem. Soc.* **2012**, *134*, 8388–8391. [CrossRef] [PubMed]
41. Das, M.; Bandyopadhyay, D.; Mishra, D.; Datir, S.; Dhak, P.; Jain, S.; Maiti, T.K.; Basak, A.; Pramanik, P. "Clickable", trifunctional magnetite nanoparticles and their chemoselective biofunctionalization. *Bioconjugate Chem.* **2011**, *22*, 1181–1193. [CrossRef] [PubMed]
42. Beal, D.M.; Albrow, V.E.; Burslem, G.; Hitchen, L.; Fernandes, C.; Lapthorn, C.; Roberts, L.R.; Selby, M.D.; Jones, L.H. Click-enabled heterotrifunctional template for sequential bioconjugations. *Org. Biomol. Chem.* **2012**, *10*, 548–554. [CrossRef] [PubMed]
43. Clavé, G.; Volland, H.; Flaender, M.; Gasparutto, D.; Romieu, A.; Renard, P.-Y. A universal and ready-to-use heterotrifunctional cross-linking reagent for facile synthetic access to sophisticated bioconjugates. *Org. Biomol. Chem.* **2010**, *8*, 4329–4345. [CrossRef] [PubMed]
44. Ornelas, C.; Weck, M. Construction of well-defined multifunctional dendrimers using a trifunctional core. *Chem. Commun.* **2009**, 5710–5712. [CrossRef] [PubMed]
45. Mari, C.; Pierroz, V.; Ferrari, S.; Gasser, G. Combination of Ru(II) complexes and light: New frontiers in cancer therapy. *Chem. Sci.* **2015**, *6*, 2660–2686. [CrossRef]
46. Antoni, P.M.; Naik, A.; Albert, I.; Rubbiani, R.; Gupta, S.; Ruiz-Sánchez, P.; Munikorn, P.; Mateos, J.M.; Luginbuehl, V.; Thamyongkit, P.; *et al*. (Metallo) porphyrins as potent phototoxic anti-cancer agents after irradiation with red light. *Chem. Eur. J.* **2015**, *21*, 1179–1183. [CrossRef] [PubMed]
47. Mion, G.; Gianferrara, T.; Bergamo, A.; Gasser, G.; Pierroz, V.; Rubbiani, R.; Vilar, R.; Leczkowska, A.; Alessio, E. Phototoxic activity and DNA interactions of water-soluble porphyrins and their rhenium(I) conjugates. *ChemMedChem* **2015**, *10*, 1901–1914. [CrossRef] [PubMed]
48. Gianferrara, T.; Spagnul, C.; Alberto, R.; Gasser, G.; Ferrari, S.; Pierroz, V.; Bergamo, A.; Alessio, E. Towards matched pairs of porphyrin–Re^{I}/$^{99m}Tc^{I}$ conjugates that combine photodynamic activity with fluorescence and radio imaging. *ChemMedChem* **2014**, *9*, 1231–1237. [CrossRef] [PubMed]
49. Frei, A.; Rubbiani, R.; Tubafard, S.; Blacque, O.; Anstaett, P.; Felgenträger, A.; Maisch, T.; Spiccia, L.; Gasser, G. Synthesis, characterization, and biological evaluation of new Ru(II) polypyridyl photosensitizers for photodynamic therapy. *J. Med. Chem.* **2014**, *57*, 7280–7292. [CrossRef] [PubMed]
50. Mari, C.; Pierroz, V.; Rubbiani, R.; Patra, M.; Hess, J.; Spingler, B.; Oehninger, L.; Schur, J.; Ott, I.; Salassa, L.; *et al*. DNA intercalating Ru^{II} polypyridyl complexes as effective photosensitizers in photodynamic therapy. *Chem. Eur. J.* **2014**, *44*, 14421–14436. [CrossRef] [PubMed]
51. Leonidova, A.; Pierroz, V.; Rubbiani, R.; Heier, J.; Ferrari, S.; Gasser, G. Towards cancer cell-specific phototoxic organometallic rhenium(I) complexes. *Dalton Trans.* **2014**, *43*, 4287–4294. [CrossRef] [PubMed]
52. Naik, A.; Rubbiani, R.; Gasser, G.; Spingler, B. Visible-light-induced annihilation of tumor cells with platinum–porphyrin conjugates. *Angew. Chem. Int. Ed.* **2014**, *53*, 6938–6941. [CrossRef] [PubMed]
53. Gasser, G.; Hüsken, N.; Köster, S.D.; Metzler-Nolte, N. Synthesis of organometallic PNA oligomers by click chemistry. *Chem. Commun.* **2008**, 3675–3677. [CrossRef] [PubMed]
54. Gasser, G.; Pinto, A.; Neumann, S.; Sosniak, A.M.; Seitz, M.; Merz, K.; Heumann, R.; Metzler-Nolte, N. Synthesis, characterisation and bioimaging of a fluorescent rhenium-containing PNA bioconjugate. *Dalton Trans.* **2012**, *41*, 2304–2313. [CrossRef] [PubMed]

55. Leonidova, A.; Pierroz, V.; Adams, L.A.; Barlow, N.; Ferrari, S.; Graham, B.; Gasser, G. Enhanced cytotoxicity through conjugation of a "clickable" luminescent Re(I) complex to a cell-penetrating lipopeptide.*ACS Med. Chem. Lett.* **2014**, *5*, 809–814. [CrossRef] [PubMed]
56. Viehweger, K.; Barbaro, L.; Pombo García, K.; Joshi, T.; Geipel, G.; Steinbach, J.; Stephan, H.; Spiccia, L.; Graham, B. EGF receptor-targeting peptide conjugate incorporating a near-IR fluorescent dye and a novel 1, 4, 7-triazacyclononane-based ^{64}Cu(II) chelator assembled via click chemistry. *Bioconjugate Chem.* **2014**, *25*, 1011–1022. [CrossRef] [PubMed]
57. Choy, T.H.; Ozawa, K.; Tuck, K.L.; Barlow, N.; Huber, T.; Otting, G.; Graham, B. Lanthanide tags for site-specific ligation to an unnatural amino acid and generation of pseudocontact shifts in proteins. *Bioconjugate Chem.* **2013**, *24*, 260–268.
58. Loh, C.-T.; Graham, B.; Abdelkader, E.H.; Tuck, K.L.; Otting, G. Generation of pseudocontact shifts in proteins with lanthanides using small "clickable" nitrilotriacetic acid and iminodiacetic acid tags. *Chem. Eur. J.* **2015**, *21*, 5084–5092. [CrossRef] [PubMed]
59. Abdelkader, E.H.; Feintuch, A.; Yao, X.; Adams, L.A.; Aurelio, L.; Graham, B.; Goldfarb, D.; Otting, G. Protein conformation by EPR spectroscopy using gadolinium tags clicked to genetically encoded *p*-azido-L-phenylalanine. *Chem. Commun.* **2015**, 15898–15901. [CrossRef] [PubMed]
60. Choi, W.-T.; Liu, H.-W.; Lo, K.K.-W. Rhenium(I) polypyridine dibenzocyclooctyne complexes as phosphorescent bioorthogonal probes: Synthesis, characterization, emissive behavior, and biolabeling properties. *J. Inorg. Biochem.* **2015**, *148*, 2–10. [CrossRef] [PubMed]
61. Candelon, N.; Hadade, N.D.; Matache, M.; Canet, J.-L.; Cisnetti, F.; Funeriu, D.P.; Nauton, L.; Gautier, A. Luminogenic "clickable" lanthanide complexes for protein labelling. *Chem. Commun.* **2013**, *49*, 9206–9208. [CrossRef] [PubMed]
62. Mastarone, D.J.; Harrison, V.S.R.; Eckermann, A.L.; Parigi, G.; Luchinat, C.; Meade, T.J. A modular system for the synthesis of multiplexed magnetic resonance probes. *J. Am. Chem. Soc.* **2011**, *133*, 5329–5337. [CrossRef] [PubMed]
63. Lebedev, A.Y.; Holland, J.P.; Lewis, J.S. Clickable bifunctional radiometal chelates for peptide labelling. *Chem. Commun.* **2010**, *46*, 1706–1708. [CrossRef] [PubMed]
64. Mindt, T.L.; Struthers, H.; Brans, L.; Anguelov, T.; Schweinsberg, C.; Maes, V.; Tourwé, D.; Schibli, R. "Click to chelate": Synthesis and installation of metal chelates into biomolecules in a single step. *J. Am. Chem. Soc.* **2006**, *128*, 15096–15097. [CrossRef] [PubMed]
65. Abraham, B.; Kelly, L.A. Photooxidation of amino acids and proteins mediated by novel 1,8-naphthalimide derivatives. *J. Phys. Chem. B* **2003**, *107*, 12534–12541. [CrossRef]
66. Zhang, J.; Woods, R.J.; Brown, P.B.; Lee, K.D.; Kane, R.R. Synthesis and photochemical protein crosslinking studies of hydrophilic naphthalimides. *Bioorg. Med. Chem. Lett.* **2002**, *12*, 853–856. [CrossRef]
67. Rogers, J.A.; Weiss, S.J.; Kelly, L.A. Photoprocesses of naphthalene imide and diimide derivatives in aqueous solutions of DNA. *J. Am. Chem. Soc.* **2000**, *122*, 427–436. [CrossRef]
68. Aveline, B.A.; Matsugo, S.; Redmond, R.W. Photochemical mechanisms responsible for the versatile application of naphthalimides and naphthaldiimides in biological systems. *J. Am. Chem. Soc.* **1997**, *119*, 11785–11795. [CrossRef]
69. Saito, I.; Takayama, M.; Sugiyama, H.; Nakatani, K. Photoinduced DNA cleavage via electron transfer: Demonstration that guanine residues located 5′ to guanine are the most electron-donating sites. *J. Am. Chem. Soc.* **1995**, *117*, 6406–6407. [CrossRef]
70. Saito, I.; Takayama, M. Photoactivatable DNA-cleaving amino acids: Highly sequence-selective DNA photocleavage by novel L-lysine derivatives. *J. Am. Chem. Soc.* **1995**, *117*, 5590–5591. [CrossRef]
71. Matsugo, S.; Kawanishi, S.; Yamamoto, K.; Sugiyama, H.; Matsuura, T.; Saito, I. Bis(hydroperoxy)naphthaldiimide as a "photo-Fenton reagent": Sequence-specific photocleavage of DNA. *Angew. Chem. Int. Ed.* **1991**, *30*, 1351–1353. [CrossRef]
72. Stasiuk, G.J.; Long, N.J. The ubiquitous DOTA and its derivatives: The impact of 1,4,7,10-tetraazacyclododecane-1,4,7,10-tetraacetic acid on biomedical imaging. *Chem. Commun.* **2013**, *49*, 2732–2746. [CrossRef] [PubMed]
73. Caravan, P.; Ellison, J.; McMurry, T.; Lauffer, R. Gadolinium(III) chelates as MRI contrast agents: Structure, dynamics, and applications. *Chem Rev.* **1999**, *99*, 2293–2352. [CrossRef] [PubMed]

74. Sherry, A.D.; Caravan, P.; Lenkinski, R.E. Primer on gadolinium chemistry. *Magn. Reson. Med.* **2009**, *30*, 1240–1248. [CrossRef] [PubMed]
75. Vives, E.; Brodin, P.; Lebleu, B. A truncated HIV-1 Tat protein basic domain rapidly translocates through the plasma membrane and accumulates in the cell nucleus. *J. Biol. Chem.* **1997**, *272*, 16010–16017. [CrossRef] [PubMed]
76. Raghunand, N.; Guntle, G.P.; Gokhale, V.; Nichol, G.S.; Mash, E.A.; Jagadish, B. Design, synthesis, and evaluation of 1,4,7,10-tetraazacyclododecane-1,4,7-triacetic acid derived, redox-sensitive contrast agents for magnetic resonance imaging. *J. Med. Chem.* **2010**, *53*, 6747–6757. [CrossRef] [PubMed]
77. Cha, T.R.; Hilgraf, R.; Sharpless, K.B.; Fokin, V.V. Polytriazoles as copper(I)-stabilizing ligands in catalysis. *Org. Lett.* **2004**, *6*, 2853–2855.
78. Hong, V.; Presolski, S.I.; Ma, C.; Finn, M.G. Analysis and optimization of copper-catalyzed azide-alkyne cycloaddition for bioconjugation. *Angew. Chem. Int. Ed.* **2009**, *48*, 9879–9883. [CrossRef] [PubMed]
79. Sawa, M.; Hsu, T.-L.; Itoh, T.; Sugiyama, M.; Hanson, S.R.; Vogt, P.K.; Wong, C.-H. Glycoproteomic probes for fluorescent imaging of fucosylated glycans *in vivo*. *Proc. Natl. Acad. Sci. USA* **2006**, *103*, 12371–12376. [CrossRef] [PubMed]
80. Melhuish, W.H. Quantum efficiencies of fluorescence of organic substances: Effect of solvent and concentration of the fluorescent solute. *J. Phys. Chem.* **1961**, *65*, 229–235. [CrossRef]
81. Sturzu, A.; Klose, U.; Echner, H.; Beck, A.; Gharabaghi, A.; Kalbacher, H.; Heckl, S. Cellular uptake of cationic gadolinium-DOTA peptide conjugates with and without *N*-terminal myristoylation. *Amino Acids* **2009**, *37*, 249–255. [CrossRef] [PubMed]

Sample Availability: Not available.

Supplementary Information

Cellular Uptake and Photo-Cytotoxicity of a Gadolinium(III)-DOTA-Naphthalimide Complex “Clicked” to a Lipidated Tat Peptide

William I. O’Malley, Riccardo Rubbiani, Margaret L. Aulsebrook, Michael R. Grace, Leone Spiccia, Kellie L. Tuck, Gilles Gasser, and Bim Graham

Contents **Page(s)**

NMR spectra of reported compounds

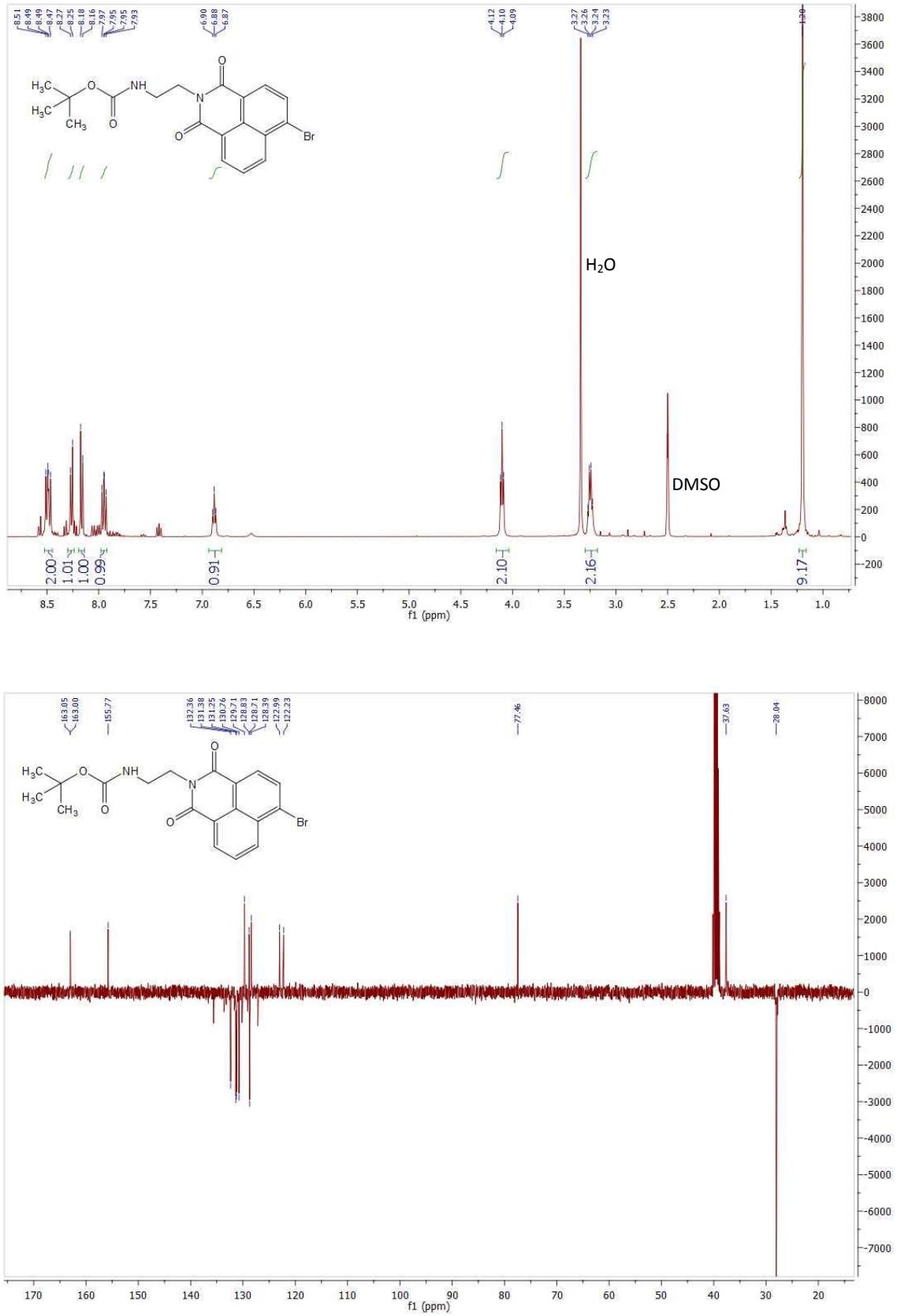

Figure S1. ^{1}H and ^{13}C NMR spectra of compound 1 in DMSO-d_6.

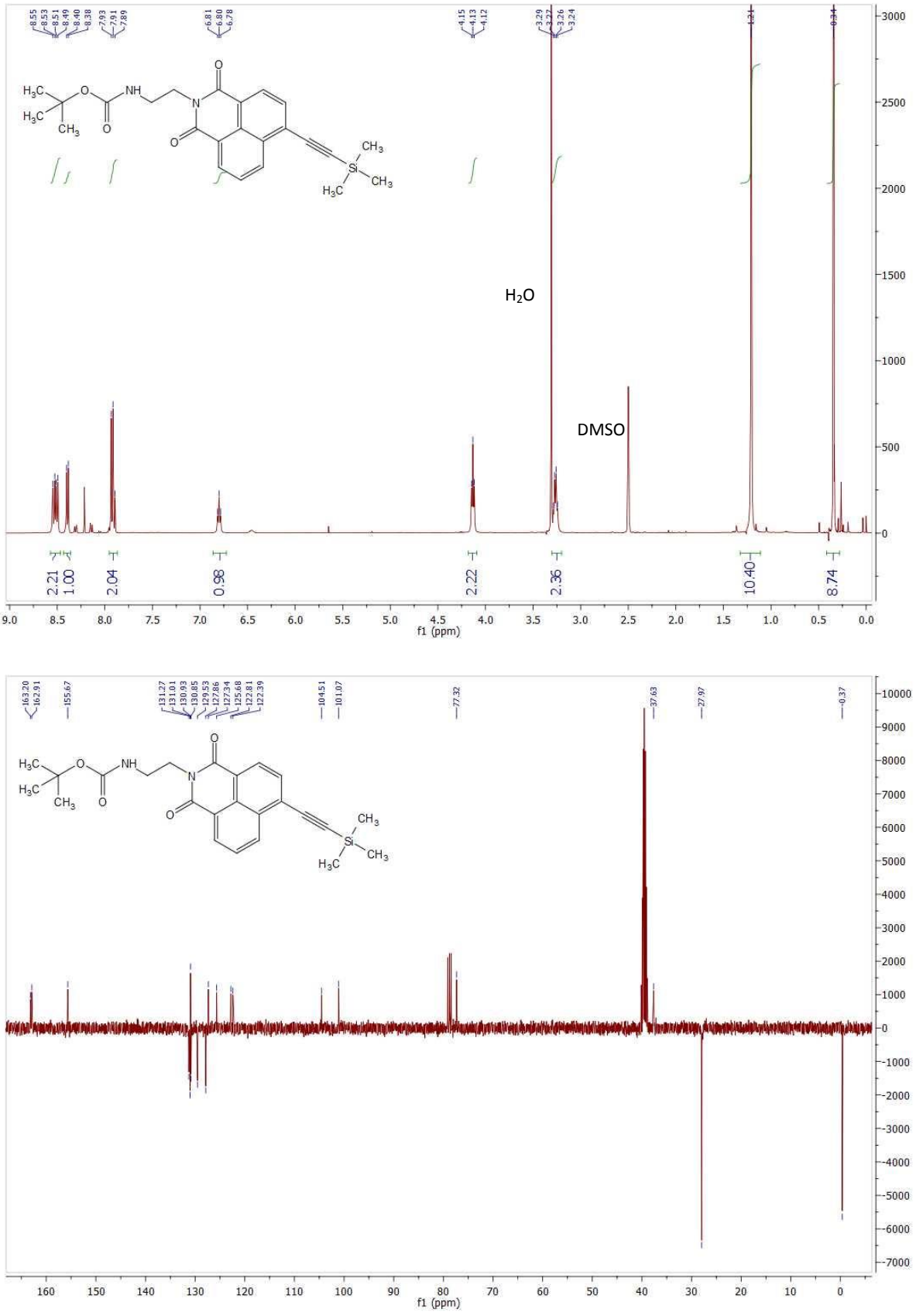

Figure S2. ^{1}H and ^{13}C NMR spectra of compound 2 in DMSO-d_6.

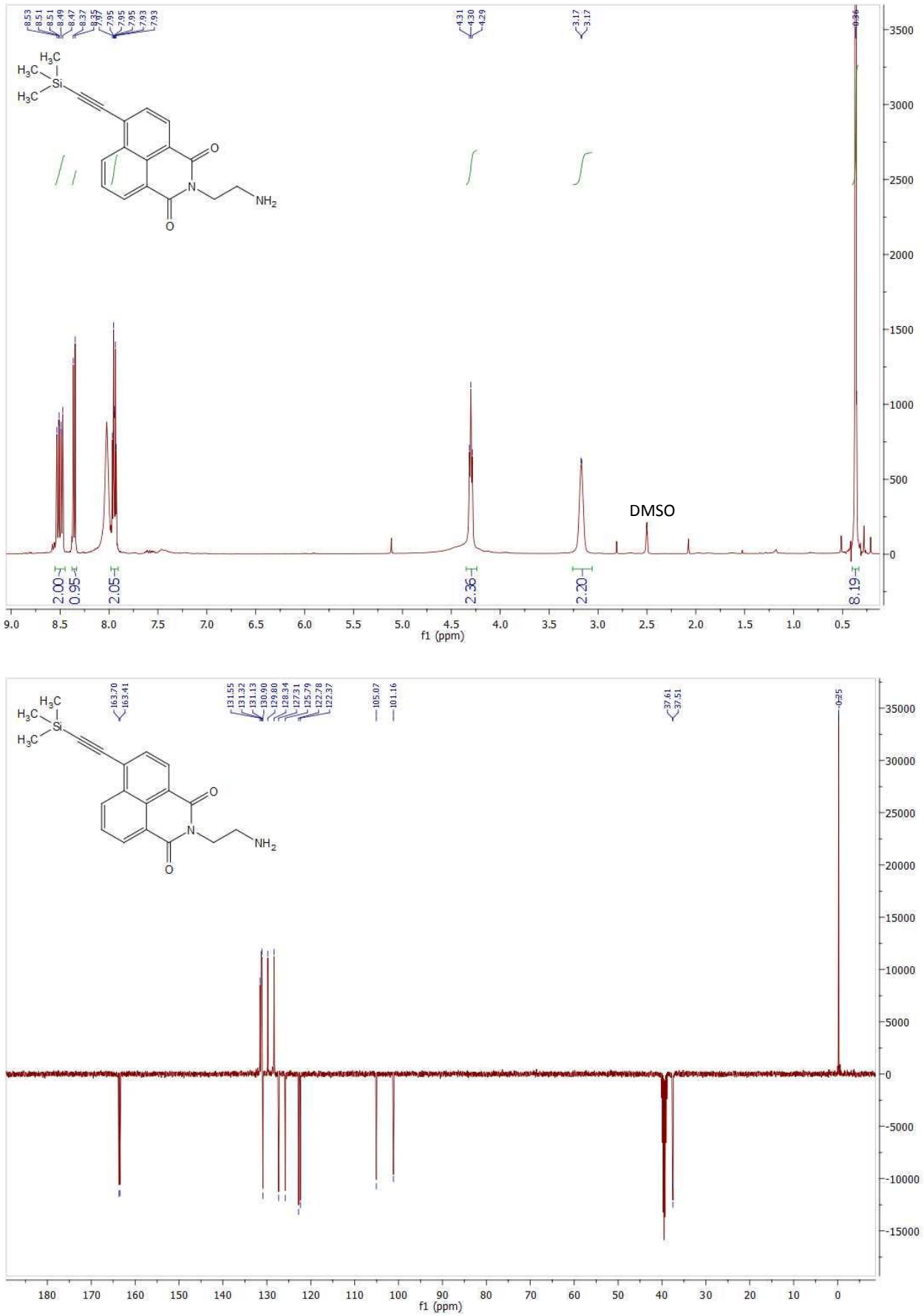

Figure S3. ^{1}H and ^{13}C NMR spectra of compound 3 in DMSO-d_6.

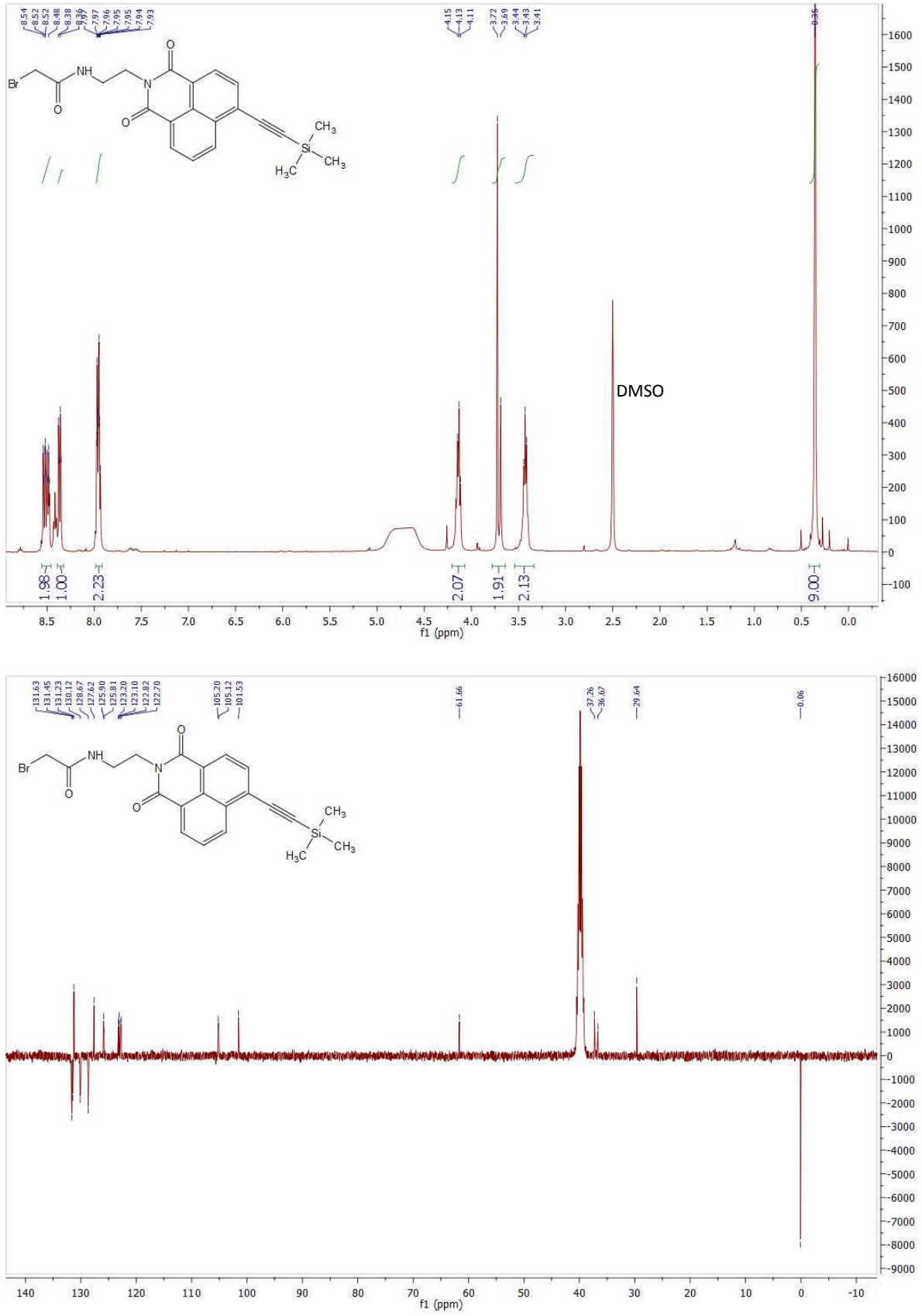

Figure S4. ^{1}H and ^{13}C NMR spectra of compound 4 in DMSO-d_6.

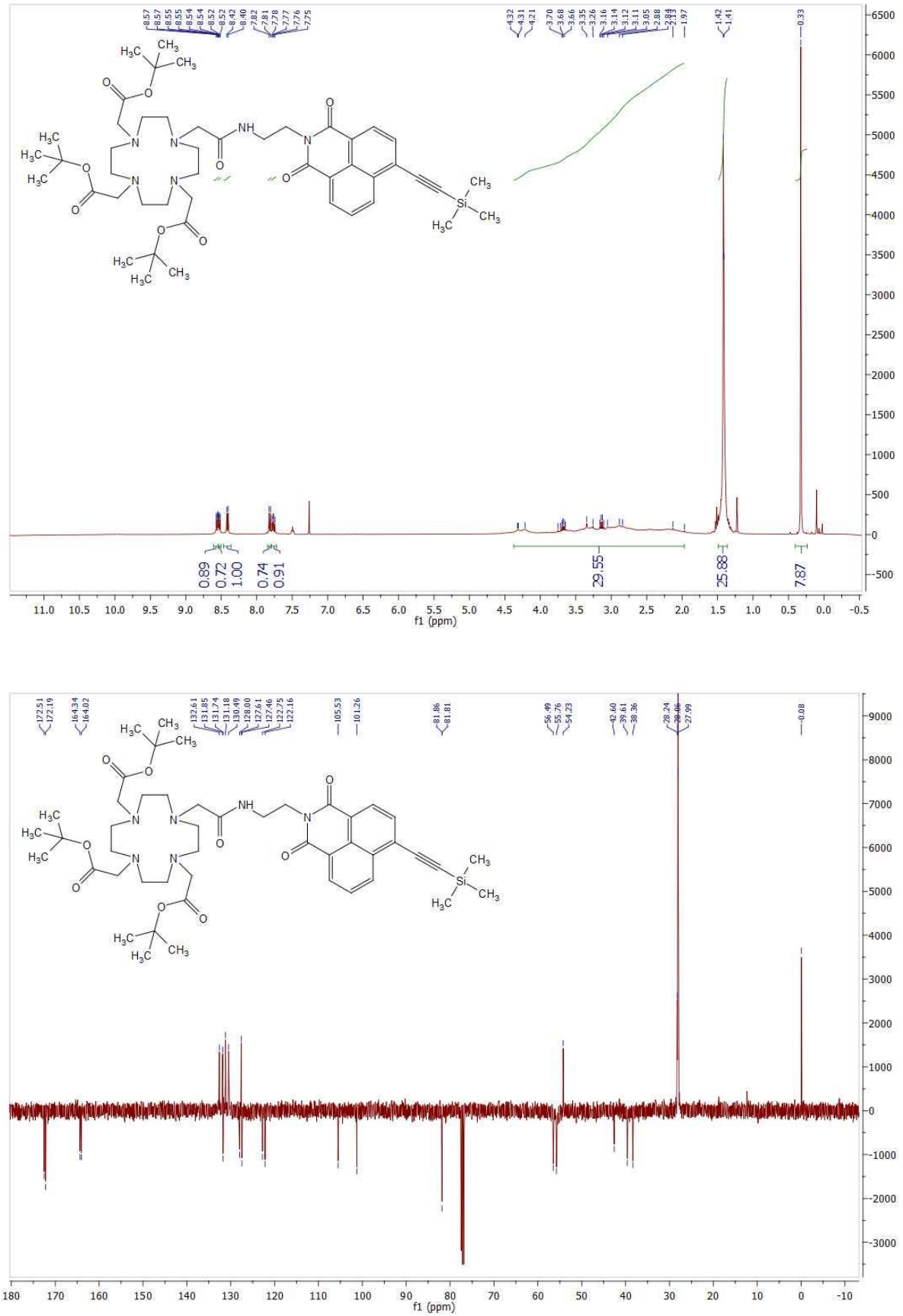

Figure S5. ^{1}H and ^{13}C NMR spectra of compound 5 in $CDCl_3$.

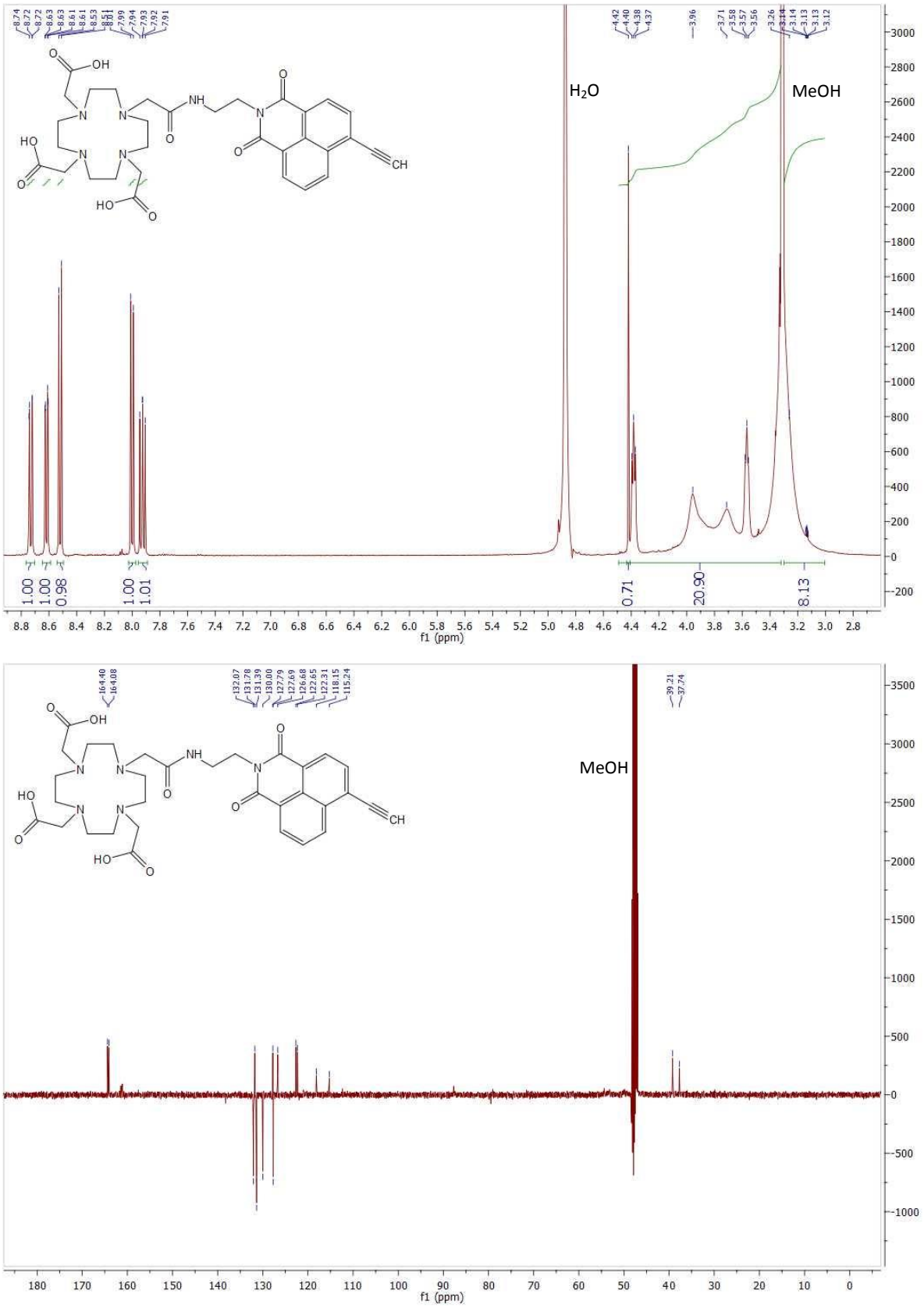

Figure S6. ^{1}H and ^{13}C NMR spectra of ligand L in CD_3OD.

LC traces for final ligand and Gd(III) complexes

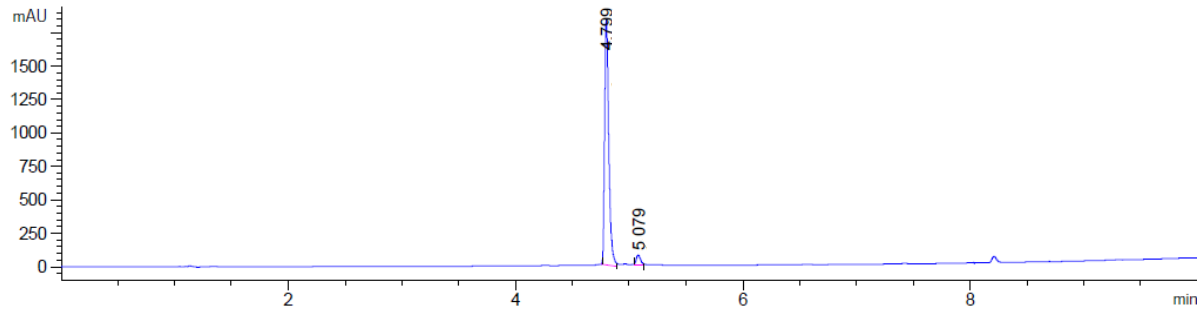

Figure S7. LC trace for ligand L (254nm).

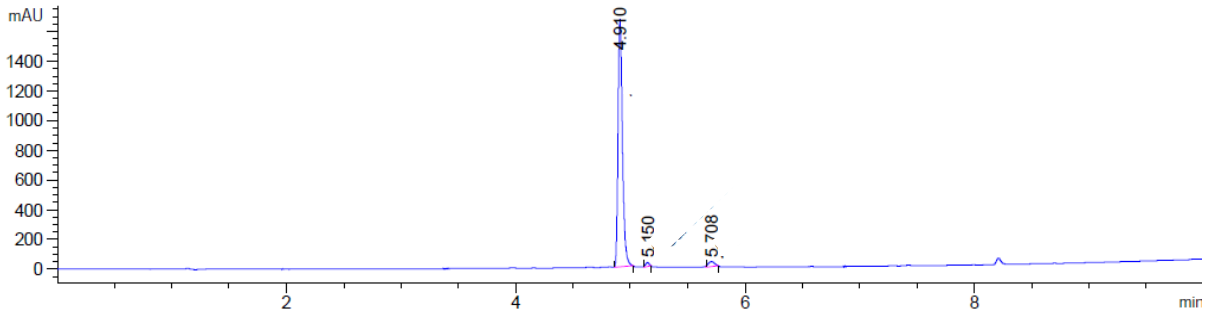

Figure S8. LC trace for Gd-L (254nm).

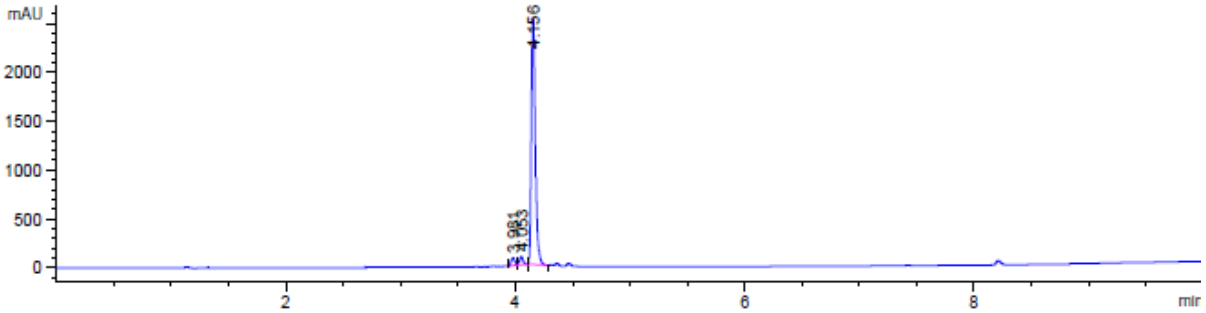

Figure S9. LC trace for “clicked” Gd-L (254nm).

LC trace for peptide conjugate

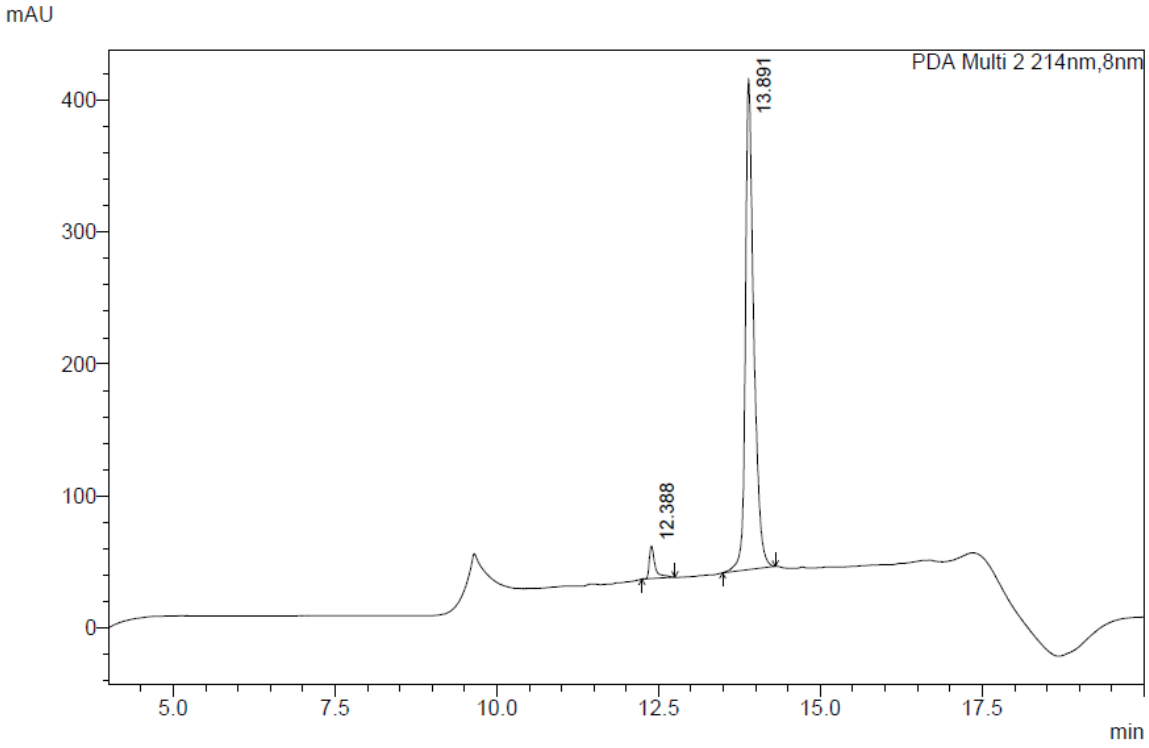

Figure S10. LC trace for Gd-L-Tat peptide conjugate (214 nm

CHAPTER 4:

SYNTHETIC EFFORTS TOWARDS TO THE DEVELOPMENT OF ADDITIONAL "CLICKABLE" LANTHANIDE COMPLEXES

4.1 Introduction

As part of the studies detailed in Chapters 2 and 3, efforts were made to develop a third luminescent lanthanide chelate (LLC) and a second gadolinium(III)-DOTA-naphthalimide tag (**Figure 1A**). These efforts were not discussed in either of the published manuscripts, hence this additional work is presented separately here.

The LLC shares similar design features to those described in **Chapter 2**, incorporating terbium as the lanthanide ion and an alkyne-functionalised pendant group for potential conjugation to (bio)molecules *via* click chemistry. The chelation domain, however, is based on a functionalised 1,4,7-triazacyclononane (TACN) macrocycle, rather than the cyclen macrocycle utilised previously. Three picolinate groups are attached to the TACN ring, contributing to a total of nine donor atoms that saturate the coordination sphere of the metal ion and ensure the absence of coordinated water molecules which can quench lanthanide luminescence.[1] Such a design has already been described in the literature (**Figure 1B**),[2,3] with the picolinate groups demonstrated to act as efficient "antenna" groups for sensitisation of terbium luminescence (quantum yield, $\Phi = 0.60$ in H_2O). However, the incorporation of a "clickable" alkyne functionality into such a structure has not been explored previously.

The gadolinium(III)-DOTA-naphthalimide tag differs from the design reported in **Chapter 3** in that the naphthalimide group is reversed in orientation with respect to the Gd-DOTA moiety.

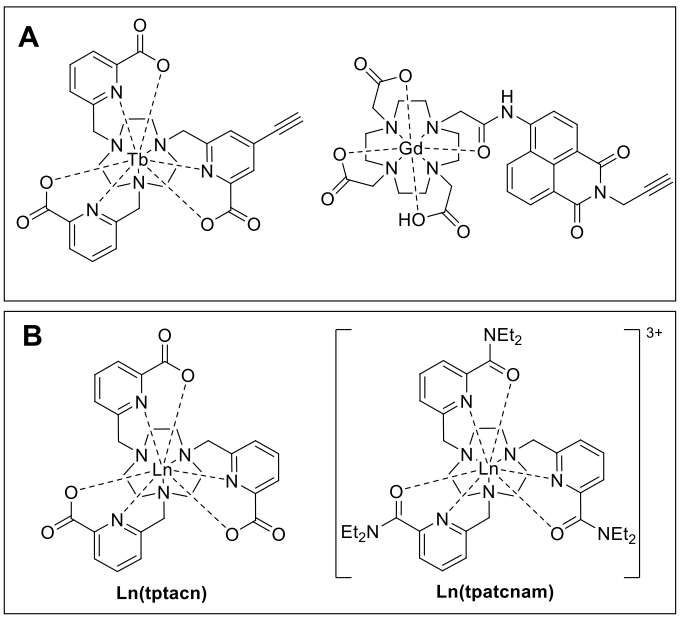

Figure 1. (**A**) Structures of the "clickable" TACN-based terbium(III) complex (left) and gadolinium(III)-DOTA-naphthalimide complex (right) described in this chapter. (**B**) Structures of the previously reported compounds, [Ln(tptacn)][2] and [Ln(tpatcnam)]$^{3+}$,[3] upon which the terbium(III) complex design was based (Ln = Eu^{3+} or Tb^{3+}).

4.2 Synthesis of a "clickable" luminescent TACN-based terbium(III) complex

Synthesis of the supporting ligand, **4**, (**Scheme 1**) began with the production of the TMS-protected alkyne-functionalised picolinate derivative **1**, the full synthesis of which has been previously detailed on page 49 of **Chapter 2**. This group was coupled to the sole unprotected amine of di-*tert*-butyloxycarbonyl-protected TACN (Boc_2TACN),[4] yielding compound **2** in 85% yield. Treatment with a trifluoroacetic acid/dichloromethane (TFA/DCM) mixture afforded the Boc-deprotected intermediate **3**, which was used without purification after the removal of solvent and excess TFA. The two newly exposed secondary amines were then subjected to a base-mediated nucleophilic reaction with ethyl 6-(bromomethyl)picolinate, prepared *via* an adapted literature procedure,[5] to yield the protected *tris*-picolinate intermediate in 52% yield. Global hydrolysis of the ethyl ester groups and removal of the TMS protective group using 2 M sodium hydroxide afforded the final ligand, **4**. The high polarity of this compound as well as the desire for high purity necessitated purification by preparative HPLC, providing **4** in greater than 95% purity but low overall yield (27% over last two steps).

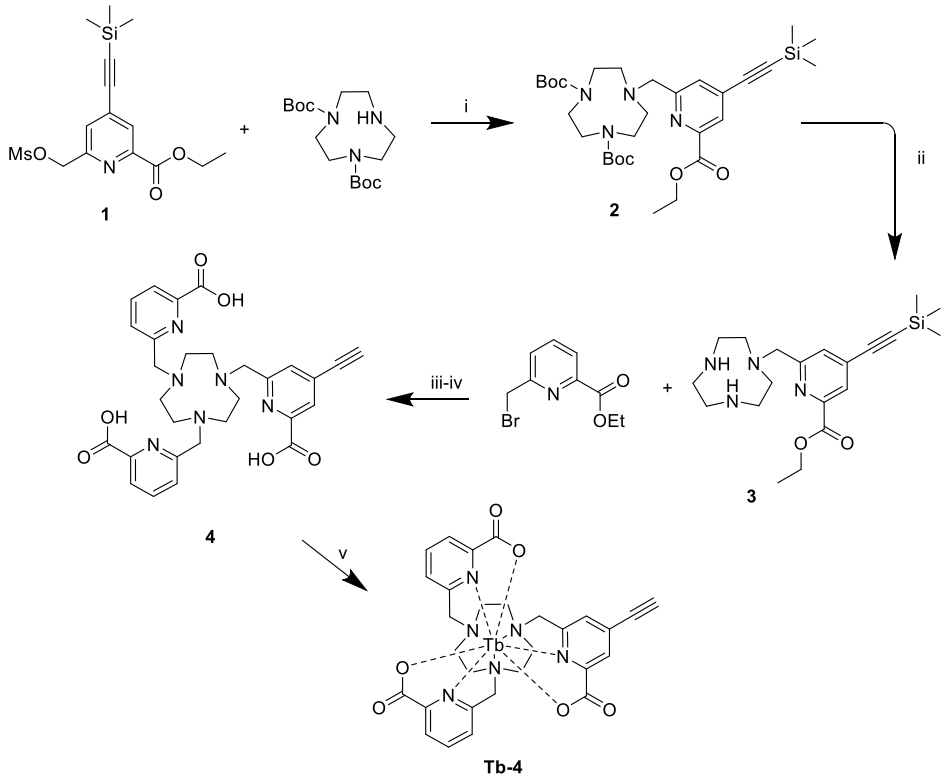

Scheme 1. Synthesis of the luminescent lanthanide complex **Tb-4**. i) DIPEA, MeCN, reflux, O/N, 85%; TFA, RT, O/N, quant.; iii) DIPEA, MeCN, reflux, O/N; iv) NaOH, RT, 3 h, 27% (over steps iii–iv); v) $Tb(OTf)_3$, H_2O, NaOH (pH 8–9), 90°C, 2h, quant. (29% isolated).

The ^1H nuclear magnetic resonance (NMR) spectrum of **4** in deuterated methanol (**Figure 2**) displays a broad set of unresolved resonances between *ca.* 3–3.5 ppm, attributable to the CH_2 groups of the TACN ring. Overlapping resonances at 8.05–7.96 ppm and 7.62–7.53 ppm correspond to the aromatic protons present in the *meta* positions of the picolinic acid groups, while the triplet at 7.90 ppm corresponds to the *para*-CH protons present in the two picolinic acid groups without the alkyne substituent. Sharp singlets at 4.23 and 4.17 ppm represent the protons of the methylene groups linking the pyridine (Py) rings to the TACN ring, while a single resonance at 3.96 ppm confirms the presence of the alkyne. Confirmation that the desired product had been synthesised was further evidenced by the high-resolution mass spectrometry (HRMS) *m/z* signal at 559.2301, agreeing well with that expected for the $[M+H]^+$ species (559.2300).

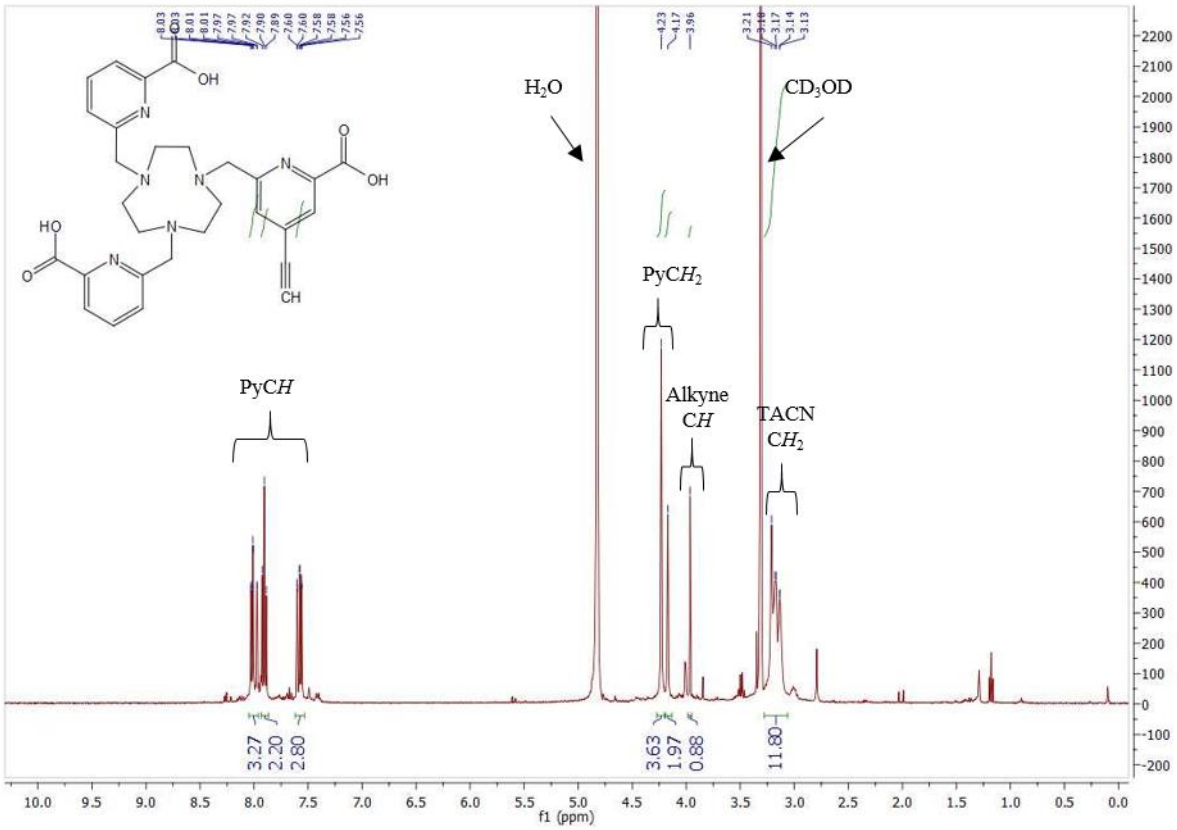

Figure 2. ^{1}H NMR spectrum of **4** in CD_3OD.

The lanthanide complex, **Tb-4**, was generated by stirring **4** with 1.5 equivalents of terbium(III) triflate under mildly basic conditions (pH 8–9) and isolated *via* preparative HPLC in greater than 95% purity. Complex formation was confirmed by high-resolution mass spectrometry (HRMS), with observation of a signal at *m/z* = 715.1342 corresponding to the $[M+H]^+$ species.

The absorbance and emission spectra of **Tb-4**, recorded in aqueous media buffered to a pH of 7.4 with 100 mM 4-(2-hydroxyethyl)-1-piperazineethanesulfonic acid (HEPES), are shown in **Figures 3** and **4**, respectively. The multiple overlapping absorbance bands observed between 245 and 305 nm are assigned mainly to $\pi\rightarrow\pi^*$ and $n\rightarrow\pi^*$ ligand-centred transitions. The luminescence emission profile is typical for a terbium complex, showing four distinct bands between *ca.* 470 and 630 nm ascribable to transitions from the $^{5}D_4$ excited state to the

^7F_J (J = 6–3) levels, with the most intense band at 545 nm corresponding to the $^5D_4 \rightarrow {}^7F_5$ transition.

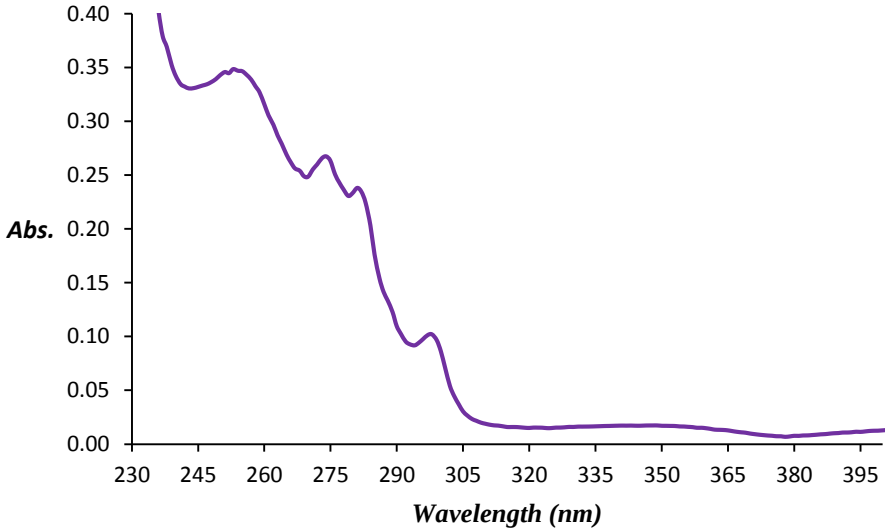

Figure 3. Absorbance spectrum of **Tb-4** (25 μM) in 100 mM HEPES, pH 7.4 (298 K).

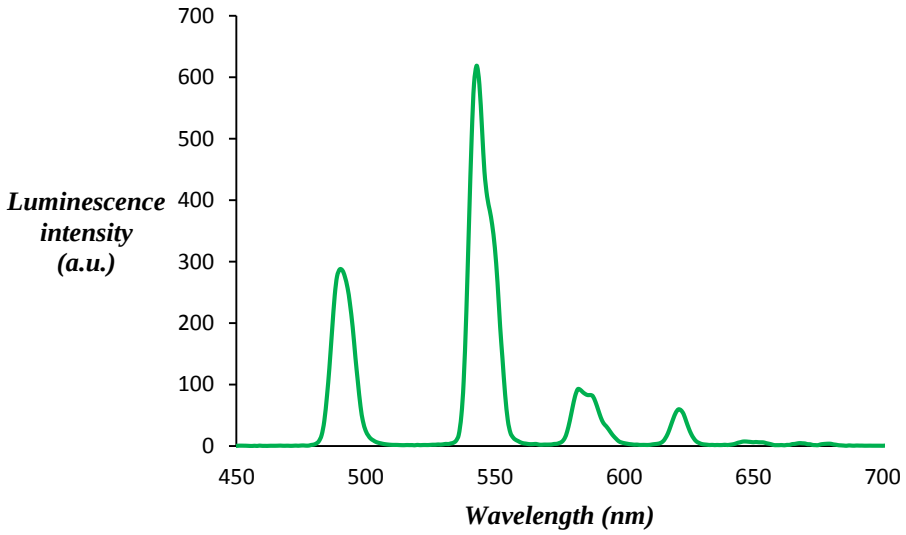

Figure 4. Emission spectrum of **Tb-4** (25 μM) in 100 mM HEPES, pH 7.4 (298 K), excited at 278 nm.

Only a very small quantity of **Tb-4** was able to be synthesised in the timeframe available due, in particular, to difficulties encountered with the preparation of sufficient quantities of compound **1** and ethyl 6-(bromomethyl)picolinate. Synthesis of **1** required six

steps, many of them inefficient and incorporating a non-trivial purification procedure, while preparation of ethyl 6-(bromomethyl)picolinate *via* a reported radical bromination procedure[5] was rendered difficult by a scarcity of carbon tetrachloride, a solvent being phased out due to its toxicity, ozone depletion and greenhouse gas properties.[6] In view of these challenges, a decision was made to focus efforts on examining the properties and utility of the LLCs reported in **Chapter 2**.

4.3 Attempted synthesis of "clickable" gadolinium(III)-DOTA-naphthalimide complex

Synthetic efforts towards a second DOTA-naphthalimide ligand, **11** (**Scheme 2**), began with the construction of a naphthalimide derivative, **8**, featuring an alkyne group attached to the imide nitrogen. This involved, firstly, conversion of commercially available acenaphthene to 4-amino-1,8-naphthalic anhydride (**7**) according to a published three-step procedure.[7] Subsequent condensation reaction with propargyl amine allowed for installation of the alkyne conjugation handle in 80% yield. Conversion to a bromoacetimide derivative, in preparation for coupling to the cyclen ring of tri-*tert*-butyl-protected 1,4,7,10-tetraazacyclododecane-1,4,7-triacetic acid ($^{t}Bu_3$DO3A),[8] was achieved through reaction with bromoacetyl bromide, employing Na_2CO_3 as a base. Despite the addition of nearly 10 equivalents of bromoacetyl bromide, only *ca.* 70% conversion to **9** was achieved, and the highly insoluble nature of the product prevented purification. Impure **9** was subsequently coupled to $^{t}Bu_3$DO3A to give **10** in 73% yield after flash silica gel chromatography. A final treatment with TFA facilitated removal of the protective *tert*-butyl groups and was followed by purification with preparative HPLC, affording the final ligand **11** in 42% yield, with a less-than-optimal purity of 85%, as evaluated *via* HPLC analysis.

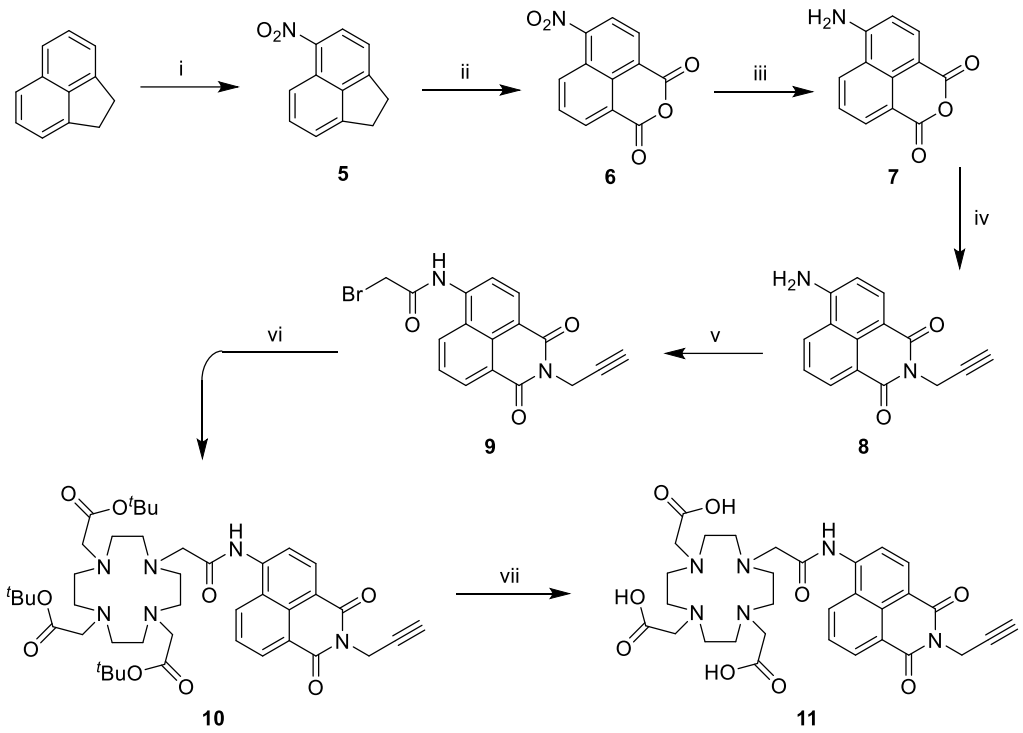

Scheme 2: Synthesis of the DOTA-naphthalimide ligand **11**. i) HNO_3, AcOH, RT, 3h, 79%; ii) $Na_2Cr_2O_7$, AcOH, reflux, 5 h, 72%; iii) $SnCl_2 \cdot 2H_2O$, conc. HCl, EtOH, reflux, 2 h, 72%; iv) propargyl amine, 1,4-dioxane, reflux, O/N, 80%; v) bromoacetylbromide, Na_2CO_3, DCM, reflux, 85%; vi) ^{t}Bu$_3$DO3A, DIPEA, MeCN, reflux, O/N, 73%; vii) TFA, DCM, RT, O/N, 42%.

The ^{1}H NMR spectrum of the penultimate compound, **10**, in $CDCl_3$ (**Figure 5**) displays an extremely broad set of unresolved signals between *ca.* 2.5–5.0 ppm, which correspond to the CH_2 groups of the cyclen macrocycle, as well as the methylene protons within the "arms" of the DO3A chelator and the CH_2 group linking the naphthalimide unit to the macrocycle. Resonances between 7.5 and 9 ppm correspond to the five aromatic protons within the naphthalimide group. A doublet with a very low coupling constant (2.4 Hz) at 4.93 ppm represents the CH_2 adjacent to the alkyne, while a triplet at 2.20 ppm with the same coupling constant corresponds to the alkyne proton. Further signals include a broad, downfield signal at 11.17 ppm, corresponding to the aromatic secondary amine (N*H*Ar), and two intense singlets at 1.45 and 1.28 ppm, due to the ^{t}Bu protons. A signal at *m/z* = 365.28 in the electrospray mass spectrum corresponds to the $[M+H]^{2+}$ species.

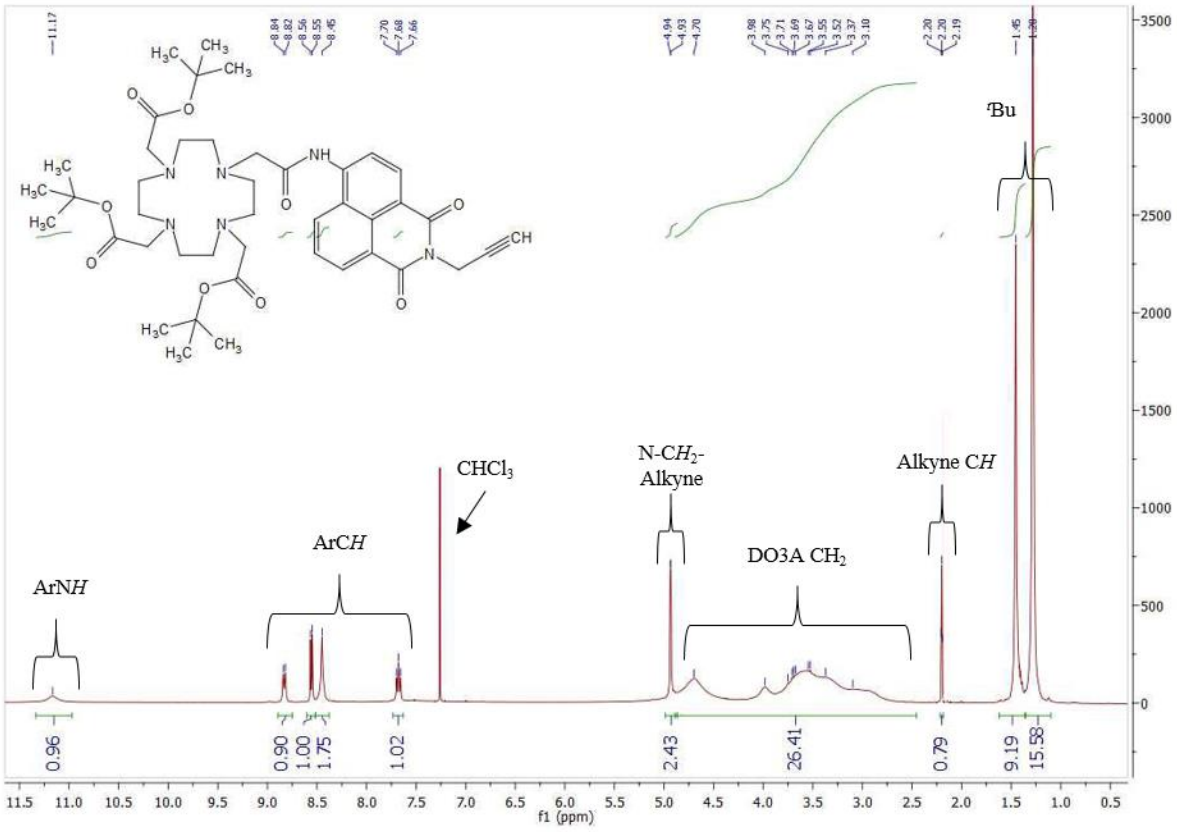

Figure 5. ^{1}H NMR spectrum of **10** in $CDCl_3$.

Purification of **11** proved highly problematic, with characterisation being solely performed through LC-MS. Attempts were made to install a Gd(III) ion under slightly basic conditions (pH 9), as per the other lanthanide complexes. However, it was quickly discovered that the amide bond between the chelating domain and the naphthalimide group was undergoing rapid hydrolysis under these conditions, due to the naphthalimide acting as good leaving group. This shed some light on why the ligand was so difficult to purify in the first place; as during ligand purification *via* preparative HPLC, significant hydrolysis was also occurring. Complexation was more successful under near-neutral pH conditions (according to LC-MS analysis), but again, purification by preparative HPLC proved to be a major issue, with cleavage of the naphthalimide group occurring once more. Given these significant issues, a decision was made to abandon the synthesis of this complex and to focus efforts on the study of the Gd-DOTA-naphthalimide complex reported in **Chapter 3**.

4.4 Conclusion

Synthetic efforts directed towards the development of two new "clickable" tags analogous to those described in chapters **2** and **3** have been detailed. A new chelator design, **4**, consisting of three picolinate groups attached to a central TACN macrocycle proved successful in stably chelating and sensitising Tb(III) ions. However, difficulties encountered during synthesis of this ligand resulted in only a small amount being produced. As such, in depth photophysical studies and an assessment of the suitability of this LLC as a "clickable" reagent were not fully explored. It is expected that if a more efficient synthetic route can be established, further investigation of this LLC will likely prove worthwhile. A new Gd(II) chelating DOTA-naphthalimide ligand, **11**, was also synthesised and investigated. Unfortunately, the ligand demonstrated very poor stability in aqueous conditions and therefore did not warrant further investigation.

Experimental

Experimental procedures for compound **1** can be found on pages 52 and 53 as part of the **Chapter 2** experimental section.

Materials and reagents

All chemicals were purchased from Sigma-Aldrich Pty, Matrix Scientific, or Merck Group Ltd and used without purification. All solvents were reagent grade. Di-*tert*-butyloxycarbonyl-protected 1,4,7-triazacyclononane (Boc_2TACN)[4] and tri-*tert*-butyl-protected 1,4,7,10-tetraazacyclododecane-1,4,7-triacetic acid ($^tBu_3DO3A$)[8] were synthesised according to literature procedures.

Instrumentation

Flash chromatography was carried out using Merck 38 Silica gel 60, 230–400 mesh ASTM. *Thin layer chromatography (TLC)* was performed on Merck Silica Gel 60 F254 plates. TLC plates were visualised using a UV lamp at 254 nm or through the use of $KMnO_4$ or ninhydrin staining agent. *^1H and ^{13}C nuclear magnetic resonance (NMR)* spectra were recorded using an Avance III Nanobay 400 MHz Bruker spectrometer coupled to the BACS 60 automatic sample changer at 400.13 MHz and 100.61 MHz, respectively. Data acquisition and processing was managed using Topspin software package version 3. Additional processing was handled with MestReNova software (PC). Chemical shifts (δ) were measured in parts per million (ppm) referenced to an internal standard of residual solvent. Spectroscopic data are given using the following abbreviations: s, singlet; d, doublet; dd, doublet-of-doublets; t, triplet; q, quartet; m, multiplet; br, broad; *J*, coupling constant. *Analytical high-performance liquid chromatography (HPLC)* was carried out on an Agilent 1260 series modular HPLC equipped with the following modules: G1312B binary pump, G1316A thermostated column compartment equipped with an Agilent Eclipse Plus C18 3.5 µm, 4.6 x 100 mm column and a G1312B diode array detector.

The following elution protocol was used: 0–10 min, gradient from 5% solvent B/95% solvent A to 100% solvent B (solvent A = 99.9% H_2O, 0.1% TFA, and solvent B = 99.9% MeCN, 0.1% TFA. *Preparative HPLC purification* was carried out on an Agilent 1260 modular Prep HPLC equipped with the following modules: G1361A prep pump, G2260A prep automatic liquid sampler, G1364B fraction collector, G1315D diode array detector, and a Luna C8 5 µm, 100 Å AXIA, 250 x 21.2 mm column. The following elution protocol was used: 0–5 min, 100% solvent C; 5–30 min, gradient from 100% solvent C to 20% solvent C/80% solvent D (solvent C = 99.9% H_2O, 0.1% formic acid; solvent D = 99.9% MeCN, 0.1% formic acid); flow rate = 20 mL min^{-1}. *High-resolution mass spectrometric (HRMS)* analyses were performed on a Waters LCT TOF LC-MS mass spectrometer coupled to a 2795 Alliance Separations module. All data was acquired and mass corrected *via* a dual-spray Leucine Enkephaline reference sample. Mass spectra were generated by averaging the scans across each peak and background subtraction of the TIC. Acquisition and analysis were performed using the MassLynx software version 4.1. The mass spectrometer conditions were as follows: electrospray ionisation mode, desolvation gas flow of 550 L h^{-1}, desolvation temperature of 250^{o}C, source temperature of 110^{o}C, capillary voltage of 2400 V, sample cone voltage of 60 V, scan range acquired between 100–1500 *m/z*, one sec scan times and internal reference ions for positive ion mode (Leucine Enkephaline) of 556.2771. *Liquid chromatography-mass spectrometry (LC-MS)* was performed using an Agilent 6100 Series Single Quad LC-MS coupled to an Agilent 1200 Series HPLC with the following conditions and equipment for MS: 1200 Series G1311A quaternary pump, 1200 Series G1329A thermostated autosampler, 1200 Series G1314B variable wavelength detector. MS conditions: quadrupole ion source, multimode-ES ion mode, 300^{o}C drying gas temperature, 200^{o}C vaporising temperature, capillary voltage of 2000 V (positive), capillary voltage of 4000 V (negative), scan range between 100–1000 *m/z* with an 0.1 sec step size and a 10 min acquisition time. LC equipment and conditions were as follows: reverse-

phase HPLC analysis on a Luna C8(2) 5 µm, 50 x 4.6 mm column using a column temperature of 30°C, an injection volume of 5 µL, and the following elution protocol: 0–4 min, gradient from 5% solvent C/95% solvent D to 100% solvent D; 4–7 min, 100% solvent D; 4–7 min, gradient from 100% solvent D to 95% solvent C/5% solvent D. Detection was at 254 nm. *Reversed-phase silica dry column vacuum chromatography (RP-DCVC)* was performed using reversed-phase silica (C18 bonded, 10 µm, 60 Å) purchased from Grace Davison and loaded into a sintered Buchner funnel (50 x 50 mm ID). Elution was performed with 100% solvent C (200 mL), followed by a 5% incremental stepwise gradient from 0 to 80% solvent D (50 mL of each solvent C/D mixture). Fractions were collected under vacuum into a separating funnel and then into test tubes. Collected fractions were analysed by analytical HPLC. *Absorbance spectra* were recorded on a Varian Cary 50 Bio UV−vis spectrophotometer using a 1 cm path length quartz cuvette. *Luminescence emission spectra* were acquired using a Varian Cary Eclipse fluorescence spectrophotometer using a 1 cm path length quartz cuvette and the following settings: phosphorescence mode, total decay time = 0.02 s, number of flashes = 1, delay time = 0.1 ms, gate time = 5 ms, excitation slit width = 1 nm, emission slit width = 1 nm, data interval = 1 nm, averaging time = 0.015 s.

Ethyl 6-(bromomethyl)picolinate[5]

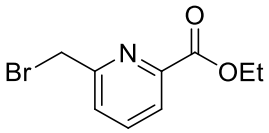

Ethyl-6-methyl-2-pyridine carboxylate (7.50 g, 45.4 mmol), *N*-bromosuccinimide (8.89 g, 49.5 mmol) and benzoyl peroxide (550 mg, 2.27 mmol) were dissolved in CCl_4 (25 mL). The resulting reaction solution was heated to 95°C and stirred overnight (O/N) under a nitrogen atmosphere. After cooling to room temperature (RT), the solution was filtered to remove any precipitated material, and the precipitates were washed with $CHCl_3$ until they appeared white

in colour. Removal of solvent from the filtrate *in vacuo* yielded an orange oil, which was purified *via* silica gel chromatography (30% EtOAc in PET spirits) to yield the product (R_f = 0.5) as a yellow oil. Yield: 3.58 g, 33%. ^{1}H NMR ($CDCl_3$) δ 8.03 (dd, *J* = 7.7, 1.0 Hz, 1H), 7.87 (t, *J* = 7.8 Hz, 1H), 7.69 (dd, *J* = 7.8, 1.0 Hz, 1H), 4.67 (s, 2H), 4.46 (q, *J* = 7.1 Hz, 2H), 1.42 (t, *J* = 7.1 Hz, 3H). ^{13}C NMR ($CDCl_3$) δ 164.60, 157.44, 147.67, 138.58, 127.32, 124.52, 62.31, 32.94, 14.38. LC-MS (ESI): *m/z* 244.10 $[M+H]^+$ (100%). Analytical HPLC: 92% purity (254 nm).

Di-*tert*-butyl 7-((6-(ethoxycarbonyl)-4-((trimethylsilyl)ethynyl) pyridin-2-yl)methyl)-1,4,7- triazacyclononane-1,4-dicarboxylate (2).

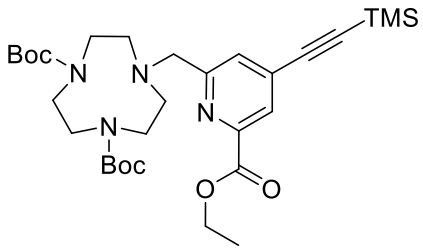

Compound **1** (320 mg, 900 µmol), Boc_2TACN (198 mg, 600 µmol), and *N*,*N*-diisopropylethylamine (DIPEA) (233 mg, 314 µL, 1.80 mmol) were dissolved in MeCN (50 mL) and stirred at reflux O/N. Removal of solvent *in vacuo* gave a thick, dark brown oil that was purified *via* silica gel chromatography (5% MeOH in DCM) to give the product (R_f = 0.2) as a glassy brown solid. Yield: 302 mg, 85%. ^{1}H NMR ($CDCl_3$) δ 8.07 (s, 1H), 7.71 (s, 1H), 4.76 (s, 2H), 4.42 (q, *J* = 7.1 Hz, 2H), 3.86 (s, 4H), 3.48 (d, *J* = 6.7 Hz, 8H), 1.67–1.31 (m, 21H), 0.26 (s, 9H). ^{13}C NMR ($CDCl_3$) δ 163.89, 161.71, 161.32, 160.94, 160.56, 150.32, 148.17, 135.01, 130.27, 127.58, 120.14, 117.27, 114.40, 111.53, 104.22, 100.07, 82.37, 82.08, 62.38, 58.51, 28.43, 28.30, 14.34, -0.50. LC-MS (ESI): *m/z* 589.310 $[M+H]^+$ (100%). Analytical HPLC: 99% purity (254 nm).

Ethyl 6-((1,4,7-triazacyclononan-1-yl)methyl)-4-((trimethylsilyl)ethynyl)picolinate (3)

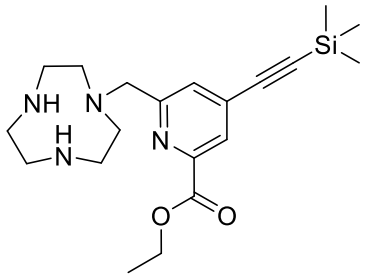

Compound **2** (600 mg, 1.02 mmol) was dissolved in neat TFA (10 mL) and stirred O/N at RT. The TFA was then removed under a stream of nitrogen to yield an off-white solid that was used without purification. Yield: 396 mg, quant. LC-MS (ESI): *m/z* 389.30 $[M+H]^+$ (100%)

6,6'-((7-((6-Carboxy-4-ethynylpyridin-2-yl)methyl)-1,4,7-triazacyclononan-1,4-diyl)bis(methylene))dipicolinic acid (4)

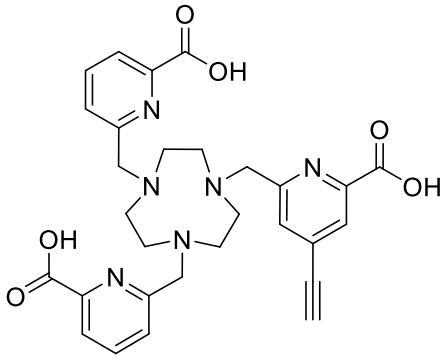

Compound **3** (396 mg, 1.02 mmol), ethyl 6-(bromomethyl)picolinate (622 mg, 2.55 mmol) and DIPEA (527 mg, 710 µL, 4.08 mmol) were dissolved in MeCN (50 mL) and stirred under reflux O/N. Removal of solvent *in vacuo* gave a yellow solid. This crude material was purified *via* silica gel chromatography (5% MeOH in DCM) to give the intermediate as a glassy yellow solid that was used without purification. Yield: 379 mg, 52%. To a solution of the intermediate (150 mg, 210 µmol) in MeCN (10 mL) was added 1.0 M NaOH (2.1 mL) and the resulting solution stirred at RT for 3 h. Purification *via* RP-DCVC gave the product as a fluffy off-white solid. Yield: 62 mg, 27%, over 2 steps. ^{1}H NMR (CD_3OD) δ 8.05–7.96 (m, 3H), 7.90 (t, *J* =

7.7 Hz, 2H), 7.62–7.53 (m, 3H), 4.23 (s, 4H), 4.17 (s, 2H), 3.96 (s, 1H), 3.28–3.06 (m, 12H). HRMS (ESI): *m/z* calc'd for $[M+H]^+$, M = $C_{29}H_{30}N_6O_6$: 559.2300, found: 559.2301. Analytical HPLC: 95% purity (254 nm).

Tb-4

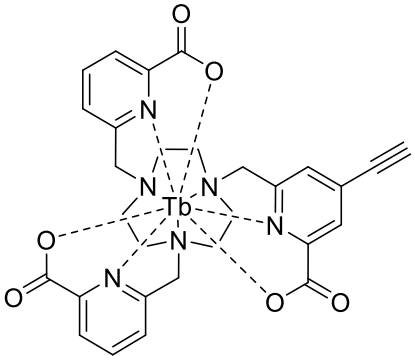

Compound **4** (30 mg, 54 μmol) and $Tb(OTf)_3$ (49 mg, 81 μmol) were dissolved in MilliQ H_2O (5 mL) and the pH adjusted to between 8 and 9 with 2 M NaOH. The resulting solution was heated at 90°C with stirring for 2 h, after which time LC-MS analysis showed near-quantitative complexation. Purification *via* preparative HPLC gave the desired product as fluffy white solid. Yield: 11 mg, 29%. HRMS (ESI): *m/z* calc'd for $[M+H]^+$, M = $C_{29}H_{27}N_6O_6Tb$: 715.1318, found: 715.1342. HPLC: 97% purity (254 nm).

5-Nitro-1,2-dihydroacenaphthylene (5)[7]

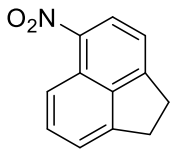

Acenaphthene (10.00 g, 64.85 mmol) was dissolved in glacial AcOH (78 mL), set stirring and placed in a bath of flowing water. 95% fuming nitric acid (10.22 g, 6.77 mL, 162.1 mmol) was added dropwise and the resulting solution stirred at RT for 3 h. Water (200 mL) was added, and the resulting precipitate collected *via* vacuum filtration to give the crude product as an orange solid. Recrystallisation from glacial AcOH and then from EtOH gave the pure product

as needle-like yellow crystals. Yield: 10.97 g, 79%. ^{1}H NMR ($CDCl_3$) δ 8.58 (d, *J* = 8.6 Hz, 1H), 8.52 (d, *J* = 7.7 Hz, 1H), 7.79–7.71 (m, 1H), 7.47 (d, *J* = 7.0 Hz, 1H), 7.35 (d, *J* = 7.7 Hz, 1H), 3.54–3.49 (m, 2H), 3.49–3.44 (m, 2H). ^{13}C NMR ($CDCl_3$) δ: 132.02, 127.78, 121.26, 120.18, 117.97, 33.16, 30.64, 30.60. LC-MS (ESI): *m/z* 200.02 $[M+H]^+$ (100%). Analytical HPLC: 85% purity (254 nm).

6-Nitro-1*H*,3*H*-benzo[de]isochromene-1,3-dione (6)[7]

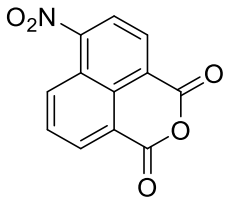

Compound **5** (8.30 g, 37.7 mmol) and sodium dichromate (27.29 g, 104.2 mmol) were dissolved in glacial AcOH (140 mL) and the resulting solution heated with stirring at reflux for 5 h. Water (300 mL) was added and the resulting orange precipitate collected *via* filtration. Purification *via* silica gel chromatography (2% MeOH in DCM) gave the product (R_f = 0.8) as an orange solid. Yield: 7.25 g, 72%. ^{1}H NMR (DMSO-D_6) δ 8.75 (dd, *J* = 8.7, 0.8 Hz, 1H), 8.66 (dd, *J* = 7.3, 0.8 Hz, 1H), 8.63 (d, *J* = 8.0 Hz, 1H), 8.56 (d, *J* = 8.0 Hz, 1H), 8.12 (dd, *J* = 8.7, 7.4 Hz, 1H). ^{13}C NMR (DMSO-D_6) δ 160.06, 159.45, 149.55, 133.20, 131.07, 130.58, 130.29, 129.79, 124.39, 124.08, 122.78, 120.05. LC-MS (ESI): *m/z* 244.03 $[M+H]^+$ (100%). Analytical HPLC: 89% purity (254 nm).

4-Amino-1,8-napthalic anhydride (7)[7]

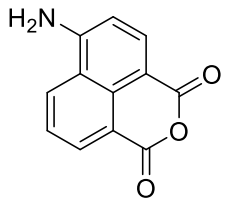

A solution of tin(II) chloride (5.85 g, 30.8 mmol) in concentrated HCl (32 %, 5.25 mL) was added dropwsie to a solution of compound **6** (1.50 g, 6.17 mmol) in EtOH (5 mL) and the resulting mixture refluxed for 2 h. The precipitate formed during this time was collected *via* vacuum filtration and washed consecutively with water, EtOH and Et_2O (10 mL each) to give the desired product as an orange solid. Yield: 953 mg, 72%. ^{1}H NMR (DMSO-D_6) δ 8.66 (d, *J* = 8.3 Hz, 1H), 8.40 (d, *J* = 7.2 Hz, 1H), 8.16 (d, *J* = 8.5 Hz, 1H), 7.76 (s, 2H), 7.66 (t, *J* = 7.8 Hz, 1H), 6.85 (d, *J* = 8.5 Hz, 1H). ^{13}C NMR (DMSO-D_6) δ 162.00, 160.31, 153.90, 135.87, 132.98, 132.56, 130.68, 124.35, 119.29, 118.23, 108.72, 102.21. LC-MS (ESI): *m/z* 214.09 $[M+H]^+$ (100%). Analytical HPLC: 80% purity (254 nm).

6-Amino-2-(prop-2-ynyl)-1*H*-benzo[de]isoquinoline-1,3(2*H*)-dione (8)

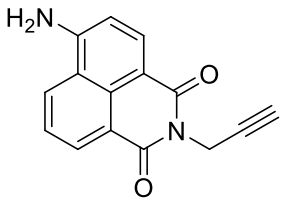

Compound **7** (500 mg, 2.35 mmol) and propargyl amine (142 mg, 178 µL, 2.58 mmol) were dissolved in 1,4-dioxane (100 mL) and stirred under reflux O/N. The solvent was removed *in vacuo* to produce a dark brown residue, which was dissolved EtOAc (150 mL) and washed with water (2 x 150 mL). The organic layer was dried over $MgSO_4$ and concentrated *in vacuo* to yield the product as a dark brown solid. Yield: 470 mg, 80%. ^{1}H NMR (DMSO-D_6) δ 8.63 (d, *J* = 8.1 Hz, 1H), 8.43 (d, *J* = 7.0 Hz, 1H), 8.20 (d, *J* = 8.4 Hz, 1H), 7.65 (t, *J* = 7.8 Hz, 1H), 7.53 (s, 2H), 6.85 (d, *J* = 8.4 Hz, 1H), 4.73 (d, *J* = 2.3 Hz, 2H), 3.07 (s, 1H). ^{13}C NMR (DMSO-D_6) δ 163.08, 162.01, 153.14, 134.27, 131.31, 129.74, 124.05, 121.39, 119.38, 108.32, 106.97, 80.00, 72.45, 28.64. LC-MS (ESI): *m/z* 250.10 $[M+H]^+$ (100%). Analytical HPLC: 90% purity (254 nm).

2-Bromo-*N*-(1,3-dioxo-2-(prop-2-ynyl)-2,3-dihydro-1*H*-benzo[de]isoquinolin-6-yl)acetamide (9)

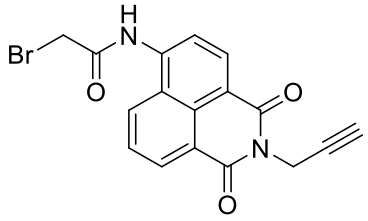

Compound **8** (620 mg, 2.48 mmol), Na_2CO_3 (1.31 mg, 12.4 mmol) and bromoacetylbromide (5.00 g, 2.16 mL, 24.8 mmol) were combined in DCM (150 mL) and the mixture refluxed O/N. After washing with water (2 x 100 mL) and drying over $MgSO_4$, the DCM was removed *in vacuo*, producing a beige residue that was used without purification. Yield: 784 mg, 85%. LC-MS (ESI): *m/z* 369.1 $[M+H]^+$ (100%). Analytical HPLC: 72% purity (254 nm).

Tri-*tert*-butyl 2,2',2''-(10-(2-((1,3-dioxo-2-(prop-2-yn-1-yl)-2,3-dihydro-1*H*-benzo[de]isoquinolin-6-yl)amino)-2-oxoethyl)-1,4,7,10-tetraazacyclododecane-1,4,7-triyl)triacetate (10)

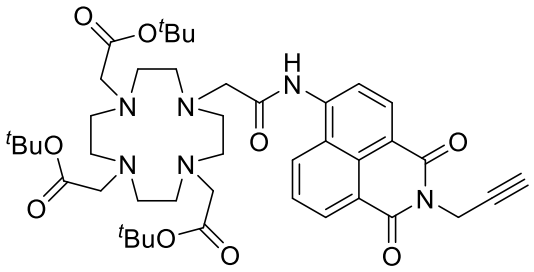

Compound **9** (200 mg, 539 µmol), ^{t}Bu$_3$DO3A·HBr (266 mg, 449 µmol) and DIPEA (174 mg, 235 µL, 1.35 mmol) were dissolved in MeCN (50 mL) and the mixture refluxed O/N. The solvent was then removed *in vacuo*, producing a dark brown oily residue. Purification *via* silica gel chromatography (5% MeOH in DCM) yielded the product (R_f = 0.1) as a yellow solid. Yield: 262 mg, 73%. ^{1}H NMR ($CDCl_3$) δ 11.17 (br, 1H), 8.83 (d, *J* = 8.5 Hz, 1H), 8.56 (d, *J* = 7.2 Hz, 1H), 8.45 (s, 2H), 7.68 (t, *J* = 7.9 Hz, 1H), 4.93 (d, *J* = 2.2 Hz, 2H), 4.89–2.45 (m,

24H), 2.20 (t, *J* = 2.4 Hz, 1H), 1.45 (s, 9H), 1.28 (s, 16H). ^{13}C NMR ($CDCl_3$) δ 163.60, 163.15, 161.80, 161.44, 161.09, 160.74, 140.07, 131.92, 129.56, 128.95, 126.88, 124.17, 122.27, 120.98, 118.77, 118.08, 115.17, 112.27, 78.88, 70.59, 31.06, 29.51, 28.12, 27.97. LC-MS (ESI): *m/z* 365.28 $[M+H]^{2+}$ (100%). Analytical HPLC: 92% purity (254 nm).

2,2',2''-(10-(2-((1,3-Dioxo-2-(prop-2-yn-1-yl)-2,3-dihydro-1*H*-benzo[de]isoquinolin-6-yl)amino)-2-oxoethyl)-1,4,7,10-tetraazacyclododecane-1,4,7-triyl)triacetic acid (11)

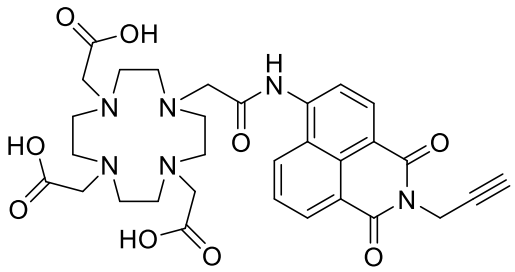

Compound **10** (150 mg, 205 µmol) was dissolved in a 1:1 mixture of TFA/DCM (5 mL) and stirred O/N at RT. A gentle stream of nitrogen was used to remove the DCM and the bulk of the TFA. The resulting dark brown oily residue was purified *via* preparative HPLC to yield the product as a fluffy yellow solid. Yield: 54 mg, 42%. LC-MS (ESI): *m/z* 637.1 $[M+H]^{+}$ (100%). Analytical HPLC: 85% purity (254 nm).

Appendix

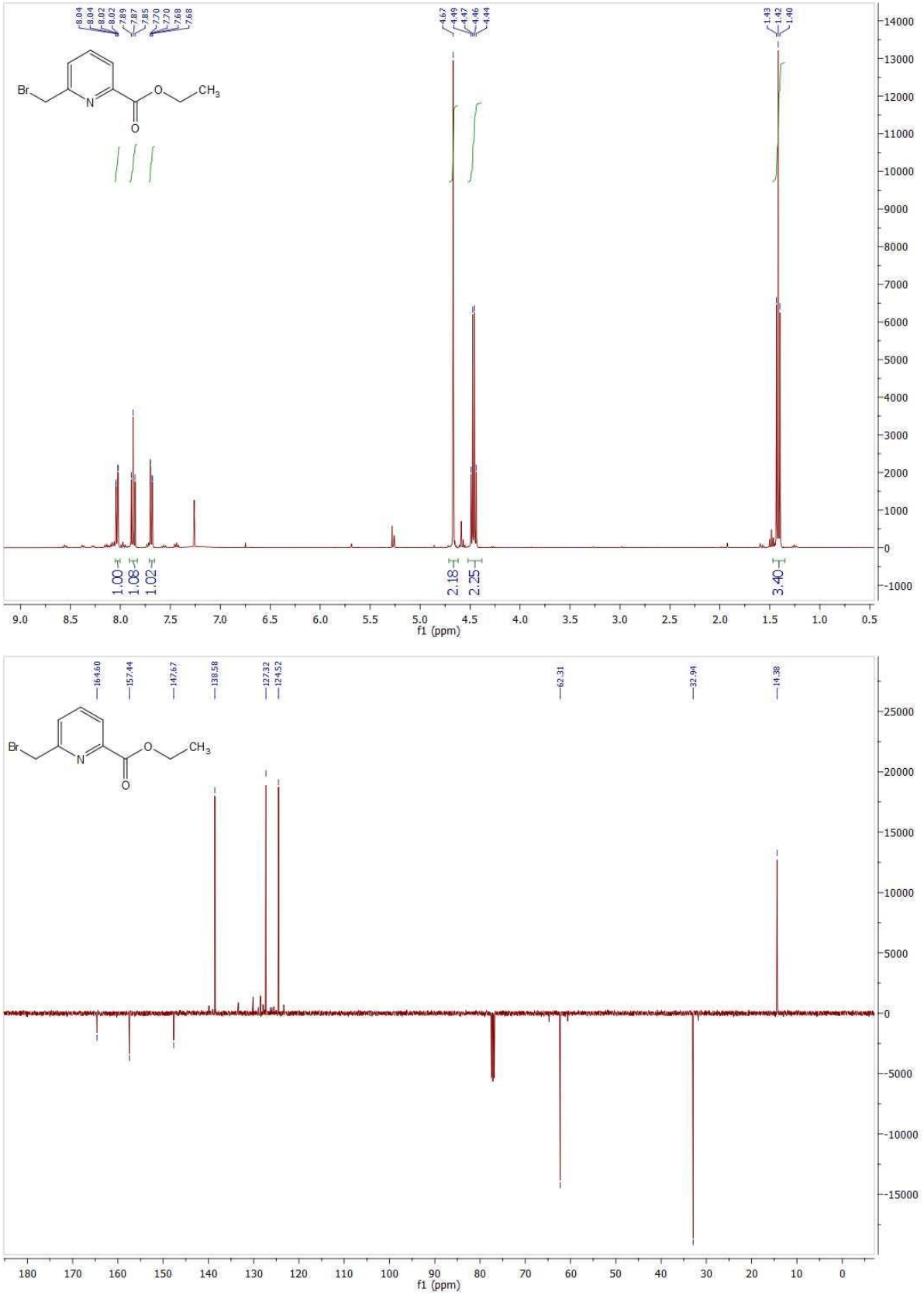

Figure A1. ^{1}H and ^{13}C NMR spectra for ethyl 6-(bromomethyl)picolinate in $CDCl_3$.

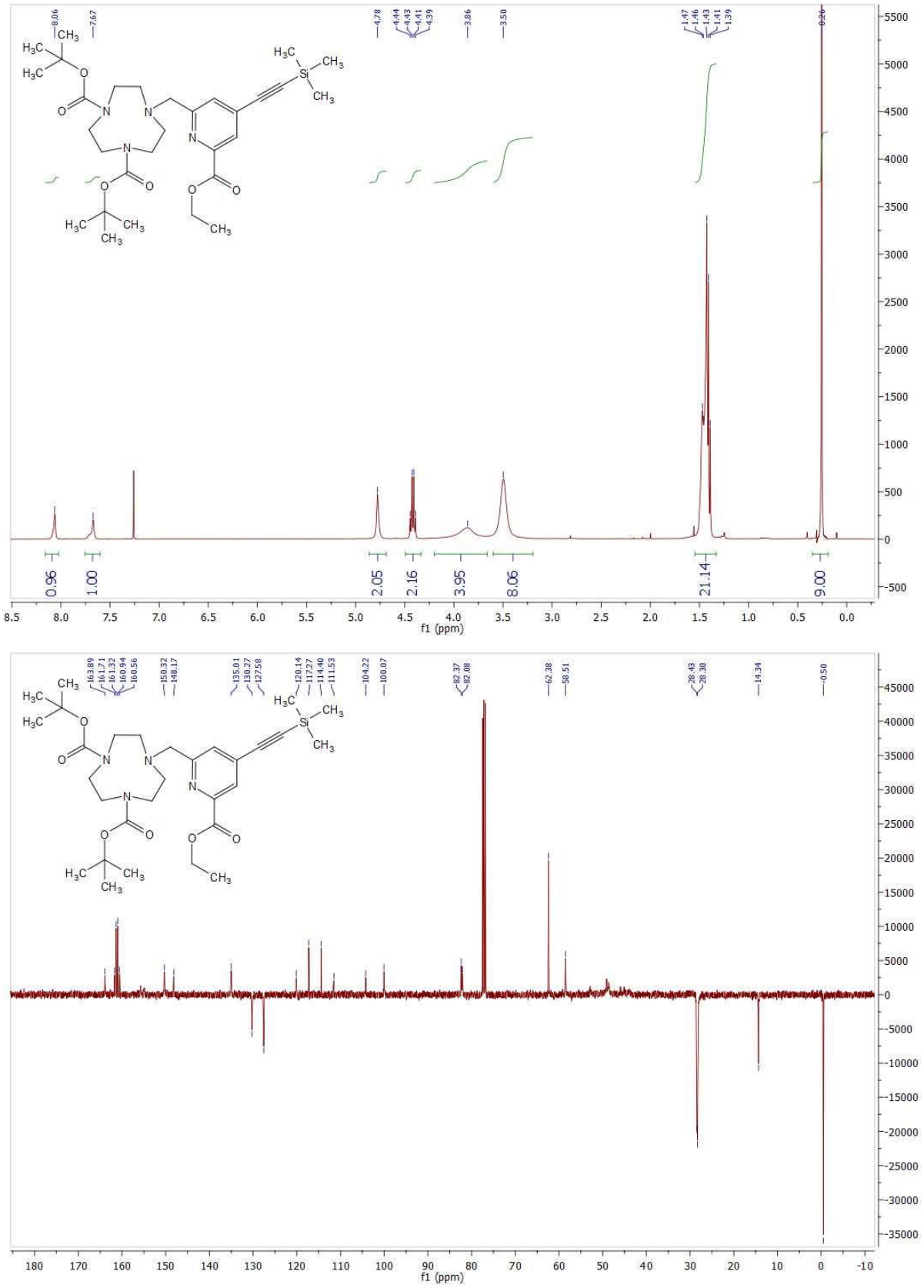

Figure A2. ^{1}H and ^{13}C NMR spectra for **2** in $CDCl_3$.

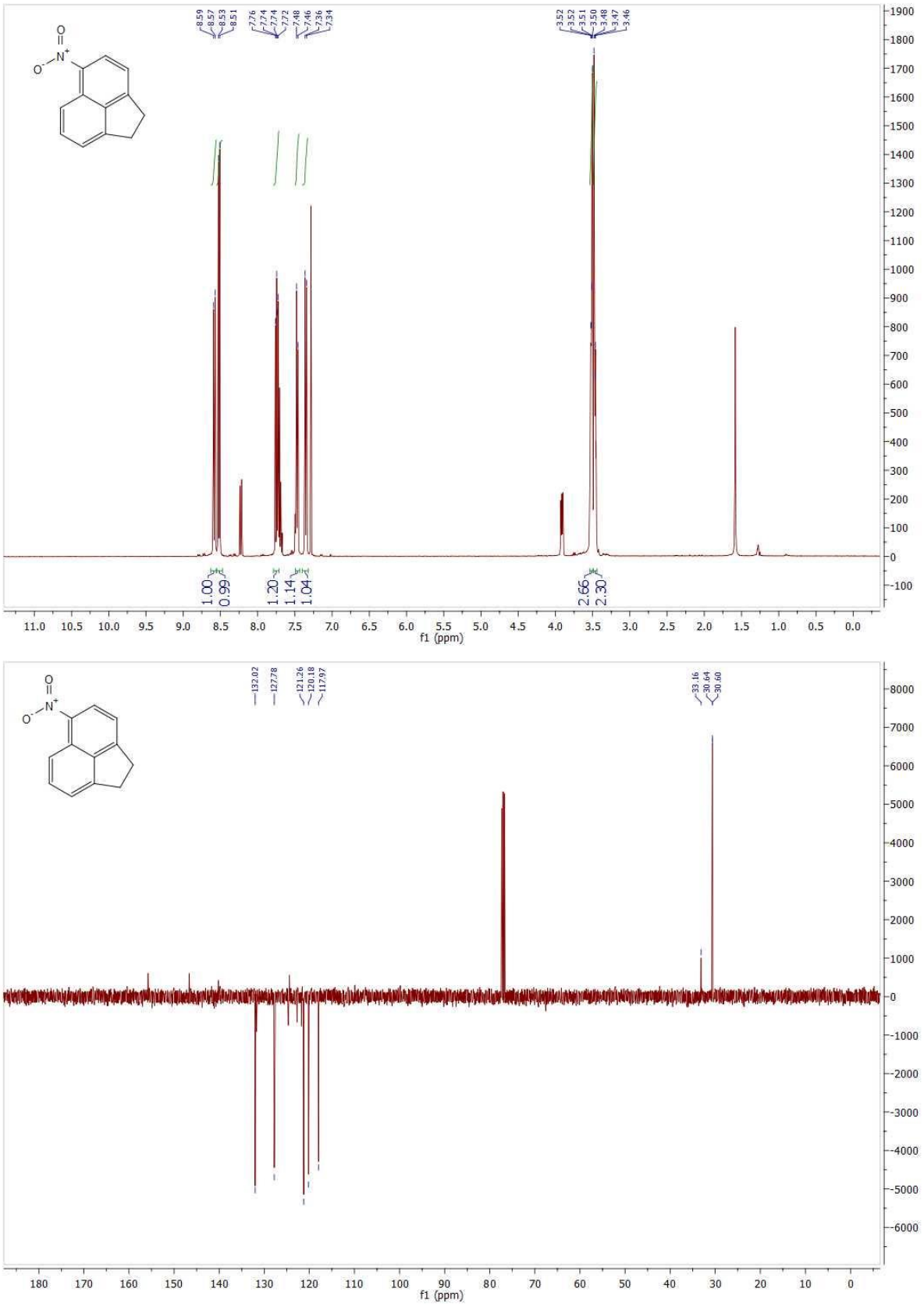

Figure A3. ^{1}H and ^{13}C NMR spectra for **5** in $CDCl_3$.

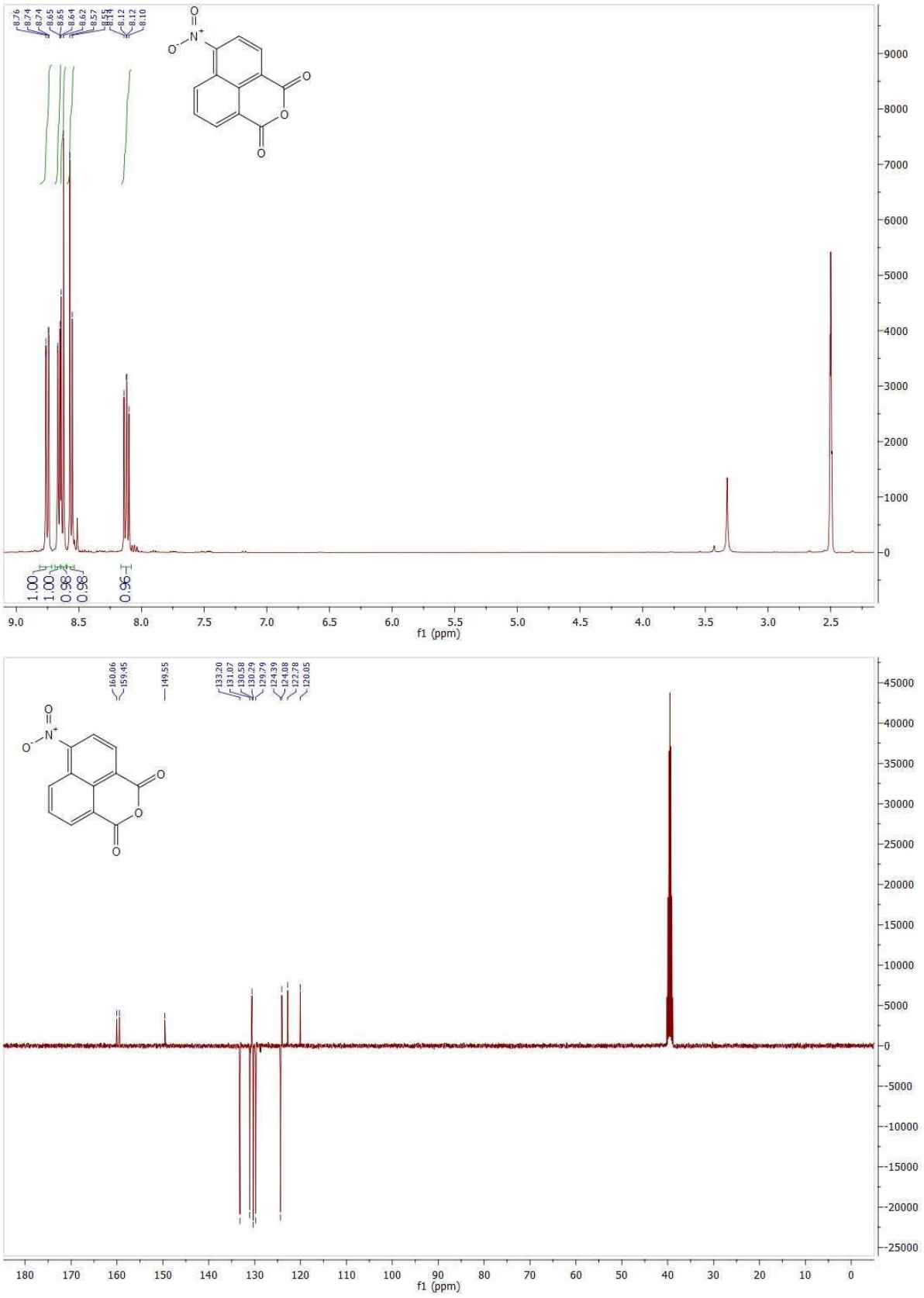

Figure A4. ^{1}H and ^{13}C NMR spectra for **6** in DMSO-D_6.

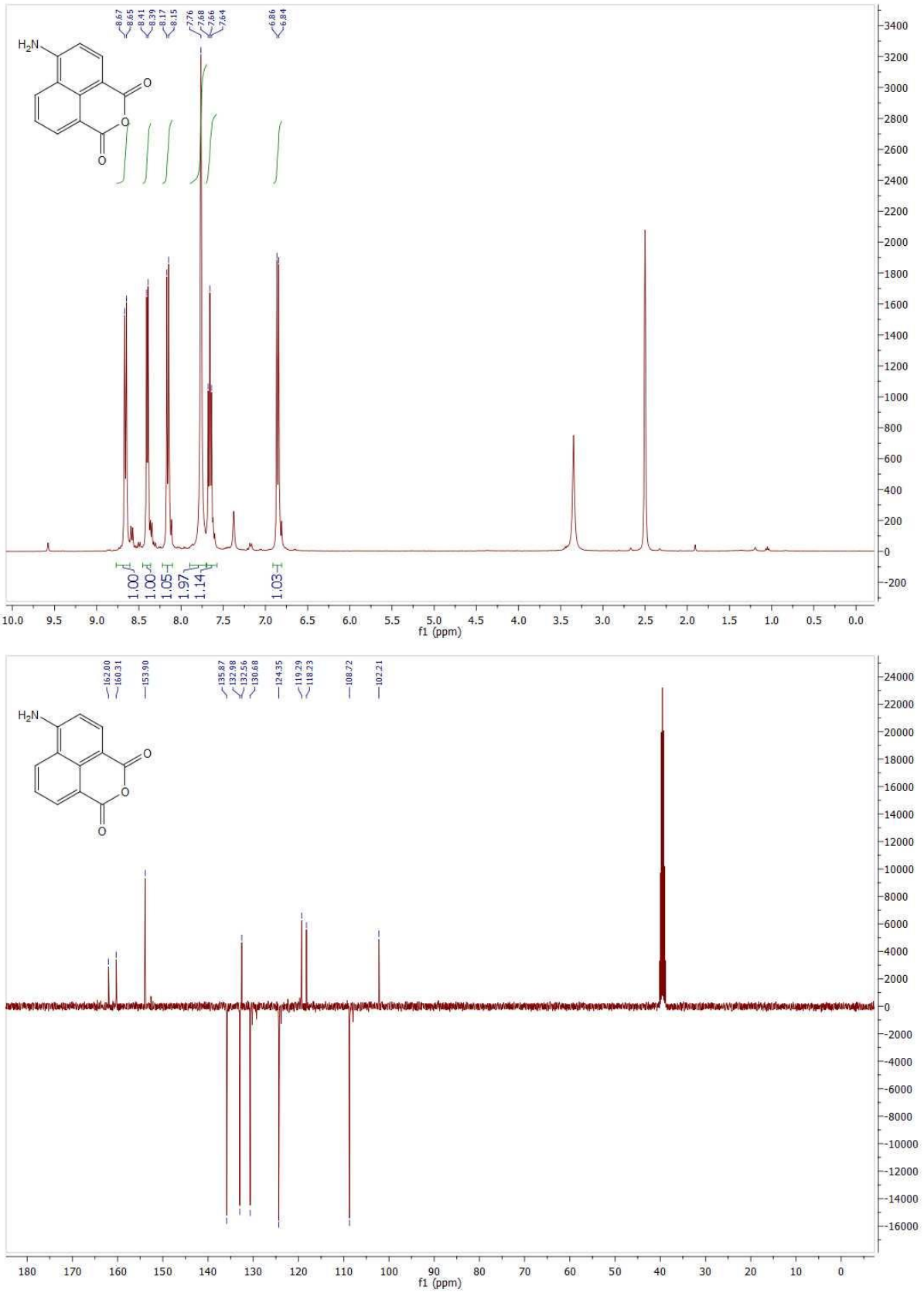

Figure A5. ^{1}H and ^{13}C NMR spectra for **7** in DMSO-D_6.

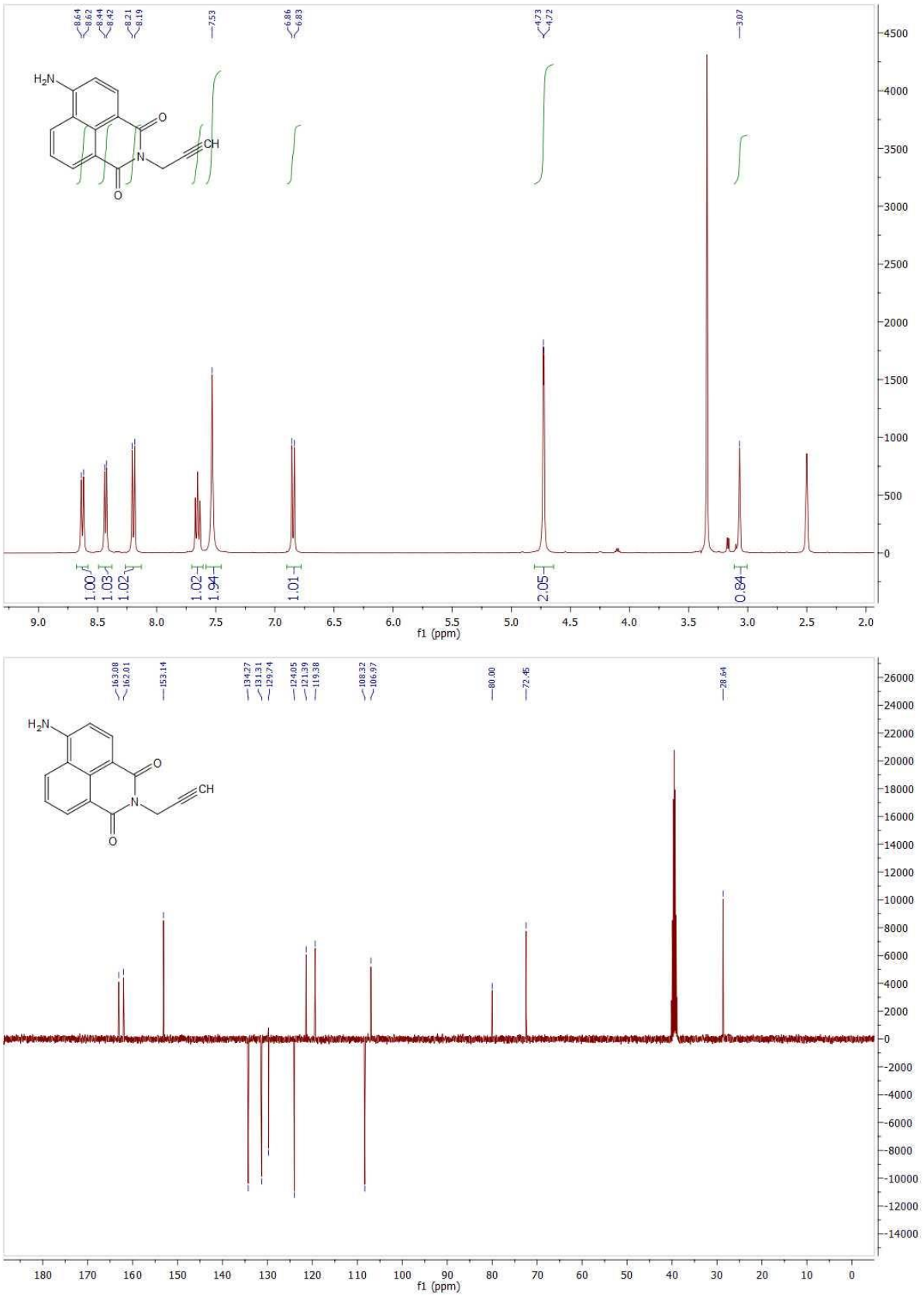

Figure A6. ^{1}H and ^{13}C NMR spectra for **8** in DMSO-D_6.

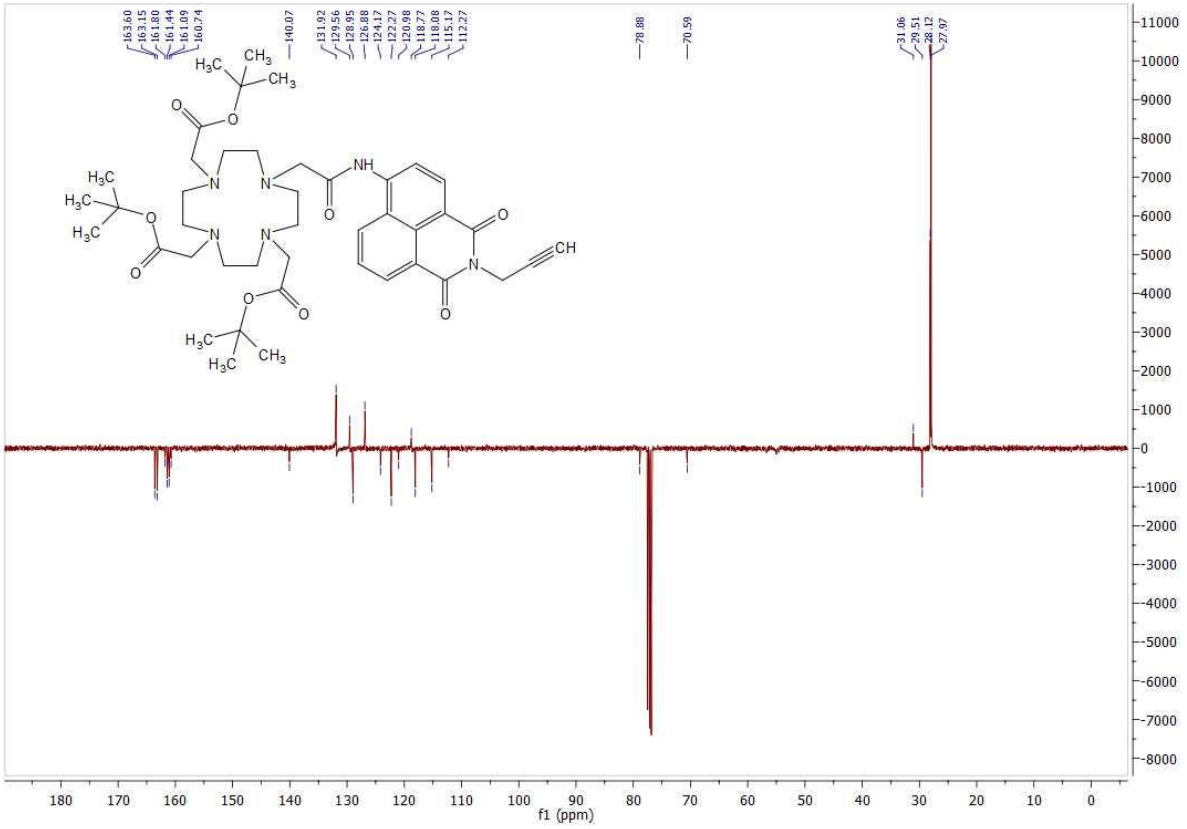

Figure A7. ^{13}C NMR spectrum for **10** in $CDCl_3$.

References

(1) Beeby, A.; Clarkson, I. M.; Dickins, R. S.; Faulkner, S.; Parker, D.; Royle, L.; de Sousa, A. S.; Williams, J. A. G.; Woods, M. *J. Chem. Soc. Perkin Trans. 2* **1999**, *2* (3), 493–504.

(2) Gateau, C.; Mazzanti, M.; Pécaut, J.; Dunand, F. A.; Helm, L. *Dalt. Trans.* **2003**, No. 12, 2428–2433.

(3) Nocton, G.; Nonat, A.; Gateau, C.; Mazzanti, M. *Helv. Chim. Acta* **2009**, *92* (11), 2257–2273.

(4) Kovacs, Z.; Sherry, A. D. *Tetrahedron Lett.* **1995**, *36* (51), 9269–9272.

(5) Rajakumar, P.; Selvam, S. *Tetrahedron* **2007**, *63* (36), 8891–8901.

(6) Evans, W. F. J.; Puckrin, E. *Geophys. Res. Lett.* **1996**, *23* (14), 1769–1772.

(7) Zhang, L.; Duan, D.; Liu, Y.; Ge, C.; Cui, X.; Sun, J.; Fang, J. *J. Am. Chem. Soc.* **2014**, *136* (1), 226–233.

(8) Raghunand, N.; Guntle, G. P.; Gokhale, V.; Nichol, G. S.; Mash, E. A; Jagadish, B. *J. Med. Chem.* **2010**, *53* (18), 6747–6757.

CHAPTER 5:

ASSEMBLY OF BOMBESIN CONJUGATES FOR BIMODAL PET-FLUORESCENCE IMAGING USING "CLICKABLE" 1,4,7-TRIAZACYCLONONANE DERIVATIVES

5.1 Introduction

Nuclear medicine is a medical discipline in which small amounts of radioisotopes are injected intravenously, swallowed or inhaled in gaseous form for the purpose of imaging internal organs, evaluating various physiological functions or treating various diseases. Nuclear imaging is one the oldest imaging techniques, predating computer-assisted tomography (CT) and magnetic resonance imaging (MRI). The radioactive material typically consists of a biologically active compound (e.g., tumour-targeting antibody or peptide) labelled with a radioisotope. Depending on the type and application of the radioisotope, these compounds can be used for therapy, diagnosis, or both.

Within the nuclear medicine field, radioactive metal ions have found particularly extensive application. This has seen the development of a wide range of metal chelators ("bifunctional chelators") that can be conjugated to peptides, antibodies, etc. It is of utmost importance that these chelates form highly stable complexes with the metal to prevent the release of radioactive material into normal tissue. A secondary requirement is that the ligand-metal complex is formed quickly, so that full advantage can be made of the limited time dictated by the half-life of the radionuclides. Ligands that have been investigated previously to fulfil these requirements are typically amine-containing polydentates. Some specific examples are those belonging to the triamine and tetraamine family of macrocyclic compounds,[1] such as 1,4,8,11-tetraazacyclotetradecane (cyclam, **1**), 1,4,7,10-tetraazacyclododecane (cyclen, **2**), 1,4,7-triazacyclononane-1,4,7-triacetic acid (NOTA, **3**), 1,4,7,10-tetraazacyclododecane-1,4,7,10-tetraacetic acid (DOTA, **4**) and 1,4,8,11-tetraazacyclotetradecane-1,4,8,11-tetraacetic acid (TETA, **5**) shown in **Figure 1**.[2–5] A range of conjugatable derivatives of these and other metal chelators have been developed,[6–8] several of which are now commercially available through companies such as Macrocyclics Inc.

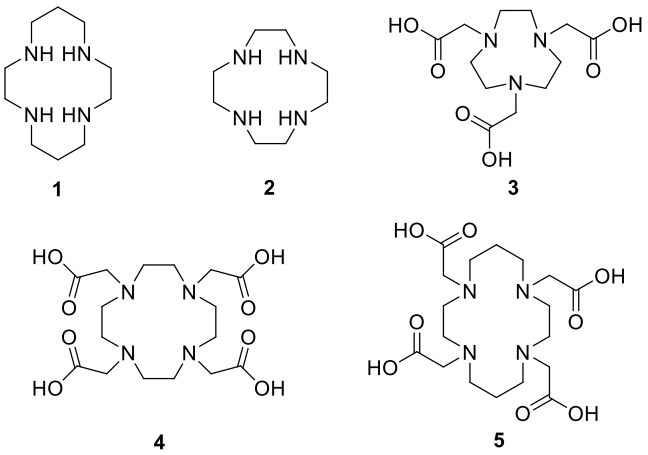

Figure 1. Examples of copper-chelating ligands.

Our group has been particularly interested in the development of chelators of copper radioisotopes. Of the available copper radioisotopes (^{60}Cu, ^{61}Cu, ^{62}Cu, ^{64}Cu and ^{67}Cu), ^{64}Cu ($t_{1/2}$ = 12.7 h) and ^{67}Cu ($t_{1/2}$ = 61.8 h) are most heavily applied within the field of radiopharmacy due to their favourable decay characteristics. Through the utilisation of radionuclide chelating ligands, radiopharmaceuticals have successfully been generated and applied, in conjunction with positron emission tomography (PET) (**Figure 2**), to image and treat various pathologies including cardiovascular disease, inflammation and cancer.[8]

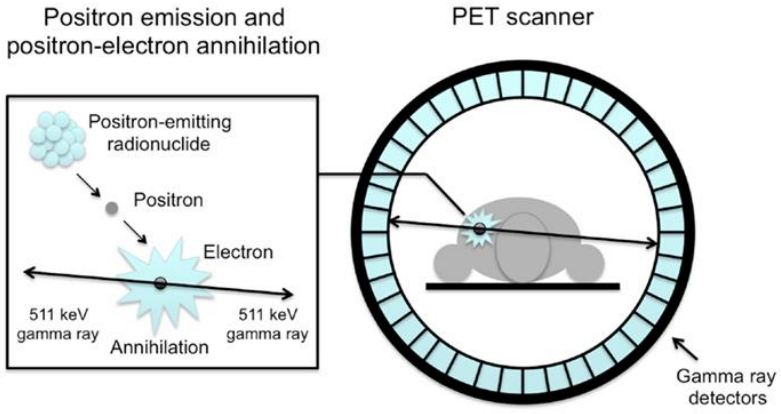

Figure 2. Image acquisition *via* positron emission tomography (PET): Emission of positrons from the radionuclide collide and annihilate with electrons within the surrounding tissue, causing the release of two photons of 511 keV at approximately 180° of each other. These emitted photons are detected by scintillation crystals. Based upon when and where these photons are detected, three-dimensional images showing the localisation of the radionuclide can be constructed *via* computer analysis. Image reproduced from van der Velt *et al*.[9]

In collaboration with the Spiccia group from Monash University, Clayton, and the Stephan group at the Helmholtz Institute in Dresden, Germany, our group have developed a number of Cu(II)-chelating functionalised 1,4,7-triazacyclononane (TACN) macrocycles for PET applications over the years. Examples of some such compounds are shown in **Figure 3**.[10–18] Many of the chelators have been utilised in various applications, including the radiolabelling of magnetic nanoparticles[14,19] and dendrimers,[17] imaging of cancers through conjugation to targeting peptides,[10,11,18] or represent useful building blocks for future applications.[16]

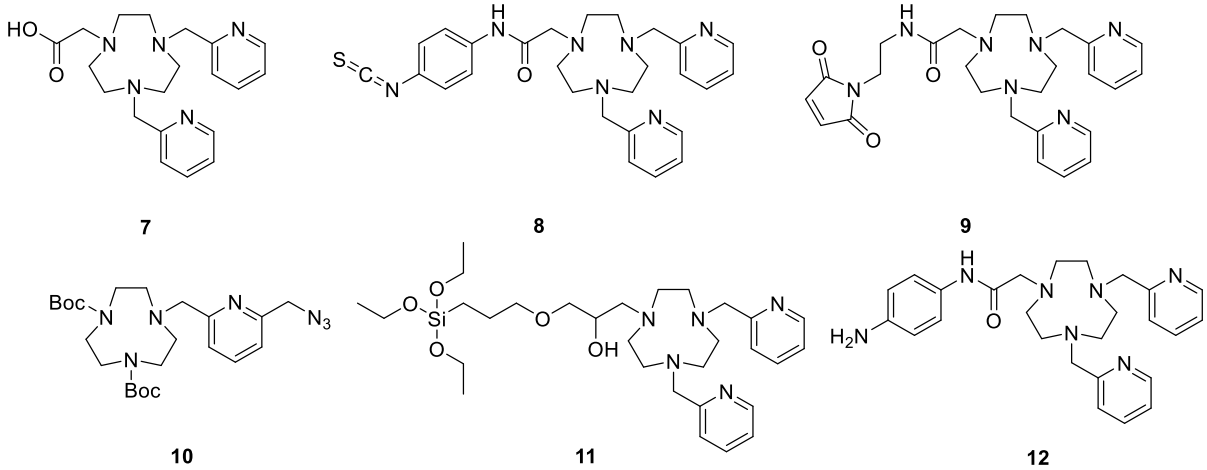

Figure 3. Selected Cu(II)-chelating TACN derivatives developed for PET applications: 2-(4,7-*bis*(pyridin-2-ylmethyl)-1,4,7-triazacyclononan-1-yl)acetic acid (**7**),[10] 2-(4,7-*bis*(pyridin-2-ylmethyl)-1,4,7-triazacyclononan-1-yl)-*N*-(4-isothiocyanatophenyl)acetamide (**8**),[17] 2-(4,7-*bis*(pyridin-2-ylmethyl)-1,4,7-triazacyclononan-1-yl)-*N*-(2-(2,5-dioxo-2,5-dihydro-1H-pyrrol-1-yl)ethyl)acetamide (**9**),[17] di-*tert*-butyl 7-((6-(azidomethyl)pyridin-2-yl)methyl)-1,4,7-triazacyclononane-1,4-dicarboxylate (**10**),[18] 1-(4,7-*bis*(pyridin-2-ylmethyl)-1,4,7-triazacyclononan-1-yl)-3-(3-(triethoxysilyl)propoxy)propan-2-ol (**11**),[14] *N*-(4-aminophenyl)-2-(4,7-*bis*(pyridin-2-ylmethyl)-1,4,7-triazacyclononan-1-yl)acetamide (**12**).[19]

A feature of most of the bifunctional chelators shown in **Figure 3** is that they are designed to react with amine groups, and so are typically incorporated into peptides during solid-phase peptide synthesis, before cleavage off the resin support and deprotection. The exception is the pro-chelator **10**, which features an azide group. This was successfully incorporated into a peptide-based probe targeting the epidermal growth factor receptor using a Cu(I)-catalysed click reaction.[18]

Bio-orthogonal reactions such as the click reaction have begun to find increasing application in the field of nuclear medicine. This is because they provide an elegant means of rapidly introducing radioactive labels to biologically active molecules in a highly controlled fashion and without the need for complex protection group strategies, as previously discussed in section 1.5.3.

In this chapter, the synthesis and utilisation of two new "clickable" TACN-based pro-chelator building blocks (**17** and **23**, **Figure 4**) is reported. These are comprised of a di-protected TACN ring with a single pyridine pendant group incorporating an alkyne in the case of **17** and a single picolinic acid pendant group incorporating an alkyne in the case of **23**. It was envisaged that these pro-chelators would both ultimately produce pentadentate ligand motifs once attached to a targeting vector and fully deprotected (**Figure 4**). Based on previous work,[18] it was considered likely that the triazole ring formed upon "clicking" **17** would provide a fifth donor atom within the coordination sphere.

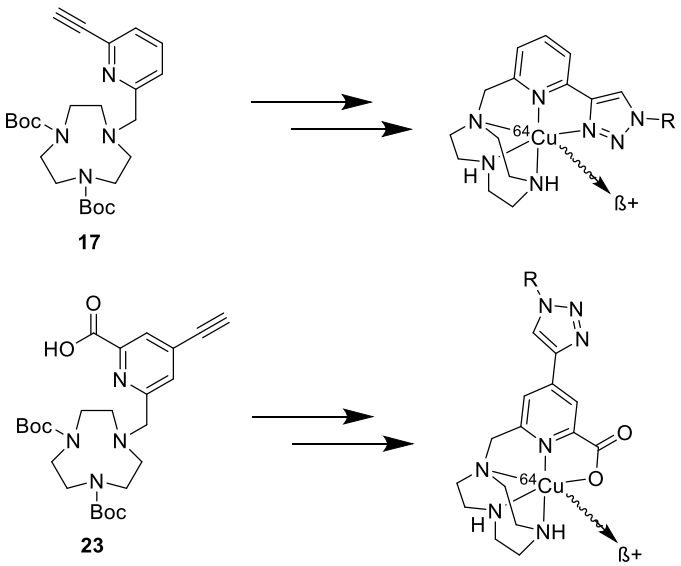

Figure 4. Structures of "clickable" pro-chelators and their envisaged mode of ^{64}Cu chelation following "clicking" and deprotection.

For this study, it was proposed to assess the utility and suitability of the pro-chelators through the construction of two tumour-imaging agents targeting the gastrin-releasing peptide

(GRP) receptor.[20] The mammalian gastrin-releasing peptide receptor (GRPr) is one of four receptor subtypes belonging to the bombesin receptor family, and the most widely studied since the discovery of the membrane-bound bombesin receptor system. It has been demonstrated that activation of this system by GRP or bombesin can stimulate cancer growth as well as induce an autocrine feedback system that upregulates the expression of the stimulating peptides and associated receptors.[21–24] The bombesin receptor system was heavily investigated by Anastasi *et al*.[25] following the isolation of the tetradecapeptide bombesin from the skin of the *Bombina bombina* frog skin in 1971. Further work in the field by McDonald *et al.*[26] in 1979 saw the isolation of the bombesin mammalian counterpart from porcine gastric tissue as a 27 amino acid-long peptide called GRP. These two peptides, GRP and bombesin, have a homologous peptide sequence, -Trp-Ala-Val-Gly-His-Leu-Met-NH_2, at the C-terminus.

Work done more recently has demonstrated that a variety of human carcinomas, including prostate, breast and small cell lung cancers over-express GRPr, allowing them to be actively targeted.[21,27–30] Targeting of these cancers is often performed with the aid of antibodies, which typically exhibit highly selective binding to antigens and are comparatively easy to initially develop. However, they can present quite high immunogenicity and slow diffusion rates, and although the initial development may be relatively fast, specialist equipment is required for antibody synthesis and isolation.

Another option available for active targeting is the use of relatively short-chain peptides. Advantages of such a targeting system include fast diffusion rates as well as low immunogenicity when compared with much larger antibodies and proteins. These peptides can typically be synthesised on non-specialist equipment and easily modified for various purposes, e.g., inclusion of non-natural amino acids to facilitate conjugation. Initial use of the bombesin (BBN) peptide as a GRPr-targeting agent involved use of the full 14 amino acid-long amphibian chain (Pyr-Gln-Lys-Leu-Gly-Asn-Gln-Trp-Ala-Val-Gly-His-Leu-Met-NH_2)

conjugated to a ^{99m}Tc-DADT (diaminodithol) radiocomplex. Very high receptor-binding affinity was demonstrated.[31] It has since been discovered that a shortened sequence, BBN (7-14-NH_2) (Gly-Asn-Gln-Trp-Ala-Val-Gly-His-Leu-Met-NH_2), can also provide excellent selectivity and affinity for tumour cells. ^{18}F, ^{68}Ga and ^{99m}Tc derivatives of this sequence have been utilised successfully for imaging GRPr-positive prostate cancer cell lines.[20,32–35] Another bombesin derivative that has been applied to ^{99m}Tc radio imaging is panbomesin, a 6-14 bombesin chain characterised by the replacement of Asn(6), Leu(13) and Met(14) by d-Phe(6), Leu-NHEt(13) and desMet(14), which functions as a fully competitive agonist.[36]

The specific bombesin analogue that was selected for this work was [Cha(13), Nle(14)]BBN(7-14). Conjugates of this particular peptide with ^{99m}Tc(CO_3) radiocomplexes show increased metabolic stability in blood and tumour cells when compared to native BBN(7-14). The addition of a *β*Ala, *β*Ala spacer further adds to this stability.[35,37] The investigation of this particular peptide with a ^{64}Cu radiolabel had been reported by Gasser *et al.*,[10] as well as Bergmann *et al.*[11] As part of the current study, a goal was to extend on this work by seeking to assemble two BBN-based probes suitable for combined PET and fluorescence imaging. The envisaged strategy was to synthesise the *β*Ala-*β*Ala-[Cha(13),NLe(14)]BBN(7-14) (= *β*Ala-*β*Ala-Gln-Tpr-Ala-Val-Gly-His-Cha-Nle-NH_2) peptide on resin and to incorporate a non-natural azido-ornithine amino acid residue to facilitate attachment of the pro-chelator groups *via* click conjugation. A sulfonated near-infrared fluorescent cyanine dye ("sulfo-Cy5") could then be appended to the *N*-terminus of the peptide (**Figure 5**). The synthesis of the two probes, and an initial assessment of the utility of one of them for *in vivo* PET imaging studies, is presented.

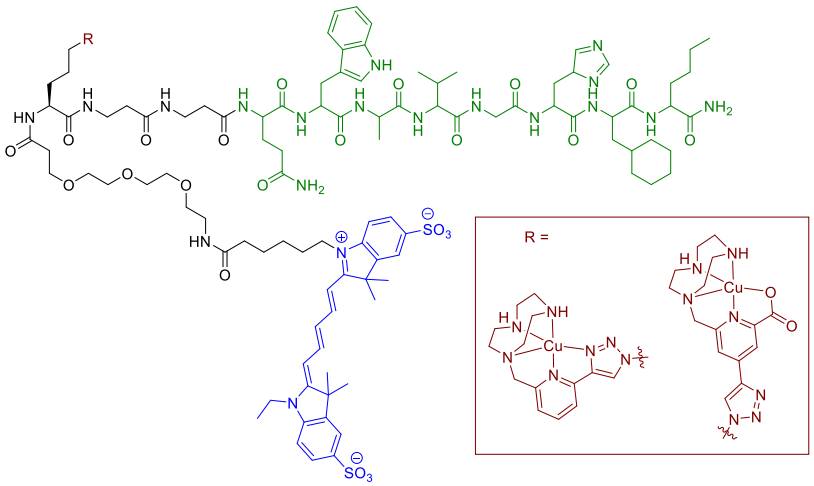

Figure 5. Structure of the two bimodal imaging probes prepared as part of this work. Green: bombesin derivative targeting the GRPr. Blue: near-IR emitting sulfo-Cy5 dye. Red: positron-emitting ^{64}Cu chelate.

5.2 Synthesis of "clickable" TACN-based derivatives

The preparation of the two TACN-based pro-chelators, **17** and **23**, commenced with the preparation of two pyridine compounds, **15** and **21**, designed to serve as the "clickable" conjugation handles as well as provide additional binding sites for a ^{64}Cu(II) ion. These pyridine compounds are the same as those used in the construction of the terbium complexes described in **Chapter 2**. Synthesis of the first pro-chelator (**Scheme 1**) proceeded with coupling of **15** to the macrocyclic ring of di-*tert*-butyloxycarbonyl-protected 1,4,7-triazacyclononane (Boc_2TACN)[38,39] yielding intermediate **16** in 66% yield after separation from unreacted starting materials *via* silica flash chromatography. The trimethylsilyl (TMS) protecting group was then removed by treatment with KF to afford the pro-chelator in 65% yield and greater than 95% purity after reverse-phase dry column vacuum chromatography (RP-DCVC). The ^{1}H nuclear magnetic resonance (NMR) spectrum of the TFA salt of **17** in $CDCl_3$ (**Figure 6**) showed a broad set of unresolved resonances corresponding to the CH_2 groups of the TACN ring between *ca.* 3–4 ppm, as well as the expected three aromatic proton signals corresponding to the pyridine (Py) ring at 7.49, 7.55 and 7.74 ppm. A single sharp resonance at 3.15 ppm confirmed the TMS deprotection of the alkyne, and signals corresponding to the C*H*$_2$Py and ^{t}Bu group

protons were observed at 4.67 and *ca.* 1.5 ppm, respectively. Formation of the desired product was also evidenced by the signal at *m/z* = 445.27 in the electrospray mass spectrum, corresponding to the $[M+H]^+$ species.

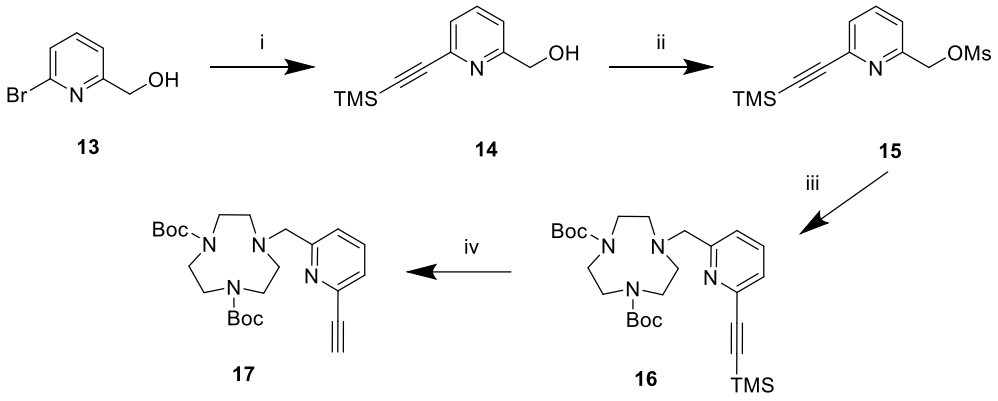

Scheme 1. Synthesis of pro-chelator **17**. i) $Pd(PPh_3)_2Cl_2$, TMS acetylene, CuI, Et_3N, THF, N_2 atmosphere, RT, 2 h, 75%; ii) MsCl, DIPEA, DCM, 0ºC to RT, 30 min, 96%; iii) Boc_2TACN, *N*,*N*-diisopropylethylamine (DIPEA), MeCN, reflux, O/N, 66%; iv) KF, H_2O/MeCN, RT, 2 h, 65%.

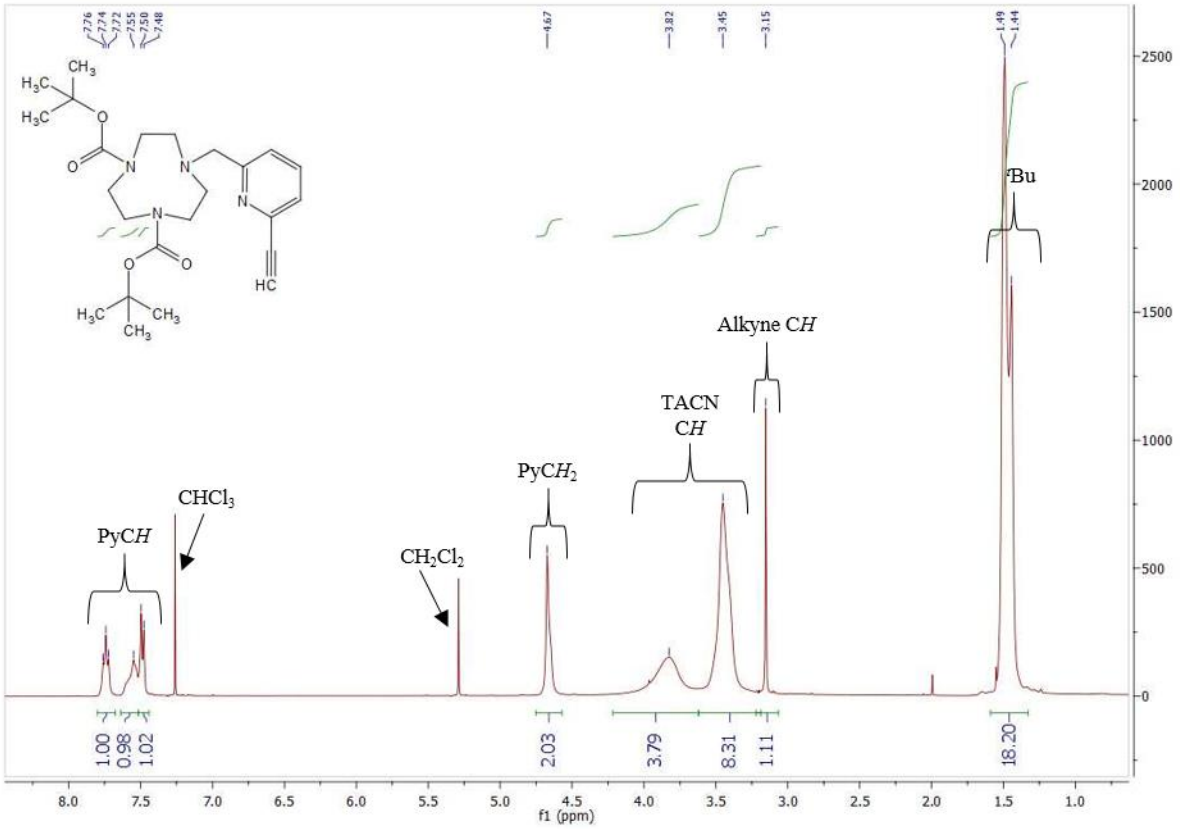

Figure 6. ^{1}H NMR spectrum for **17** in $CDCl_3$.

The synthesis of the second pro-chelator **23** (**Scheme 2**) involved attachment of the functionalised picolinate ester **21** to Boc_2TACN, to afford compound **22** in 85% yield after purification *via* silica flash chromatography. Treatment with NaOH removed the TMS protective group and hydrolysed the ethyl ester, giving the pro-chelator **23** in 41% yield and greater than 95% purity following isolation *via* RP-DCVC.

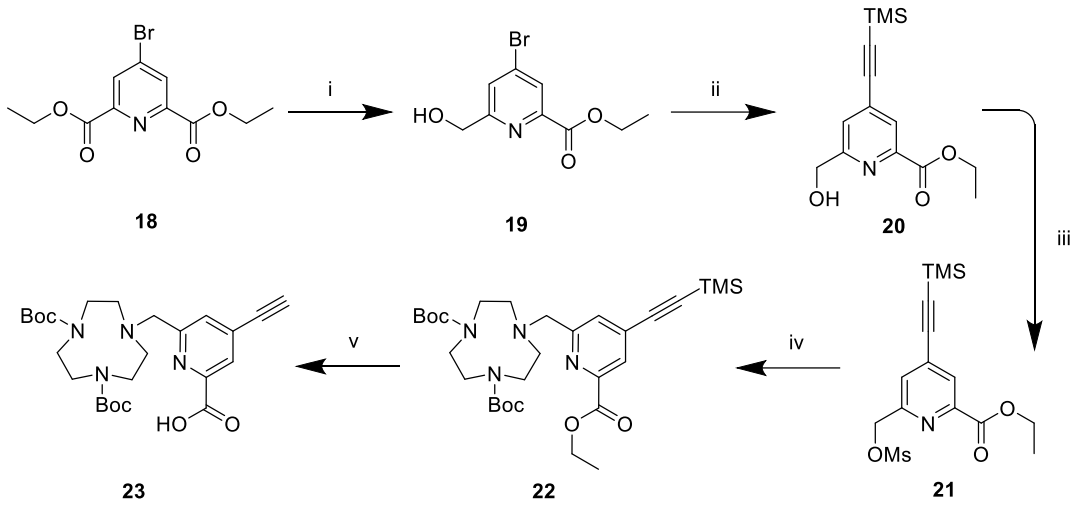

Scheme 2. Synthesis of pro-chelator **23**. i) $NaBH_4$, EtOH, reflux, 15 min, 48%; ii) $Pd(PPh_3)_2Cl_2$, TMS acetylene, CuI, Et_3N, THF, N_2 atmosphere, RT, 2 h, 85%; iii) MsCl, DIPEA, DCM, 0°C to RT, 30 min, quant.; iv) Boc_2TACN, DIPEA, MeCN, reflux, O/N, 85%; v) NaOH, H_2O/MeCN, RT, 2h, 41%.

Similar to **17**, the ^{1}H NMR spectrum of **23** in $CDCl_3$ (**Figure 7**) showed a broad set of unresolved signals corresponding to the CH_2 protons between *ca.* 3–4 ppm, a sharp signal attributed to the alkyne proton at 3.51 ppm, and signals at 4.78 and *ca.* 1.5 ppm corresponding to the C*H*$_2$Py and ^{t}Bu group protons, respectively. The two expected pyridyl CH singlet resonances were observed at 7.67 and 8.06 ppm. A signal corresponding to the $[M+H]^+$ species was observed at *m/z* = 489.20 in the electrospray mass spectrum.

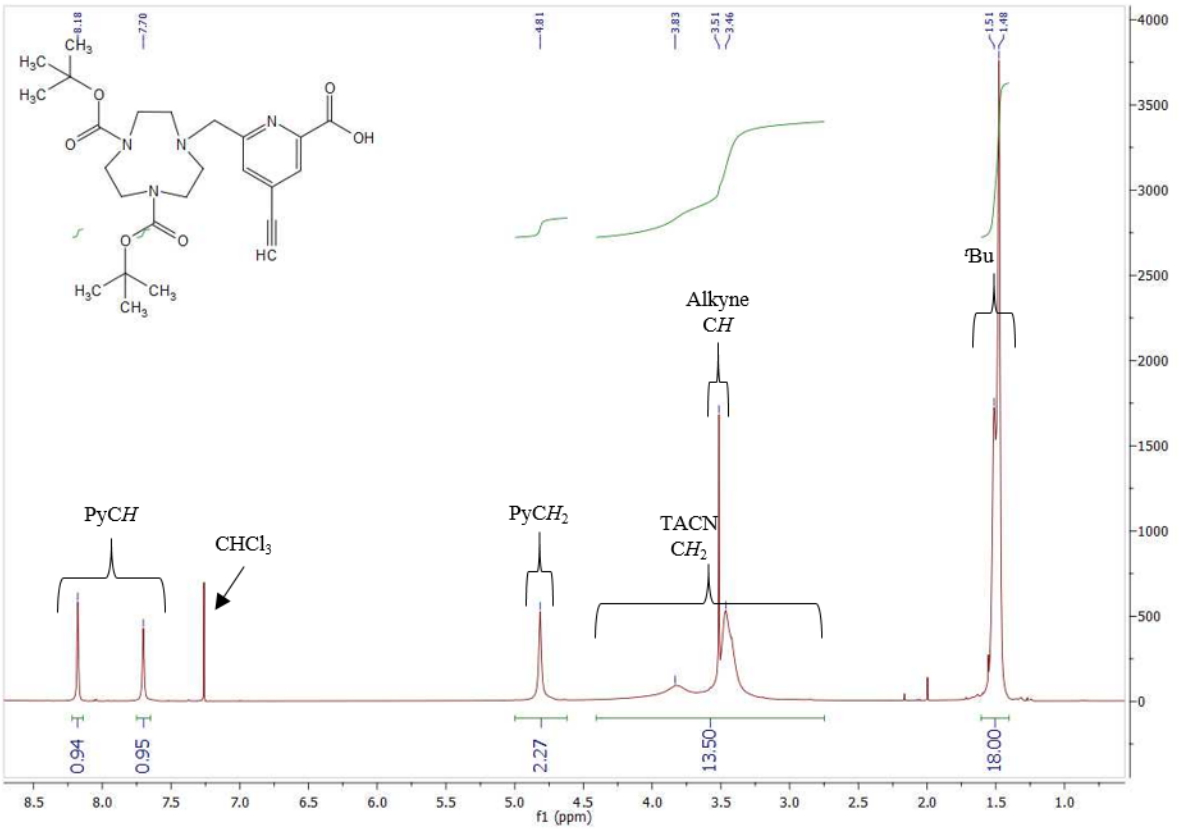

Figure 7. ^{1}H NMR spectrum for **23** in $CDCl_3$.

5.3 "Click" ligation to a model azide

In order to investigate the Cu(II)-binding properties of the chelator motifs that would be formed after clicking the pro-chelators to an azide-bearing compound, it was decided to ligate them to 3-azidopropanol as a small "model" azide in the first instance (**Scheme 3**). Ligation was carried out in a water/acetonitrile mixture using a two-fold excess of azide, $CuSO_4$ (0.1 equiv.) as the copper source, sodium ascorbate (2.0 equiv.) as the reducing agent, and *tris*(3-hydroxypropyl-triazolylmethyl)amine (THTPA)[40,41] (0.2 equiv.) as a Cu(I)-stabilising ligand. It was necessary to perform the copper-catalysed "click" reactions with the Boc-protected forms of the pro-chelators in order to avoid complexation of the copper catalyst (an undesirable outcome given that it would preclude subsequent binding of ^{64}Cu by the chelator motifs).

LC-MS analysis indicated near-quantitative reaction for both pro-chelators after stirring overnight at room temperature. The two pure products, **24** and **26** were isolated in 58% and 28% yield, respectively, following purification *via* RP-DCVC. The low isolated yields reflect the fact that there was significant co-elution of the products with the Cu(I)-stabilising agent, THPTA. Subsequent treatment with TFA to remove the Boc groups gave **25** and **27** in 65% and 60% yield, respectively. Preparative HPLC was again utilised to afford the model "clicked" ligands in greater than 95% purity.

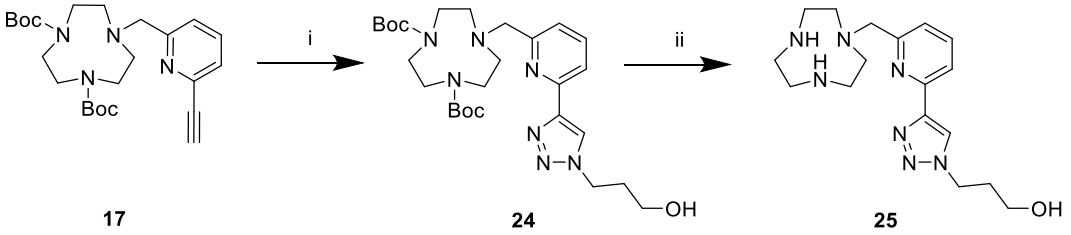

Scheme 3. Synthesis of "clicked" TACN derivative **25**. i) 3-azido-1-propanol, $CuSO_4$, THPTA, sodium ascorbate, water/MeCN, pH 7, RT, O/N, quant. (53% isolated); ii) TFA, DCM, RT, O/N, 63%.

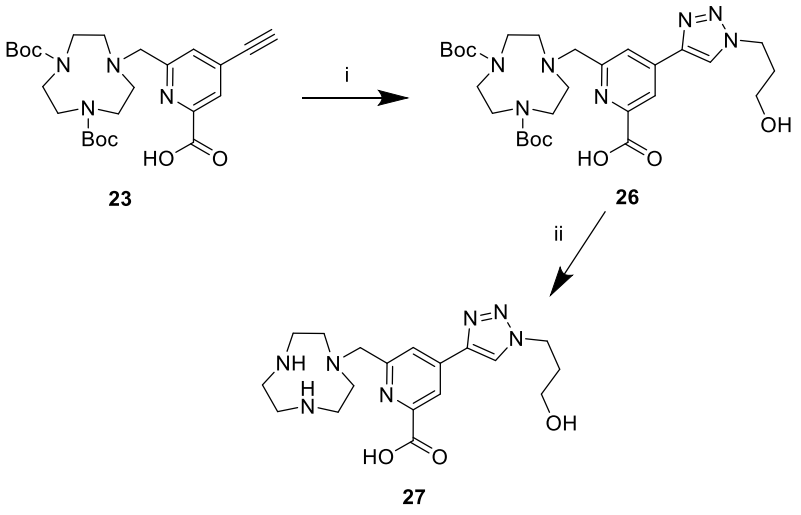

Scheme 4. Synthesis of "clicked" TACN derivative **27**. i) 3-azido-1-propanol, $CuSO_4$, THPTA, sodium ascorbate, H_2O/MeCN, pH 7, RT, O/N, quant. (28% isolated); ii) TFA, DCM, RT, O/N, 60%.

The ^1H NMR spectrum of **25** in D_2O (**Figure 8**) was surprisingly well resolved compared to those of **17** and **23**. A set of well separated signals with defined splitting patterns were observed between 2.0 and 4.6 ppm for the various methylene protons present in the TACN

ring and pendant arm of the molecule. The most diagnostic of these is the apparent quintet at 2.14 ppm, corresponding to the central CH_2 group of the propanol chain, which indicated successful "clicking" of the 3-azidopropanol. Four aromatic proton signals were observed – three corresponding to the pyridine ring (7.40, 7.75 and 7.98 ppm) and one to the newly-formed triazole ring (8.54 ppm). Some small signals corresponding to a low-level impurity were also apparent, though the analytical HPLC showed only a single peak (254 nm detection) and indicated a purity of 98%. The ^{13}C NMR spectrum showed the expected number of resonances, and high-resolution mass spectrometry (HRMS) confirmed the identity of the product, with a signal observed at *m/z* = 346.2353 comparing favourably with that expected for the $[M+H]^+$ species (346.2350).

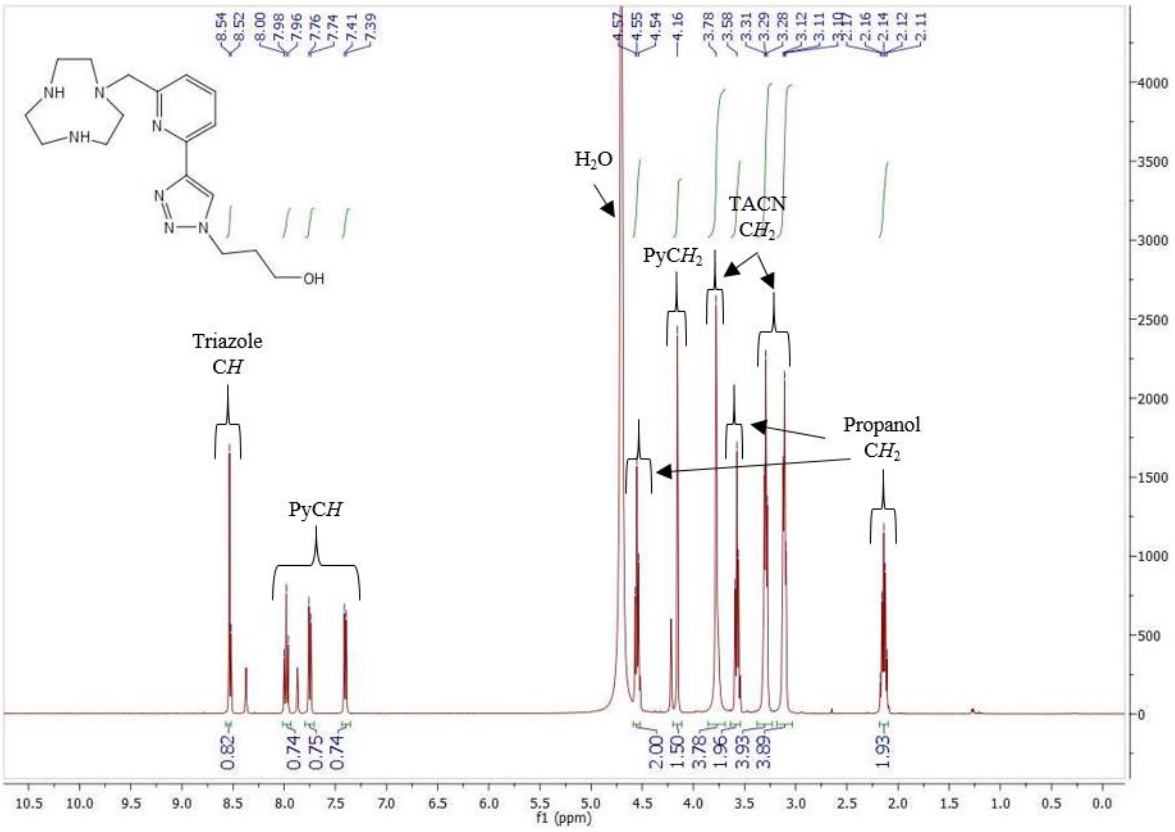

Figure 8. ^1H NMR spectrum for **25** in D_2O.

The ^1H NMR spectrum of **27** in D_2O (**Figure 9**) was also well resolved, with the number, positioning, integration and splitting of the signals consistent with the predicted

structure. In particular, successful coupling of the 3-azidopropanol to the picolinic acid pendant group was evident from the sharp singlet at 8.71 ppm, corresponding to the triazole CH proton. Interestingly, both the ^{1}H and ^{13}C NMR spectra of **27** were of considerably poorer quality in terms of resolution and signal strength (particularly for the TACN methylene groups) when recorded in deuterated methanol. The ^{13}C NMR spectrum of **27** in D_2O showed the expected number of resonances, and successful formation of the product was also supported by HRMS, with an observed signal at *m/z* = 390.2255 consistent with that expected for the $[M+H]^+$ species (390.2248).

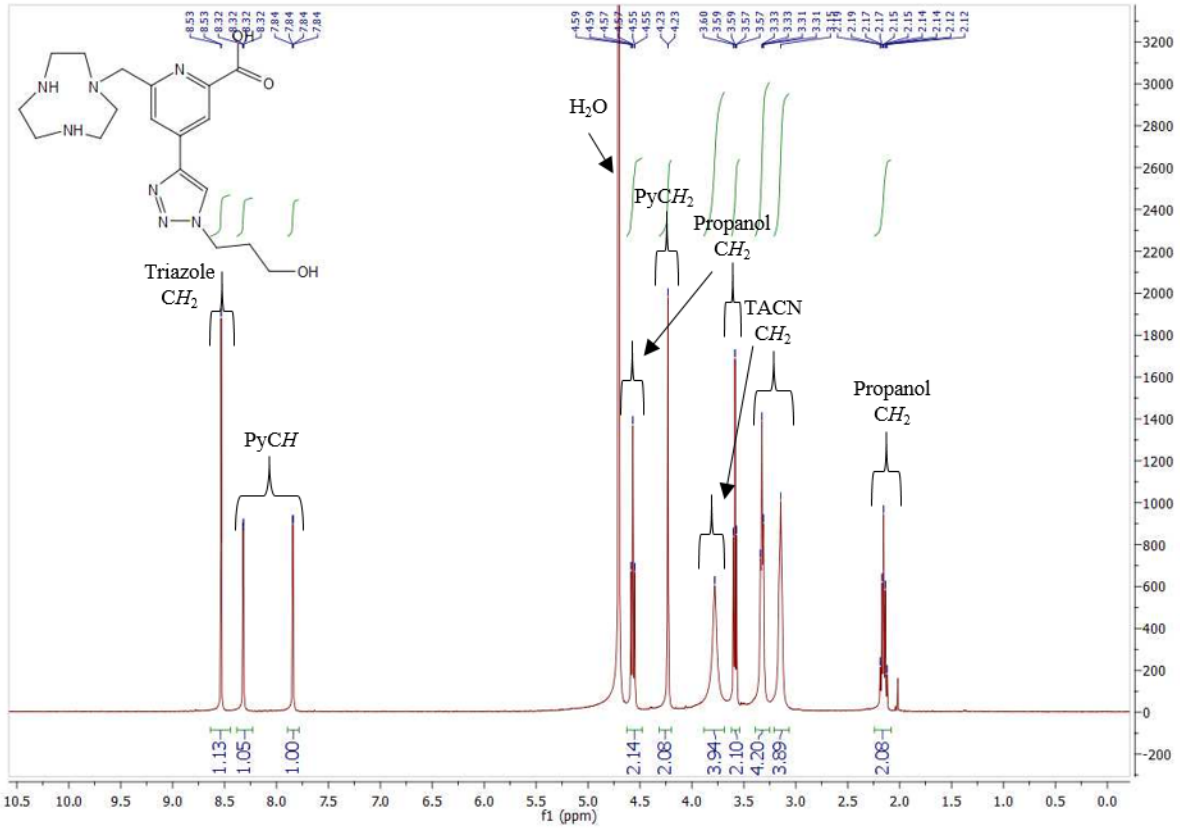

Figure 9. ^{1}H NMR spectrum for **27** in D_2O.

5.4 Radiolabelling and stability of model ^{64}Cu(II) complexes

Next, a series of ^{64}Cu radiolabelling experiments were performed upon the prepared model "clicked" conjugates **25** and **27**. It was important to establish how quickly complexation

occurs, as well as the stability of the ^{64}Cu(II) complexes once formed. These assessments are necessary to help determine if the complexes are safe for use *in vivo*, as leaching/scavenging of radioactive metal ions from radiolabelled compounds into healthy tissue is highly dangerous. ^{64}Cu(II) complexes were prepared by adding $^{64}Cu^{2+}$ ions to a solution containing one of the two ligands dissolved in 0.1 M 2-(*N*-morpholino)ethanesulphonic acid (MES) buffer (pH 5.5). The mixtures were then incubated with agitation at 37°C for half an hour. Radio-purity of the formed complexes was assessed *via* radio-TLC, revealing a single species in each of the two traces corresponding to the two ^{64}Cu(II)-ligand complexes (^{64}Cu(II)-**25**: R_f = 0.82, ^{64}Cu(II)-**27**: R_f = 0.84) and no evidence of any remaining free $^{64}Cu^{2+}$ ions (R_f = 0) (**Figure 10**).

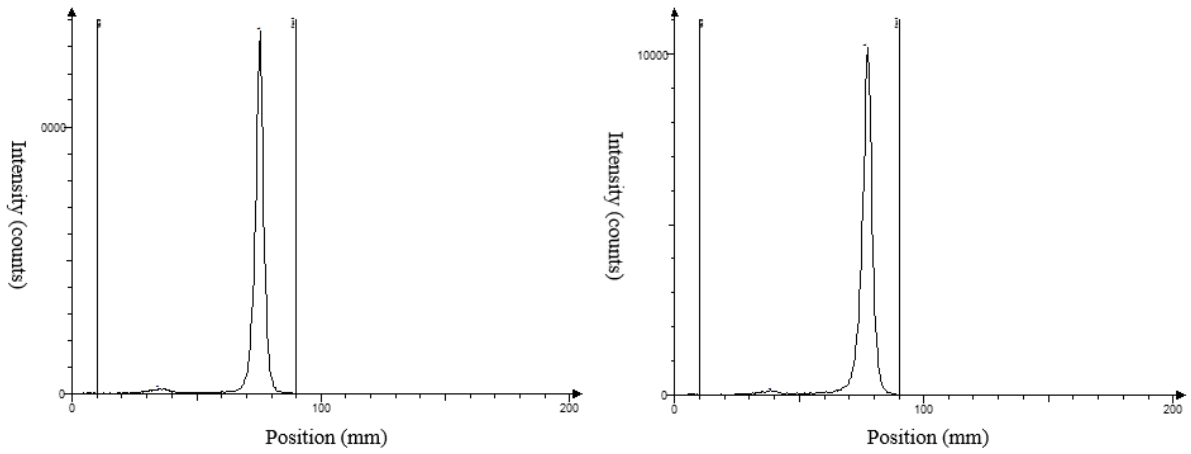

Figure 10. Radio-TLC of ^{64}Cu(II)-**25** (left) and ^{64}Cu(II)-**27** (right) after 30 min incubation at 37°C in 0.1 M MES buffer (pH 5.5). Vertical lines represent the beginning and end of an 80 mm-long plate.

Rapid complexation kinetics are very desirable for PET imaging, as it reduces the amount of radioisotope that is lost to decay prior to injection into a specimen/patient. To investigate the ^{64}Cu(II)-binding kinetics of the model ligands, aliquots of ^{64}Cu(II)-ligand mixtures incubated in MES buffer at 25°C were taken at different time points and analysed *via* radio-TLC. This study revealed that after just one minute, greater than 95% radiochemical yield of the ^{64}Cu(II) complexes of both ligands was achieved, i.e. > 95% of the total initial radioactivity was present within the complexes (**Figure 11**). From the perspective of their

Cu(II)-binding kinetics, the two triazole-bearing TACN chelators are thus eminently well suited to PET imaging applications.

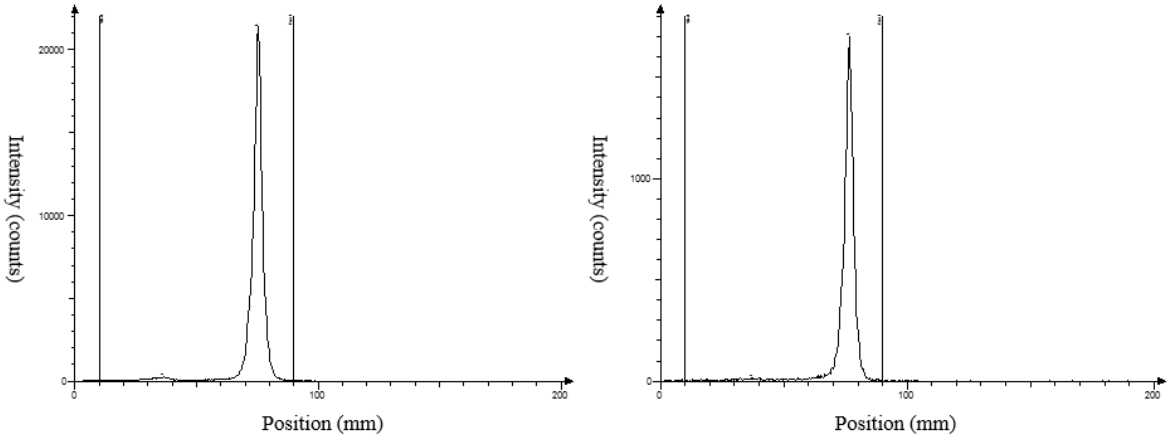

Figure 11. Radio-TLC of ^{64}Cu(II)-**25** (left) and ^{64}Cu(II)-**27** after 1 min incubation at 37°C in 0.1 M MES buffer (pH 5.5, 298 K). Vertical lines represent the beginning and end of an 80 mm-long plate.

The incubated mixtures were left for a full 24 h to observe whether any degradation of the complexes takes place over this timeframe. Promisingly, in both cases no difference was observed between the initial radio-TLC trace and that obtained after 24 h.

"Challenge" experiments were performed to assess the relative stability of the ^{64}Cu(II) complexes. These studies involved adding a large excesses of a known Cu(II) chelator to the prepared ^{64}Cu(II) complexes and then measuring the degree of trans-chelation, i.e., scavenging of the ^{64}Cu(II) by the added ligand. Typically, cyclam is employed for these assessments, however its Cu(II) complex was found to have very a similar R_f to the complexes of **25** and **27** and thus proved unsuitable in this instance. Another common chelator, 1,4,8,11-tetraazacyclotetradecane-1,4,8,11-tetraacetic acid (TETA), was therefore used for the challenge experiments. As before, the radio-complexes were prepared by adding $^{64}Cu^{2+}$ ions to the ligands in MES buffer and incubating with agitation at 37°C for 30 min. The solutions were then exposed to a 20-fold excess of TETA and further incubated at 37°C. After 4 h, no

noticeable trans-chelation was observed, as shown in **Figure 12**, indicating the ^{64}Cu(II) complexes of the new TACN-based ligands possess high stability.

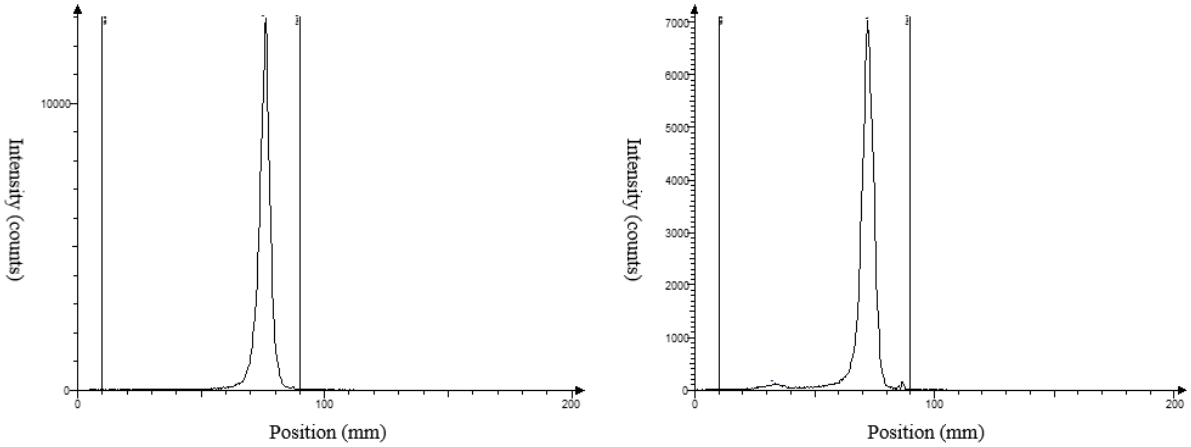

Figure 12. Radio-TLC of ^{64}Cu(II)-**25** (left) and ^{64}Cu(II)-**27** (right) after 4 h incubation with 20-fold excess of TETA at 37ºC in 0.1 M MES buffer (pH 5.5). Vertical lines represent the beginning and end of an 80 mm-long plate.

To further assess radiocomplex stability, samples of ^{64}Cu(II)-**25** and ^{64}Cu(II)-**27** were incubated in human plasma for 4 h and 37ºC. Again, no degradation of the complexes was observed (**Figure 13**), providing further evidence that these ligands may be suitable for PET imaging.

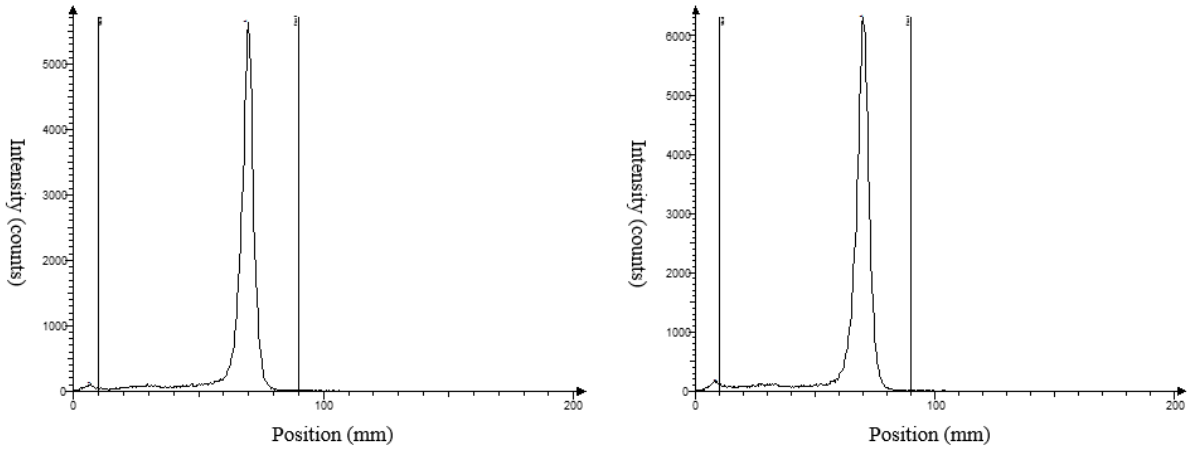

Figure 13. Radio-TLC of ^{64}Cu(II)-**25** (left) and ^{64}Cu(II)-**27** (right) after 4 h incubation in human plasma at 37ºC. Vertical lines represent the beginning and end of an 80 mm-long plate.

5.5 Synthesis of bombesin conjugates

The selected BBN analogue, (Orn(N_3)-*β*Ala-*β*Ala-Gln-Tpr-Ala-Val-Gly-His-Cha-Nle-NH_2), was prepared on an automated solid-phase peptide synthesiser (SPPS) using standard fluorenylmethyloxycarbonyl chloride/ 2-(6-chloro-1H-benzotriazole-1-yl)-1,1,3,3-tetramethylaminium hexafluorophosphate (Fmoc/HCTU) protocols, on a Rink amide resin, with the unnatural amino acid azido-ornithine (Orn(N_3)) incorporated to provide a site for attachment of the pro-chelator building blocks *via* click chemistry. Attachment of the poly(ethylene glycol) (PEG-3) linker chain was achieved under the same conditions, after synthesis of the peptide had been confirmed by a small-scale cleavage (< 2 mg of resin) and peptide LCMS analysis. Attempts to couple the sulfo-Cy5 dye to the end of the PEG linker using the commercially-available sulfo-Cy5 *N*-hydroxysuccinimide (NHS) ester (even freshly purchased) proved troublesome, with either no or very limited reaction observed. However, the use of the "free" carboxylic acid form of sulfo-Cy5, along with benzotriazol-1-yl-oxytripyrrolidinophosphonium hexafluorophosphate (PyBOP) as a coupling reagent, gave near-complete ligation following overnight reaction.

As a strong focus of this thesis as a whole was the simplified construction of multi-functional conjugates, it was desirable to establish conditions to couple the pro-chelator building blocks to the modified bombesin peptide while it was still attached to the resin. The literature is somewhat limited in this regard, with various authors utilising differing copper sources, including copper(I) bromide, copper(I) iodide and copper(II) sulphate, various copper(I)-stabilising ligands, including 2-[4-({*bis*[(1-*tert*-butyl-1H-1,2,3-triazol-4-yl)methyl]amino}methyl)-1H-1,2,3-triazol-1-yl]acetic acid (BTTAA) and THPTA, as well as other additives, including tetramethylammonium fluoride (TMAF) and 2,6-lutidine.[42–45] As there was no apparent consensus on the best conditions for on-resin clicking, and because the combination of reagents used seemed to be quite specific depending upon application, a small

series of test reactions were conducted to determine which combination would be most suited in this instance. Given that **25** and **27** involved lengthy syntheses and were only available in limited quantities, a simple model alkyne, propargyl alcohol, was used for these experiments. Also, these experiments were conducted on the peptide pre-sulfo-Cy5 coupling, given the expense of the sulfo-Cy5 reagent. The initial reaction conditions trialled involved combining 0.1 equivalents of the copper source, 2 equivalents of sodium ascorbate as the reducing agent, 0.2 equivalents of copper(I)-stabilising ligand and 2 equivalents of the model alkyne in DMSO, addition of peptide-resin and gentle mixing overnight at room temperature. Following cleavage of the peptide using a standard cleavage cocktail, the extent of reaction was established *via* peptide LCMS analysis, comparing the relative areas of the product and starting peptide signals. The results are summarised in **Table 1**.

Table 1. Results for on-resin "click" experiments conducted at room temperature. Percentage values correspond to the extent of product formation using the combination of reagents listed, as determined by peptide LCMS analysis.

	2,6-Lutidine	TBAF	THPTA	BTTAA
CuI	40%	30%	36%	39%
CuBr	22%	28%	25%	32%
$CuSO_4$	29%	27%	33%	27%

These results were promising, as they indicated that there was some conversion to the desired clicked product, even if conversion was fairly low. Copper(I) iodide as the copper source generally gave the best levels of conversion. In order to see if further improvements could be made, a second series of trial reactions were conducted, with mild heating applied, using copper(I) iodide as the sole copper source. The results are summarised in **Table 2**.

Table 2. Results for on-resin "click" experiments conducted at 50°C. Percentage values correspond to the extent of product formation using the reagents listed, as determined by peptide LCMS analysis.

	2,6-Lutidine	THPTA	BTTAA
Heating (50°C)	23%	48%	35%

The combination of copper(I) iodide with THPTA and mild heating at 50°C gave the best results, with approximately 50% conversion to the desired click product. Whilst this could most likely be improved upon, these conditions were deemed suitable for attempts to couple the pro-chelators themselves to the peptide.

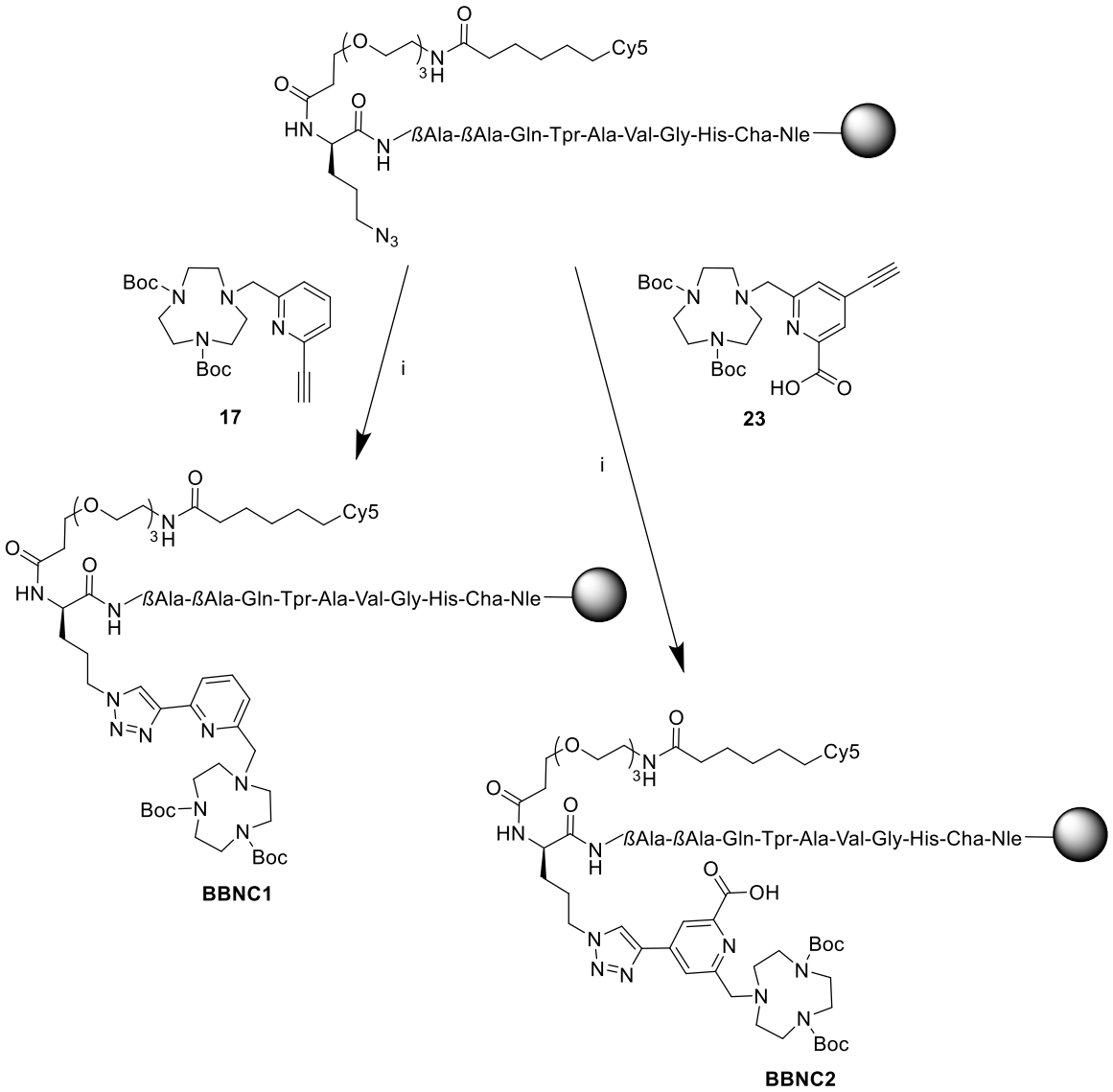

Scheme 5. On-resin "click" coupling of pro-chelators to the bombesin peptide derivative, yielding the conjugates **BBNC1** and **BBNC2**. i) Cu(I), THPTA, sodium ascorbate, 50°C, O/N.

The click reactions with the pro-chelators were performed on the resin following coupling of the sulfo-Cy 5 dye, i.e., as the penultimate step of the synthesis of the target peptide conjugates, **BBNC1** and **BBNC2**, as shown in **Scheme 5**.

Following the click reactions, the resins were washed as per the standard SPPS synthesis protocol, followed by a small-scale cleavage to assess the reaction progress. LC-MS analysis revealed the presence of significant amounts of a Cu(II) adduct in each case, meaning that some copper had remained on the resin post-clicking, despite extensive washing, and had become incorporated into the TACN chelator motifs upon removal of the Boc protective groups during cleavage of the peptide from the resin. To avoid this outcome, the synthesis was modified to include a wash step after the click reaction, in which the resin was agitated with a vast excess of cyclen (> 100 equiv.) in DMF to chelate any residual copper, allowing it be easily washed away prior to peptide cleavage. With the inclusion of this step, **BBNC1** and **BBNC2** could be obtained in greater than 95% purity following preparative HPLC. The peptide LC-MS traces of these final constructs (**Figure 14**) were consistent with the predicted structures, as evidenced by the observation of signals at *m/z* = 778 and 1167 m/z, corresponding to +2 and +3 charge states for **BBNC1**, and *m/z* = 793 and 1189, representing the +2 and +3 charges species for **BBNC2**.

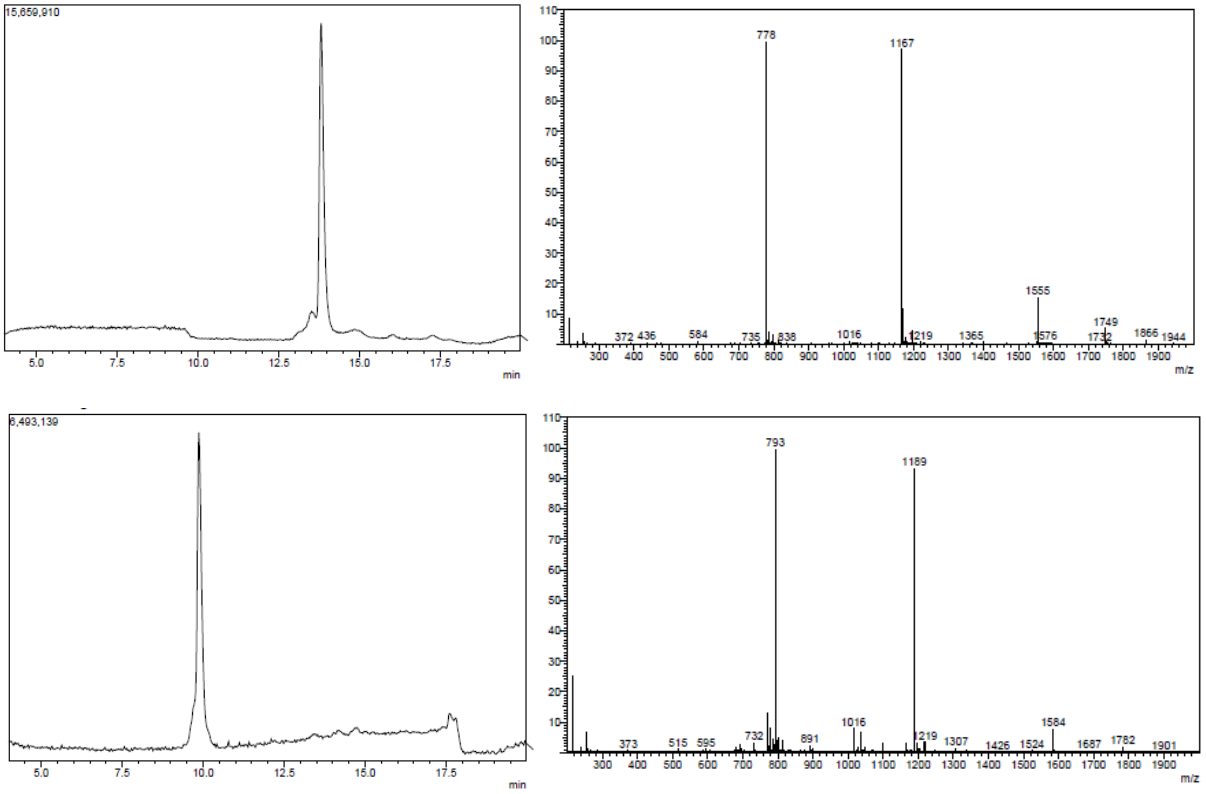

Figure 14. LC traces (left) and mass spectra (right) for **BBNC1** (top) and **BBNC2** (bottom). Major mass peaks are the +2 and +3 charged species in both cases. The large difference in elution times between **BBNC1** and **BBNC2** is due to the use of different elution protocols.

5.6 Radiolabelling and *in vivo* PET imaging of BBNC1 construct

Having successfully synthesised the two copper-chelating, sulfo-Cy5-labelled bombesin constructs, the next stage was to assess their performance as PET imaging agents. In this section we describe the testing and results for one of the constructs, **BBNC1** (the reason why no testing was performed on **BBNC2** will be discussed towards the end of this chapter). The $^{64}Cu^{2+}$ -binding capacity of **BBNC1** was assessed by radio-TLC as well as radio-HPLC. Labelling was achieved by adding $^{64}Cu^{2+}$ ions to a solution of **BBNC1** in 0.1 M MES buffer (pH 5.5) containing 10% ethanol and incubating with agitation at 37°C for 2 h. A radiochemical yield of approximately 90% was observed after this time, under two separate radio-TLC conditions (**Figure 15**) as well as by radio-HPLC analysis (**Figure 16**).

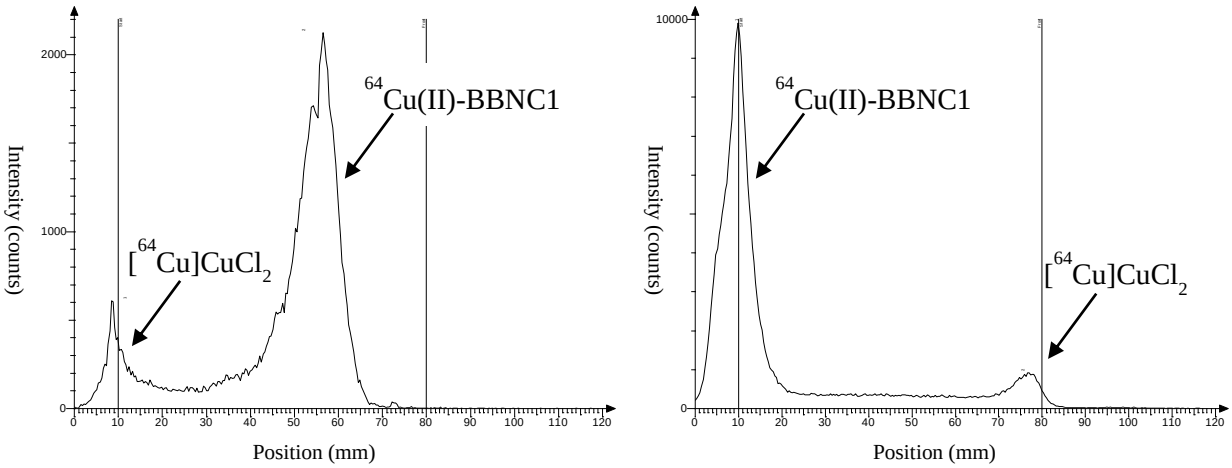

R_f = 0.00 Integral [%] = 13.3%
R_f = 0.67 Integral [%] = 86.7%

R_f = 0.00 Integral [%] = 90.5%
R_f = 0.95 Integral [%] = 9.5%

Figure 15. Radio-TLCs of ^{64}Cu(II)-**BBNC1** after 2 h incubation at 37°C in 0.1 M MES buffer (pH 5.5) Left: aluminium oxide TLC plate run with a 2 M ammonium acetate in ethanol mobile phase. Right: instant thin layer chromatography silica gel (ITLC-SG) plate run with a 0.9 % sodium chloride + 5 % acetic acid aqueous mobile phase. Values below the radio-TLCs show relative integration of the peaks.

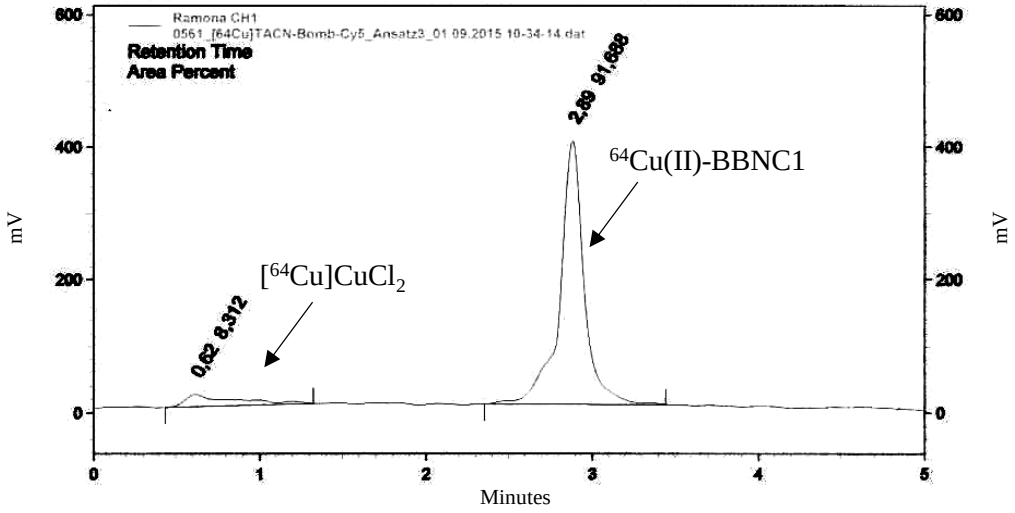

Ramona
CH1
Results

Pk #	Retention Time	Area	Area Percent	Height	Height Percent
1	0,617	371270	8,312	17934	4,317
2	2,887	4095352	91,688	397531	95,683
Totals		4466622	100,000	415465	100,000

Figure 16. Radio-HPLC chromatogram of ^{64}Cu(II)-**BBNC1** after 2 h incubation at 37°C in 0.1 M MES buffer (pH 5.5).

To assess the biodistribution and kinetics of uptake and removal of ^{64}Cu(II)-**BBNC1**, *in vivo* experiments involving dynamic small-animal PET imaging of NMRI nude immunodeficient (nu/nu) mice with subcutaneous injections of PC-3 (prostate cancer cell line-3) cells. Studies were conducted on two groups of mice. One group of six mice were injected with ^{64}Cu(II)-**BBNC1**, whilst another group of six mice were simultaneously injected with both ^{64}Cu(II)-**BBNC1** and 4 mg/kg body weight of GRP as a GRPr blocking agent, in order to allow an assessment of the targeting effectiveness of **BBNC1**. PET images (representative of both groups) taken 2 h after a single intravenous injection are shown in **Figures 17** and **18**.

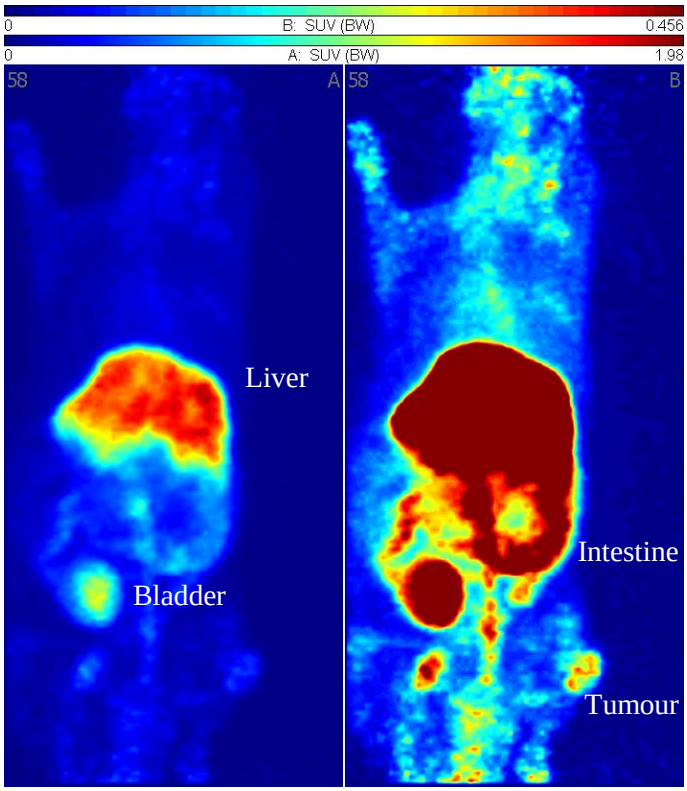

Figure 17. Typical biodistribution of ^{64}Cu(II)-**BBNC1** at 2 h after a single intravenous injection into a PC3 tumour-bearing mouse.

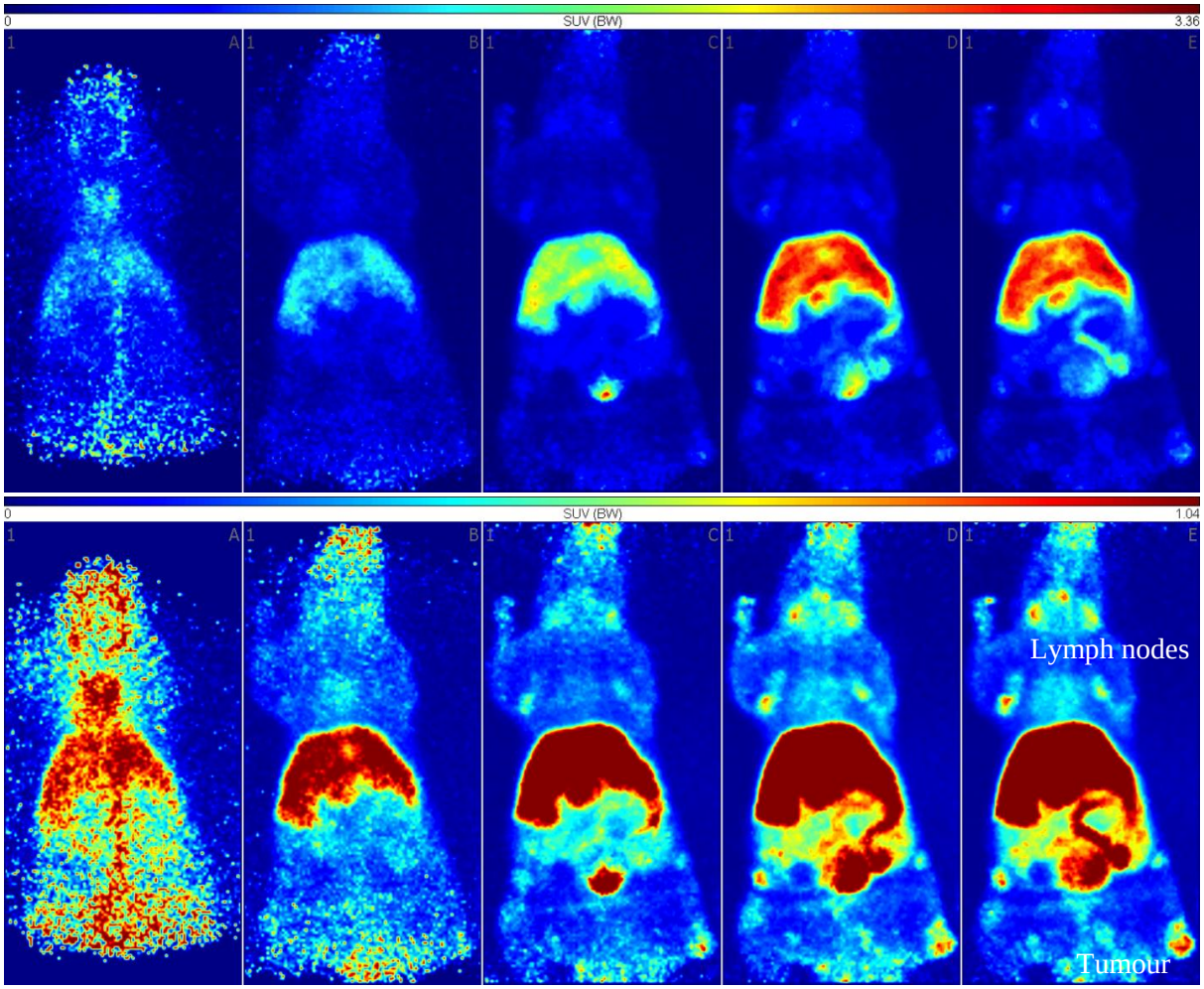

Figure 18. Typical biodistribution of ^{64}Cu(II)-**BBNC1** at 2 h after a single intravenous co-injection with GRP into a PC3 tumour-bearing mouse.

The PET images revealed clear visualisation of the tumour in the mice after one hour. Unfortunately, direct comparison between the control and blocked mice showed an identical tumour-to-blood standard uptake ratio (SUR, measured as a function of tissue radioactivity concentration over the injected activity) of approximately 1.5 (**Figure 19, A**). Further refinement of the data to give absolute uptake values (SUV_{mean}) reinforces this finding, providing strong evidence that that **BBNC1** has no active targeting properties (**Figure 19, B**), instead expressing distribution properties typical of non-specific lipophilic interactions. **BBNC1** also experienced extremely rapid accumulation in the liver, causing the absolute accumulation in the tumour to be very low.

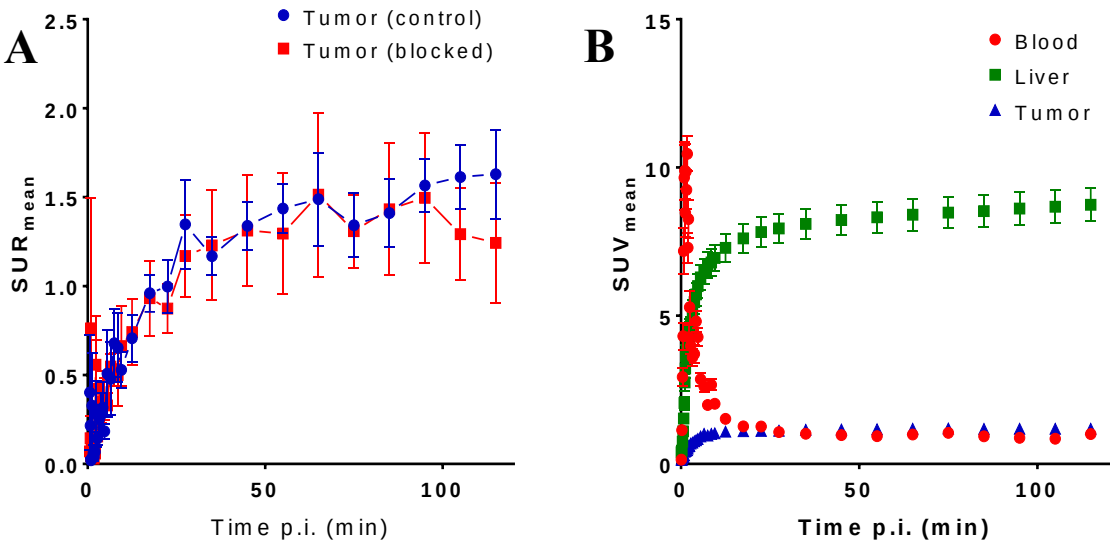

Figure 19. (**A**) Standard uptake ratio of ^{64}Cu(II)-**BBNC1** in mice without (n = 6) and with GRPr blocking (n = 6) (mean +/- standard error of the mean) (**B**) Absolute uptake (SUV_{mean}) of ^{64}Cu(II)-**BBNC1** in PC3 tumour-bearing mice (n = 12, mean +/- standard error of the mean).

Interestingly, the radiotracer presented lymph node accumulation, although the precise reason for this is unknown. The mouse in question may have been presenting some generalised inflammation, as it is very unlikely that the mouse was experiencing metastasis in all larger lymph nodes. Some lipophilic compounds have been known to accumulate in lymph nodes,[46–48] which may be the active mechanism in this case. Still, it presents an interesting finding, indicating that this compound and those of its ilk may be of use in imaging "excited" lymph nodes, even after intravenous injection. Typically, such lymph node imaging with high-molecular weight compounds is only possible after localised subcutaneous injection near the nodes.

The findings for the ^{64}Cu(II)-**BBNC1** conjugate differ markedly from those reported by Gasser *et al.*[10] and Bergmann *et al.*[11] for BBN derivatives featuring a di(methylpyridyl)-TACN (DMPTACN) chelator (**Figure 20**). In both of these cases, successful GPRr targeting was demonstrated. Structurally, the conjugates are very similar to that **BBNC1**, except for the obvious absence of the sulfo-Cy5 dye. Thus, it is strongly suspected that the relatively high

lipophilicity of the sulfo-Cy5 moiety may be exerting a dominant effect upon the *in vivo* distribution characteristics of **BBNC1**. In fact, a recent study reported by Guo *et al.*[49] has highlighted the inherent issues with dyes such as Cy5 in radio-probe design, including unwanted and non-specific interactions with proteins and peptides. Within their paper, Guo *et al.* describe the construction and evaluation of an integrin-binding multifunctional probe in which the non-specific interactions of a Cy5.5 dye were mitigated through the incorporation of a 5 kDa PEG chain designed to act as a "shielding cloud". This approach could provide an interesting further direction for the project.

In view of the results obtained with the **BBNC1** conjugate, **BBNC2** was not tested, however it is expected that the bio-distribution results would be very similar.

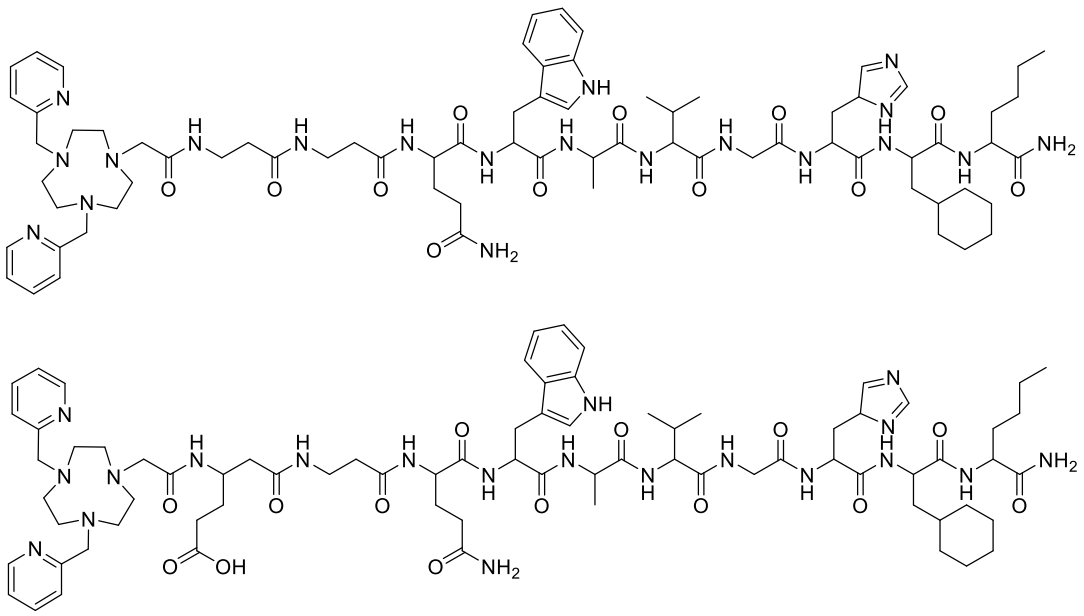

Figure 20. Structures of GPRr-targeting DMPTACN-BBN conjugates reported by Gasser *et al.*[10] (top) and Bergmann *et al.*[11] (bottom).

.

5.7 Conclusion

Two new "clickable" alkyne-bearing pro-chelator compounds based on the TACN macrocycle have been successfully synthesised. These are designed to enable ready installation of a ^{64}Cu(II)-binding ligand into new PET imaging designs. The pro-chelators were clicked to 3-azidopropanol to produce two "model" ligands, **25** and **27**, which demonstrated excellent ^{64}Cu(II)-binding properties. A radiochemical yield in excess of 95% was obtained for both ligands within 1 min. The resulting ^{64}Cu(II) complexes were stable in pH 5.5 buffer and human plasma, and also proved to be highly resistant to trans-chelation during challenge experiments with TETA. The utility of the pro-chelators for multi-modal probe construction was successfully demonstrated through the on-resin assembly of two Cu(II)-chelating, sulfo-Cy5-bearing bombesin peptide conjugates designed to target GRPr-overexpressing tumours. Whilst *in vivo* testing of one of these conjugates in tumour-bearing mice showed disappointing results, likely attributable to the lipophilicity of the sulfo-Cy5 dye, it is clear that the new pro-chelators provide useful building blocks for future probe construction.

Experimental

Experimental procedures for compounds **14**–**15** and **18**–**21** can be found on pages 52 and 53 as part of the **Chapter 2** experimental section. The experimental procedure for **22** can be found on page 113 as part of the **Chapter 4** experimental section.

Materials and reagents

All chemicals were purchased from Sigma-Aldrich Pty, Matrix Scientific, or Merck Group Ltd and used without purification. All solvents were reagent grade. Di-*tert*-butyloxycarbonyl-protected 1,4,7-triazacyclononane (Boc_2TACN) was synthesised according to a literature procedure.[38] ^{64}Cu was produced with a "Cyclone 18/9" PET cyclotron at the Helmholtz-Zentrum Dresden-Rossendorf *via* the $^{64}Ni(p.n) \rightarrow {}^{64}Cu$ nuclear reaction.

Instrumentation

Peptide synthesis was, unless otherwise indicated, performed on a PS3 automated peptide synthesizer (protein technologies Inc.) using standard Fmoc/HCTU/piperidine protocols for all coupling and deprotection cycles. *Flash chromatography* was carried out using Merck 38 Silica gel 60, 230–400 mesh ASTM. *Thin layer chromatography (TLC)* was performed on Merck Silica Gel 60 F254 plates. TLC plates were visualised using a UV lamp at 254 nm or through the use of $KMnO_4$ or ninhydrin staining agent. *^{1}H and ^{13}C nuclear magnetic resonance (NMR)* spectra were recorded using an Avance III Nanobay 400 MHz Bruker spectrometer coupled to the BACS 60 automatic sample changer at 400.13 MHz and 100.61 MHz, respectively. Data acquisition and processing was managed using Topspin software package version 3. Additional processing was handled with MestReNova software (PC). Chemical shifts (δ) were measured in parts per million (ppm) referenced to an internal standard of residual solvent. Spectroscopic data are given using the following abbreviations: s, singlet; d, doublet; app. t, apparent triplet; q, quartet; app. p, apparent pentet; m, multiplet; br, broad; *J*, coupling constant.

Analytical high-performance liquid chromatography (HPLC) was carried out on an Agilent 1260 series modular HPLC equipped with the following modules: G1312B binary pump, G1316A thermostated column compartment equipped with an Agilent Eclipse Plus C18 3.5 µm, 4.6 x 100 mm column and a G1312B diode array detector. The following elution protocol was used: 0–10 min, gradient from 5% solvent B/95% solvent A to 100% solvent B (solvent A = 99.9% H_2O, 0.1% TFA, and solvent B = 99.9% MeCN, 0.1% TFA. *Preparative HPLC purification* was carried out on an Agilent 1260 modular Prep HPLC equipped with the following modules: G1361A prep pump, G2260A prep automatic liquid sampler, G1364B fraction collector, G1315D diode array detector, and a Luna C8 5 µm, 100 Å AXIA, 250 x 21.2 mm column. The following elution protocol was used: 0–5 min, 100% solvent C; 5–30 min, gradient from 100% solvent C to 20% solvent C/80% solvent D (solvent C = 99.9% H_2O, 0.1% formic acid; solvent D = 99.9% MeCN, 0.1% formic acid); flow rate = 20 mL min^{-1}. *High-resolution mass spectrometric (HRMS)* analyses were performed on a Waters LCT TOF LC-MS mass spectrometer coupled to a 2795 Alliance Separations module. All data was acquired and mass corrected *via* a dual-spray Leucine Enkephaline reference sample. Mass spectra were generated by averaging the scans across each peak and background subtraction of the TIC. Acquisition and analysis were performed using the MassLynx software version 4.1. The mass spectrometer conditions were as follows: electrospray ionisation mode, desolvation gas flow of 550 L h^{-1}, desolvation temperature of 250°C, source temperature of 110°C, capillary voltage of 2400 V, sample cone voltage of 60 V, scan range acquired between 100–1500 *m/z*, one sec scan times and internal reference ions for positive ion mode (Leucine Enkephaline) of 556.2771. *Liquid chromatography-mass spectrometry (LC-MS)* was performed using an Agilent 6100 Series Single Quad LC-MS coupled to an Agilent 1200 Series HPLC with the following conditions and equipment for MS: 1200 Series G1311A quaternary pump, 1200 Series G1329A thermostated autosampler, 1200 Series G1314B variable wavelength detector.

MS conditions: quadrupole ion source, multimode-ES ion mode, 300°C drying gas temperature, 200°C vaporising temperature, capillary voltage of 2000 V (positive), capillary voltage of 4000 V (negative), scan range between 100–1000 *m/z* with an 0.1 sec step size and a 10 min acquisition time. LC equipment and conditions were as follows: reverse-phase HPLC analysis on a Luna C8(2) 5 µm, 50 x 4.6 mm column using a column temperature of 30°C, an injection volume of 5 µL, and the following elution protocol: 0–4 min, gradient from 5% solvent C/95% solvent D to 100% solvent D; 4–7 min, 100% solvent D; 4–7 min, gradient from 100% solvent D to 95% solvent C/5% solvent D. Detection was at 254 nm. *Reversed-phase silica dry column vacuum chromatography (RP-DCVC)* was performed using reversed-phase silica (C18 bonded, 10 µm, 60 Å) purchased from Grace Davison and loaded into a sintered Buchner funnel (50 x 50 mm ID). Elution was performed with 100% solvent C (200 mL), followed by a 5% incremental stepwise gradient from 0 to 80% solvent D (50 mL of each solvent C/D mixture). Fractions were collected under vacuum into a separating funnel and then into test tubes. Collected fractions were analysed by analytical HPLC. *Analysis of the peptide conjugates* was performed on a Shimadzu modular LC-MS system equipped with the following modules: LC-20AD liquid chromatograph system, SPD-M20A diode array detector, CTO-20A column oven equipped with a Luna 3 micron C8(2) 3 µm, 100 Å, 100 x 2.0 mm column and a LC-MS-2020 system, operating in positive mode with an *m/*z scan range of 200–2000. The mass spectrometer conditions were as follows: ES+ polarity, capillary voltage of 1000–4500 V, sample cone voltage of 50–200 V, desolvation gas flow of 450 L h^{-1}, desolvation temperature of 150°C and source temperature of 80°C. Acquisition and analysis were performed using the MassLynx software version 4.1. *Radio-TLC* chromatograms were scanned using a radioisotope thin layer analyser (Rita Star, Rayset). *Radio-HPLC* was performed on a Kanuer HPLC fitted with a radio-detector using a Phenomenex Aqua C-18 column (125 Å, 5 µm, 250 x 4.6 mm).

Di-*tert*-butyl 7-((6-((trimethylsilyl)ethynyl)pyridin-2-yl)methyl)-1,4,7-triazacyclononane-1,4-dicarboxylate (16)

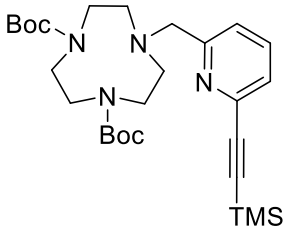

Compound **15** (180 mg, 635 µmol), Boc_2TACN (174 mg, 529 µmol), and DIPEA (137 mg, 184 µL, 1.06 mmol) were dissolved in MeCN (25 mL) and stirred under reflux overnight (O/N). Removal of solvent *in vacuo* gave a thick dark brown oil that was purified *via* silica gel chromatography (5% MeOH in DCM) to 8give the product (R_f = 0.15) as a glassy brown solid. Yield: 180 mg, 66%. ^{1}H NMR ($CDCl_3$) δ 7.72 (t, *J* = 7.9 Hz, 1H), 7.61–7.50 (m, 1H), 7.46 (d, *J* = 7.7 Hz, 1H), 4.65 (s, 2H), 3.82 (s, 4H), 3.44 (s, 8H), 1.64–1.37 (m, 18H), 0.26 (s, 9H). ^{13}C NMR ($CDCl_3$) δ 170.16, 152.05, 142.61, 137.83, 127.37, 123.95, 103.36, 95.74, 81.80, 59.22, 55.97, 49.84, 47.26, 39.64, 28.20, -0.29. LC-MS (ESI): *m/z* 517.30 $[M+H]^+$ (100%). Analytical HPLC: 91% purity (254 nm).

Di-*tert*-butyl 7-((6-ethynylpyridin-2-yl)methyl)-1,4,7-triazacyclononane-1,4-dicarboxylate triacetic acid (17)

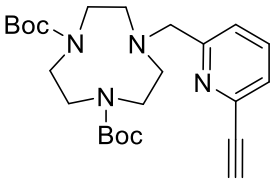

Compound **16** (200 mg, 387 µmol) was dissolved in a 1:1 (v/v) mixture of H_2O/MeCN (5 mL). To this was added 1.0 M KF solution (1.16 mL, 1.16 mmol) and the resulting solution was stirred for 2 h at room temperature (RT). RP-DCVC was used to separate the product as a fluffy, off white solid after lyophilisation. Yield: 111 mg, 65%. ^{1}H NMR ($CDCl_3$) δ 7.74 (t, *J*

= 7.4 Hz, 1H), 7.64–7.51 (m, 1H), 7.49 (d, *J* = 7.6 Hz, 1H), 4.67 (s, 2H), 3.82 (s, 4H), 3.45 (s, 8H), 3.18 (d, *J* = 18.2 Hz, 1H), 1.59–1.33 (m, *J* = 18.8 Hz, 18H). ^{13}C NMR ($CDCl_3$) δ 162.01, 161.63, 161.26, 160.88, 155.68, 154.82, 150.34, 142.43, 138.19, 128.29, 125.57, 120.28, 117.40, 114.52, 111.64, 82.31, 81.92, 78.34, 58.99, 52.27, 48.79, 48.11, 45.67, 44.49, 43.55, 28.50, 28.32. LC-MS (ESI): *m/z* 445.27 $[M+H]^+$ (100%). Analytical HPLC: 99% purity (254 nm).

6-((4,7-*bis*(*tert*-Butoxycarbonyl)-1,4,7-triazacyclononan-1-yl)methyl)-4-ethynylpicolinic acid (23)

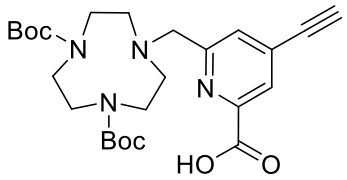

Compound **22** (344 mg, 513 µmol) was dissolved in a 1:2 (v/v) mixture of H_2O/MeCN (5 mL). To this was added 2.0 M NaOH solution (1.02 mL, 2.05 mmol) that was stirred for 2 h at RT. RP-DCVC was used to separate the product as a fluffy off white solid following lyophilisation. Yield: 118 mg, 41%. ^{1}H NMR ($CDCl_3$) δ 8.06 (s, 1H), 7.67 (s, 1H), 4.78 (s, 2H), 4.42 (q, *J* = 7.1 Hz, 2H), 3.86 (s, 4H), 3.50 (s, 8H), 1.54–1.33 (m, 21H), 0.26 (s, 9H). ^{13}C NMR ($CDCl_3$) δ 164.31, 162.28, 161.91, 161.53, 161.16, 149.55, 147.99, 134.82, 129.33, 127.20, 120.28, 117.40, 114.53, 111.64, 85.73, 82.42, 79.29, 57.23, 51.83–28.30 (broad set of peaks). LC-MS (ESI): *m/z* 489.20 $[M+H]^+$ (100%). Analytical HPLC: 99% purity (254 nm).

Di-*tert*-butyl 7-((6-(1-(3-hydroxypropyl)-1H-1,2,3-triazol-4-yl) pyridin-2-yl)methyl)-1,4,7-triazacyclononane-1,4-dicarboxylate (24)

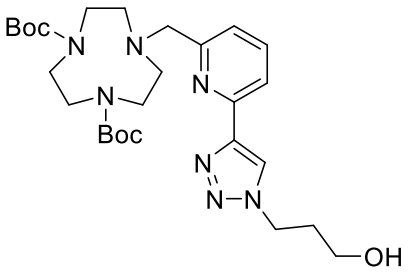

17 (154 mg, 346 µmol) was dissolved in a 1:2 (v/v) mixture of H_2O/MeCN (10 mL). To the resulting solution was added 3-azidopropan-1-ol (70 mg, 693 µmol), sodium ascorbate (137 mg, 693 µmol), copper (II) sulphate (5.5 mg, 35 µmol) and THPTA (30 mg, 70 µmol) and the resulting mixture stirred at RT O/N, after which time LC-MS showed complete click ligation. RP-DCVC was used to isolate the product as an off-white solid following lyophilization. Yield: 100 mg, 53%. ^{1}H NMR (CD_3OD) δ 8.76 (s, 1H), 8.01 (s, 2H), 7.56–7.38 (m, 1H), 4.82 (s, 2H), 4.62 (t, *J* = 7.1 Hz, 2H), 3.88 (s, 4H), 3.63 (t, *J* = 6.0 Hz, 2H), 3.51 (s, 8H), 2.20 (app. p, *J* = 6.5 Hz, 2H), 1.52 (s, 18H). ^{13}C NMR (CD_3OD) δ: 157.22, 151.31, 151.06, 147.90, 140.40, 125.28, 124.12, 121.62, 82.83, 60.67, 59.26, 52.66, 48.61 (overlapping with solvent peak), 45.19, 33.93, 28.58. LC-MS (ESI): *m/z* 546.30 $[M+H]^+$ (100%). Analytical HPLC: 98% purity (254 nm).

3-(4-(6-((1,4,7-Triazacyclononan-1-yl)methyl)pyridin-2-yl)-1H-1,2,3-triazol-1-yl)propan-1-ol (25)

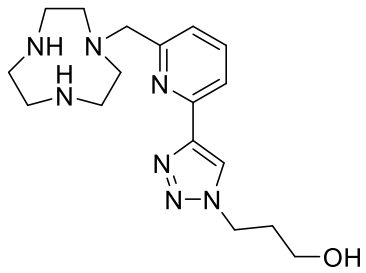

Compound **24** (24 mg, 55 µmol) was dissolved in a 1:1 (v/v) mixture of TFA/DCM (5 mL) and stirred at RT O/N. Excess TFA and remaining DCM were removed by gently bubbling N_2 gas through the solution to yield a dark brown crude solid that was purified *via* preparative HPLC

to yield a colourless crystalline product following lyophilisation. Yield: 12 mg, 63%. ^{1}H NMR (D_2O) δ 8.54 (s, 1H), 7.98 (t, *J* = 7.8 Hz, 1H), 7.75 (d, *J* = 7.8 Hz, 1H), 7.40 (d, *J* = 7.8 Hz, 1H), 4.55 (t, *J* = 6.8 Hz, 2H), 4.16 (s, 2H), 3.78 (s, 4H), 3.58 (t, *J* = 6.3 Hz, 2H), 3.29 (t, *J* = 5.8 Hz, 4H), 3.11 (t, *J* = 5.7 Hz, 4H), 2.14 (app. p, *J* = 6.5 Hz, 2H). ^{13}C NMR (D_2O) δ 157.43, 147.48, 145.20, 140.95, 124.89, 123.46, 121.30, 58.22, 57.30, 48.43, 44.23, 42.82, 31.77. HRMS (ESI): *m/z* calc'd for $[M+H]^+$, M = $C_{17}H_{27}N_7O$: 346.2350, found: 346.2353. Analytical HPLC: 96% purity (254 nm).

6-((4,7-*bis*(*tert*-Butoxycarbonyl)-1,4,7-triazacyclononan-1-yl)methyl)-4-(1-(3-hydroxypropyl)-1H-1,2,3-triazol-4-yl)picolinic acid (26)

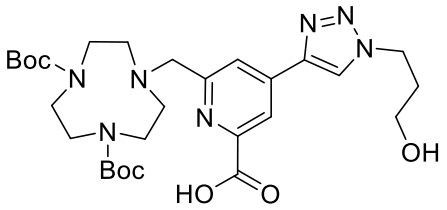

Compound **23** (80 mg, 164 µmol) was dissolved in a 1:2 (v/v) mixture of H_2O/MeCN (6 mL). To the resulting solution was added 3-azidopropan-1-ol (33 mg, 327 µmol), sodium ascorbate (65 mg, 327 µmol), copper (II) sulphate (2.6 mg, 16 µmol) and THPTA (14.3 mg, 33 µmol) and the mixture stirred at RT O/N, after which time LC-MS analysis showed complete click ligation. RP-DCVC was used to isolate the product as an off-white solid after lyophilisation. Yield: 27 mg, 28%. ^{1}H NMR (CD_3OD) δ 8.74 (s, 1H), 8.60 (d, *J* = 1.2 Hz, 1H), 8.19 (s, 1H), 4.90 (s, 2H), 4.62 (t, *J* = 7.0 Hz, 2H), 3.89 (s, 4H), 3.62 (t, *J* = 6.0 Hz, 2H), 3.53 (s, 8H), 2.18 (app. p, *J* = 6.6 Hz, 2H), 1.52 (s, 18H). ^{13}C NMR (CD_3OD) δ 162.40, 157.22, 152.41, 150.25, 144.75, 143.46, 125.50, 122.40, 82.98, 60.41, 59.24, 48.70, 45.18, 33.87, 28.58. LC-MS (ESI): *m/z* 590.30 $[M+H]^+$ (100%). Analytical HPLC: 98% purity (254 nm).

6-((1,4,7-Triazacyclononan-1-yl)methyl)-4-(1-(3-hydroxypropyl)-1H-1,2,3-triazol-4-yl)picolinic acid (27)

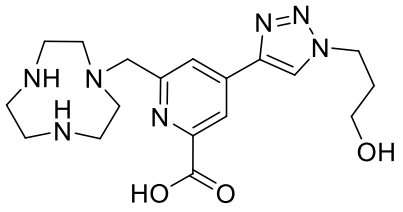

Compound **26** (20 mg, 34 µmol) was dissolved in a 1:1 (v/v) mixture of TFA/DCM (5 mL) and stirred at RT O/N. Excess TFA and remaining DCM were removed by gently bubbling N_2 gas through the solution to yield a dark brown crude solid that was purified *via* preparative HPLC to yield a colourless crystalline product following lyophilisation. Yield: 8 mg, 60%. ^{1}H NMR (D_2O) δ 8.53 (s, 1H), 8.32 (d, *J* = 1.2 Hz, 1H), 7.84 (d, *J* = 1.1 Hz, 1H), 4.57 (t, *J* = 7.0 Hz, 2H), 4.23 (s, 2H), 3.78 (s, 4H), 3.59 (t, *J* = 6.2 Hz, 2H), 3.33 (t, *J* = 5.7 Hz, 4H), 3.15 (s, 4H), 2.15 (app. p, *J* = 6.7 Hz, 2H). ^{13}C NMR (D_2O) δ 168.43, 160.07, 149.26, 143.97, 140.65, 124.67, 121.66, 120.47, 58.15, 57.35, 48.66, 47.66, 44.50, 43.05, 31.75. HRMS (ESI): *m/z* calc'd for $[M+H]^+$, M = $C_{18}H_{27}N_7O_3$: 390.2248, found: 390.2255. Analytical HPLC: 99% purity (254 nm).

On-resin "clicking" experiments

The bombesin peptide sequence Orn(N_3)-*β*Ala-*β*Ala-Gln-Tpr-Ala-Val-Gly-His-Cha-Nle-NH_2 was constructed on resin *via* automated SPSS, following standard Fmoc chemistry. 15 mg of resin, which was estimated to be equivalent to 4 mg of peptide by calculating the difference in mass between the blank and peptide-loaded resin, was placed in a 1.5 mL plastic vial and allowed to swell in DMSO (1 mL) for 30 min. A separate vial was prepared for each reaction. 100 mM stocks of sodium ascorbate, CuI, CuBr, $CuSO_4$, 2,6-lutidine, $(CH_3)_4NF$ (TBAF), THPTA, BTTAA and propargyl alcohol were prepared. To each prepared vial was added 1 equivalent of sodium ascorbate (32 µL), 2 equivalents of progaryl alcohol (64 µL), 0.1 equivalents of a copper source (3.2 µL) and 0.2 equivalents of copper(I)-stabilising ligand (6.4 µL). The resulting solutions were agitated either at RT or 50°C O/N. Resin was pelleted *via*

centrifugation followed by washing with MeOH (2 x 1 mL) and Et_2O (2 x 1 mL). Treatment of the resin using a cleavage cocktail of 95% TFA, 2.5% water and 2.5% triisopropylsilane (TIPS) gave the deprotected peptides, which were analysed by peptide LC-MS to determine the extent of conversion to the product.

Synthesis of sulfo-Cy5-(PEG-3)-bombesin peptide conjugate

The PEGylated bombesin peptide sequence (PEG-3)-Orn(N_3)-*β*Ala-*β*Ala-Gln-Tpr-Ala-Val-Gly-His-Cha-Nle-NH_2 was constructed on resin *via* automated SPSS, following standard Fmoc chemistry. To resin-bound peptide (100 mg resin, equivalent to *ca.* 38 µmol of peptide) swollen in DMF (5 mL) was added sulfo-Cy5-COOH (30 mg, 45 µmol), DIPEA (92 mg, 16 µL, 56 µmol) and PyBOP (30 mg, 46 µmol) and the resulting solution agitated at RT O/N. The resin was washed with MeOH (2 x 10 mL), followed by Et_2O (2 x 10 mL). A small-scale cleavage was conducted (cleavage cocktail: 95 % TFA, 2.5% water and 2.5% TIPS) to confirm the formation of the product. Peptide LC-MS (ESI): *m/z* 1044.30 $[M+H]^{2+}$.

Synthesis of BBNC1

To resin-bound sulfo-Cy5-(PEG-3)-bombesin (40 mg resin, equivalent to *ca.* 9.5 µmol of peptide) swollen in DMSO (3 mL) for 30 min was added **17** (8.8 mg, 20 µmol), sodium ascorbate (4 mg, 20 µmol), CuI (0.2 mg, 1.0 µmol) and THPTA (0.9 mg, 2.0 µmol). The resulting solution was agitated at 50^{o}C O/N. The resin was then washed as described previously, with an additional washing step of 100 mM cyclen solution (2 x 10 mL) before cleavage from the resin using a cocktail of 95 %TFA, 2.5% water and 2.5% TIPS. The crude product was purified *via* preparative HPLC to give the final product as a fluffy dark blue solid after lyophilisation. Peptide LC-MS (ESI) : *m/z* 1166.50 $[M+H]^{2+}$, 778.10 $[M+H]^{3+}$.

Synthesis of BBNC2

To resin-bound sulfo-Cy5-(PEG-3)-bombesin (40 mg resin, equivalent to *ca.* 9.5 µmol of peptide) swollen in DMSO (3 mL) for 40 min was added **23** (9.8 mg, 20 µmol), sodium ascorbate (4 mg, 20 µmol), CuI (.2 mg, 1.0 µmol) and THPTA (0.9 mg, 2.0 µmol). The resulting solution was agitated at 50°C O/N. The resin was then washed as described previously, with an additional washing step of 100 mM cyclen (2 x 10 mL) solution before cleavage from the resin using a cocktail of 95% TFA, 2.5% water and 2.5% TIPS. The crude product was purified *via* preparative HPLC to give the final product as a fluffy dark blue solid after lyophilisation. Peptide LC-MS (ESI): *m/z* 1189.50 $[M+H]^{2+}$, 792.70 $[M+H]^{3+}$.

$^{64}Cu^{2+}$ radiolabelling kinetic studies for ligands 25 and 27

Compound **25** or **27** (0.02 µmol) was combined with 5 MBq of $[^{64}Cu]CuCl_2$ in 0.1 M MES buffer (pH 5.5) to make up a final volume of 200 µL. The resulting mixtures were incubated with agitation at 25°C and the extent of complexation monitored at various time intervals (1, 2, 5, 10, and 30 min, and 1, 4, and 24 h) *via* radio-TLC using silica TLC plates with a 2 M NH_4OAc/MeOH (1:1) mobile phase.

Assessment of stability of the $^{64}Cu(II)$ complexes of 25 and 27 using TETA challenge experiments

Compound **25** or **27** (0.02 µmol) was combined with 5 MBq of $[^{64}Cu]CuCl_2$ in 0.1 M MES buffer (pH 5.5) to make up to a final volume of 200 µL. These mixtures were incubated at 37°C for 30 min prior to the addition of 20 equivalents of TETA (173 µg, 0.40 µmol). The resulting mixtures were incubated with agitation at 25°C, and the amount of intact $^{64}Cu(II)$ complexes determined at various time intervals (5, 10, 30, 60, 120 and 240 min) *via* radio-TLC using silica TLC plates with a 2M NH_4OAc/MeOH (1:1) mobile phase.

Assessment of stability of the ^{64}Cu(II) complexes of 25 and 27 in human serum

Compound **25** or **27** (0.02 μmol) were combined with 5 MBq of [^{64}Cu]$CuCl_2$ in 0.1 M MES buffer (pH 5.5) to make up to a final volume of 50 μL. These mixtures were incubated at 37^{o}C for 30 min. To these solutions was added 450 μL human serum to make up to a final volume of 500 μL. The solutions were incubated with agitation at 25^{o}C, and the amount of intact ^{64}Cu(II) complexes determined at various time intervals (10, 30, 60, 120 and 240 min) *via* radio-TLC using silica TLC plates with a 2 M NH_4OAc/MeOH (1:1) mobile phase.

Synthesis of ^{64}Cu(II)-BBNC1 radiocomplex

BBNC1 (50 μg, 0.02 μmol) was dissolved in 0.1 M MES buffer (pH 5.5) (50 μL) with 20% ethanol. To this was added 53 Mbq of [^{64}Cu]$CuCl_2$ and 0.1 M MES buffer (pH 5.5) added to make up to a final volume of 150 μL. The resulting solution was incubated with agitation at 37^{o}C for 2 h. The extent of radiolabelling was assessed *via* radio-TLC under two different conditions: 1) aluminium oxide TLC plates with a 2 M ammonium acetate in ethanol mobile phase, 2) silica gel TLC plate with a 0.9 % sodium chloride + 5 % acetic acid aqueous mobile phase.

Appendix

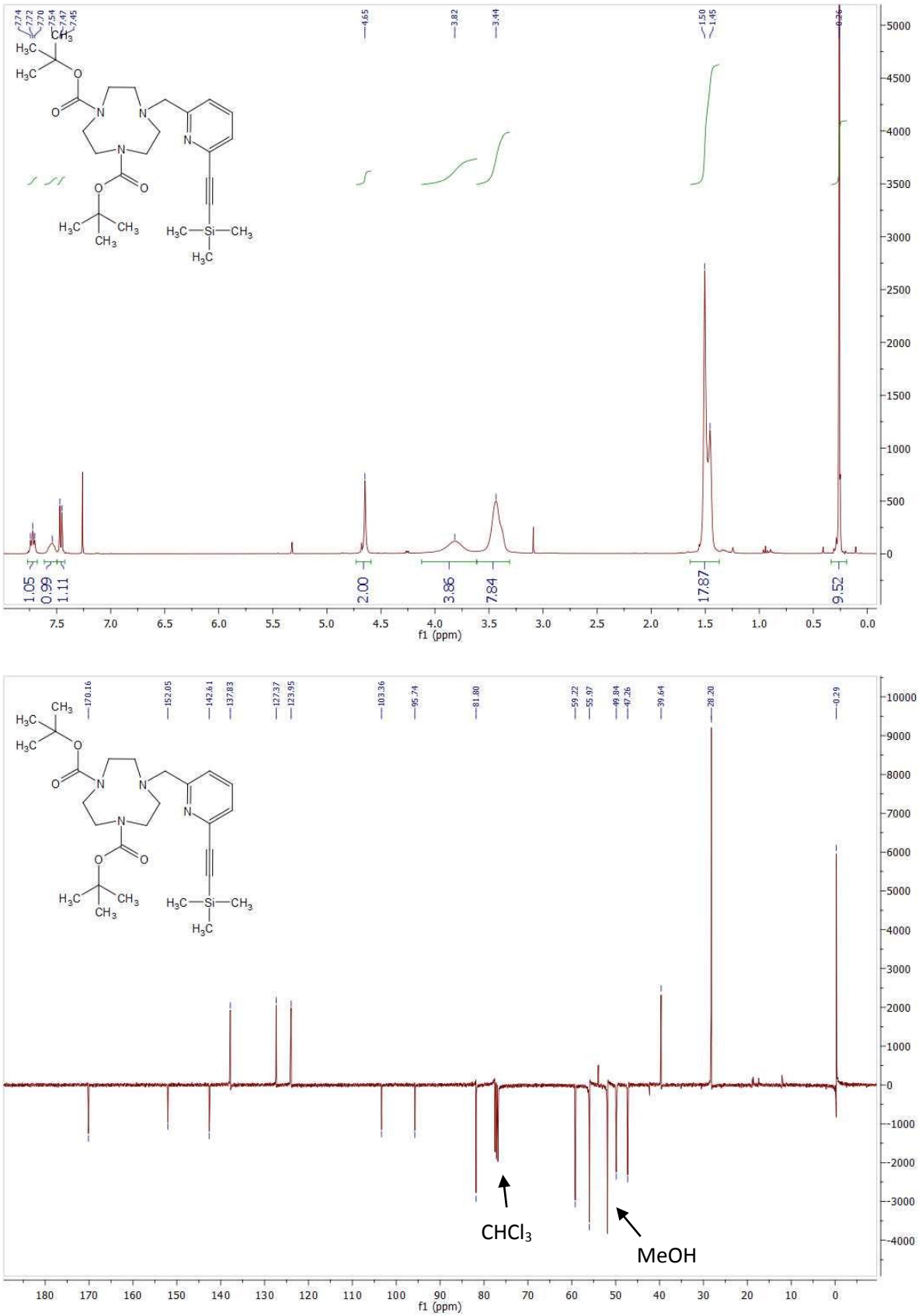

Figure A1. ^{1}H and ^{13}C NMR spectra for **16** in $CDCl_3$.

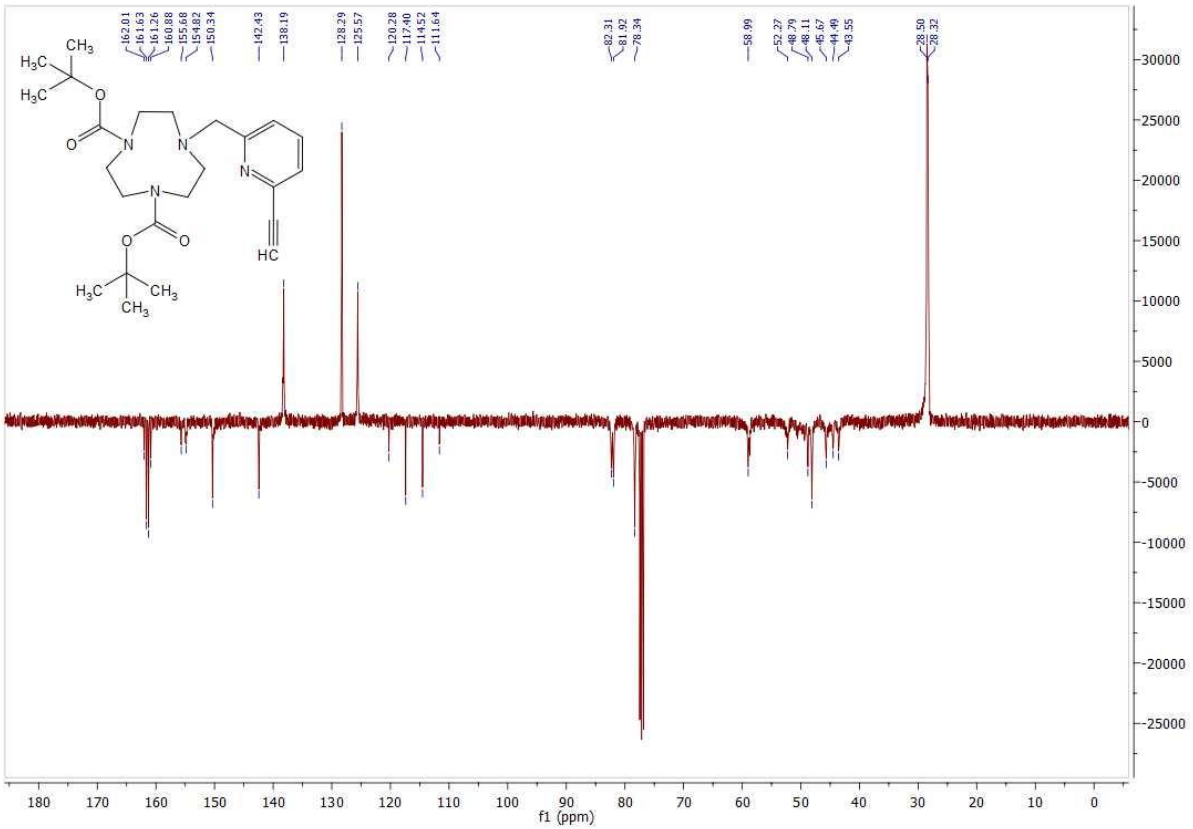

Figure A2. ^{13}C NMR spectra for **17** in $CDCl_3$.

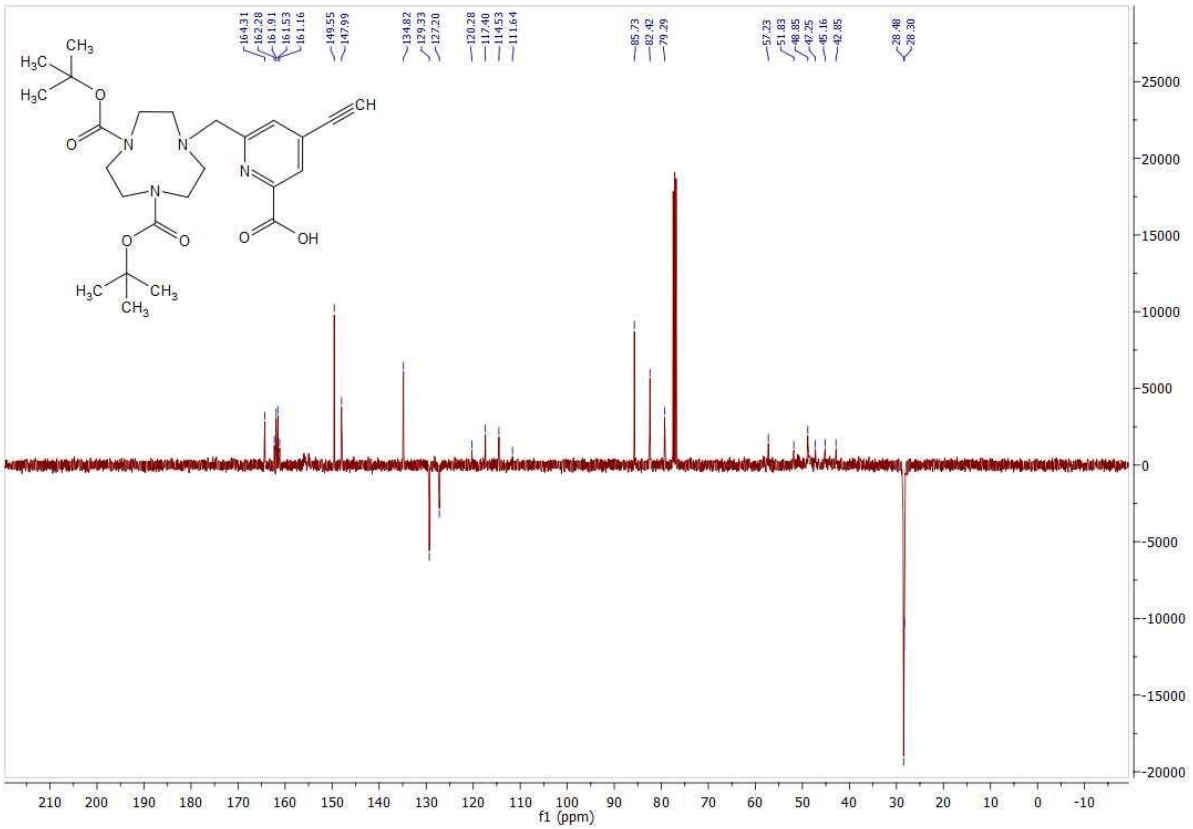

Figure A3. ^{1}H and ^{13}C NMR spectra for **23** in $CDCl_3$.

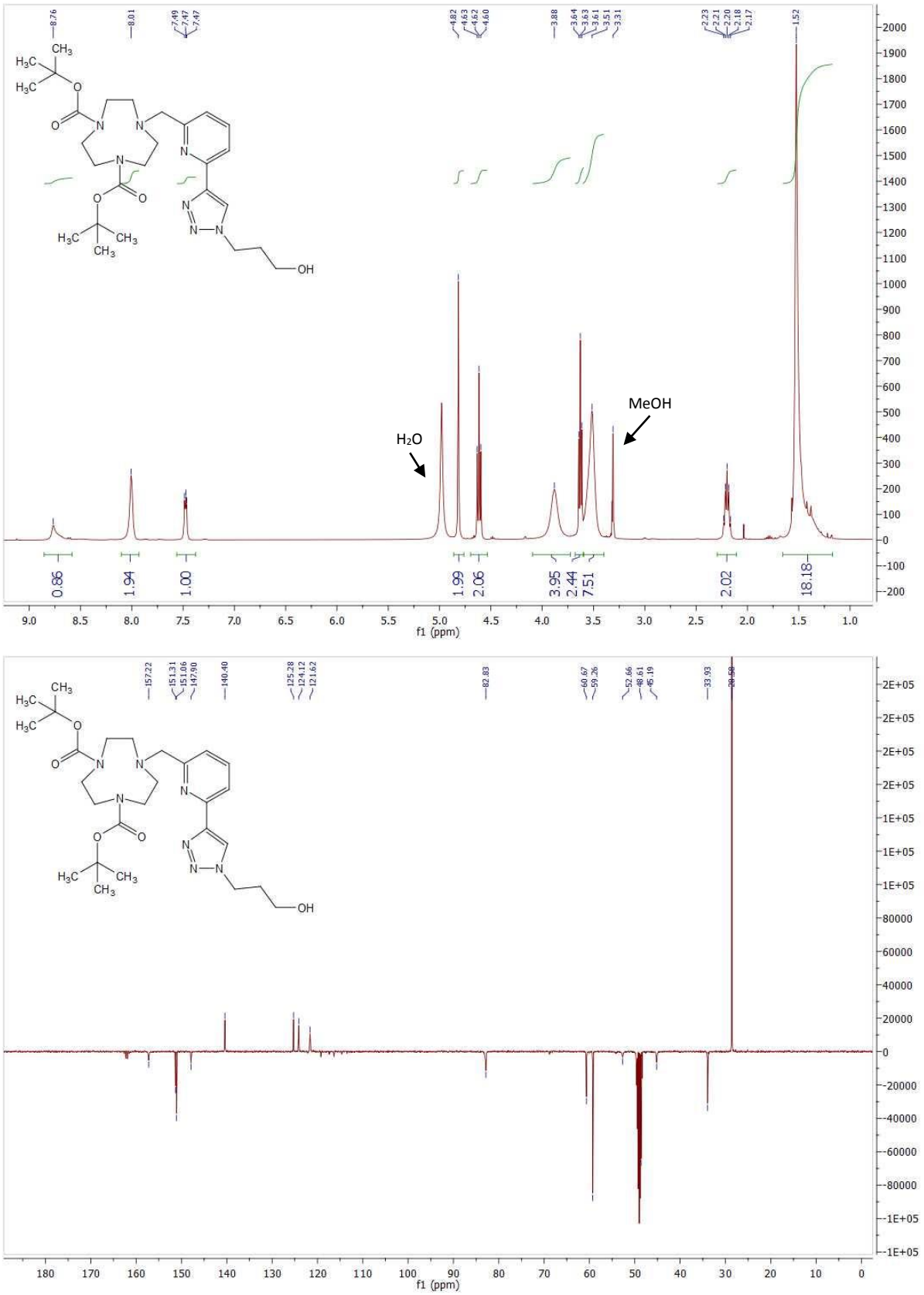

Figure A4. ^{1}H and ^{13}C NMR spectra for **24** in CD_3OD.

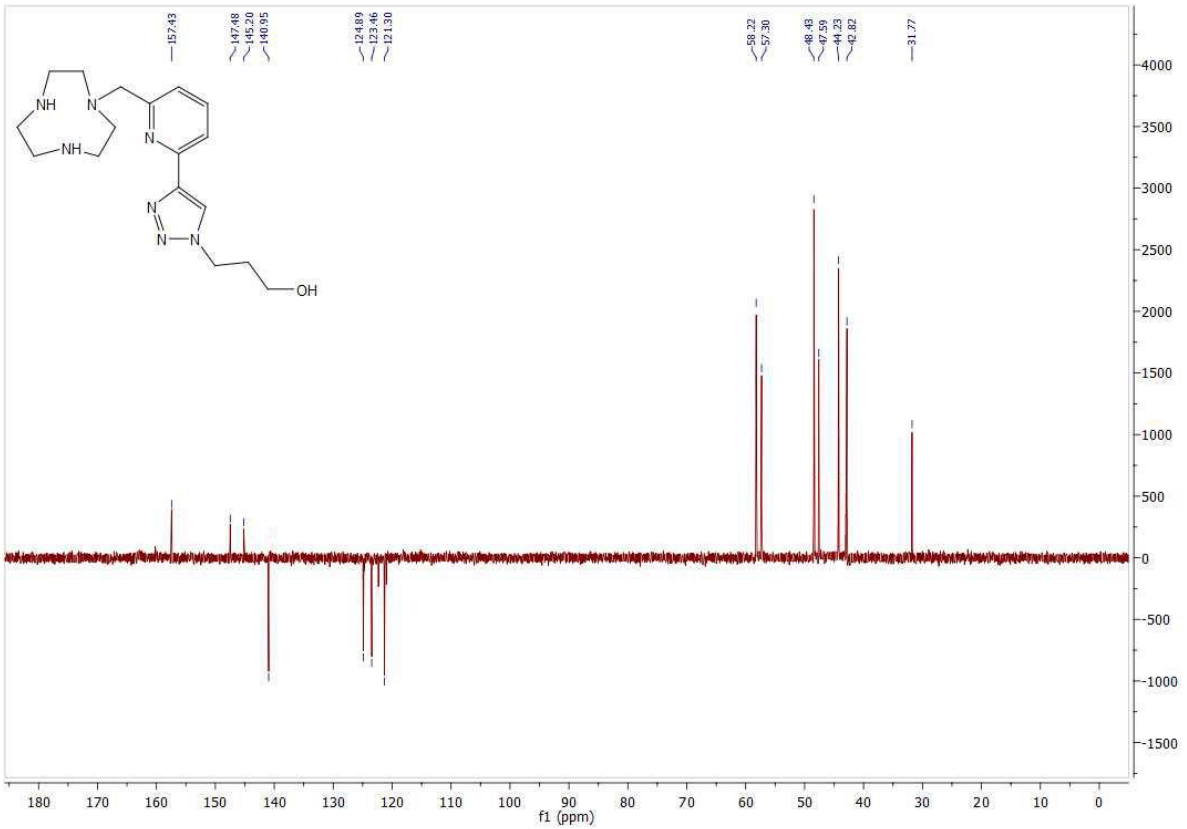

Figure A5. ^{13}C NMR spectrum for **25** in D_2O.

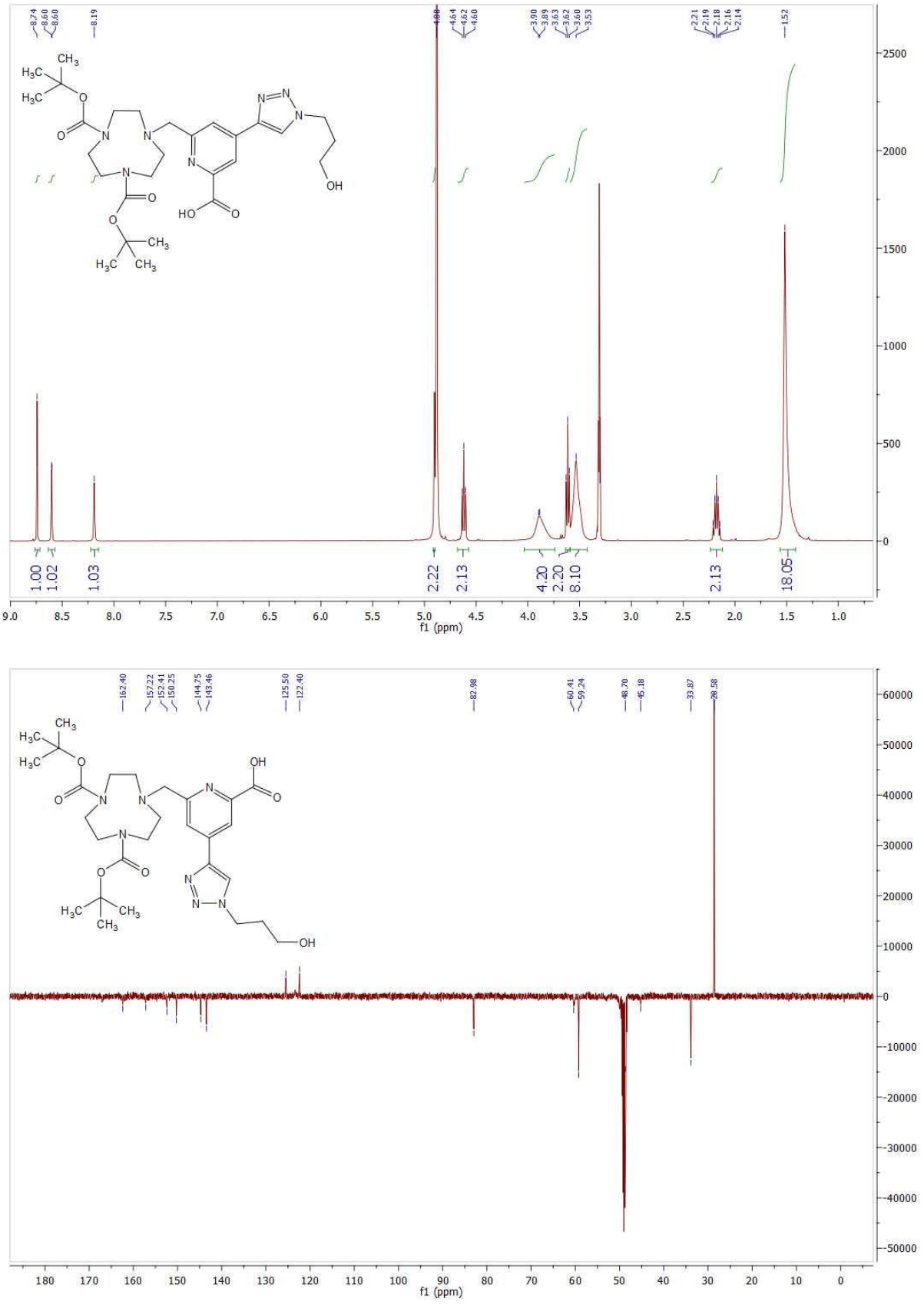

Figure A6. ^{1}H and ^{13}C NMR spectra for **26** in CD_3OD.

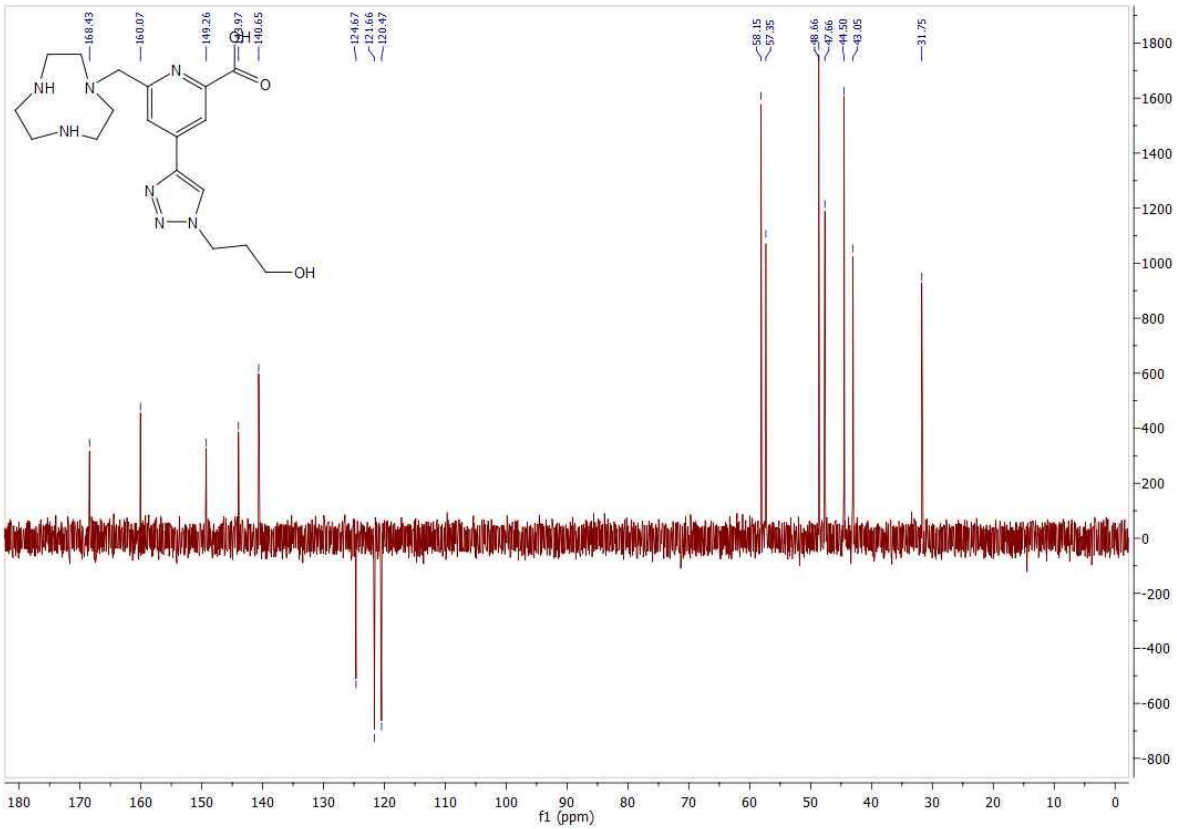

Figure A7. ^{13}C NMR spectrum for **27** in D_2O.

References

(1) Delgado, R.; Felix, V.; Lima, L. M. P.; Price, D. W. *Dalt. Trans.* **2007**, No. 26, 2734.

(2) Parker, D. *Chem. Soc. Rev.* **1990**, *19* (3), 271–291.

(3) Bernhardt, P. V.; Sharpe, P. C. *Inorg. Chem.* **2000**, *39* (18), 4123–4129.

(4) Rogers, B. E.; Anderson, C. J.; Connett, J. M.; Guo, L. W.; Edwards, W. B.; Sherman, E. L.; Zinn, K. R.; Welch, M. J. *Bioconjugate Chem.* **1996**, *7* (4), 511–522.

(5) Anderson, C. J.; Dehdashti, F.; Cutler, P. D.; Schwarz, S. W.; Laforest, R.; Bass, L. A; Lewis, J. S.; McCarthy, D. W. *J. Nucl. Med.* **2001**, *42* (2), 213–221.

(6) Smith, S. V. *J. Inorg. Biochem.* **2004**, *98* (11), 1874–1901.

(7) Shokeen, M.; Anderson, C. J. *Acc. Chem. Res.* **2009**, *42* (7), 832–841.

(8) Sun, X.; Anderson, C. J. In *Methods in Enzymology*; **2004**; Vol. 386, pp 237–261.

(9) van der Veldt, A. A. M.; Smit, E. F.; Lammertsma, A. A. *Front. Oncol.* **2013**, *3* (August), 1–7.

(10) Gasser, G.; Tjioe, L.; Graham, B.; Belousoff, M. J.; Juran, S.; Walther, M.; Künstler, J. U.; Bergmann, R.; Stephan, H.; Spiccia, L. *Bioconjugate Chem.* **2008**, *19* (3), 719–730.

(11) Bergmann, R.; Ruffani, A.; Graham, B.; Spiccia, L.; Steinbach, J.; Pietzsch, J.; Stephan, H. *Eur. J. Med. Chem.* **2013**, *70*, 434–446.

(12) Comba, P.; Hunoldt, S.; Morgen, M.; Pietzsch, J.; Stephan, H.; Wadepohl, H. *Inorg. Chem.* **2013**, *52* (14), 8131–8143.

(13) Brox, D.; Comba, P.; Herten, D.-P.; Kimmle, E.; Morgen, M.; Rühl, C. L.; Rybina, A.; Stephan, H.; Storch, G.; Wadepohl, H. *J. Inorg. Biochem.* **2015**, *148*, 78–83.

(14) Barreto, J. A.; Matterna, M.; Graham, B.; Stephan, H.; Spiccia, L. *New J. Chem.* **2011**, *35* (11), 2705.

(15) Juran, S.; Walther, M.; Stephan, H.; Bergmann, R.; Steinbach, J.; Kraus, W.; Emmerling, F.; Comba, P. *Bioconjugate Chem.* **2009**, *20* (2), 347–359.

(16) Kubeil, M.; Zarschler, K.; Pietzsch, J.; Kraus, W.; Comba, P.; Stephan, H. *Eur. J. Inorg. Chem.* **2015**, *2015* (24), 4013–4023.

(17) Pant, K.; Gröger, D.; Bergmann, R.; Pietzsch, J.; Steinbach, J.; Graham, B.; Spiccia, L.; Berthon, F.; Czarny, B.; Devel, L.; Dive, V.; Stephan, H.; Haag, R. *Bioconjugate Chem.* **2015**, *26* (5), 906–918.

(18) Viehweger, K.; Barbaro, L.; García, K. P.; Joshi, T.; Geipel, G.; Steinbach, J.; Stephan, H.; Spiccia, L.; Graham, B. *Bioconjugate Chem.* **2014**, *25* (5), 1011–1022.

(19) Pombo-García, K.; Zarschler, K.; Barreto, J. A.; Hesse, J.; Spiccia, L.; Graham, B.; Stephan, H. *RSC Adv.* **2013**, *3* (44), 22443.

(20) Smith, C. J.; Volkert, W. A.; Hoffman, T. J. *Nucl. Med. Biol.* **2003**, *30* (8), 861–868.

(21) Cuttitta, F.; Carney, D. N.; Mulshine, J.; Moody, T. W.; Fedorko, J.; Fischler, A.; Minna, J. D. *Nature* **1985**, *316* (6031), 823–826.

(22) Carney, D. N.; Cuttitta, F.; Moody, T. W.; Minna, J. D. *Cancer Res.* **1987**, *47* (3), 821–825.

(23) Thomas, S. M.; Grandis, J. R.; Wentzel, A. L.; Gooding, W. E.; Lui, V. W. Y.; Siegfried, J. M. *Neoplasia* **2005**, *7* (4), 426–431.

(24) Moody, T. W.; Cuttitta, F. *Life Sci.* **1993**, *52* (14), 1161–1173.

(25) Anastasi, A.; Erspamer, V.; Bucci, M. *Arch. Biochem. Biophys.* **1972**, *148* (2), 443–446.

(26) McDonald, T. J.; Jörnvall, H.; Nilsson, G.; Vagne, M.; Ghatei, M.; Bloom, S. R.; Mutt, V. *Biochem. Biophys. Res. Commun.* **1979**, *90* (1), 227–233.

(27) Sun, B.; Halmos, G.; Schally, A. V.; Wang, X.; Martinez, M. *Prostate* **2000**, *42* (4), 295–303.

(28) Markwalder, R.; Reubi, J. C. *Cancer Res.* **1999**, *59* (5), 1152–1159.

(29) Gugger, M.; Reubi, J. C. *Am. J. Pathol.* **1999**, *155* (6), 2067–2076.

(30) Moody, T. W.; Bertness, V.; Carney, D. N. *Peptides* **1983**, *4* (5), 683–686.

(31) Baidoo, K. E.; Lin, K. S.; Zhan, Y.; Finley, P.; Scheffel, U.; Wagner, H. N. *Bioconjugate Chem.* **1998**, *9* (2), 218–225.

(32) Smith, C. J.; Volkert, W. A.; Hoffman, T. J. *Nucl. Med. Biol.* **2005**, *32* (7), 733–740.

(33) Dimitrakopoulou-Strauss, A.; Hohenberger, P.; Haberkorn, U.; Macke, H. R.; Eisenhut, M.; Strauss, L. G. *J. Nucl. Med.* **2007**, *48* (8), 1245–1250.

(34) Brans, L.; García-Garayoa, E.; Schweinsberg, C.; Maes, V.; Struthers, H.; Schibli, R.; Tourwé, D. *ChemMedChem* **2010**, *5* (10), 1717–1725.

(35) Schweinsberg, C.; Maes, V.; Brans, L.; Bläuenstein, P.; Tourwé, D. A.; Schubiger, P. A.; Schibli, R.; Garayoa, E. G. *Bioconjugate Chem.* **2008**, *19* (12), 2432–2439.

(36) Cescato, R.; Maina, T.; Nock, B.; Nikolopoulou, A.; Charalambidis, D.; Piccand, V.; Reubi, J. C. *J. Nucl. Med.* **2008**, *49* (2), 318–326.

(37) García Garayoa, E.; Rüegg, D.; Bläuenstein, P.; Zwimpfer, M.; Khan, I. U.; Maes, V.; Blanc, A.; Beck-Sickinger, A. G.; Tourwé, D. A.; Schubiger, P. A. *Nucl. Med. Biol.* **2007**, *34* (1), 17–28.

(38) Kovacs, Z.; Sherry, A. D. *Tetrahedron Lett.* **1995**, *36* (51), 9269–9272.

(39) Chong, H. S.; Ma, X.; Le, T.; Kwamena, B.; Milenic, D. E.; Brady, E. D.; Song, H. A; Brechbiel, M. W. *J. Med. Chem.* **2008**, *51* (2), 118–125.

(40) Chan, T. R.; Hilgraf, R.; Sharpless, K. B.; Fokin, V. V. *Org. Lett.* **2004**, *6* (27), 2853–2855.

(41) Hong, V.; Presolski, S.; Ma, C.; Finn, M. A. G. *Angew. Chem Int. Ed.* **2009**, *48* (52), 9879–9883.

(42) Baccile, J. A.; Morrell, M. A.; Falotico, R. M.; Milliken, B. T.; Drew, D. L.; Rossi, F. M. *Tetrahedron Lett.* **2012**, *53* (15), 1933–1935.

(43) Ingale, S.; Dawson, P. E. *Org. Lett.* **2011**, *13* (11), 2822–2825.

(44) Serim, S.; Mayer, S. V.; Verhelst, S. H. L. *Org. Biomol. Chem.* **2013**, *11* (34), 5714.

(45) Strack, M.; Metzler-Nolte, N.; Albada, H. B. *Org. Lett.* **2013**, *15* (12), 3126–3129.

(46) Phillips, W. T.; Klipper, R.; Goins, B. *J. Pharmacol. Exp. Ther.* **2000**, *295* (1), 309–313.

(47) Misselwitz, B. *Eur. J. Radiol.* **2006**, *58* (3), 375–382.

(48) Kalchenko, V.; Shivtiel, S.; Malina, V.; Lapid, K.; Haramati, S.; Lapidot, T.; Brill, A.; Harmelin, A. *J. Biomed. Opt.* **2006**, *11* (5), 050507.

(49) Guo, Y.; Yuan, H.; Rice, W. L.; Kumar, A. T. N.; Goergen, C. J.; Jokivarsi, K.; Josephson, L. *J. Am. Chem. Soc.* **2012**, *134* (47), 19338–19341.

CHAPTER 6:

SUMMARY AND FUTURE DIRECTIONS

6.1 General summary

This thesis described the design, synthesis and evaluation of a series of new metal complex-based tags that can be conjugated to other molecules *via* bioorthogonal copper-catalysed azide alkyne cycloaddition (CuAAC) or "click" reactions for various biological and medical applications. A major focus of this work was to use these tags to enable site-specific labelling of biological entities with different chemical functionalities, with imaging and utilisation as assay components representing the ultimate future applications. Three separate classes of click-conjugatable tags were investigated. Each chapter within this thesis focused on a different class of tags, namely i) luminescent lanthanide complexes, ii) an MRI-active probe incorporating a fluorescent pendant, and iii) ^{64}Cu radionuclide-binding tags. This last chapter provides a summary of the major results and discusses potential future directions for each of the developed tags.

6.2 Terbium(III)-based luminescent lanthanide complexes for bioorthogonal labelling

The first section of this thesis (**Chapter 2**) established a synthetic pathway to two novel luminescent lanthanide complexes (Tb-$\mathbf{L^1}$ and Tb-$\mathbf{L^2}$), each incorporating an alkyne reaction handle for "click" bioconjugation. A third terbium complex (Tb-**4**, **Chapter 3**) was also produced, however synthetic challenges resulted in the focus of this work being directed towards Tb-$\mathbf{L^1}$ and Tb-$\mathbf{L^2}$. The suitability of these two complexes for click labelling was initially demonstrated through the successful and rapid conjugation to a small model azide. In evaluation of their photophysical properties, Tb-$\mathbf{L^1}$ and Tb-$\mathbf{L^2}$ exhibited quantum yields of Φ_{H2O} = 13% and 22%, respectively. Additionally, Tb-$\mathbf{L^1}$ displayed a significant increase in quantum yield to Φ_{H2O} = 21% post-clicking, due to the newly formed triazole both evicting a co-ordinated water molecule and creating a ninth co-ordination site to the Tb ion, establishing the usefulness of this complex as a "light up" tagging reagent. Both Tb-$\mathbf{L^1}$ and Tb-$\mathbf{L^2}$ proved

"click"-compatible in the labelling of a *E. coli* aspartate/glutamate-binding protein that had been engineered to contain either an *p*-azido-*L*-phenylalanine or *p*-(azidomethyl)-*L*-phenylalanine unnatural amino acid. Given that these two tags are luminescent, can be ligated in near-quantitative yields and can be introduced to proteins in a site-specific manner, it is anticipated that will ultimately prove useful for luminescent assay applications. Future work may involve, for example, the development of a system to detect protein conformational changes. Such a system could potentially utilise one of these complexes functioning in tandem with a cysteine-reactive acceptor fluorophore (which can also be selectively installed into proteins, due to the rarity of protein surface cysteine residues) to form a luminescence resonance energy transfer (LRET) pair that responds to conformational changes in proteins. Such a system would have applications in drug discovery and inhibitor screening.[7,8]

It should be noted that whilst the tags are luminescent, they are not well suited to cellular imaging applications. The two tags, as well as their clicked counterparts, exhibit absorption maxima between 275 and 300 nm. Irradiating living tissue or cells at such low wavelengths is less than ideal, resulting in poor penetration and potential damage.[1,2] Additionally, whilst the complexes' quantum yields compare favourably with many other terbium-based LLCs, the low molar extinction coefficients of Tb-$\mathbf{L^1}$ and Tb-$\mathbf{L^2}$ mean that they lack the brightness of the fluorophores typically used for cellular imaging. Although not reported within this thesis, Tb-$\mathbf{L^1}$ and Tb-$\mathbf{L^2}$ were successfully conjugated to a small viral cell-penetrating peptide (Tat peptide)[3] and attempts made to image these conjugates *via* confocal fluorescence microscopy. These, however, proved unsuccessful due the lack of brightness and the fact that the microscope employed lacked the capacity to perform time-gated experiments to eliminate background fluorescence.[4–6] Further work may involve re-engineering of the complexes to increase brightness and the excitation wavelength.

6.3 Gadolinium(III) complexes incorporating a fluorophore for multi-modal theranostic applications

The second part of this thesis concerned the development of two new alkynyl-napthalimide fluorophore-bearing bifunctional Gd(III) chelates. Unfortunately, ligand **11** (**Chapter 4**), proved to be unstable in aqueous media, resulting in difficulty producing the corresponding Gd(III) complex. **L** (**Chapter 3**), however, proved highly stable, allowing for the formation of a Gd(III) complex and ligation to a small model azide. Post-clicking, Gd-**L** demonstrated an increased quantum yield, from Φ_{H2O} = 35% to 59%. Additionally, a large shift of 54 nm was observed in the maximal emission. The cellular imaging capabilities and cytotoxicity of Gd-**L** were assessed by clicking it to an azide-bearing, cell-penetrating viral Tat peptide. Incubation of this construct (Gd-**L**-**Tat**) with CAL-33 cells demonstrated its ability to enter cells. In addition, irradiation experiments revealed an increase in cytotoxicity upon exposure to UV-A radiation.

Future work will involve experiments to establish the MRI contrast capabilities of Gd-**L**. Such experiments would involve first establishing that a simple solution of the material is MRI-active. This would then be followed by the conjugation of Gd-**L** to a targeting agent, which would enable the probe to accumulate at a site of interest in small animal MRI studies.

6.4 Bombesin conjugates for biomodal PET-fluorescence imaging applications

The final section of this thesis involved the synthesis and evaluation of two bombesin constructs incorporating functionalities for both PET and fluorescence detection, to be applied as a bimodal prostate cancer imaging probes.[9–12] The bulk of this work involved the development and synthesis of **17** and **23**, two new alkyne-bearing ^{64}Cu pro-chelators based upon the TACN macrocycle. **17** and **23** were successfully ligated to a model azide and, following deprotection, gave the model

clicked ligands **25** and **27**. Both of these ligands demonstrated rapid complexation of the ^{64}Cu radionuclide, with the resulting complexes exhibiting high stability when exposed to human plasma and a strong resistance to trans-chelation in challenge experiments, a prerequisite for *in vivo* PET imaging applications. Pro-chelators **17** and **23** were evolved into prostate cancer imaging probes through clicking to a resin bound bombesin peptide containing an azido-ornithine unnatural amino acid, and previously labelled with a fluorescent sulfo-Cy5 dye. Of the two constructs, **BBNC1** and **BBNC2**, only **BBNC1** was assessed, displaying a radiochemical yield of 90% before injection into NMRI nude immunodeficient (nu/nu) mice, pre-injected with subcutaneous prostate cancer cells. Unfortunately, assessment of biodistribution and uptake/removal kinetics of ^{64}Cu(II)-**BBNC1** from these mice, *via* small-animal PET imaging, revealed that the radiotracer exhibited no active targeting properties. These disappointing results are throught to be the result of the lipophilic nature of the sulfo-Cy5 dye exhibiting a dominant effect upon *in vivo* distribution characteristics.[13] Accumulation of ^{64}Cu(II)-**BBNC1** was noted in the lymph nodes of some mice, although the precise mechanism remains unknown, indicating that this compound may have application in the imaging of "excited" lymph nodes.[14–16] This observation may warrant further investigation, possibly through the development of an excited lymph animal model as well as metabolic studies and observation of tumour and lymph node accumulation in various tumour entities. More likely continuation of this project would involve the revaluation of the constructs themselves to incorporate a "PEG cloud", which has been demonstrated to provide shielding against the non-specific lipophilic binding imparted by the Cy5 dye.[13] Introduction of such a PEG cloud would require the revaluation of copper-binding properties, to ensure that the PEG presents no undesired copper chelation, followed by *in vivo* testing.

To conclude, this work has delivered a versatile series of new tags that can be easily incorporated into bio-entities with the aid of click chemistry. Their utility, including as detectable and/or potential therapeutic moieties, has been demonstrated through preparation of a number of "model" conjugates. It is hoped that these tags will serve as convenient building blocks for the construction of a wide range of new (bio)conjugates for imaging and assay applications, thereby helping to advance our understanding of biological process, both in healthy and diseased states.

References

(1) Stephens, D. J. *Science (80).* **2003**, *300* (5616), 82–86.

(2) Wang, Y.; Shyy, J. Y.-J.; Chien, S. *Annu. Rev. Biomed. Eng.* **2008**, *10* (1), 1–38.

(3) Vives, E.; Brodin, P.; Lebleu, B. *J. Biol. Chem.* **1997**, *272* (25), 16010–16017.

(4) Soini, A. E.; Kuusisto, A.; Meltola, N. J.; Soini, E.; Seveus, L. *Microsc. Res. Tech.* **2003**, *62* (5), 396–407.

(5) Connally, R. *Anal. Chem.* **2011**, *83* (12), 4782–4787.

(6) Connally, R.; Jin, D.; Piper, J. *Cytom. Part A* **2006**, *69A* (9), 1020–1027.

(7) Kupcho, K. R.; Stafslien, D. K.; DeRosier, T.; Hallis, T. M.; Ozers, M. S.; Vogel, K. W. *J. Am. Chem. Soc.* **2007**, *129* (44), 13372–13373.

(8) Heyduk, T. *Curr. Opin. Biotechnol.* **2002**, *13* (4), 292–296.

(9) Schweinsberg, C.; Maes, V.; Brans, L.; Bläuenstein, P.; Tourwé, D. A.; Schubiger, P. A.; Schibli, R.; Garayoa, E. G. *Bioconjugate Chem.* **2008**, *19* (12), 2432–2439.

(10) García Garayoa, E.; Rüegg, D.; Bläuenstein, P.; Zwimpfer, M.; Khan, I. U.; Maes, V.; Blanc, A.; Beck-Sickinger, A. G.; Tourwé, D. A.; Schubiger, P. A. *Nucl. Med. Biol.* **2007**, *34* (1), 17–28.

(11) Gasser, G.; Tjioe, L.; Graham, B.; Belousoff, M. J.; Juran, S.; Walther, M.; Künstler, J. U.; Bergmann, R.; Stephan, H.; Spiccia, L. *Bioconjugate Chem.* **2008**, *19* (3), 719–730.

(12) Bergmann, R.; Ruffani, A; Graham, B.; Spiccia, L.; Steinbach, J.; Pietzsch, J.; Stephan, H. *Eur. J. Med. Chem.* **2013**, *70*, 434–446.

(13) Guo, Y.; Yuan, H.; Rice, W. L.; Kumar, A. T. N.; Goergen, C. J.; Jokivarsi, K.; Josephson, L. *J. Am. Chem. Soc.* **2012**, *134* (47), 19338–19341.

(14) Phillips, W. T.; Klipper, R.; Goins, B. *J. Pharmacol. Exp. Ther.* **2000**, *295* (1), 309–313.

(15) Misselwitz, B. *Eur. J. Radiol.* **2006**, *58* (3), 375–382.

(16) Kalchenko, V.; Shivtiel, S.; Malina, V.; Lapid, K.; Haramati, S.; Lapidot, T.; Brill, A.; Harmelin, A. *J. Biomed. Opt.* **2006**, *11* (5), 050507.